OPTIMIZATION OF 1ST-LINE ANTITUBERCULOSIS DOSING REGIMENS USING A POPULATION PHARMACOKINETIC APPROACH: FOOD EFFECTS, DRUG COMBINATIONS AND PHARMACOLOGICAL EFFECTS

By

SIMBARASHE PETER ZVADA

Division of Clinical Pharmacology, Department of Medicine

UNIVERSITY OF CAPE TOWN

A thesis in fulfillment of the requirements for the degree of Doctor of Philosophy (PhD)

Main Supervisor: Associate Professor Helen McIlleron

Co-Supervisor: Associate Professor Ulrika S.H. Simonsson

FEBRUARY 2014

“You only live once, but if you do it right, once is enough.”— Mae West

Contributions to the field

This thesis includes some of the contributions to the fields listed below

Full length original articles:

1. Simbarashe P. Zvada, Paolo Denti, Peter R. Donald, Simon H. Schaaf, Stephanie Thee, James A. Seddon, Heiner I. Seifart, Peter J. Smith, Helen M. McIlleron, and Ulrika S. H. Simonsson. Population pharmacokinetics of rifampicin, pyrazinamide and isoniazid in children with tuberculosis: in silico evaluation of currently recommended doses. *Journal of Antimicrobial Chemotherapy*. 2014 Jan; doi: 10.1093/jac/dkt524.

2. Simbarashe P. Zvada, Paolo Denti, Frederick A. Sirgel, Emmanuel Chigutsa, Mark Hatherill, Salome Charalambous, Stanlely Mungofa, Lubbe Wiesner, Ulrika S.H. Simonsson US, Amina Jindani, Thomas Harrison, Helen McIlleron. Moxifloxacin population pharmacokinetics and model-based comparison of efficacy between moxifloxacin and ofloxacin in African patients. *Antimicrobial Agents and Chemotherapy*. 2014 Jan; 58(1):503-10.

3. Simbarashe P. Zvada, Paolo Denti, Hennie Geldenhuys, Sandra Meredith, Sandra van Dyk, Mark Hatherill, Willem Hanekom, Lubbe Wiesner, Ulrika S.H. Simonsson, Amina Jindani, Thomas Harrison, Helen McIlleron. Moxifloxacin population pharmacokinetics in patients with pulmonary tuberculosis and the effect of intermittent high-dose rifapentine. *Antimicrobial Agents and Chemotherapy*. 2012 Aug; 56(8):4471-3.

4. Simbarashe P. Zvada, Jan-stefan Van Der Walt, Peter J. Smith, Benard P Fourie P, Giorgio Roscigno, Dennis Mitchison, Ulrika S.H. Simonsson, Helen McIlleron. Effects of four different meal types on the population pharmacokinetics of single-dose rifapentine in healthy male volunteers. *Antimicrobial Agents and Chemotherapy*. 2010 Aug; 54(8):3390-4.

Scientific conference presentations:

1. Simbarashe P. Zvada, Paolo Denti, Frederick A. Sirgel, Emmanuel Chigutsa, Mark Hatherill, Salome Charalambous, Stanlely Mungofa, Lubbe Wiesner, Ulrika S.H. Simonsson US, Amina Jindani, Thomas Harrison, Helen McIlleron. Moxifloxacin population pharmacokinetics and model-based comparison of efficacy between moxifloxacin and ofloxacin in African patients. *6th International Workshop on Clinical Pharmacology of Tuberculosis Drugs*. Denver, USA. September 2013.

2. Simbarashe P. Zvada, Paolo Denti, Peter R. Donald, Simon H. Schaaf, Stephanie Thee, James A. Seddon, Heiner I. Seifart, Peter J. Smith, Helen M. McIlleron, and Ulrika S. H. Simonsson. Population pharmacokinetics of rifampicin, pyrazinamide and isoniazid in children with tuberculosis. Model-based evaluation of currently recommended doses. *5th International Workshop on Clinical Pharmacology of Tuberculosis Drugs*. San Francisco, USA. September 2012.

3. Simbarashe P. Zvada, Ulrika S. H. Simonsson, Paolo Denti, Peter R. Donald, Simon H. Schaaf, Peter J. Smith, Helen M. McIlleron. Population Pharmacokinetics of Isoniazid in Children with Pulmonary Tuberculosis. *Population Approach Group Europe (PAGE) Twentieth Meeting*. Anthens, Greece. June 2011.

4. Simbarashe P. Zvada, Ulrika S. H. Simonsson, Paolo Denti, Peter R. Donald, Simon H. Schaaf, Peter J. Smith, Helen M. McIlleron. A Population Pharmacokinetic Model for Rationalizing

Rifampicin Dose in Childhood Tuberculosis. *South African Congress for Pharmacology and Toxicology.* Cape Town, South Africa. October 2010.

5. Simbarashe P. Zvada, Ulrika S. H. Simonsson, Paolo Denti, Peter R. Donald, Simon H. Schaaf, Peter J. Smith, Helen M. McIlleron. Population pharmacokinetics of rifampicin in childhood tuberculosis and the need for dose adjustment. *3rd International Workshop on Clinical Pharmacology of Tuberculosis Drugs*. Boston, United States. September 2010.

6. Simbarashe P. Zvada, Jan-stefan Van Der Walt, Peter J. Smith, Benard P Fourie P, Giorgio Roscigno, Dennis Mitchison, Ulrika S.H. Simonsson, Helen McIlleron. Effect of Various Meals on the Population Pharmacokinetics of Rifapentine. *Population Approach Group Europe (PAGE) Nineteenth Meeting.* Berlin, Germany. June 2010.

7. Simbarashe P. Zvada, Jan-stefan Van Der Walt, Peter J. Smith, Benard P Fourie P, Giorgio Roscigno, Dennis Mitchison, Ulrika S.H. Simonsson, Helen McIlleron . Effect of Four Different Meal Types on the bioavailability of a single 900 mg Dose of Rifapentine in Healthy Male Volunteers. *Annual Medicine Research Day*. University of Cape Town, South Africa. October 2009.

8. Simbarashe P. Zvada, Jan-stefan Van Der Walt, Peter J. Smith, Benard P Fourie P, Giorgio Roscigno, Dennis Mitchison, Ulrika S.H. Simonsson, Helen McIlleron. Effect of bulk and fat content meals on the bioavailability of a single 900 mg Dose of Rifapentine in Healthy Male Volunteers. *5th International Conference on Pharmaceutical and Pharmacological Sciences.* North-West University, Potchefstroom, South Africa.

ABSTRACT

OPTIMIZATION OF 1ST-LINE ANTITUBERCULOSIS DOSING REGIMENS USING A POPULATION PHARMACOKINETIC APPROACH: FOOD EFFECTS, DRUG COMBINATIONS AND PHARMACOLOGICAL EFFECTS

Simbarashe Peter Zvada – 2014

The aim of this thesis was to evaluate optimal doses of 1st-line antituberculosis dosing regimens using a population pharmacokinetic approach, quantify food effects, drug combinations and pharmacological effects. The population pharmacokinetics of rifampicin, isoniazid and pyrazinamide in 76 children with tuberculosis were described using a population pharmacokinetic approach, and then Monte Carlo simulation were performed to evaluate adequacy of newly recommended weight band based doses in World Health Organisation (WHO) guidelines. Food effect (breakfast) was evaluated on rifapentine pharmacokinetic data in 35 healthy male volunteers. Effect of co-administered intermittent rifapentine on the pharmacokinetics of moxifloxacin was evaluated in 28 patients with pulmonary tuberculosis, who participated in a multicenter controlled clinical trial evaluating high dose rifapentine in combination with moxifloxacin. The moxifloxacin pharmacokinetic model, together with a previously published ofloxacin pharmacokinetic model, was used to evaluate the efficacy between moxifloxacin and ofloxacin. Furthermore, pharmacokinetic summary variables of rifapentine and moxifloxacin were evaluated as predictors of treatment outcome.

Simulations based on the final models suggested that with the new guidelines, and utilizing available paediatric fixed dose combinations, children will receive adequate rifampicin exposures when compared to adults, but with a larger degree of variability. However, pyrazinamide and isoniazid exposures in many children will be lower than in adults. For food effect, all meals compared with the fasting state, high fat meal had the greatest effect on rifapentine oral bioavailability, increasing it by 86%; bulky low-fat, bulky-high-fat, and chicken soup resulted in 33%, 46%, and 49% increases in rifapentine oral bioavailability, respectively. Similar trends were observed for the metabolite 25-desacetyl rifapentine. For drug-resistant tuberculosis, using a target ratio of ≥100 for multidrug-resistant strains (without resistance to injectable agents or fluoroquinolones), the cumulative fraction of response (CFR) was 88% for moxifloxacin and only 43% for ofloxacin. The higher dose of 800 mg moxifloxacin was needed to achieve a CFR target of ≥90%. In terms of drug-interaction, rifapentine increased the clearance of moxifloxacin by 8% during antituberculosis treatment compared to that after treatment completion without rifapentine. Also, the effect moxifloxacin and rifapentine pharmacokinetics indices on outcome treatment outcome support that combined effect of longer treatment duration and higher rifapentine exposures are associated with better treatment response.

In summary, the newer WHO doses for children may give lower pyrazinamide and isoniazid exposures in many children than in adults. Meals have a substantial impact on rifapentine exposure. Rifapentine did not result in a clinically significant change in moxifloxacin exposure. Moxifloxacin is more efficacious than ofloxacin in the treatment of MDR-TB. The combined effect of longer treatment duration, higher rifapentine exposures are associated with better treatment outcome, but could not differentiate which major factor needed for favourable outcome.

ACKNOWLEDGEMENTS

I am highly thankful to the following whom/which have contributed towards the success my work.

Supervision

- Associate Prof Helen McIlleron – For giving me the opportunity to study under her determined supervision, creation of opportunities to present my work at both local and international scientific conferences/workshops, encouragement, and guidance throughout the course of the work, timely interaction, and a conducive working environment.
- Associate Prof Ulrika Simonsson – For tireless and timely guidance throughout the project, feedback, patience and couching on pharmacokinetic model building and evaluation at Uppsala University in Sweden.

Funding

Wellcome Trust funded the pharmacokinetic data collection of RIFAQUIN study, and additionally supported me for 3.5 years (grant number WT081199/Z/06/Z). Additional support was obtained from the Division of Clinical Pharmacology.

The RIFAQUIN trial study team

Special thanks to Dr. Amina Jindani and Prof Thomas Harrison for helping in monitoring the enrollment of patients into the pharmacokinetic study. I also like to thank the South African Tuberculosis Vaccine Initiative (SATVI), South Africa Aurum Institute for Health Research, Johannesburg, South Africa; Biomedical Research and Training Institute, Harare, Zimbabwe; and Harare City Health Department, Harare, Zimbabwe, for hosting the RIFAQUIN clinical study. Many thanks also to Manshil Misra (Cape Town site), Ronnie Matambo (Harare site), and Marietha Luttig (Johannesburg site), who were responsible for daily capturing of patient data at the sites.

The University of Cape Town Division of Clinical Pharmacology

I would like to thank Prof Gary Maartens, Prof Peter Smith, Dr Lubbe Weisner, Sandra Medereth, Jennifer Norman, Marilyn Solomons and the entire Pharmacometrics Group at Division of Clinical Pharmacology for the creation of enlightening and interactive environment where exchange of fruitful ideas enabled enjoyable progress with my work.

Modeling advice and guidance

The success of my modeling work was through advice and guidance from my supervisors, and inconceivable mentoring and feedback from Dr Paolo Denti. More advice and input was also from Prof. Mats Karlsson, Prof NHG Holford, Dr Jan-Stefan van der Walt.

Collaborations

- A/Prof Rada Savic for giving me the opportunity and facilities to carry out the pharmacometrics analysis of pharmacokinetic and pharmacodynamics data from the RIFAQUIN trial, under her directional supervision, guidance and feedback. I also like to thanks everyone in A/Prof Rada Savic's group for creating a lively working environment.
- Prof Goonaseelan (Colin) Pillai for giving me the wonderful opportunity to participate in the Novartis Next Generation Scientist Program 2012. Special thanks to Dr Thomas Bouillon for daily mentoring on building pharmacokinetic-pharmacodynamic models, Dr Jean-Louis Steimer and Prof Steven Kern for exchange of scientific ideas during internship, and all the Novartis Pharma Department of Modeling and Simulation for stimulating environment.

Personal

To Prynet, Tinotenda and Tanatswa Zvada, you stood by me all the time. Thanks to my twin brother and family members for all your support.

TABLE OF CONTENTS

ABSTRACT v
TABLE OF CONTENTS viii
LIST OF ABBREVIATIONS xii
LIST OF FIGURES xv
1 INTRODUCTION AND LITERATURE REVIEW 1
1.1 Tuberculosis 1
1.1.1 Burden of tuberculosis 2
1.1.2 Host and pathogen factors affecting disease progression/treatment 3
1.2 Treatment of tuberculosis 9
1.2.1 Drug resistant tuberculosis 10
1.2.2 Novel regimens in the treatment of tuberculosis 11
1.3 Pharmacology of drugs for treatment of tuberculosis 13
1.3.1 Mechanism of action for drugs used for the treatment of tuberculosis 14
1.3.2 Pharmacokinetics of drugs for the treatment of tuberculosis 17
1.3.3 Factors influencing drug pharmacokinetics 25
1.3.4 Pharmacokinetics and pharmacodynamics (PKPD) relationships 32
2 PROBLEM STATEMENT AND JUSTIFICATION 41
3 AIM 47
4 METHODOLOGY 48
4.1 Declaration of work 48
4.2 Patient population and studies used in this thesis 49
4.2.1 Studies of pharmacokinetics of first-line antituberculosis drugs 49
4.2.2 Healthy male volunteer study 49
4.2.3 RIFAQUIN clinical trial 50
4.2.4 MIC of moxifloxacin and ofloxacin 50
4.2.5 Population pharmacokinetics and pharmacodynamics of ofloxacin. 51
4.3 Plasma sample handling and drug concentration determination 51
4.4 Determination of moxifloxacin and ofloxacin MICs in patient sputum isolates 54

4.5 General pharmacometric methodology 55

4.5.1 Classification NAT2 polymorphism 55
4.5.2 Calculation of arm muscle area and arm fat area in children (Lee 2001) 56
4.5.3 Population pharmacokinetic analysis 57

5 Population pharmacokinetics of rifampicin, pyrazinamide and isoniazid in children with tuberculosis, *in silico* evaluation of currently recommended doses 64

5.1 Introduction 64

5.2 Setting and Study Design 65

5.2.1 Pharmacokinetic data analysis 67
5.2.2 Simulations 69

5.3 Results 70

5.3.1 Simulations 78

5.4 Discussion 84

5.4.1 Limitation 89

5.5 Conclusion 89

6 Effects of Four Different Meal Types on the Population Pharmacokinetics of Single-Dose Rifapentine in Healthy Male Volunteers 90

6.1 Introduction 90

6.2 Setting and Study Design 91

6.2.1 Population pharmacokinetic analysis 94

6.3 Results 96

6.4 Discussion 100

6.5 Conclusion 103

7 Moxifloxacin Population Pharmacokinetics in Patients with Pulmonary Tuberculosis and the Effect of Intermittent High-Dose Rifapentine 104

7.1 Introduction 104

7.2 Setting and Study Design 105

7.3 Population Pharmacokinetic analysis 105

7.4 Results 107

7.5 Discussion 110

7.6 Conclusion 111

8 Moxifloxacin population pharmacokinetics and model-based comparison of efficacy between moxifloxacin and ofloxacin in African patients 112

8.1 Introduction 112

8.2 Setting and Study Design 114

8.2.1 Population pharmacokinetic analysis. 115

8.2.2 Pharmacokinetic simulations and probability of target attainment 117

8.3 Results 118

8.4 Discussion 125

8.4.1 Limitations 129

8.5 Conclusion 129

9 Investigation of population pharmacokinetic summary variables of rifapentine and moxifloxacin as of predictors of treatment outcome 131

9.1 Introduction 131

9.2 Setting and Study design 133

Adequacy of treatment 135

9.3 Population pharmacokinetic analysis 135

9.4 Parametric hazard modeling (Pharmacokinetic-pharmacodynamic (PKPD) analysis) 137

9.5 Results 138

9.6 Discussion 146

9.7 Conclusion 149

10 Overall discussion and conclusions 150

10.1 Using population pharmacokinetic models to optimize dosing regimens 152

10.2 Understanding what drives efficacy 154

10.3 How to improve treatment of drug resistant tuberculosis 155

10.4 Conclusion..... 156

REFERENCES 159
APPENDICES 174
Appendix 1- Rifampicin run record and control stream 174
Appendix 2- Pyrazinamide run record and control stream 179
Appendix 3 - Isoniazid run record and control stream 183
Appendix 4- Rifapentine and 25-desacetyl rifapentine in healthy volunteer run record and control stream 188
Appendix 5- Moxifloxacin run records and control streams 194
Appendix 6- Rifapentine run records and control streams (RIFAQUIN study) 203
Appendix 7- Parametric hazard modeling 209

LIST OF ABBREVIATIONS

AA – Upper Arm Area

AADAC – human arylacetamide deacetylase

ALT – Alanine transaminase

AMA – Arm muscle area

ARR – Acquired rifamycin monoresistance

AUC – Area under the curve

AUC_{0-6} - Area under the curve from 0-6 hours

AUC_{0-12} - Area under the curve from 0-12 hours

AUC_{0-24} - Area under the curve from 0-24 hours

AUC_{0-48} - Area under the curve from 0-48 hours

$AUC_{0-\infty}$ - Area under the curve from 0-infinity hours

BC – Before Christ

BMI – Body Mass Index

BSA –Body surface area

CAR – Constitutive androstane receptor

CDC – United States Centers for Disease Control and Prevention

CFU – Colony forming unit

CI – Confidence interval

CL – Clearance

Cmax – Peak plasma concentration

CrCl – Creatinine clearance

CWRES – Conditional weighted residuals

CYP3A – Cytochrome P450 subfamily 3A

DNA – Deoxyribonucleic acid

DOTS – Direct observed therapy

DST – Drug-susceptibility testing

EBA – Early Bactericidal Activity

ELF – Epithelial lining fluid

F – Oral bioavailability

fAUC – Unbound fraction of the area-under-the-curve

fAUC/MIC – Ratio of the unbound fraction of the area-under-the-curve to the minimum

FDA – (United States of America) Food and Drug Administration

FDC – Fixed dose Combination

FFM – fat-free mass

FOCE – First Order Conditional Estimation

GOF – Goodness of fit

h - Hour

HIV – Human immunodeficiency virus

HIV+ – Human immunodeficiency virus infected

HPLC – High-performance tandem liquid chromatography

IGRA – Interferon gamma release assay

IIV –interindividual variability

inhA – Enoyl-acyl carrier protein reductase

IOV – Interoccasional variability

ka – First order absorption rate constant

katG – Bacterial catalase peroxidase

kg - kilogram

L - Litre

LJ – Lowenstein-Jensen

LLOQ – Lower limit of quantification

LOD – Lower limit of detection

LOQ – Lower limit of quantification

m - Metre

M. tuberculosis – *Mycobacterium tuberculosis*

MDR-TB – multidrug resistant tuberculosis

MED – Minimum effective dose

MF – maturation factor

mg - milligram

MGIT – Mycobacterial growth indicator tube

MIC – Minimum inhibitory concentrations

min - Minute

MRC –Medical Research Council

MSG – Monosodium Glutamate

MTIME – Model event time

MTT – Mean transit time

MUAC – Mid upper arm circumference

NAT2 – arylamine N-acetyltransferase 2

NCA – non-compartmental analysis

NLME – Non-linear mixed effects

OFV – Objective Function Value

p – probability of rejecting the null hypothesis when it is true (false positive result)

PAS – Para-aminosalicylic acid

pdf – probability density function

P-gp – p-glycoprotein

PKPD – Pharmacokinetic-Pharmacodynamic

PMA – post menopausal age

PsN – Perl Speaks NONMEM

PTA – Probability of Target Attainment

PTB – Pulmonary tuberculosis

PXR –pregnane X receptor

Q – intercompartmental clearance

QC – Quality control

RNA – ribonucleic acid

rpoB – Beta subunit of bacterial ribonucleic acid polymerase

RSE – Relative standard error

RUV - residual unexplained variability

SCM – Stepwise covariate model

SE – Standard errors

SLCO1B1 – Solute Carrier Organic Anion Transporter Family 1B1

SM –Streptomycin

SNP – Single Nucleotide Polymorphism

TAMIC –Time above MIC

TM_{50} – The age at which maturation reaches 50% of the adult value

Tmax – time to peak plasma concentration

TSF – Skinfold thickness

USA – United States of America

Vc – volume of distribution in plasma

Vp – volume of distribution in peripheral compartment

VPC – Visual Predictive Check

WHO – World Health Organization

WT – Total body weight

XDR-TB – Extensively drug resistant tuberculosis

LIST OF FIGURES

Figure 1.1: Illustration of time points at which drugs were developed and stages of those in developmental pipeline (adapted from Wong AB et al (Wong et al. 2013).....12

Figure 5.1: Maturation of oral clearance (CL) and mean transit time (MTT) of rifampicin and CL/F of isoniazid in a typical patient with post-natal age. The plot is not adjusted for covariate effects or allometric scaling. 72

Figure 5.2: Visual predictive checks for the final model of rifampicin. The lower, middle and upper lines (dotted/solid) are the 5^{th}, median, and 95^{th} percentiles of the observed data, respectively. The shaded areas are the 95% confidence intervals for the 5^{th} percentile, median and the 95^{th} percentile of the simulated data. 73

Figure 5.3: Visual predictive checks for the final model of pyrazinamide. The lower, middle and upper lines (dotted/solid) are the 5^{th}, median, and 95^{th} percentiles of the observed data, respectively. The shaded areas are the 95% confidence intervals for the 5^{th} percentile, median and the 95^{th} percentile of the simulated data. 75

Figure 5.4: Visual predictive checks for the final model of isoniazid. The lower, middle and upper lines (dotted/solid) are the 5^{th}, median, and 95^{th} percentiles of the observed data, respectively. The shaded areas are the 95% confidence intervals for the 5^{th} percentile, median and the 95^{th} percentile of the simulated data. 78

Figure 5.5: Box plot of simulated steady-state area under the concentration-time curve (AUC) of rifampicin across different age and weight bands, obtained adhering as closely as possible to the revised guidelines in dose per unit weight according to World Health Organisation 2010 dosing guidelines. Each box shows the 25^{th}-75^{th} percentile of simulated AUC and the symbol "x" shows data falling outside 1.5 times the interquartile range (25^{th}-75^{th}). The lower, middle, and upper dashed lines are the derived 5^{th} (9.0 mg·h/L), median (30.7 mg·h/L) and 95^{th} (52.4 mg·h/L) percentiles of the adult AUC, respectively. The grey shaded area is the 25^{th}-75^{th} (21.9 -39.5 mg·h/L) percentile of adult AUC. 79

Figure 5.6: Box plot of simulated steady-state area under the concentration-time curve of pyrazinamide across different age and weight bands, obtained adhering as closely as possible to the revised guidelines in dose per unit weight according to World Health Organisation 2010 dosing guidelines. Each box shows the 25^{th}-75^{th} percentile of simulated AUC and the symbol "x" shows data falling outside 1.5 times the interquartile range (25^{th}-75^{th}). The lower, middle, and upper dashed lines are the derived 5^{th} (244.0 mg·h/L), median (427.0 mg·h/L), and 95^{th} (675.0 mg·h/L) percentiles of the adult AUC, respectively. The grey shaded area is the 25^{th}-75^{th} (346-547 mg·h/L) percentile of adult exposure. 80

Figure 5.7: Box plot of simulated steady-state area under the concentration-time curve (AUC) of isoniazid in slow (S), intermediate (I) and fast (F) acetylators across different age and weight bands, obtained adhering as closely as possible to the revised guidelines in dose per unit weight according to World Health Organisation 2010 dosing guidelines. Each box shows the 25^{th}-75^{th} percentile of simulated AUC and the symbol "x" shows data falling outside 1.5 times the interquartile range (25^{th}-75^{th}). The lower, middle, and upper dashed lines are the derived 5^{th} (9.8 mg·h/L), median (23.4 mg·h/L), and 95^{th} (55.6 mg·h/L) percentiles of the adult AUC, respectively. The grey shaded area is the 25^{th}-75^{th} (15.6-35.5 mg·h/L) percentile of adult exposure. 81

Figure 5.8: Scatter plot of simulated rifampicin steady state area under the concentration-time curve (AUC) versus post-natal age, based on the final model. AUCpop (black triangles) are the population predicted values for each individual, obtained under the assumption that each subject is characterised by the typical parameter values of the population, i.e. no random effects are included. AUCi (grey open circles) are the individual simulated predictions, obtained by including the random effects, generated according to the level of variability identified in the population. Data from the 5.0-7.9 kg weight band is shown. Age was included as a covariate in the final model. 82

Figure 5.9: Scatter plot of simulated pyrazinamide steady state area under the concentration-time curve (AUC) versus post-natal age, based on the final model. AUCpop (black triangles) are the population predicted values for each individual, obtained under the assumption that each subject is characterised by the typical parameter values of the population, i.e. no random effects are included. AUCi (grey open circles) are the individual simulated predictions, obtained by including the random effects, generated according to the level of variability identified in the population. Data from the 5.0-7.9 kg weight band is shown. Age was included as a covariate in the final model.....83

Figure 5.10: Scatter plot of simulated isoniazid steady state area under the concentration-time curve (AUC) versus post-natal age, based on the final model. AUCpop (black triangles) are the population predicted values for each individual, obtained under the assumption that each subject is characterised by the typical parameter values of the population, i.e. no random effects are included. AUCi (grey open circles) are the individual simulated predictions, obtained by including the random effects, generated according to the level of variability identified in the population. Data from the 5.0-7.9 kg weight band is shown. Please note that for isoniazid the simulations were repeated three times, assuming fast, intermediate, or slow metaboliser status, thus the separate trends visible in the charts for AUCpop. Age was included as a covariate in the final model.....84

Figure 6.1: Illustration of the parent metabolite model. All rifapentine is assumed to be converted to the major metabolite (25-desacetylrifapentine). N_1represents the first hypothetical transit compartment up to N_n compartment. k_{tr} is the transit rate constant. k_a is the absorption rate constant from the hypothetical drug depot compartment to plasma. *k* (calculated as CL/*Vc*) is the elimination rate constant of rifapentine. CL*m* is the time-varying metabolite clearance. V_m represents volume of distribution of the metabolite. k34 is the first-order rate constant of the metabolite from plasma to the peripheral compartment, and k43 is the first-order rate constant of the metabolite from the peripheral compartment back to plasma.....97

Figure 6.2: Visual predictive check for the final (left) and metabolite (right) models. The lower, middle, and upper solid lines are the 5th, 50th, and 95th percentiles of the observed data, respectively. The dotted and dashed-dotted (50th percentile) lines around each percentile show the 95% confidence interval from the model prediction. The circles are the observed concentration-time data points.....98

Figure 7.1: Illustration of the final moxifloxacin pharmacokinetic model (bottom). N_1 to $N_n$represents a series of hypothetical transit compartments used to model the delay in onset of absorption, and k_{tr} is the transit rate constant. k_a is the absorption rate constant from the hypothetical drug absorption site (depot) compartment to plasma. V_c, V_p, CL, and Q are the central and peripheral volumes of distribution and the oral and intercompartmental clearance, respectively. (Top) Visual predictive check of the final moxifloxacin pharmacokinetic model. The lower, middle, and upper solid lines are the 5th percentiles, medians, and 95th percentiles of the observed data, respectively. The shaded areas are the 95% confidence intervals for the 5th percentile, median, and 95th percentile of the simulated data. The open black circles are the observed concentrations. 108

Figure 8.1: Visual predictive check (VPC) for the final moxifloxacin population pharmacokinetic model. In the upper panel, the lower, middle and upper solid lines are the 2.5th, median, and 97.5th percentiles of the observed plasma concentration, respectively, while the shaded areas are the 95% confidence intervals for the same percentiles of the simulated data. The lower panel shows the fraction of observed data below lower limit of quantification (LOQ) which is represented by the solid line. The shaded area shows simulation based 95% confidence interval around the median of LOQ data. 121

Figure 8.2: Probability of target attainment for 400 mg moxifloxacin and 800 mg ofloxacin. 122

Figure 8.3: Probability of target attainment (target *f*AUC_{0-24}/MIC≥ ratio 53) versus *Mycobacterium tuberculosis* isolates minimum inhibitory concentrations (MIC) for 400 mg and 800 mg moxifloxacin dose. MDR and XDR are MIC distributions from multidrug resistant and extensive drug resistant isolates, respectively. MDR+INJ and MDR+FLQ are MIC distributions from isolates resistant to injectables and fluroroquinolones, respectively. The distributions of these MICs are represented by right side y-axis.....123

Figure 8.4: Probability of target attainment (target *f*AUC_{0-24}/MIC≥ ratio 53 or 100) versus *Mycobacterium tuberculosis* isolates minimum inhibitory concentrations (MIC) for 800 mg ofloxacin dose. MDR and XDR are MIC distributions from multidrug resistant and extensive drug resistant isolates, respectively. MDR+INJ and MDR+FLQ are MIC distributions from isolates resistant to injectables and fluroroquinolones, respectively. The distributions of these MICs are represented by right side y-axis. 124

Figure 9.1: Visual predictive check (VPC) for the final rifapentine population pharmacokinetic model. The lower, middle and upper solid lines are the 2.5th, median, and 97.5th percentiles of the observed plasma concentration, respectively, while the shaded areas are the 95% confidence intervals for the same percentiles of the simulated data. 140

Figure 9.2: Box plots of area under curve (AUC) from 0-infinity hours and peak concentration (Cmax) for rifapentine for different time interval. Each box shows the 25^{th}-75^{th} percentile of AUC and the symbol "·" shows data falling outside 1.5 times the interquartile range (25^{th}-75^{th}). 'Total" refers to whole duration of continuation phase of treatment. 143

Figure 9.3: Box plots of area under curve (AUC) from 0-infinity hours and peak concentration (Cmax) for moxifloxacin for different time interval. Each box shows the 25^{th}-75^{th} percentile of AUC and the symbol "·" shows data falling outside 1.5 times the interquartile range (25^{th}-75^{th}). 'Total" refers to whole duration of continuation phase of treatment. 144

LIST OF TABLES

Table 1.1: Rifampicin pharmacokinetics (since year 2000) in adults with tuberculosis including those who are HIV positive (HIV+), where 22

Table 1.2: Pyrazinamide pharmacokinetics (since year 2000) in adults with tuberculosis including those who are HIV positive (HIV+), where 23

Table 1.3: Isoniazid pharmacokinetics (since year 2000) in adults and children with tuberculosis including those who are HIV positive (HIV+) 24

Table 5.1: Demographic and clinical characteristics of children with tuberculosis 66

Table 5.2: Parameter estimates of the final rifampicin pharmacokinetic model 71

Table 5.3: Parameter estimates of the final pyrazinamide pharmacokinetic model 74

Table 5.4: Final parameter estimates for isoniazid pharmacokinetics 76

Table 6.1: Description of different meals ingested 30 minutes before administration of a single 900 mg dose of rifapentine 92

Table 6.2: Demographic and clinical characteristics of healthy male volunteers 93

Table 6.3: Final parameter estimates for rifapentine 98

Table 6.4: Different meal effects, relative to fasted state, estimated from parent (rifapentine) model 99

Table 6.5: Final parameter estimates for 25-desacetyl rifapentine 100

Table 7.1: Parameter estimates of the final moxifloxacin pharmacokinetic model[a] 109

Table 7.2: Pharmacokinetic values for different moxifloxacin dosing regimens 110

Table 8.1: The MIC distribution of moxifloxacin and ofloxacin in 197 *Mycobacterium tuberculosis* isolates 116

Table 8.2: Characteristics of patients who received moxifloxacin in the RIFAQUIN trial, and those who were on ofloxacin in a previous study 119

Table 8.3: Final parameter estimates for moxifloxacin population pharmacokinetic model 120

Table 8.4: PTA values of ofloxacin and moxifloxacin for different target ratios 122

Table 8.5: The cumulative fraction of response (CFR) for daily doses of 400 mg and 800mg moxifloxacin, and 800 mg ofloxacin for target $fAUC_{0\text{-}24}$/MIC ratio of 53 (Gumbo et al. 2004) and 100 (Schaaf et al. 2009a, Schentag et al. 2003a,b) 125

Table 9.1: Baseline characteristics of pharmacokinetic-pharmacodynamic (PKPD) patient subset in 4-month and 6-month arms 134

Table 9.2: Final parameter estimates for rifapentine population pharmacokinetic model 139

Table 9.3: Parameter estimates for of the final parametric hazard model. 141

Table 9.4: Summary of pharmacokinetic variable for rifapentine and moxifloxacin, and significance test for differences in these variables between 4-month and 6-month arms 145

1 INTRODUCTION AND LITERATURE REVIEW

1.1 Tuberculosis

Tuberculosis is a contagious, more frequently a chronic disease, caused by phenotypically and genotypically diverse acid-fast tubercle bacillus (Jindani et al. 1980, Wayne & Hayes 1996) called *Mycobacterium* tuberculosis *(M.tuberculosis).* The disease burden is high amongst the poor especially those in Sub-Saharan Africa and across all age groups; human immunodeficiency virus (HIV) infection being an important risk factor (WHO 2013). Tuberculosis largely affects the lung parenchyma or the tracheobronchial tree in about 90% of the cases (Lawn & Zumla 2012), and in South Africa about 80% of cases are classified as pulmonary tuberculosis. The most common clinical features of active tuberculosis infection include chronic cough, sputum production, weight loss, fever, night sweats, and hemoptysis (Lawn & Zumla 2012). The recommended methods for *M.tuberculosis* diagnosis are sputum microscopy and culture in liquid or solid medium (solid more cost-effective in resource-limited settings), with consequent drug-susceptibility testing (DST), but treatment sometimes has to be started without a microbiological confirmation of *M.tuberculosis* especially in children. Treatment of tuberculosis requires administration of multiple antibiotics over a long period of time, and is may be complicated by emergence of drug-resistant strains, co-infection with HIV, and severity of disease in children. Tuberculosis has existed for millions of years, yet it continues to be major contributor to high mortality and morbidity.

In the history of tuberculosis, pictures of people suffering from the disease were seen in Egyptian art and amplification of skeletal remains discovered in Egyptian tombs suggests that the disease existed for more 3000-2400 “Before Christ” (years BC) (Haas et al. 2000, Zink et al. 2003); making tuberculosis different from other diseases due to its long co-existence with humans. Tuberculosis spread to the rest of the world, surged in major epidemics and then subsided, similar to other infectious diseases. At that time death rates in cities like London, Stockholm, and Hamburg approached 800 - 1000 per 100 000 population per year (Daniel 2006). A likely explanation for these figures is that tuberculosis transmission increased due to increased population density and crowded living conditions, while other risk factors, such as poor nutrition, increased the risk of progressing from latent to active disease (Lonnroth et al. 2009). In those early years, the discovery of the tubercle bacillus in 1882, and the discovery of X-rays by Wilhelm Konrad Röntgen in 1895 were two breakthrough events followed by the development of the Bacillus Calmette–Guérin vaccine in 1921 in France (Bonah 2005), as well as effective medical treatment. In 1923, the British Medical Research Council was established mainly focusing on tuberculosis research (Grig 1958). Improvements in public health began significantly reducing rates of tuberculosis by 90% even before the discovery of streptomycin and other antibiotics for treatment of tuberculosis. Since these early years, significant progress has been made with discovery of drugs for treatment of tuberculosis, and management of the disease. With this long history, the disease continues to be a major pandemic.

1.1.1 Burden of tuberculosis

In spite of falling incidence rates of tuberculosis in many countries, the annual incidence of tuberculosis remains high. In 2012 there were an estimated 8.6 million incident cases of tuberculosis and 1.3 million (320 000 had HIV) deaths from the disease. Among these

deaths, were an estimated 170 000 from multi-drug resistant tuberculosis (MDR-TB) (WHO 2012a). In children less than 15 years of age, there were an estimated 530 000 new cases and 74 000 deaths among children who were HIV negative. The estimates of tuberculosis morbidity and mortality were estimated to be slightly higher than those reported in 2012 (WHO 2013).

In 2012, it was estimated that there were 310 000 incident cases of MDR-TB. MDR-TB occurs when *M.tuberculosis* organisms became resistant to at least isoniazid and rifampin. More than 60% of these patients were in China, India, the Russian Federation, Pakistan, and South Africa (WHO 2012a). A total of 84 countries have reported cases of Extensively drug-resistant tuberculosis (XDR-TB) tuberculosis, a subset of MDR-TB with added resistance to all fluoroquinolones plus any of the three injectable antituberculosis drugs, kanamycin, amikacin, and capreomycin (WHO 2012a).

Worrying is the case of children, who are often neglected when optimizing therapeutic regimens but experience severe forms of tuberculosis. They comprise 10-20% of the total cases of tuberculosis in high burden areas (Marais et al. 2006, Walls & Shingadia 2004). Thus, childhood tuberculosis represents a significant but still neglected clinical and public health problem. An additional complication is dissemination of drug resistance that may also occur in children, and which may be facilitated by lack of optimised doses of first-line drugs in children (McIlleron et al. 2009, Schaaf et al. 2009b, Thee et al. 2008).

1.1.2 Host and pathogen factors affecting disease progression/treatment

There are several important factors which are associated with susceptibility to tuberculosis treatment.

Standards of living and nutrition

An improved standard of living and nutrition is proposed to be among factors that were associated with declining mortality rates due to tuberculosis before chemotherapy was available in the mid-19th century (Lonnroth et al. 2009). Improved working conditions and socioeconomic factors (Weber 1948), along with improved health care programs were among the factors. Also importantly, ill patients were housed in sanitoria. These sanitoria prevented ill patients from spreading tuberculosis to others and the patients found them comforting and relieving. The first sanatorium devoted to treatment of tuberculosis was built in 1859 by Herman Brehmer, where rest, rich diet and supervised exercises was important components of the management of tuberculosis.

Strains of M.tuberculosis

The *M.tuberculosis* was first described by Robert Koch on 24 March 1882 (Sakula 1982). *M.tuberculosis* is an aerobic, small, non-encapsulated, non-spore forming, and nonmotile bacillus characterised by high lipid content which probably results in its virulence and intrinsic resistance to antibiotics (Southwick 2007). Also, due to the high lipid-rich and mycolic acid content of the cell wall, *M.tuberculosis* does not retain any bacteriological stain hence Ziehl-Neelsen staining, or acid-fast staining, is used. In terms of multiplication, the mycobacterium divides at an extremely low rate (every 16-20 hours) compared with other bacterium like *Escherichia coli* (every 20 minutes). This slow replication rate and ability to persist in a latent state leads to long durations of both drug therapies of tuberculosis and for preventive therapy in people with *M.tuberculosis* infection. *M.tuberculosis* is genetically diverse, and different strains of *M.tuberculosis* are associated with different geographic regions. Even though there are many strains,

studies of the phylogeny and biogeography of *M.tuberculosis* have discovered six main strain lineages that are linked with particular geographical regions (Gagneux & Small 2007). It is speculated that, the Beijing family of strains originated in Asia. This family of strains is distributed worldwide and is able to spread in large clonal clusters. Lineage of strains may affect outcomes of treatment of tuberculosis. A recent study in 2013 by Reiling et al., identified clade-specific virulence patterns in human primary macrophages and in mice infected by the aerosol route. The authors' analysis identified 3 different pathogenic profiles: strains of the East Asian lineage lineage characterized by low uptake by macrophages, low cytokine induction, and a high replicative potential; strains of the Haarlem lineage by high uptake, high cytokine induction, and high growth rates; and East African Indian strains by low uptake, low cytokine induction, and a low replicative potential (Reiling et al. 2013). Furthermore, the characteristics of Beijing strain could be associated with relapse after treatment. A prospective study conducted among 1068 Vietnamese with tuberculosis (23 relapse cases), the Beijing strain was significantly associated with relapse (Huyen et al. 2013). These findings support are in agreement with a study by Visser et al which identified W-Beijing genotype as a moderate baseline predictor for sputum conversion (Visser et al. 2012).

Immunity, cavitation and smoking

The main sources of *M.tuberculosis* are patients with active pulmonary tuberculosis (PTB). After infection, progression to active tuberculosis does not immediately occur in the majority of immunocompetent people; in 95% of them, the immune system can successfully contain the *M.tuberculosis* but as asymptomatic latent infection (Long & Shwartzman 2007). The latent infection may persist in the host for years without symptoms or experiencing adverse effects. . However, risk of progression to active tuberculosis from latent stage was estimated to be 5% in 18 months from first infection

(Andrews et al. 2012). In the approximately 5% of immunocompetent individuals whose immune system cannot contain the infection, the probability of developing primary disease after infection is also much greater in immunocompromised individuals (Long & Shwartzman 2007).

When *M.tuberculosis* reaches lungs, mostly by inhalation, it begins to multiply within alveolar macrophages. In response, cell-mediated and delayed type hypersensitivity immunity is activated by the host if the innate response is not capable of destroying the bacterium (Flynn 2006, Long & Shwartzman 2007).. The CD4+ T cells secrete mainly interferon-γ capable of inducing macrophages into inducing intracellular killing of mycobacteria. Thereafter, inflammatory response includes the formation of granulomas by the host immune system that work to limit the spread of infection. In the majority of infected individuals, the infection is contained and tuberculosis disease does not develop. Screenings for latent infection is therefore indicated in people at high risk, especially those living in regions with high disease burden. . The Mantoux tuberculin skin test (Escalante 2009) and Interferon gamma release assays (IGRAs) are recommended in those who tested positive Mantoux test. Because treatment is based upon diagnosis, it should be known that a false-positive Mantoux test can occur in those previously immunized while false-negative test may occur in those with malnutrition (Kumar et al. 2007).

Once the granuloma is formed, it assumes a solid caseous center surrounded by immature macrophages. The caseous material is not favourable for bacterial growth due to acidic pH, and low oxygen tension. Even though the mycobacterium cannot multiply, it can survive for years in this environment. Liquefaction and cavitation occurs as the disease progresses. Immunocompromised individuals and/or infants may be deficient in granuloma formation and thus are not efficient at containing the infection. Without the

formation of granulomas to control the bacteria, the infection cannot be contained (Flynn 2006). Cavitation is a well-known risk factor associated with treatment failure or delayed sputum conversion (Telzak et al. 1997, Visser et al. 2012), and relapse (Benator et al. 2002), possibly due to inability of the drugs to penetrate the cavities. Other factors such as high bacillary load, host immunity and bacterial physiology are other plausible explanations. Also *M.tuberculosis* can migrate to other extrapulmonary infection sites including the pleura, central nervous system, the lymphatic system, the genitourinary system, the bones and joints. In these areas, successful treatment may be limited by the ability of the drugs to penetrate to the infected sites. Failure of drugs to infiltrate to affected areas especially necrotic lesions may possibly result in localised monotherapy and emergency of drug resistance.

Even though some studies show smoking as a risk factor to lack of sputum culture conversion, these findings are still conflicting. A study by Slama et al., failed to find sufficient evidence to support an association of smoking and delay, default, slower smear conversion, greater severity of disease or drug-resistant TB or of second-hand tobacco smoke exposure and infection (Slama et al. 2007). But a recent reported that, ever smokers had longer time-to-culture conversion than those who never smoked (Visser et al. 2012). Also, smokers have been shown to have cavitary more lesions, compared with non-smokers (Altet-Gômez et al. 2005). However, further studies may be needed to evaluate the relationship between smoking and time-to-culture conversion.

Genetic variability of human leukocyte antigen

Other contributors to susceptibility include polymorphisms in genes including human leukocyte antigen (HLA) alleles and other non-major histocompatibility complex genes (Yim & Selvaraj 2010). These polymorphisms may provide genetic markers to predict

an individual's vulnerability to the development of tuberculosis. Work on genetic variability in relation to tuberculosis noted that immunological adaptations, specifically different forms of T-cell immune responses, in addition to socioeconomic factors may influence susceptibility to tuberculosis (Larcombe et al. 2005).

Vitamin D deficiency

There is growing interest in the link between susceptibility to tuberculosis and vitamin D deficiency; this has multiple effects on the immune system (Wang et al. 2004) including macrophage activation and induction of the antimycobacterial peptide LL37 (Martineau et al. 2011). A randomised clinical trial demonstrated that vitamin D supplementation was associated with more rapid sputum-culture conversion (from positive to negative) in a subset of individuals with specific vitamin D receptor polymorphisms even though further clinical trials of vitamin D supplementation in the treatment and prevention of tuberculosis are warranted (Martineau et al. 2011).

Diagnosis of tuberculosis in resource-limited countries

Importantly, in resource-constrained settings where there is a high burden of tuberculosis and HIV, an estimated 30% of all patients with tuberculosis and more than 90% of those with multidrug-resistant and extensively drug-resistant tuberculosis do not receive a diagnosis (WHO 2012b), which severely impacts on timely intervention with chemotherapy. Even though the new molecular diagnostic test called Xpert MTB/RIF has been developed, it is not readily available in resource limited countries. The Xpert In children, diagnosis often starts after presenting with signs and symptoms, with the likelihood of exposure at the forefront of predictive value of subsequent investigations.

Even though microscopical examination of sputum smears is the cornerstone of diagnosis in most countries, the paucibacillary nature of the disease disrupts its usefulness in young children due to low expectorant capability, albeit gastric aspiration and sputum induction can improve diagnostic yield (Nicol & Zar 2011).

1.2 Treatment of tuberculosis

Treatment of tuberculosis and emergence of drug-resistant strains dates back to 1940s after the discovery of streptomycin by Albert Schatz (Schatz et al. 1944). Streptomycin was administered as monotherapy and resulted in a dramatic decrease in mortality (MRC 1948). However, 5 years later it was increasingly evident that *M.tuberculosis* became resistant to streptomycin as patients on monotherapy died in similar proportions to those not on treatment (Fox et al. 1954), and combination with para-aminosalicylic acid (PAS) significantly reduced the emergence of streptomycin resistance (Fox et al. 1954). A year after the discovery of PAS, isoniazid emerged as a better drug due to tolerability in humans and low minimum inhibitory concentration. Therapy with streptomycin, PAS, and isoniazid prevented the selection of streptomycin-resistant mutants and resulted in the cure of patients with 18 months of treatment. During those times, the exploration of isoniazid monotherapy or combination with streptomycin and/or PAS continued, and led to the widely acceptable regimen of first 3 months streptomycin, PAS and isoniazid followed by 9 months of PAS and isoniazid. However, the regimen was only available in Europe due to the cost of PAS (Lonnroth et al. 2010).

The issue of cutting treatment expenses in hospitals come to light in 1960 after a study under the direction of Fox which showed that domiciliary chemotherapy could be as effective as treatment in expensive hospitals or sanatoria (Andrews et al. 1960). The study resulted in finding ways to ensure regular drug taking during a year of domiciliary

treatment and led to establishment of the DOTS (Directly Observed Therapy Short course) strategy by WHO in 1995, DOTS was subsequently updated by the with the formulation of the Stop TB strategy (Lonnroth et al. 2010). Beginning in the 1970s, combination therapy with streptomycin, isoniazid, and PAS was progressively replaced by combinations that included isoniazid, rifampin, pyrazinamide, and ethambutol. Rifamycins and pyrazinamide played an important role in reducing the duration of treatment to 6 months. A remarkable number of well-controlled randomized clinical trials established the efficacy of "short-course" treatment regimens utilizing these agents (Fox et al. 1999). These short-course regimens are able to cure multibacillary forms of active tuberculosis after 6 months of administration and have become the standard of care throughout the world. This classical therapy for pulmonary tuberculosis consists of rifampicin, isoniazid, pyrazinamide and ethambutol for 2 months followed by a continuation phase of rifampicin and isoniazid. When adequately administered, the standard regimens are capable of relapse-free cure rates of 95% or more in patients with drug sensitive organisms (Fox et al. 1999, Jindani et al. 2004). Shortening the duration of tuberculosis treatment or administering therapy intermittently (i.e., once weekly or even less frequently) without lowering efficacy is a plausible option in reducing the burden of supervised drug therapy and could improve treatment success. In the context of the HIV epidemic and emergency of drug resistance, new drugs and novel strategies to complement current efforts are desirable.

1.2.1 Drug resistant tuberculosis

Due to the limited number of randomized controlled clinical trials, the treatment of MDR-TB, on top of using data from large observational studies, is also based on expert opinion and requires the creation of combination drug regimens which are very costly and prolonged. However, successful outcomes for MDR-TB are achievable in about

two-thirds of patients, though for XDR-TB the outcomes are very heterogeneous (Orenstein et al. 2009). In most parts of the world, access to such therapy is very poor, with less than 2% of patients with MDR-TB worldwide treated according to WHO standards (WHO 2009). As part of treatment of MDR-TB, a fluoroquinolone (e.g., moxifloxacin) and an injectable agent (e.g., kanamycin or capreomycin) should routinely be included to provide a regimen with at least four second-line drugs that will have certain or nearly certain effectiveness, as well as pyrazinamide. Such therapy should be administered for at least 20 months in patients who have not received previous treatment for MDR-TB and for up to 30 months in those who have received previous treatment. Encouragingly, an observational study showed that a shorter regimen, with treatment given for 9 to 12 months (the so-called Bangladesh regimen), had acceptable efficacy with fewer adverse reactions (Van Deun et al. 2004) in a population with no previous exposure to second-line drugs. However, MDR-TB remains a cause of concerns leading to development of new drugs, development and optimization of novel regimens, and other therapeutic alternatives.

1.2.2 Novel regimens in the treatment of tuberculosis

Faced with these treatment option challenges, future successes in the control of tuberculosis will depend on the development of novel treatment strategies with regimens that are shorter, easier to deliver, safe, easy to monitor and low in cost. After decades of neglect, ten new drugs for the treatment of tuberculosis are in the clinical development pipeline of which six are being specifically developed for tuberculosis (Figure 1.1).

The Novel regimens for the treatment of tuberculosis are aiming at reducing the duration of standard therapy from 6 months but without compromising the efficacy of the drugs.. Clinical trials involving rifapentine conducted in humans indicate that higher doses of rifapentine may be beneficial in preventing rifamycin resistance, and this is supported by

in vitro studies of rifamycin activity (Gumbo et al. 2007a). The trials demonstrated that in patients with HIV infection, severe or advanced tuberculosis (as evidenced by cavitations on chest x-ray), once weekly rifapentine plus isoniazid, at the currently used standard dosage of 600 mg (Blumberg et al. 2003), was inferior to the thrice-weekly rifampicin comparator (Benator et al. 2002, Tam et al. 2002).

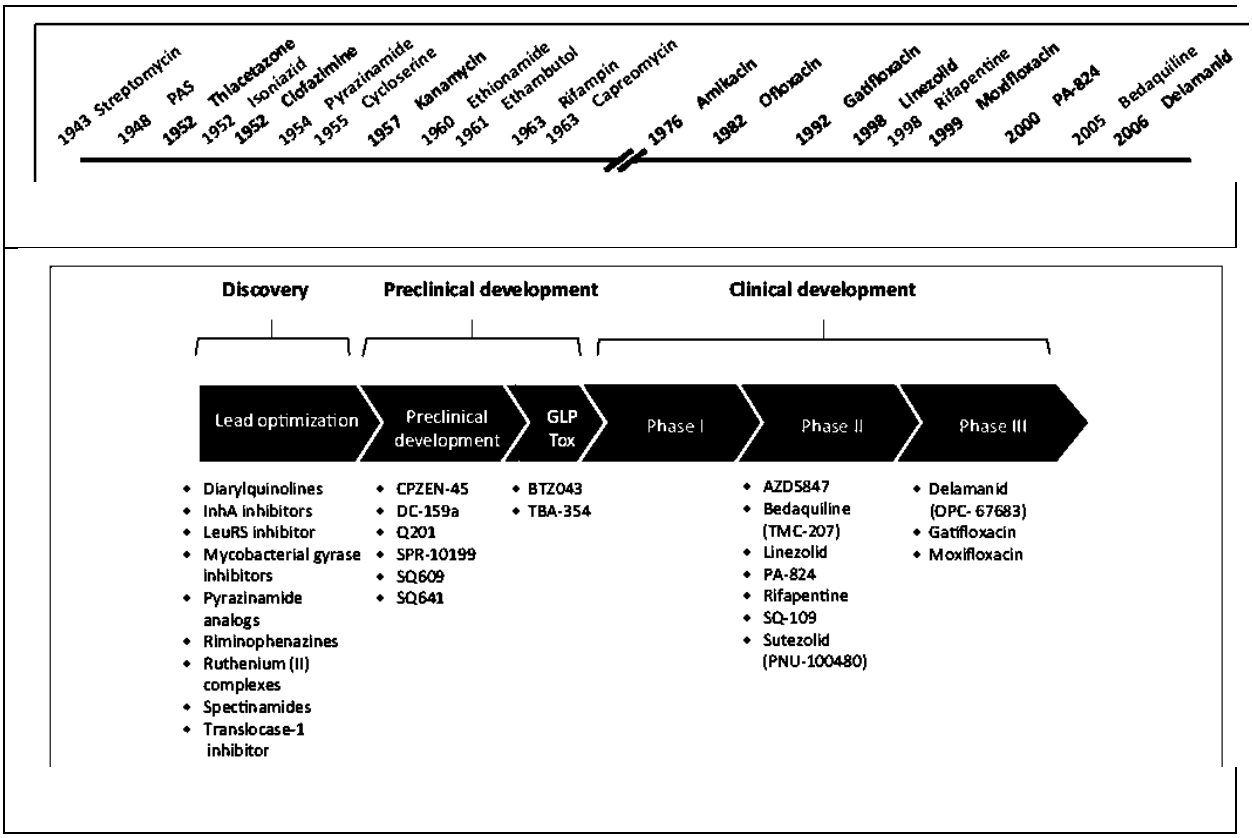

Figure 1.1: Illustration of time points at which drugs were developed and stages of those in developmental pipeline (adapted from Wong AB et al (Wong et al. 2013)

In a study conducted in the United States of America (USA), emergence of acquired rifamycin monoresistance (ARR) was reported in four out of 5 HIV sero-positive patients who relapsed. The highly protein-bound nature of rifampicin (97%) is assumed to have played a role in relapse or failure since low unbound drug levels will be available for bactericidal activity (Mitchison 1998, Sirgel et al. 2005). Low unbound

concentrations of rifapentine were thought to have led to a small pulse size and to the re-growth of bacilli during the interval between doses when active levels are very low.

Despite the fact that no association between low isoniazid concentration and failure rate was found in the Hong-Kong study (Tam et al. 1998), in Center for Disease Control (CDC) Study 22 (Weiner et al. 2005) where patients were on regimen of once weekly RFP plus isoniazid, an association was found between low isoniazid plasma concentrations and the occurrence of relapse suggesting that isoniazid might have been ineffective in preventing rifamycin resistance. Moxifloxacin which has demonstrated potent bactericidal and sterilizing activity in vitro and in mouse models (Ji et al. 1998, Yoshimatsu et al. 2002) could be a better potential companion drug for rifapentine regimen. Moxifloxacin has a long serum half-life (9-12 hours) in humans (Siefert et al. 1999) giving a longer duration of drug activity and ultimately reduction in frequency of drug administration matching very well with rifapentine. In support of moxifloxacin as a potential companion to rifapentine, a mouse study has led to the suggestion that the efficacy of the once weekly isoniazid plus rifapentine in the continuation phase can be increased by substituting moxifloxacin for isoniazid and by increasing the dose size of rifapentine to 15 mg/kg (Lounis et al. 2001).

1.3 Pharmacology of drugs for treatment of tuberculosis

The activity of anti-tuberculosis drugs either in combination or alone during the first 14 days of treatment were widely studied by Jindani et al (Jindani et al. 1980, 2003). These early bactericidal (EBA) studies take into account the viable bacterium content of the sputum. Even with EBA studies extended to 14 days, their role in predicting treatment shortening potential is unclear. Another improvement in describing EBA results was

inclusion of calculation of the therapeutic margin, defined as the ratio between therapeutic dose and minimum effective dose (MED) correspondingly for each drug. The MED is determined as the lowest dose that failed to produce a kill, and for isoniazid the MED is 15 giving a therapeutic margin of 20 when a dose of 300 mg is given (Donald et al. 1997).

1.3.1 Mechanism of action for drugs used for the treatment of tuberculosis

The mechanism of action of rifampicin and rifapentine is through binding to and inhibition of the deoxyribonucleic acid (DNA)-dependent ribonucleic acid (RNA) polymerase beta subunit (rpoB), thus preventing formation of new proteins (Wehrli 1983). Therefore mutation in rpoB results in resistance to rifampicin. In terms of activity, rifampicin has a low therapeutic margin of only 4 (Sirgel et al. 2005) at the standard dose of 10 mg/kg presumably due to highly protein bound nature of rifampicin resulting in 20% unbound concentrations in lesions (Acocella 1978). Rifampicin gave an average rate of decline in the count of bacteria per mL of sputum per day of 0.17 log10 colony-forming units (CFU) in the first two days when administered at standard doses (Jindani et al. 2003).. Isoniazid is important for actively diving bacteria (Jindani et al. 2003). Nonetheless, rifampicin is an important drug throughout the entire course of treatment. Rifampicin is a key sterilizing drug and is important for shortening the duration of treatment.

Importantly, complete sterilization takes 6 months for tuberculosis lesions in the lungs of patients, an occurrence which has been attributed to the presence of slowly replicating bacteria (persisters) particularly those in the stationary phase of growth (Mitchison &

Selkon 1956). Peak serum concentrations of rifampicin may be important in the sterilization of these persisters (Mitchison 2012). Only in vitro, persisters were reported to go through the non-replicating phases, nrp1 and nrp2, lasting approximately 3 weeks, when they acquire tolerance to isoniazid and minimally to rifampicin (Wayne & Hayes 1996). Following further incubation for about 3 months, they become the bacilli of the Hu/Coates model (Hu et al. 2000) with a failure to grow on solid media and marked antibiotic tolerance.

Bacilli which fail to grow on solid media are killed rapidly by pyrazinamide (Hu et al. 2006). There are different theories with regards to how pyrazinamide or pyrazinoic acid (pyrazinamide's active moiety) exerts bacterial activity. Pyrazinamide is deaminated to pyrazinoic acid by the *M.tuberculosis* amidases-encoded by the pncA gene (Zhang & Mitchison 2003). Hence mutations in pncA result in drug resistant to pyrazinamide (Sreevatsan et al. 1997). Pyrazinoic acid is reabsorbed by passive diffusion (not requiring energy) in a highly pH-dependent manner once it reaches the exterior of bacilli. Pyrazinoic acid then accumulates inside the bacilli due to inefficient energy requiring efflux pump, acidifying the interior, and membrane damage or inhibition of trans-translation in persisting cells is probably how it kills the bacilli (Shi et al. 2011). With this mechanism, pyrazinamide is particularly effective in killing dormant bacilli.

Isoniazid is most important for rapidly dividing bacilli. Isoniazid is activated to isonicotinyl-NAD by the bacterial catalase-peroxidase (*katG*). The activated Isoniazid irreversibly binds and inhibits the bacterial enoyl-acyl carrier protein reductase (*inhA*). *inhA* is the key bacterial enzyme responsible for fatty acid synthesis and production of cell wall mycolic acid (Lei et al. 2000). Resistance usually arises by mutation in *katG* most commonly at S315T, which confers partial loss of isoniazid activation and is associated with high-levels of resistance; whereas *inhA* mutations lead to target

alteration in the gene product and altered affinity for isoniazid-NAD adducts (Almeida Da Silva & Palomino 2011, Warren et al. 2009). Unlike rifampicin, isoniazid has a high therapeutic margin of 20 (Donald et al. 1997), but has much slower action against non-multiplying cells. From EBA studies, a typical curve in the log CFU counts is obtained which starts with a rapid fall and then levels off as an exponential kill from about day 7 (Brindle et al. 2001). An alternative explanation for little or no activity of isoniazid could be selection or physiological changes in the baseline populations. The initial rapid part of the kill could be due to the action of isoniazid on an initially multiplying part of the bacterial population.

The general mechanism of action of action of moxifloxacin on *M.tuberculosis* is inhibition of bacterial DNA gyrase (topoisomerase IV), which is essential for bacterial DNA replication and growth (Sato et al. 1986)(Sato *et al.* 1986). Resistance to fluoroquinolones is a result of mutations in the genes encoding for the DNA gyrase subunits A and B (*gyrA* and *gyrB*), particularly *gyrA* (Kocagoz *et al.* 1996). The best predictor of *in vivo* efficacy for this class of drugs is the area under curve (AUC/minimum inhibitory concentration (MIC) (Shandil et al. 2007). Several studies have shown that the optimal kill rates and low probability of development of resistance will occur when the AUC/MIC ratio for the fluoroquinolones is at least 100 (Ginsburg et al. 2003, Schentag et al. 2003a,b). The EBA of an 800 mg dose ofloxacin is reported to be about half that of a 300 mg dose of isoniazid (Sirgel et al. 2000). Among fluoroquinolones, ofloxacin has been widely used in developing countries, and the use of moxifloxacin as a replacement is advised. Ofloxacin is known to be less potent than the other fluoroquinolones used for the treatment of tuberculosis both *in vitro* and *in* vivo (Hu et al. 2003, Rustomjee et al. 2008). In 2012, Chigutsa et al., demonstrated that ofloxacin might be ineffective even with doubled dose to 1600 mg daily (Chigutsa et al.

2012). Based on in vitro potency, it has been demonstrated that moxifloxacin was more bactericidal against slowly growing bacilli and also had sterilizing activity against persisters that are tolerant of high rifampin concentrations (Hu et al. 2003), hence moxifloxacin might be superior to gatifloxacin. Moreover, levofloxacin is more promising among fluoroquinolones, its activity has been shown to be slightly lower than moxifloxacin (Ahmad et al. 2013), making moxifloxacin and levofloxacin as attractive candidates.

1.3.2 Pharmacokinetics of drugs for the treatment of tuberculosis

Rifampicin pharmacokinetics are influenced by polymorphisms in drug transporting enzymes (Chigutsa et al. 2011) and autoinduction of rifampicin systemic metabolism (Strolin Benedetti & Dostert 1994). Rifampicin induces the majority of phase I and phase II drug metabolising enzymes and drug transporters such as p-glycoprotein (P-gp) through binding to and subsequent activation of the constitutive androstane receptor (CAR) and pregnane X receptor (PXR) (Chen & Raymond 2006, Rae et al. 2001), also inducing its own metabolism. The bioavailability of rifampicin has been reported to be 93% after single administration of rifampicin but with chronic administration the bioavailability reduces to only 68% (Loos et al. 1985), which is a clear indication of autoinduction of first-pass metabolism as was described by (Smythe et al. 2012). Smythe et al. study determined that it takes 40 days for the autoinduction of rifampicin to reach its steady-state and causing more than 40% reduction in AUC (Smythe et al. 2012). In vitro experiments using human hepatocytes determined that rifampicin has the highest reported induction potential among rifamycins, followed by rifapentine (Li et al. 1997).

Rifampicin pharmacokinetics is marked by high between subject variability (Wilkins et al. 2008), influenced by factors like age, weight, HIV infection, and nutrition, polymorphisms in drugs transporters, food, sex (detailed under section 1.3.3: Factors influencing drug pharmacokinetics). The absorption of rifampicin was reported to be quite variable (Wilkins et al. 2008) with two subgroups of 'fast absorbers' and 'slow absorbers' reported previously (Peloquin et al. 1997). Rifampicin is rapidly absorbed with maximum time (Tmax) to reach peak concentrations (Cmax) within 2-3 hours (Table 1.1). In humans, rifampicin is about 80% bound mainly to albumin, and distributes well throughout the body and body fluids (Acocella 1978). About 50% of the rifampicin dose is eliminated unchanged through biliary, whilst the other 50% is found in the urine as a combination of unchanged drug (10%) and metabolites. Rifampicin is metabolized by arylacetamide deacetylase, AADAC (Nakajima et al. 2011), and its main metabolite is 25-desacety rifampicin, which is active against *M.tuberculosis*. The expected half-life, Cmax and area under concentration-time curve (AUC) are summarized in Table 1.1. Rifampicin elimination is dose-dependent. At doses higher than 450 mg daily, there is decreased elimination of rifampicin (Acocella 1978), which could be attributed to saturation of the biliary transport mechanisms (Acocella 1983). Also, sex difference has been shown to alter pharmacokinetics of rifampicin, males had 19.3% (95% CI, 3.6, 35.1) lower AUC_{0-12} than females (McIlleron et al. 2012).

The pharmacokinetics of rifapentine is similar and also different from that of rifampicin and some of the factors influencing its pharmacokinetics gave opposite effects when compared with rifampicin. Rifapentine pharmacokinetics is influenced by age, weight, HIV infection, and nutrition, polymorphisms in drugs transporters, food, and sex . Rifapentine is well absorbed and less rapid than rifampicin with Tmax reached within 5

h (Langdon et al. 2004). The relative bioavailability reported after oral administration is 70%. Rifapentine has a longer half-life than rifampicin, which is approximately 12 hours in humans (Burman et al. 2001, Keung et al. 1999). The primary metabolic pathways for rifapentine are deacetylation and nonenzymatic hydrolysis forming a main primary enzymatic metabolite, 25-desacetyl rifapentine, and two secondary nonenzymatic metabolites, 3-formyl rifapentine and 3-formyldesacetyl rifapentine (Reith et al. 1998). Protein binding of rifapentine was estimated to be 98% (mainly to albumin) and 93% for 25-desacetyl rifapentine (Sirgel et al. 2005, Weiner et al. 2004). Even though rifampicin has higher induction potential in vitro (Li et al. 1997), at clinically relevant doses encountered routinely, rifapentine had a higher induction potential on cytochrome P450 subfamily 3A (CYP3A) (Bliven-Sizemore et al. 2011). The autoinduction effect of rifapentine has been described, with the mean AUC_{0-48} after seven thrice-weekly doses decreased by 20.3% ($p = 0.0035$) compared to the AUC_{0-48} after the first dose, and the mean $t_{1/2}$ decreased from 18.5 to 14.8 h ($p = 0.0004$). The mean AUC_{0-48} for the 25-desacetyl-rifapentine metabolite diminished by 21% (Dooley et al. 2008).

Pyrazinamide is rapidly absorbed following oral administration with Tmax reached with 1 h (Table 1.2). The pharmacokinetics of pyrazinamide have been shown to be less variable than that for the other first-line drugs (McIlleron et al. 2006). Pyrazinamide is reported to have an oral clearance of about 3.4 L/h and a volume of distribution of about 29 L (Wilkins et al. 2006) with relatively low protein binding of 10-20%. It is mainly eliminated through metabolism to pyrazinoic acid by a hepatic microsomal deamidase (Lacroix et al. 1989). Pyrazinoic acid is further metabolised to 5-hydroxy-pyrazinoic acid by xanthine oxidase (Lacroix et al. 1989). The main metabolite of pyrazinamide is pyrazinoic acid which is about 30% of the dose, whilst other metabolites and unchanged

drug account for the rest of its elimination from the body (Ellard 1969). Table 1.2 summarises different studies and expected half-life and exposures of pyrazinamide. Pyrazinamide pharmacokinetics is marked by high between subject variability (Wilkins et al. 2006). Similar to rifampicin, males on pyrazinamide had 14.0% (95% CI, 5.6, 22.4) lower AUC_{0-12} than females (McIlleron et al. 2012).

Isoniazid pharmacokinetics is very variable with the major source of variability between subjects being contributed by NAT-2 genetic polymorphism (McIlleron et al. 2009). Isoniazid is rapidly absorbed with a Tmax of about 1 h (Peloquin et al. 1997) and distributes well into tissues. Table 1.3 summarises some of the recent studies where Cmax and AUC were reported for isoniazid. Isoniazid undergoes first pass metabolism in the liver and intestines (Back & Rogers 1987) which has been shown to occur to a greater extent in fast than in slow acetylators, thus giving rise to differences in bioavailability between the 2 subpopulations; hence slow acetylators have higher Cmax compared with fast acetylators (Peloquin et al. 1997). With a dose of 5 mg/kg/day, peak serum concentrations of 3-5 mg/L were observed in humans (Weber & Hein 1979). The half-life of isoniazid in South African tuberculosis patients has been reported to be 2.8 hours (McIlleron et al. 2006) although up to 8 fold differences between patients has been observed.

Moxifloxacin is rapidly absorbed and the major fraction of the dose reaches the systemic circulation within 2 h (Dooley et al. 2008, Siefert et al. 1999). It has a long half-life of 9-12 hours in humans (Dooley et al. 2008, Siefert et al. 1999) with moderate renal excretion of 6-20% of total elimination after intravenous administration (Siefert et al. 1999). Moxifloxacin is widely distributed throughout the body, with tissue

concentrations often exceeding plasma concentrations. Moxifloxacin is a not substrate of cytochrome P450 enzyme but of the inducible drug-transporter p-glycoprotein (P-gp) , recently named ABCB1 (Brillault et al. 2009), sulfotransferases (Senggunprai et al. 2009), and glucuronyltransferases (Tachibana et al. 2005). The pharmacokinetics of moxifloxacin are influenced by rifamycins (due to induction of metabolising enzymes) resulting in low exposures (Dooley et al. 2008). The sulfate conjugate (M1) accounts for approximately 38% of the dose, and is eliminated primarily in the faeces. Approximately 14% of an oral or intravenous dose is converted to a glucuronide conjugate, which is excreted exclusively in the urine. Peak plasma concentrations of glucuronide conjugate are close to 40% those of the parent drug, while plasma concentrations of sulfate conjugate are generally less than 10% those of moxifloxacin.

Ofloxacin is rapidly absorbed with peak concentrations reached within 2 h and with a half-life of 6 h, which is comparable between healthy volunteers (Yuk et al. 1991) and patients (Belousov et al. 1996). The primary route of elimination of ofloxacin is renal with only 4% being metabolized (Lode *et al.* 1987) (Lode et al. 1987). Ofloxacin has been shown to have linear pharmacokinetics with concentrations reported to increase linearly with dose, but elimination of ofloxacin decreases with declining renal function and increasing age (Stambaugh et al. 2002).

Table 1.1: Rifampicin pharmacokinetics (since year 2000) in adults with tuberculosis including those who are HIV positive (HIV+), where Tmax, Cmax and AUCs were reported.

Dose, (mg/kg/day)	Sample size		T_{max}(h)	C_{max} (mg/L)[a]	AUC (mg·h/L)[a]	Source
10.5 (6.9, 14.1)	13		2.4 (1.7, 3.1)	7.2 (5.5, 8.9)	33.0 (26.7, 39.4)	(Gurumurthy et al. 2004a)[b]
10.7 (7.3, 19.6)	15 (HIV+)		3.6 (2.7, 4.5)	3.4 (2.7, 4)	16.5 (12.4, 20.6)	
9.6 (6.6, 14.7)	34		5.6 (2.0, 10.0)	5.5 (1.1, 11.2)	17.0 (3.7, 47.7)	(Perlman et al. 2005)[c]
8.7 (6.1, 15.2)	21 (HIV+)		2.2 (2.0, 8.0)	5.44 (2.2, 14.0)	22.3 (4.6, 49.1))	
10	58 (HIV+)		2.0 (1.8, 6.3)	5.6 (0, 13.7)	24.0 (7.0, 52.4)	(Tappero et al. 2005)[d]
10	28		2.0 (1.8, 6.1)	6.0 (2.2, 14.6)	21.7 (7.1, 52.9)	
3	8		2.8 (±0.5)	1.5 (±0.4)	7.8 (±1.6)	(Sirgel et al. 2005)[e]
6	8		3.4 (±0.5)	2.9 (±0.5)	15.5 (±2.6)	
12	8		2.1 (±0.6)	9.5 (±1.8)	65.2 (±9.6)	
10.9 (8.8, 14.2)	88		2.5 (2.0, 3.0)	5.9 (4.2, 8.4)	21.5 (15.3, 31.7)	(McIlleron et al. 2006)[b]
Children						
	Sample size	Median age (years)				
9.6 (±2.3)	21 (HIV+)	3.73	1.8 (±0.9)	4.9 (±2.0)	14.9 (±7.3)	(Schaaf et al. 2009b)[d]
9.6 (±2.3)	33	4.05	1.7 (±0.9)	6.9 (±5.9)	18.1 (±12.5)	

Tmax, time to reach peak plasma concentrations. [a]Area under concentration-time curve (AUC) and peak plasma concentration (Cmax) reported as median (interquartile range), mean (±standard deviation). [b]AUC until 8-h time point. [c]AUC calculated using 2-6 h concentrations. [d]AUC until 6-h time point. [e]AUC up to infinity hours.

Table 1.2: Pyrazinamide pharmacokinetics (since year 2000) in adults with tuberculosis including those who are HIV positive (HIV+), where Tmax, Cmax and AUCs were reported.

Dosage, (mg/kg)	Sample size		T_{max}(h)	C_{max} (mg/L)	AUC (mg·h/L),	Source
31	47 (HIV+)		2.3(±1.0)	41.8 (±11.3)	277 (±78)	(Perlman et al. 2004)[a]
35[b]	24 (HIV+)		2.7(±1.5)	52.8 (±17.6)	328 (±92)	
30 or 50	59 (HIV+)		2.0 (2, 6.3)	48.7 (35.6, 118.8)	219 (156, 519)	(Tappero et al. 2005)[c]
30 or 50	28		2.0 (1.8, 6.3)	55.5 (36.7, 78.9)	241 (156, 372)	
35.7 (25.2, 47.3)	142		2.0 (0.5, 4.1)	52.7 (2, 92)	288 (246, 335)	(McIlleron et al. 2006)[d]
Children						
	Sample size	age (years)				
30.5	15	0 - 4	3.5	27.5 (±16.6)	327 (±335)	(Graham et al. 2006a)[e]
35.0	12	>5	3.3	47.9 (±17.7)	416 (±333)	
25	20	5 - 12	1.7 (0.2)	42.4 (±3.3)	453 (±67)	(Gupta et al. 2008)[c]
15	20	5 - 12	1.8 (0.1)	38.6 (±3.9)	385 (±43)	
23.1	34	1.5 - 5.2	0.75 (0.75, 1.5)	30.7 (25.5, 35.0)	138 (121, 157)	(McIlleron et al. 2011)[a]

Tmax, time to reach peak plasma concentrations. [a]Area under concentration-time curve (AUC) and peak plasma concentration (Cmax) reported as median (interquartile range), or mean (±standard deviation). [a]AUC reported using 2-10 h concentrations. [a]Intermittent dose. [c]AUC until 6-h time point. [d]AUC until 8-h time point. [e]AUC until 24-h time point.

Table 1.3: Isoniazid pharmacokinetics (since year 2000) in adults and children with tuberculosis including those who are HIV positive (HIV+)

Dosage, (mg/kg/day)	Sample size		C_{max} (mg/L)[d]	AUC (mg·h/L)[d]	Source
14.3 (9.7, 26.1)[a]	8		12.9 (10.6, 15.2)	61.1 (50.0, 72.3)	(Gurumurthy et al. 2004b)
14.3 (9.7, 26.1)[a]	7 (HIV+)		10.1 (8.3, 11.8)	52.4 (44.9, 59.8)	
14.0 (9.2, 18.8)[b]	5		11.0 (7.6, 14.3)	39.0 (23.7, 54.4)	
14.0 (9.2, 18.8)[b]	8 (HIV+)		7.0 (5.5, 8.6)	22.9 (17.8, 28.0)	
6.5 (4.8, 8.8)	142		6.5 (4.9, 8.7)	25 (18.9, 32.8)	(McIlleron et al. 2006)[e]
Children					
	Sample size	age (years)			
<4	7	1.27 (0.41, 5.1)	0.76 (0.69, 2.24)	2.93 (1.56, 7.2)	(McIlleron et al. 2009)[f]
4 - 6	30	3.58 (1.97, 5.51)	2.39 (1.59, 3.4)	5.97 (4.0, 9.39)	
>6 to <8	2	7.0 (2.04, 11.97)	5.85 (5.7, 6.0)	11.7 (11.0, 12.4)	
8 -12	15	4.07 (1.91, 6.43)	5.71 (4.74, 7.62)	14.1 (9.4, 28.4)	
5.01 (4.35, 9.24)[a]	20		4.05 (2.72, 5.74)	10.6 (8.7, 16.1)	
5.01 (4.35, 9.24)[c]	24		2.63 (1.6, 5.3)	6.5 (4.2, 13.3)	
5.01 (4.35, 9.24)[b]	8		1.54 (1.2, 4.1)	2.3 (1.8, 6.1)	
>12	2	0.81 (0.61, 1.01)	6.46 (5.92, 6.99)	19.74	
9.4 (6.9, 12.5)	17	1.0 - 3.0	3.3 (2.4, 4.6)	14.9 (7.2, 19.5)	(Ramachandran et al. 2013)[e]
10.1 (8.6, 11.4)	22	3.1 - 6.0	6.1 (3.1, 8.4)	26.7 (12.5, 40.7)	
10 (8.8, 10.7)	23	6.1- 9.0	6.3 (4.4, 9.0)	21.9 (15.0, 28.8)	
9.1 (8.2, 10.0)	23	9.1-12	7.2 (5.6, 8.5)	28.7 (18.6, 40.6)	

[a]Slow acetylators. [b]Fast acetylators. [c]Intermdiate acetylators. [d]Area under concentration-time curve (AUC) and peak plasma concentration (Cmax) reported as median (interquartile range). [e]AUC until 8-h time point; [f]AUC

1.3.3 Factors influencing drug pharmacokinetics

Cure rates of more than 85% were reportedly achieved when rifampicin, isoniazid and pyrazinamide are administered optimally in adults (Fox et al. 1999, Jindani et al. 2004). Children still face the challenge of low exposures of rifampicin, pyrazinamide and isoniazid when compared to adults after standard doses (mg/kg), and children experience severe form of tuberculosis compared with adults. Recent systematic reviews on rifampicin (Donald et al. 2011) and pyrazinamide (Donald et al. 2012) have shown that the serum levels of rifampicin are low in patient infected with *M.tuberculosis* and children having the lowest concentrations when they receive similar mg/kg doses (Table 1.1) when compared to health volunteers; although generally similar exposures are achieved in both adults and children with tuberculosis receiving similar mg/kg doses of pyrazinamide (Table 1.2). Several factors such as HIV co-infection, weight, sex, formulation, age, pharmacogenetic and nutritional status influence the pharmacokinetics of anti-TB drugs and they needs to account for when describing the pharmacokinetics and pharmacodynamics of drugs.

HIV infection

The impact of HIV and consequently immune suppression has been shown to influence the pharmacokinetics of drugs in patients co-infected with tuberculosis (Gurumurthy et al. 2004a).. Reductions in rifampin bioavailability of ranging from 32 to 50% have been ascribed to HIV infection (Chideya et al. 2009, Gurumurthy et al. 2004a, McIlleron et al. 2006). However, since other studies found no effect of HIV status, this effect could be related to WHO stage, CD4 count and antiretroviral drugs used in the cohorts. Pyrazinamide concentrations may also be reduced among subjects with HIV, and similar trends have been described for isoniazid in association with diarrhea (Gurumurthy et al.

2004a). Decreased bioavailability of these drugs is thought to be linked to more extensive malabsorption due to HIV-mediated enteropathy and increased susceptibility to enteric infections.

Other studies evaluating the effect of HIV infection were conducted following intermittent dosing. In general, intermittent dosing of anti-TB drugs is not recommended in patients with HIV co-infection, but studies have been conducted when intermittent short course regimens were administered and have shown that high mortalities and failures occur in people co-infected with HIV (Havlir & Barnes 1999). Poor treatment outcomes have been reported in children with tuberculosis in areas highly burdened with HIV, and HIV being the most import risk factor (Rekha & Swaminathan 2007). When rifampicin has been dosed daily for at least 6 months, better treatment outcomes were reportedly achieved in patient with tuberculosis (Khan et al. 2010). Other contrary reports have shown no effect of HIV on the pharmacokinetics of anti-tuberculosis drugs (Gurumurthy et al. 2004a). In South African children infected with both HIV and *M.tuberculosis*, low rifampicin levels have been reported in children irrespective of HIV status. The respective AUC_{0-6} (standard deviation) for rifampicin were 14.9 (7.4) and 18.1 (12.5) mg·h/L for HIV infected and HIV negative children with tuberculosis (Schaaf et al. 2009a). Similarly, in a study conducted in Malawi, pyrazinamide AUC_{0-24} were not comparable between children with tuberculosis only and those infected with both HIV and tuberculosis, the respective AUC (standard deviation) for rifampicin were 411 (382) and 322 (240) mg·h/L for HIV infected and HIV negative children with tuberculosis (Graham et al. 2006a). For rifapentine, studies of differences in pharmacokinetic parameters of in HIV-positive and -negative individuals have produced mixed results, with some groups showing significant differences (Peloquin et al. 1996) and others finding no clinically significant effect (Choudhri et al. 1997). A study

conducted in South Africa (Langdon et al. 2004) showed good absorption of rifapentine and no differences in pharmacokinetic parameters when compared to HIV-negative patients. Sex was not found to influence the pharmacokinetics of rifapentine (Reith et al. 1998). Conversely, a study conducted in South Africa showed that females had low clearance of rifapentine, and there was a good correlation between rifapentine pharmacokinetics and total body weight (Langdon et al. 2005); given that females in the study had generally lower body weight, the sex effect possible was not independent of body weight

Dosage form

Drug formulation plays an important role in the pharmacokinetics of drugs. A previous study by McIlleron et al in adults have showed important differences when patients were dosed with single drugs versus fixed dose combinations (FDC) of rifampicin and isoniazid (McIlleron et al. 2006). Children often receive crushed or divided FDC tablets. Crushing and division of the FDCs may result in changes in biopharmaceutics and loss of active drug, and has been shown to result in significantly lower concentrations especially of isoniazid (Notterman et al. 1986). Absorption of drugs in children can also be affected by gastric pH, gastrointestinal surface area (Kearns 2000, Kearns et al. 2003) and other factors experienced by children including 'dislike' of the taste of drugs.

Age and body weight

Children experience varied physiological changes during growth which may affect drug absorption, distribution and metabolism leading to significantly altered pharmacokinetic profiles which could impact drug efficacy. Enzyme maturation also affects the bioavailability of drugs and failure to account for it has in part accounted for low exposures in children when mg/kg doses are used as in adults. In children gastric

emptying time appears to approach adult values within the first 6 to 8 months of life. Intestinal motor activity matures throughout early infancy with increases in the frequency, amplitude, and duration of propagating contractions and is also influenced by food (al Tawil & Berseth 1996).

A study of Zhu et al found that absorption of pyrazinamide in children was 32% slower compared to that of the adults studied and the volume of distribution of the children 32% greater than that of the adults (Zhu et al. 2002). However, when volume is normalized to weight per kilogram, the absolute value may be lower. Children also prescribed the standard 10 mg/kg body weight had lower concentrations compared to adults who received a similar dose (Schaaf et al. 2009b). The relatively low plasma concentration of rifampicin in children has been found in other studies where rifampicin prescribed at 10–12 mg/kg produced peak concentrations ranging from 3–9 mg/L (McCracken et al. 1980). In another study, ethambutol was thought to lower the exposures of rifampicin (Thee et al. 2009). Like isoniazid, the authors suggest that rifampicin doses may be calculated on the basis of body surface area rather than body weight, especially in younger children. Encouragingly, children receiving a dosage of 300 mg/m^2 body surface and at the age of 3 months to 2.5 years had mean serum concentrations of 9.1 mg/L, which is above the target of 8 mg/L and was close to the desired serum level of 10 mg/L (Thee et al. 2009).

Younger children receiving 10 mg/kg of isoniazid (dose similar to adults) had significantly lower AUC than adults, leading to the suggestion that younger children eliminate isoniazid faster than adults (Schaaf et al. 2005). The faster clearance (adjusted according to body) of isoniazid could be attributed to the higher proportion of liver size to total body weight; hence it was proposed that children should be dosed according to body surface area (BSA). In support, when serum levels of isoniazid were compared

when children were dosed according to body weight (mg/kg) and BSA, weight-based isoniazid concentrations were lower than those dosed according to BSA especially in children less than 8 years, and BSA-based doses gave similar exposures as in adults (Thee et al. 2010). Also, a study conducted in South African children with tuberculosis had showed that children who received 4-6 mg/kg dose of isoniazid had 58% lower peak versus those who received 8-10 mg/kg dose, and in about 70% of children who received 4-6 mg/kg, the peak concentrations were below the recommended range of 3 mg/L (McIlleron et al. 2009).

Similar trends of lower concentrations, exposures and shorter half-lives were reported in children on pyrazinamide (McIlleron et al. 2011, Ramachandran et al. 2013) and increase in doses has been suggested. However a study by Thee et al (Thee et al. 2008) which described the pharmacokinetics of children who received higher doses of 30 mg/kg of pyrazinamide has shown that Cmax was reached in all three groups receiving pyrazinamide 3 h after dosing and was 37.9 mg/ml, 31.3 mg/ml and 33.3 mg/ml in the age groups < 6, 6-10 and 10-14 years. There was no significant difference between the concentrations in the three age groups. Unlike isoniazid, the similar pyrazinamide concentrations found in their study across a range of ages indicated that dosing should probably be based on body weight rather than body surface area. The findings of Ellard (Ellard 1969) support the opinions of the study by Thee et al. Conversely, the results of Zhu et al in children with a mean age of four years receiving a mean pyrazinamide dosage of 25 mg/kg and those of Graham et al from children age less than four years receiving a PZA dosage of 30.5 mg/kg do suggest that any lowering of the dosage to less than 30 mg/kg will result in a significant proportion of younger children being exposed to serum Cmax concentrations of <20 mg/L (Graham et al. 2006b, Zhu et al. 2002).

Recently, a study conducted in adults with HIV co-infection showed that for 10 kg increase in body weight was associated with 14.1 % (CI, 7.5, 20.8), 14.1% (95% CI, −0.7, 31.1), and 6.1% (95% CI, 2.7, 9.6) decrease in respective AUC_{0-12} of rifampicin, isoniazid and pyrazinamide (McIlleron et al. 2012).

Nutritional Status

The association between pharmacokinetics of drugs for treatment of tuberculosis and nutritional status has long been debated. In malnourished children, it has been suggested that drugs used in current standard doses, calculated on the basis of age or body weight (mg/kg), may not produce the desired therapeutic effect (Mehta 1990). The pathophysiological changes associated with malnutrition can alter pharmacokinetic processes, drug responses and toxicity (Krishnaswamy 1989). It is common that patients with tuberculosis are often malnourished, and a significant association between malnutrition and severe forms of childhood tuberculosis has been reported (Vijayakumar et al. 1990). But, studies which evaluated the effect of malnutrition on the pharmacokinetics of anti-tuberculosis drugs have had conflicting results. A study in South Africa showed that changing conditions of disease or nutrition did not significantly influence isoniazid elimination in children (Schaaf et al. 2005).

Genetic factors

There pharmacokinetics of drugs such as rifamycins and isoniazid are influenced by genetic factors. Recent data indicate that a single nucleotide polymorphism in solute carrier organic anion transporter family, member 1B1 (SLCO1B1) gene that encodes the

OATP1B1 transmembrane receptor affects rifampin drug concentrations (Weiner et al. 2004). OATP1B1 is an influx transporter that regulates hepatic uptake of xenobiotics and is important for numerous drugs (Chigutsa et al. 2011, Kalliokoski et al. 2010, Pasanen et al. 2006). Persons with the SLCO1B1 rs11045819 gene mutation at exon 4 (variant name c463C>A) had 42% lower AUC and 34% lower Cmax values than those without it in one study (Weiner et al. 2004), and an rs4149032 C>T polymorphism was associated with 20% and 28% reductions in rifampin bioavailability in heterozygotes and homozygotes, respectively in another (Chigutsa et al. 2011). Importantly, SLCO variants appear to be more common in Black patients than White patients. The contribution of genetic factors to differences in rifapentine pharmacokinetics is unknown.

The effect of arylamine N-acetyltransferase 2 (NAT2) on pharmacokinetics of isoniazid is well known. A study conducted by Mcllleron et al. in South African children showed dose in mg/kg body weight and NAT2 genotypes to be dominant determinants of isoniazid concentrations. Hence dose reduction below 6 mg/kg body weight would disadvantage fast acetylators, while slow acetylators would require only a 3 mg/kg dose to achieve a satisfactory exposure of isoniazid (McIlleron et al. 2009). It has, therefore been suggested that the optimal dosage of isoniazid should consider age and possibly NAT2 genotype. Polymorphism in the NAT2 and its ability to metabolise isoniazid has led to three distinct trends in clearance: slow, intermediate and fast acetylators (McIlleron et al. 2009, Schaaf et al. 2005). and the effect of maturation of NAT2 on pharmacokinetics of isoniazid has been shown to be become apparent from as early as the first 3 months of life (Kiser et al. 2012). There is wide geographical variation in the distribution of *NAT-2* polymorphisms (Sabbagh et al. 2008). The NAT2 alleles NAT2*5,

*6 and *14, have been found predominantly in Africa (Matimba et al. 2009), and these polymorphism results in slow to intermediate acetylation of isoniazid. The NAT2*4 is the ancestral and is associated with a fast phenotype, while the other alleles NAT2*5, *6 and *14 are associated with slow phenotype.

Effect of food

Food has been reported to decrease the rate of absorption of rifampicin as evidenced by an increase in Tmax (Zent & Smith 1995) which may result in reduced Cmax (Jeanes *et al.* 1972). Food has also been shown to lower bioavailability of rifampicin (Zent & Smith 1995), and effect which was not found in Peloquin's study(Peloquin et al. 1999). The effect of food had been reported to lower the bioavailability of isoniazid (Zent & Smith 1995) and higher exposure may be achieved by administration of isoniazid on an empty stomach. For rifapentine, unlike rifampicin, concomitant food has a marked increase on rifampicin absorption giving high bioavailability (Chan et al. 1994). The effect of food on systemic rifapentine exposure may therefore impact treatment activity and safety. However the effects on other meal types which are often used in tuberculosis control programs remains unknown. However, delay in absorption of ofloxacin was observed which may be attributed to food effect (Stambaugh et al. 2002).

1.3.4 Pharmacokinetics and pharmacodynamics (PKPD) relationships

One descriptor of sterilizing and bactericidal activity of anti-tuberculosis drugs have been the link between pharmacokinetic exposures and MIC. Drugs such as rifampicin have reported to have concentration dependent killing where the rate of bacterial killing increases as the concentration of antibiotic increases over a wide range of concentrations. The magnitude of the pharmacokinetic/pharmacodynamic parameters required for

efficacy for such drugs may be relatively similar in animal infection models and in human infections (Craig 1998).

Dose fractionation studies for rifampicin showed that doses expected to achieve an AUC/MIC ratio of 271 in the mouse were associated with a 1 $\log_{10}$ reduction in lung CFU counts after 6 daily doses. But, these doses were on the low end of the dose-response curve. In humans, the AUC/MIC ratio associated with activity was expected to be close to 120 after a 600 mg oral dose of rifampicin (Kenny & Strates 1981). While this value meets the target values for AUC/MIC associated with efficacy for other concentration-dependent antibiotics against gram-negative bacilli, it is clear that higher doses of rifampicin or more potent rifamycins might exert substantially greater activity. Lower doses of rifampicin appear to be less effective in clinical studies. One randomized clinical trial demonstrated a decline in the activity of rifampicin with a dose reduction from 600 to 450 mg daily (Long et al. 1979). Furthermore, it has been established that rifampicin unbound AUC/MIC correlated better with killing of *M.tuberculosis* than Cmax/MIC using the hollow-fiber bioreactor system (HFS) (Gumbo et al. 2007a). The unbound Cmax (*f*Cmax)/MIC≥175 of rifampicin in plasma result in prevention of resistance to rifampicin (Gumbo et al. 2007a), while plasma AUC_{0-24}/MIC≥271 and epithelial lining fluid (ELF) AUC_{0-24}/MIC ≥665 were associated with a 1-log10-CFU reduction in the total lung bacterial load in mice(Jayaram et al. 2003). In the early phases of infection bacteria multiply in alveolar macrophages, hence concentrations of rifampicin in macrophages and ELF may be important. In alveolar cell, rifampicin concentration after 600 mg dose were more than 10 fold higher than in plasma, but in ELF it was slightly lower (Goutelle et al. 2009). As a result, the rates of target attainment estimated by the model suggested that Cmax/MIC≥175 was 95% in alveolar cell, 48.8% in plasma, and 35.9% in ELF. Furthermore, rifampicin killing effect was determined to

be 100% in plasma, while in macrophages it was 54.5%, while doubling the dose of rifampicin to 1200 mg gave improved target ratios (Goutelle et al. 2009), hence recent studies propose increasing the dose of rifampicin from 600 mg(de Steenwinkel et al. 2013, van Ingen et al. 2011).

On the other hand, rifapentine is a more promising candidate than rifampicin owing to better pharmacokinetics.. It has a long half-life (Burman et al. 2001, Keung et al. 1999) and superior *in vitro* potency against *M.tuberculosis* in comparison with rifampin (Heifets et al. 1990), making it an attractive candidate for shortening and simplifying antitubercular therapy. Like rifampicin, higher doses have been suggested to overcome development of ARR, and relapse may be associated with intermittent dosing (Burman et al. 2006, Menzies et al. 2009). The sterilising effect of rifapentine has been shown to be dose dependent in murine studies which suggest that daily doses of rifapentine may reduce treatment duration to less than 3 months (Rosenthal et al. 2006, 2007; Zhang et al. 2009). Furthermore, higher doses of rifapentine are associated with improved early bactericidal activity in humans (Sirgel et al. 2005). But in the TBTC study 29A, increase in exposure due to daily rifapentine failed to accelerate bacterial elimination in humans which was not expected following mouse studies (Dorman et al. 2012). Following this failure, Mitchison suggested that this could be due to presence of low-tolerance persisters in humans which are absent in mouse studies, hence Cmax could be important determinant of kill rather than AUC/MIC as found in mouse studies (Mitchison 2012). Rifapentine has been shown to have significantly higher intracellular concentrations since the MIC and minimal bactericidal concentrations were against *M.tuberculosis* H37Rv within macrophages were 4 times lower compared with corresponding values for extracellular bacilli (Mor et al. 1995). Consequently, rifapentine could be 8 times more potent against intracellular *M.tuberculosis* when compared with rifampicin because

rifampicin had 2 times higher intracellular MIC and minimal bactericidal concentrations (Mor et al. 1995). But, a study in guinea pigs established that rifapentine is not more active than rifampicin against chronic dosing (Dutta et al. 2012). However, little is known about the effect AUC and Cmax on the probability of failure or relapse.

Studies on PKPD of pyrazinamide are few. In a HFS study, resistance suppression has been linked to duration of time the concentration is above MIC while maximal bacterial killing in epithelial lining fluid has been associated with $AUC_{0\text{-}24}$/MIC ratio $\geq$ 209 (Gumbo et al. 2009). Also, a study conducted in Botswana has shown that pyrazinamide concentrations lower than 35 mg/L were associated with increased risk of treatment failure (Chideya et al. 2009). Furthermore a recent study based on HFS has established that peak pyrazinamide concentration (cut-off 53.8 mg/L) was the most important predictor of both 2-month sputum conversion (Pasipanodya et al. 2013), hence pyrazinamide remains an important drug in treatment of tuberculosis.

For isoniazid, activity has been proposed to be concentration dependent following a single clinical trial using divided dosing. Of interest from this study was that 400 mg daily doses of isoniazid were more effective than 200 mg given twice daily, but the 400 mg daily study only provided concentrations above the MIC for only 50–75% of the dosing interval from rapid acetylators, while the 200 mg twice daily had concentrations above the MIC for the entire dosing interval (Gangadharam et al. 1961). The efficacy of isoniazid had a demonstrated plateau interval (Gangadharam et al. 1961) but there were no significant differences in outcomes between slow and rapid acetylators or between patients receiving 400 or 700 mg isoniazid. Recent studies showed that the activity of mycobacterial kill of isoniazid is related to the AUC/MIC ratio compared to Cmax/MIC ratios or the time above MIC (Gumbo et al. 2007b). Importantly, Chigutsa et al., had

shown that isoniazid may antagonize sterilizing activity in PTB patients on standard first line regimen (Chigutsa et al. 2013), which supports mouse models suggesting antagonism (Grosset et al. 1992).

The efficacy of fluoroquinolones including moxifloxacin and ofloxacin has been related to the *f*AUC_{0-24}/MIC (Shandil et al. 2007). Based on *in vitro*, murine, and clinical studies, a *f*AUC_{0-24}/MIC ratio of at least 100–125 has been proposed as a minimum target for bactericidal activity against gram-positive and gram-negative bacteria (Schentag et al. 2003a,b). The HFS study has suggested a minimum target *f*AUC_{0-24}/MIC ratio of 53 for *M.tuberculosis* as the identified target for suppressing the outgrowth of moxifloxacin-resistant mutants and not necessarily optimal bactericidal activity (Gumbo et al. 2004). However, there is no agreed value on the target ratio to be used when fluoroquinolones are used. Fluoroquinolones generally achieve higher concentrations in ELF than in plasma (Kiem & Schentag 2008), which could be advantageous where patients had cavities. Compared with other fluoroquinolones, moxifloxacin has been found to have greater efficacy than levofloxacin in mice despite a lower plasma AUC/MIC ratio (Ahmad et al. 2013), which is due to higher intracellular concentrations of moxifloxacin. Levofloxacin penetrates into cerebrospinal fluid of patients with tuberculosis meningitis better than ciprofloxacin and gatifloxacin (Thwaites et al. 2011).

In general, the PKPD indices of either AUC/MIC or Cmax/MIC and their potential to predict clinical outcome and bacterial load remain debatable.

Tolerability of higher doses

Even though higher doses of anti-tuberculosis drugs are associated with more favorable outcomes, of concern is lack of concrete knowledge about dose-toxicity relationships. In all these drugs higher doses are proposed in children to match adult exposures (Steingart et al. 2011). It is debatable to say that rifamycin higher doses are likely to cause toxic effects. For rifampicin doses, doses above 600 mg (10 mg/kg) are not used because of concern about toxicity, but there is little evidence that higher doses of rifampicin are associated with toxicity (Acocella et al. 1971, Curci et al. 1972, Favez et al. 1972). In small-scale studies, higher doses of rifampicin have been used and were shown to have bactericidal activity which is twice that of 10 mg/kg (Diacon et al. 2007). The toxic effects of rifampicin, "flu-like" syndrome were suggested to be linked to intermittency rather than the magnitude of dose (Peloquin 2003). However, the situation might be different in children who experience various physiological changes such as maturation of enzymes and drug transporters. For rifapentine, limited studies which have been conducted using doses up to 1200 mg once weekly being used and were tolerated in humans (Weiner et al. 2004). However, convincing evidence still needs to be presented in ongoing clinical trials.

For pyrazinamide, the major limitation to increased doses is high rate of adverse reactions, frequently reported are arthralgia and hepatic toxicity (Blumberg et al. 2003, Corbella et al. 1995). Interestingly and contrary to many reports, a recent meta-analysis has shown that doses ranging from 43 to ≥60 mg/kg were associated with sporadic hepatotoxicity and there was no significant difference with those who were on lower doses (Pasipanodya & Gumbo 2010). However, the use of higher doses of isoniazid is associated with acute and chronic toxicities. Use of doses ≥20 mg/kg increase the likelihood of seizures (Lheureux et al. 2005). Elevated body temperatures, tachycardia

and tachypnea may occur due to seizure activity. Consequently, long-term sequelae include anoxic encephalopathy and dementia (McLay et al. 2005). Chronic toxic effects include hepatotoxicity and peripheral neuropathy. Peripheral neuropathy, uncommon with lower doses, has been reported after 7.8-9.6 mg/kg daily doses of isoniazid in poorly nourished patients (Devadatta et al. 1960), hence the use of pyridoxine to minimize peripheral neuropathy. The other most commonly encountered side-effects of isoniazid which are dose-related are elevated serum transaminase, biliriubinemia, jaundice, hepatitis and vomiting.

Higher doses of fluoroquinolones may increase side effects including QT interval prolongation observed even at recommended doses (Falagas et al. 2007). Given the long duration of treatment of MDR-TB, QT interval prolongation is of particular concern. However, limited studies seem to suggest safety of higher doses. A recent study by Ruslami et al. (Ruslami et al. 2013) which evaluated higher doses of moxifloxacin, 800 mg daily, did not show increased toxicity. In support, a study by Alffenar et al. showed tolerability at 600 mg and 800 mg moxifloxacin (Alffenaar et al. 2009). An ongoing clinical trial by Alffenar et al. is evaluating the safety of moxifloxacin at escalated doses of 600 and 800 mg (NCT01329250: http://clinicaltrials.gov/show/NCT01329250).

Nonlinear mixed effect modeling (pharmacometrics)

Pharmacometrics is a science that involves quantitative interpretation of pharmacological observations which help in optimization of dosing regimens, clinical trial design, efficacy of drugs, drug labeling, disease progression and responsiveness to therapy. The United States Food and Drug Administration based (FDA) extensively defined pharmacometrics as a branch of science that quantifies drug, disease and trial

information to aid efficient drug development and/or regulatory decisions where disease, trial and drug disease models are important. Disease models describe the association between biomarkers and clinical outcomes, placebo effects and time course of disease. Then trial models for the inclusion/exclusion criteria, patient discontinuation and adherence. Lastly, drug models describe the relationship between exposure (or pharmacokinetics), response (or pharmacodynamics) and individual patient characteristics (FDA 2010).

The term population pharmacokinetics is often used in pharmacometrics, which is the study of pharmacokinetics where drug concentration data from all individuals in a population are pooled together and evaluated simultaneously using a single pharmacometric model, and an association with pharmacodynamic responses may be evaluated (Sheiner & Beal 1980). The main components of describing the observed data within a population include: structural model; statistical model; covariate model; and software used. Structural models describe the median concentration time course within the population while statistical models cater for variabilities in in observed data within the population such as interindividual variability (IOV), interoccassional variability (IOV) and random unexplained variability. Covariate models explain variability predicted by individual's clinical and demographic characteristics.

The most important strength of the population approach is simulation of different scenarios which are beyond the scope of just analyzing or describing the data. Through the use of Monte-Carlo simulation, therapeutic effectiveness, toxicity, adequacy of doses or other factors which may affect clinical outcomes can be predicted and optimised for

future population. Another importance advantage of a population approach to analysis is the ability to interpret be sparsely sampled data (mostly phase 3 clinical data) such compared with a traditional standard two stage approach or the naive pooled method (Sheiner & Beal 1980, 1983).

Modeling and simulation has been shown to be an important development towards improvement of decision making in the pharmaceutical industry (Gieschke & Steimer 2000, Miller et al. 2005). The increased use of modeling and simulation as part of drug development is expected to lead to fewer drug failures and smaller numbers of studies before a drug succeeds in a new drug application (Rajman 2008). Also, The FDA recommended the use of pharmacometric approach for successful application of investigational new drug entities

Therefore, in light of the above introduction and literature highlighting the past, present and future efforts in treatment of tuberculosis, further work is still required in using pharmacometric approaches to optimise dosing regimens, understanding what drives efficacy, and how to improve treatment of drug-resistant tuberculosis.

2 PROBLEM STATEMENT AND JUSTIFICATION

South Africa has the second highest per capita annual risk of tuberculosis disease after Swaziland, and its communities have extremely high tuberculosis transmission rates. The classical therapy for pulmonary tuberculosis consists of rifampicin, isoniazid, pyrazinamide and ethambutol for 2 months followed by a continuation phase of rifampicin and isoniazid, and has been used for the past four decades. When these standard regimen is optimally administered, cure rates of 85% or more can be achieved in patients with drug sensitive organisms (Fox et al. 1999, Jindani et al. 2004). But, the cure rates in public health care programs remain worryingly lower (WHO 2012b) especially in children, making it important to optimize treatment regimens especially in children, and investigate other treatment strategies.

In high disease burden settings, children contribute 15-20% of tuberculosis cases (Marais et al. 2006). Young children (<5 years of age) and children infected with HIV are prone to rapid progression to tuberculosis disease following infection, and children are prone to severe forms of tuberculosis including disseminated disease and meningitis (Marais et al. 2006). Lack of novel and better pharmacokinetic approaches in analyzing data in children limited optimization of doses in children assuming that adults from similar ethnic populations receive therapeutic doses. Furthermore, the majority of studies which had evaluated the pharmacokinetics of drugs used for the treatment have used non compartmental analysis (NCA) methods.. The NCA method is informative only after rigorous and intensive pharmacokinetic sampling in patients, and is often limited by financial resources, ethical constraints related to burden of the research on the patient, cost and convenience due to intensive sampling schedule required. In addition NCA has

limited application outside the scope of descriptive statistics such as simulations of different scenarios or study design.

Novel regimens aiming at shortening the duration of tuberculosis treatment or offering more intermittent therapy (i.e., once weekly or even less frequently) without lowering efficacy are required in reducing the burden of supervised drug therapy. New treatment strategies are evaluating the combination of moxifloxacin and intermittent high dose rifapentine as a first-line agent. Like rifapentine, moxifloxacin has a long half-life (9 - 12 h) (Dooley et al. 2008, Siefert et al. 1999), making it an attractive companion drug to prevent selection of rifapentine-resistant strains when the drugs are administered intermittently. Hence describing the population pharmacokinetics of moxifloxacin and rifapentine help in identifying potential sources of variability (covariate effects), and also evaluating the possibility of drug-drug interactions when they are used together. Furthermore, there is limited information about the effects of pharmacokinetics parameters such as time above MIC, Cmax and AUC in relation to proportion of patients with relapse or treatment failure per regimen, adjusted for duration of treatment/study regimen.

Fluoroquinolones play an important role in the treatment of multi-drug resistant tuberculosis (MDR-TB) (Falzon et al. 2011) which is defined by resistance to both rifampicin and isoniazid (WHO 2008a). Fluoroquinolones differ from each other in their efficacy against *M.tuberculosis* as measured by $fAUC_{0\text{-}24}$/MIC, and also display differences in their clinical pharmacokinetics. New fluoroquinolones are usually preferred to the earlier-generation ones (WHO 2011), but ofloxacin is still widely used to treat MDR-TB, because of its affordability and availability. Even though the *in vitro*

bactericidal activity of moxifloxacin against *M.tuberculosis* is superior to that of ofloxacin (Hu et al. 2003), little is known as to whether this will be the case in humans where distribution of AUCs of drugs used for treatment of MDR-TB and their respective MIC distributions in relevant patient population is taken into account.

Population pharmacokinetics of rifapentine

Population pharmacokinetic studies of rifapentine are very few. The only studies conducted in Southern African populations have limited scope when evaluating steady state population pharmacokinetics (Langdon et al. 2004, 2005). Concomitant food has a marked effect on rifapentine absorption (Chan et al. 1994). The effect of food on systemic rifapentine exposure may therefore impact treatment activity and safety. The study by Chan et al was studied on English breakfast (fat meal) which may not be applicable to resource limited countries like South Africa; hence there is need for further evaluation when other meal types are considered. Additionally, rifapentine has a microbiologically active metabolite, 25-desacetyl rifapentine (Heifets et al. 1990), evaluating pharmacokinetics of this metabolite have to be considered.

The population pharmacokinetics of rifapentine is not only affected by food, but other factors like pharmacogenetics have to be considered. Recent advances in evaluating the pharmacogenetic correlates of rifamycin pharmacokinetics had determined that rifampicin drug concentrations and AUC are altered after a single nucleotide polymorphism of SLCO1B1 gene which encodes the OATP1B1 transmembrane receptor (Weiner et al. 2010). A recent study in South African population where pharmacometric approaches were used to quantify the effect of SLCO1B1 mutation showed significantly reduced bioavailability of rifampicin (Chigutsa et al. 2011). Given that rifapentine is a

rifamycin, the relative contribution of genetic differences in drug handling to these differences is unknown; hence similar pharmacometric evaluations are important.

Population pharmacokinetics of moxifloxacin and its efficacy in MDR-tuberculosis

Moxifloxacin and ofloxacin are rapidly absorbed following oral administration with peak concentrations reached within 2 h after dose, but moxifloxacin has a longer half-life of approximately 12 h (Dooley et al. 2008) versus 6 h of ofloxacin (Belousov et al. 1996). A further pharmacokinetic difference between these two drugs is that moxifloxacin has moderate renal excretion which comprise 6-20% of total elimination after intravenous administration (Siefert et al. 1999), while ofloxacin is primarily renally eliminated (Lode et al. 1987). In light of this highlighted differences in pharmacokinetics, whether it contributes to differences in efficacy between these two drugs is unclear. Hence non-linear mixed effects modelling approaches could then be used to quantify the efficacy of moxifloxacin and ofloxacin against each other when *f*AUC/MIC ratios are taken into account.

Rifapentine and moxifloxacin drug interactions

Little is known about the interaction between moxifloxacin and rifapentine. Moxifloxacin is a substrate of inducible P-gp (Brillault et al. 2009), sulfotransferases (Senggunprai et al. 2009), and glucuronosyltransferases (Tachibana et al. 2005). Co-administration of moxifloxacin with rifapentine (enzyme and transporter inducer) resulted in a 17.2% (Dooley et al. 2008) decrease in moxifloxacin exposure in healthy volunteers (dosed three times a week). Hence there is need to evaluate the extent of drug-drug interactions when moxifloxacin is administered with intermittent high dose rifapentine.

Investigation of population pharmacokinetic summary variables of rifapentine and moxifloxacin as of predictors of treatment outcome

Novel clinical trials are evaluating the combination of rifapentine and moxifloxacin as first-line therapy. Information gathered in these novel regimens is important in optimizing the doses of respective drugs used. Most importantly, risk factors that resulted in unfavorable outcome should be investigated and this information is still to be known. Hence there is need to estimate the PKPD indices of both moxifloxacin and rifapentine, among them time above MIC, Cmax, AUC either for once weekly or twice weekly regimens all at steady state, and time above MIC (TAMIC), and evaluate them as predictors of treatment outcome.

Optimization of rifampicin, isoniazid and pyrazinamide dosages in children using a population pharmacokinetic approach

The widely used daily dosages of first-line antituberculosis drugs recommended in children were derived from adult dosage based on the assumption that the same dose per kg is appropriate across all ages of patients. Even though rifampicin, isoniazid and pyrazinamide have been available for many years, the limited pharmacokinetic information in children suggests that young children receiving adult-derived dosages have drug exposures lower than adults (McIlleron et al. 2009, Schaaf et al. 2005, 2009b). The majority of the studies used NCA for analysis. In children, factors such as maturation of metabolizing enzymes and transporters, body composition, organ function, nutritional status, and the pathophysiology of severe forms of tuberculosis may contribute to changes in pharmacokinetics, drug response and toxicity (Kearns et al. 2003). WHO has recently recommended increased dosage of the first-line

antituberculosis drugs for children (WHO 2010), which are to be implemented using dispersible FDC tablets for paediatric use, manufactured according to newly recommended specifications, with each tablet containing 50 mg isoniazid, 75 mg rifampicin and 150 mg pyrazinamide (WHO 2012c). Hence there is a need to describe the population pharmacokinetics of rifampicin, pyrazinamide, and isoniazid through a pharmacometric approach non-linear mixed-effects models, and use final models to predict AUC and Cmax in a paediatric population and compare them with the corresponding pharmacokinetic measures in ethnically similar adults with tuberculosis, where adults are on standard therapy recommended by WHO.

3 AIM

The principal purpose of this work was to:

1. Describe the population pharmacokinetics of rifampicin, pyrazinamide and isoniazid in children with tuberculosis, and to evaluate the adequacy of currently recommended doses using a pharmacometric approach
2. Describe the population pharmacokinetics of rifapentine in order to quantify the effects of four different meal types on the population pharmacokinetics of single-dose rifapentine in healthy male volunteers
3. Quantify the drug interaction between moxifloxacin and intermittent high dose rifapentine
4. Describe the population pharmacokinetics of moxifloxacin, and compare moxifloxacin pharmacodynamic efficacy against widely used comparator ofloxacin
5. Investigation of population pharmacokinetic summary variables of rifapentine and moxifloxacin as predictors of treatment outcome

4 METHODOLOGY

4.1 Declaration of work

This thesis is based on the pharmacometric analysis of different studies, namely: Two studies of the pharmacokinetics of first-line antituberculosis drugs in children; a healthy male volunteer study; the RIFAQUIN clinical trial; a population pharmacokinetic study of ofloxacin in patients with multidrug-resistant TB, and an investigation of the MICs for moxifloxacin and ofloxacin in Mycobacterium tuberculosis isolates resistant to rifampicin and isoniazid. More details about the above-mentioned studies are given in section 4.2. Patient enrollment, drug administration and monitoring, pharmacokinetic sampling, follow up and all data collection for the work described in this Chapter was carried out by a study team and not by the candidate. All the drug plasma concentration determination was carried out by the University of Cape Town Division Of Clinical Pharmacology, except in 20 Children where it was carried out at Desmond Tutu Tuberculosis Centre, Department of Paediatrics and Child Health, Faculty of Health Sciences, Stellenbosch University, Tygerberg, South Africa. All the data analysis, modeling and simulation were performed by the candidate. The candidate used previously published models in adults for rifampicin (Wilkins et al. 2008), pyrazinamide (Wilkins et al. 2006) and isoniazid (Wilkins et al. 2011) to derive reference exposures in adults, and a previously published population pharmacokinetic and pharmacodynamic model for ofloxacin (Chigutsa et al. 2012) used in this thesis to compare efficacy between moxifloxacin and ofloxacin was not developed by the candidate. The determination of moxifloxacin and ofloxacin MICs in patient sputum isolates was done at DST/NRF Centre of Excellence for Biomedical Tuberculosis Research/MRC Centre for Molecular and Cellular Biology, Division of Molecular Biology and Human

Genetics, Faculty of Health Science, Stellenbosch University, Stellenbosch, South Africa.

In the RIFAQUIN study the candidate was responsible for aspects of coordination of data collection, data collation, giving updates on progress and sites needing assistance in enrolling patients, and visiting the sites to identify potential sources of confounders and variability. The candidate did all the pharmacometric analysis.

4.2 Patient population and studies used in this thesis

This thesis is based on the population pharmacokinetic and pharmacodynamic evaluation of data from the following studies:

4.2.1 Studies of pharmacokinetics of first-line antituberculosis drugs

The previously published studies used in this thesis described the plasma concentrations of rifampicin (Schaaf et al. 2009b), pyrazinamide (McIlleron et al. 2011) and isoniazid (Wilkins et al. 2011) in one cohort of 56 South African children with tuberculosis. These studies were further combined with another cohort describing the plasma concentrations of rifampicin, isoniazid and pyrazinamide in a cohort of 20 South African children (Thee et al. 2011). In addition, previously published models describing the population pharmacokinetics of rifampicin (Wilkins et al. 2008), pyrazinamide (Wilkins et al. 2006) and isoniazid (Wilkins et al. 2011) were used to derive reference exposures in adults.

4.2.2 Healthy male volunteer study

Thirty-five adult male healthy volunteers were enrolled in an open-label, randomized, sequential, five-way, crossover design study at Groote Schuur Hospital, Cape Town, South Africa. The aim of the study was to investigate the effect of four different meal types on the

population pharmacokinetics of rifapentine and its primary metabolite 25-desacetyl rifapentine.

4.2.3 RIFAQUIN clinical trial

The standard therapy of tuberculosis consists of 2 months of daily ethambutol, isoniazid, rifampicin, and pyrazinamide followed by 4 months of daily isoniazid and rifampicin (WHO 2013). The RIFAQUIN trial was a Phase 3 study (Jindani et al. 2013, RIFAQUIN 2008) which evaluated substitution (in the current standard therapy) of isoniazid with moxifloxacin in all phases in the tuberculosis treatment together with replacement of rifampicin with high dose intermittent rifapentine only in the continuation phase in standard tuberculosis treatment. The dosing schedules of two experimental arms of the RIFAQUIN study were: 1) 4-month regimen where isoniazid was replaced by 400 mg moxifloxacin daily for 2 months followed by 2 months of twice-weekly 400 mg moxifloxacin and 900mg rifapentine; 2) 6-month regimen where isoniazid was replaced by 400 mg moxifloxacin daily for 2 months followed by 4 months of once-weekly moxifloxacin and 1200mg rifapentine. The participants were followed up to 18 months with scheduled visits at 1, 2, 3, 4, 5, 6, 7, 8, 9, 10, 11, 12, 15, 18 months after starting therapy.

4.2.4 MIC of moxifloxacin and ofloxacin

The MICs for moxifloxacin and ofloxacin were obtained from a separate study comparing mutations in the quinolone resistance-determining region of the gyrA gene and flanking sequences with the MICs of ofloxacin and moxifloxacin for *M.tuberculosis* (Sirgel et al. 2012). The total number of isolates and the methodology on which how the MIC were determined is described in Section 4.4.

4.2.5 Population pharmacokinetics and pharmacodynamics of ofloxacin.

A population pharmacokinetic and pharmacodynamic model used in this thesis was previously published (Chigutsa et al. 2012). The study described ofloxacin pharmacokinetics in 56 South African patients being treated for multidrug-resistant tuberculosis and assessed the adequacy of ofloxacin drug exposure with respect to the probability of pharmacodynamic target attainment (PTA). The MIC distributions used were obtained from the study described in Section 4.2.4.

4.3 Plasma sample handling and drug concentration determination

In the studies of pharmacokinetics of first-line antituberculosis drugs, 56 children (Cohort 1), plasma concentrations of rifampicin, pyrazinamide, and isoniazid were determined by liquid chromatography tandem mass spectrometry, using an Applied Biosystems API 2000 (LC/MS/MS) as detailed previously (McIlleron et al. 2007, 2009, 2011). At each time after dose, the blood samples were immediately placed on ice, and centrifuged at 750 g for 10 min within 1 h of collection. Then 1 ml plasma from each sample was stored in polypropylene tubes at -80^{o}C and away from light until analysis was done. The analysis was done at the Division of Clinical Pharmacology, University of Cape Town, South Africa. The samples were processed with a protein precipitation method using 3 vol precipitation solution (acetonitrile) containing the appropriate internal standards. The internal standards used were rifapentine for rifampicin and sulfamethoxazole for isoniazid and pyrazinamide. The injection volume of plasma samples was 5 µL. For rifampicin, a gradient chromatographic separation was achieved with a mobile phase containing 10-90% acetonitrile in 0.1% formic acid, with 5 min run time delivered at 0.3 ml/min. For pyrazinamide and isoniazid, an isocratic elution was used; the mobile phase consisted of 80% acetonitrile in 0.1% formic acid. The selected

reaction monitoring of transitions of protonated molecular ions to product ions were: rifampicin *m/z* 823.5-791.4. For rifampicin, pyrazinamide and isoniazid, the linear ranges for standard curves were 0.1–30 mg/L, 0.2–70 mg/L and 0.1–15 mg/L. The lower limit of quantification (LLOQ) for both rifampicin and isoniazid was 0.1 mg/L and for pyrazinamide was 0.2 mg/L, and intra-and inter day assay variability was less than 10%. Data below LLOQ was handled using M3 method (Bergstrand & Karlsson 2009) where the likelihood of being below LLOQ was estimated.

In 20 children (Cohort 2), the drug determination was done at Stellenbosch University, South Africa. Rifampicin was determined by LC/MS/MS (Thee et al. 2011). However the difference with cohort 1 was that reaction monitoring of transitions of protonated molecular ions to product ions for rifampicin was at *m/z* 823.5-89.2. For isoniazid and pyrazinamide plasma concentrations were determined by high-performance liquid chromatography (HPLC) and ultra-violet (UV) detection (Thee et al. 2011). Isoniazid was derivatized with cinnamaldehyde, an approach shown to improve detection of isoniazid at 340 nm (Seifart et al. 1995). Pyrazinamide was measured directly at 269 nm. The lower limit of detection (LLOD) in Cohort 2, under which no concentration was reported, was 0.25, 0.5, and 0.15 mg/L for rifampicin, pyrazinamide and isoniazid, respectively.

In the healthy male volunteer study, plasma concentrations of rifapentine and 25-desacetyl rifapentine in health volunteer study were determined simultaneously using a validated high-performance tandem liquid chromatography (HPLC) method developed at the Division of Clinical Pharmacology, Cape Town, South Africa (Langdon et al. 2004). The drugs were extracted using 3 ml BondElut C18 solid phase extraction columns (Anatech, Sittard, The Netherlands). Detection of the drugs was at 270 nm with an isocratic flow rate of 2 ml/min using a mobile phase comprising of 50% acetonitrile and

0.1% trifluoroacetic acid in distilled water. The intra-day coefficients of variation ranges were 2.8% - 4.4% and 4.4% -5.6% for rifapentine and 25-desacetyl rifapentine, respectively. The coefficients of variation between the 3 days were 2.5% -4.7% and 4.0% -6.3% for rifapentine and 25-desacetyl rifapentine, respectively. The assay was validated over the concentration range of 0.6 to 30 mg/L for both parent and metabolite. Linearity values of the calibration curve (r^2) were 0.9975 and 0.9946 for rifapentine and 25-desacetyl rifapentine, respectively.

Plasma moxifloxacin concentrations from the RIFAQUIN study were determined using a validated liquid chromatography-tandem mass spectrometry assay method developed in the Division of Clinical Pharmacology, University of Cape Town. The samples were processed with a protein precipitation extraction method using 20 µl plasma with 200 µl precipitation solution (acetonitrile) containing the internal standard gatifloxacin at a concentration of 0.5 mg/L. Gradient chromatographic separation was achieved on a Phenomenex, Gemini-NX 5-µm C_{18} (110-A, 50-mm by 2-mm) analytical column using acetonitrile and 0.1% formic acid as the mobile phase and was delivered at a flow rate of 400 µl/min. An AB Sciex API 3200 Q-trap mass spectrometer was operated at unit resolution in the multiple-reaction-monitoring mode, monitoring the transition of the protonated molecular ions at *m/z* 402.1 to the product ions at *m/z* 358.3 for moxifloxacin and the protonated molecular ions at *m/z* 376.1 to the product ions at *m/z* 332.4 for the internal standard. The assay was validated over the concentration range of 0.063 mg/L to 16 mg/L. The accuracies for the moxifloxacin assay were 106.3%, 100.7%, and 102% at the low, medium, and high quality control (QC) levels, respectively, during interbatch validation. The precision (expressed as the percent coefficient of variation) was less than 5.5% at the low, medium, and high QC levels. The lower limit of quantification (LLOD) was 0.063 mg/L.

Plasma rifapentine concentrations from the RIFAQUIN study were determined with a validated liquid chromatography-tandem mass spectrometry assay developed in the Division of Clinical Pharmacology, University of Cape Town. Samples were processed with a protein precipitation extraction method using rifaximin as internal standard, followed by high performance liquid chromatography with MS/MS detection using an AB SCIEX API 3200 instrument. The analyte and internal standard were monitored at mass transitions of the protonated precursor ions m/z 877.3 and m/z 786.3 to the product ions m/z 845.4 and m/z 754.1 for rifapentine and rifaximin, respectively. The calibration curves fit quadratic (weighted by 1/concentration) regressions over the ranges 0.0390 – 40.0 mg/L for rifapentine. The accuracies for the moxifloxacin assay were 103.9%, 102.8%, and 97.5% at the low, medium, and high QC levels, respectively, during interbatch validation. The LLOQ was 0.156 mg/L.

4.4 Determination of moxifloxacin and ofloxacin MICs in patient sputum isolates

The *M.tuberculosis* isolates were obtained from a separate study, in patients with drug-resistant tuberculosis in the Western Cape, South Africa during the period 2007–2009 (Sirgel et al. 2012). The isolates had previously been subjected to routine drug susceptibility testing on Middlebrook 7H11 agar and had known IS6110 restriction fragment length polymorphism and spoligotype patterns. As previously described (Donald et al. 2001), the MICs were determined by quantitative drug susceptibility testing using an automated BACTEC mycobacterial growth indicator tube (MGIT) 960 instrument (BD Bioscience, Sparks, MD, USA) equipped with TBeXiST and EpiCentreTM V5.75A software (BD Bioscience, Erembodegem, Belgium). The concentrations tested were 0.5, 1.0, 2.0, 4.0, 6.0, 8.0, 10, 50.0 mg/L for ofloxacin and 0.125, 0.25, 0.5, 1.0, 2.0, 4.0, 6.0, 8.0, 10.0 mg/L for moxifloxacin (24). The 0.25 mg/L

and 2.0 mg/L concentrations of moxifloxacin and ofloxacin were used as susceptibility breakpoints to differentiate between susceptible and resistant strains as suggested by WHO (WHO 2008b).

4.5 General pharmacometric methodology

The general methods used in data analysis which forms the basis of this PhD thesis are described in this section.

4.5.1 Classification NAT2 polymorphism

On the basis of analysis of genetic polymorphisms of the NAT2 gene, the children were categorized as slow, intermediate, or fast acetylator genotypes for acetylation of isoniazid. The methods used in classification of NAT2 genotypes have been previously described for cohort 1 comprised of 56 South African children with tuberculosis (Schaaf et al. 2005) and cohort 2 comprised of 20 children (Thee et al. 2011). In both cohorts, NAT2 genotyping and categorization of alleles was done at Stellenbosch University, South Africa (Schaaf et al. 2005). The NAT2 genotypes were analyzed using polymerase chain reaction (PCR) and restricted fragment length polymorphism. Separate PCR aliquots were restricted with the *Msp*I, *Fok*I, *Kpn*I, *Taq*I, *Dde*I, and *Bam*HI restriction enzymes (according to the manufacturer's recommendations) to delineate the polymorphisms at nucleotide positions 191, 282, 481, 590, 803, and 857, respectively. The standard PCR mixture contained two primer sets, primer set I [5′-^{876nt}TTAGAGGCTATTTTTGATCACA^{897nt}-3′and 5′^{081nt}ATGTAATTCCTGCCGTCAG^{1063nt}-3′], which initiates amplification in the case of the 341C allele (a 187bp product), and primer set II [5′-^{1045nt}TTCTCCTGCAGGTGAC CAT^{1063NT}-3′ and 5′-^{1368nt}AAGATGTTGGAGA

CGTCTGC^{1349nt}-3′], which only amplifies in the case of the 341T allelic sequence (a 323bp product). In addition, outermost primers [^{876nt}TTAGAG GCTATTTTTGATCACA^{897nt} and^{1368nt}AAGATGTTGGAGACGTCTGC^{1349nt}] also amplify a gene specific PCR product (475bp) in the reaction mixture which serves as an internal amplification control. After analysing the genomic DNA for the *NAT2*5, 2*6, 2*7, 2*12, 2*13,* and *2*14* alleles, the alleles were assigned into acetylator status of isoniazid according to the Vatsis nomenclature (Vatsis et al. 1995). The wild type fast allele (F) is assigned as *NAT2*4, 2*12,* or *2*13.* These alleles confer normal enzyme activity on the NAT2 protein. The mutant slow alleles (S), classified as *NAT2*5, 2*6, 2*7,* and *2*14* in humans, confer a decreased enzyme activity on the NAT2 protein (Vatsis et al. 1995). In cohort 2, NAT2 genotyping was done at Stellenbosch University.The genomic DNA was analysed for NAT2*5, NAT2*6, NAT2*7, NAT2*12, NAT2*13, and NAT2*14 alleles. The assignment of these alleles into acetylator category was done according to the NAT2 nomenclature. The NAT2*4 allele was designated the wild-type, which together with the NAT2*12 and NAT2*13 alleles, were defined as the rapid-acetylator (F) status. The slow acetylator is defined by decreased or impaired NAT2 enzyme activity which is encoded by the mutant alleles NAT2*5, NAT2*6, NAT2*7, and NAT2*14. Hence, individuals were classified as homozygous fast (FF), heterozygous intermediate (FS), or homozygous slow (SS) acetylators, based on the combination of alleles detected.

4.5.2 Calculation of arm muscle area and arm fat area in children (Lee 2001)

Upper Arm Area (AA) was calculated as:

$$AA\ (mm^2) = \frac{MUAC^2}{4 \times \pi}$$

where MUAC is mid upper arm circumference (mm) and $\pi = 3.14$.

Arm Muscle Area (AMA) was calculated as:

$$AMA\ (mm^2) = \frac{[MUAC - (\pi \times TSF)]^2}{4 \times \pi}$$

where TSF is skinfold thickness.

Then Arm Fat Area (AFA) was calculated as:

$$AFA\ (mm^2) = AA\ (mm^2) - AMA\ (mm^2)$$

The AMA values were derived from percentiles from the United States Health and Nutrition Examination Survey I from 1971 to 1974 (Heymsfield et al. 1979), and the z-scores were derived from National Center for Health Statistics/Centers for Disease Control and Prevention/World Health Organization (NCHS/CDC/WHO) international reference standards (Gibson 2005).

4.5.3 Population pharmacokinetic analysis

The overall methodology used for the pharmacokinetic analysis is described in this section applied to all the plasma drug concentration-time data.

The concentration-time data for each drug were analyzed separately using a non-linear mixed-effects approach. Non-linear mixed effects modeling implemented in the NONMEM® software program (Icon Development Solutions, Ellicott City, MD, USA) (Beal et al. 2009) was used for analysis. NONMEM version 7.2 was used.The program was operated on a cluster of LINUX machines using an Intel Fortran Compiler. The execution of runs was through Perl-speaks-NONMEM (PsN) (Lindbom et al. 2005) and graphical diagnostics were created using Xpose 4 (Jonsson & Karlsson 1999) and Census® (Wilkins 2005).

4.5.3.1 Model building and validation

Estimation of typical population pharmacokinetic parameters, along with their random inter-individual (IIV) and inter-occasional (IOV) variability was performed using the first-order conditional estimation method with ε-η interaction (FOCE INTER) (Karlsson & Sheiner 1993). The general approach included building the base model with all the variabilities included and testing for significant relationships between parameters and covariate. Various pharmacokinetic models, including one or two compartments with first-order absorption and first- order elimination (Holford et al. 1992), incorporating either lag times (to describe the delay in the appearance of drug in plasma) or transit absorption compartments (Rousseau et al. 2004, Savic et al. 2007), time-varying clearance (Langdon et al. 2005), and enterohepatic recirculation (Roberts et al. 2002), were fitted to the data during model development. Use of additive and proportional error terms was also investigated.

Time-varying clearance was introduced into the model as:

$$CL_i = TV(\frac{CL_1}{F}).\exp\left(\eta_{i,}^{\frac{CL_1}{F}} + \kappa_i^{\frac{CL_1}{F}}\right).(1 - mpast(i)) + TV(\frac{CL_2}{F}).\exp\left(\eta_i^{\frac{CL_2}{F}} + \kappa_i^{\frac{CL_2}{F}}\right).mpast(i)$$

where CL_i is the oral clearance for the *i*th individual, $TV(\frac{CL_1}{F})$ is the typical oral clearance which later changes to $TV(\frac{CL_2}{F})$ at model event time (MTIME), $mpast(i)$ remains zero until MTIME when it changes to 1, $\eta_i^{\frac{CL_1}{F}}$ represents the IIV and $\kappa_i^{\frac{CL_1}{F}}$ represents the IOV.

In general, if there was data below lower limit of quantification (LLOQ) with the values reported, where appropriate was handled by fixing the error structure to additive with size LLOQ/2, to include these samples in the fit while accounting for the lower precision. In some cases where some LLOQ values were missing in one cohort, LLOQ values were imputed to lower limit of detection (LLOD)/2 reported from the laboratory, discarding consecutive undetectable concentrations in a series. However, if the LLOQ values were not reported at all, the M3 method (Beal 2001) was preferred, where the likelihood of being below LLOQ was estimated.

Model discrimination was based on graphical assessment of conditional weighted residuals (CWRES) versus time, basic goodness of fit (GOF) plots, and changes in the NONMEM OFV during model development. OFV is equal to approximately $-2 \times$ log likelihood, and ΔOFV is assumed to be chi squared distributed. Statistical significance was set at 5% (ΔOFV > 3.84) for a single degree of freedom (i.e., addition of one model parameter) and at 1% significance level (ΔOFV > 6.63) for deletion of one parameter (Wahlby et al. 2001). Assessment of IIV estimates and their corresponding standard errors (SE) was done to check for η shrinkage since η and ε shrinkage values above 30% result in a model with a low power to detect model and residual error misspecification, which may hide true relationships (Karlsson & Savic 2007). Precision of parameter estimates as provided by the covariance step (if successfully completed), and visual predictive checks (VPC) (Holford 2005) were also considered during model selection. In cases where the covariance step failed to run, measures of parameter uncertainty were obtained through a nonparametric bootstrap of the final model and the number of bootstrap replicates used was 200. From the VPC, the 2.5^{th}, 50^{th} and 97.5^{th} percentile from the observed data should lie within the 95% confidence interval from the model prediction.

Potential covariate relationships were identified by clinical and statistical significance. The covariate relationships were tested in the model by stepwise addition (forward step) using a ΔOFV of ≥ 3.84 ($p \leq 0.05$) as the cut-off for inclusion, followed by stepwise deletion (backward step) using ΔOFV of ≥ 6.83 ($p \leq 0.01$) as a requisite for covariate retention. Missing continuous covariate data were replaced with the individual information from the other dosing and sampling occasion, if available. The covariate analysis using the basic models was performed via forward addition and backward elimination using stepwise covariate model (SCM) building as implemented in PsN. Using SCM, one model for each relevant parameter-covariate relationship is prepared and tested in a univariate manner. In the first step the model that gives the best fit of the data according to some criteria is retained and taken forward to the next step. In the subsequent steps all remaining parameter-covariate combinations are tested until no more covariates meet the criteria for being included into the model. The forward selection can be followed by backward elimination, which proceeds as the forward selection and backwards using ΔOFV cut-offs mentioned above.

The effect of continuous covariates was parameterized as shown in equation below:

$$PAR = \theta_P \times (1 + \theta_{cov} \times (COV - COV_{med}))$$

where θ_P is the parameter (PAR) estimate in a typical individual (a median covariate value of COV_{med}), while θ_{cov} is the fractional change in PAR with each unit change in the covariate (COV) from COV_{med}.

For categorical covariates, such as acetylator genotype, a separate typical value for the parameter under test was estimated in each group. For the categorical covariates (sex and HIV status), the covariate model was expressed as a fractional change (θ_{cov}) from the estimate for a typical value (θ_P) due to covariate (COV) using the following equation:

$$PAR = \theta_P \times (1 + \theta_{cov} \times (COV))$$

COV takes the values between 0 and 1. Total body weight (WT) where relevant was included through allometric scaling was applied on oral clearance (CL) and apparent volume of distribution in plasma (Vc) according to Anderson and Holford (Anderson & Holford 2008) was used and scaled as shown below:

$$CL_i = CLstd \cdot (WT_i/WTstd)^{0.75}$$

$$Vc_i = Vstd \cdot (WT_i/ WTstd)^{1}$$

where CL_i is the scaled typical value of CL/F for individual i, CLstd is its typical CL for an individual of median weight (WTstd) in the patient population. A similar notation applies to Vc_i. In the case of a two-compartment model, allometric scaling was also applied on inter-compartmental clearance (Q) similar to CL/F and on apparent peripheral volume of distribution (Vp) similar to Vc. Normal fat mass (NFM), fat-free mass (FFM) and fat mass (FAT) were tested through allometric scaling instead of total body weight.

The FFM was calculated as follows according to Janmahasatien et al (Janmahasatian et al. 2005):

$$FFM = \frac{WHSMAX_{MAX} \times HT^2 \times WT}{WHS_{50} \times HT^2 + WT}$$

where for females $WHSMAX_{MAX}$ = 37.99 and WHS_{50}=35.98 and for males $WHSMAX_{MAX}$ = 42.92 and WHS_{50}=30.93, and HT is height (m) and WT is total body weight (kg). Then $NFM = FFM + ffat(WT - FFM)$. $ffat$ is parameter-specific fat fraction associated with size. If $ffat$ is 1 then WT is used for allometric scaling, if $ffat$ is zero (0) then FFM is used.

After allometric scaling was included, the need for including maturation models following the approach previously described by Anderson and Holford (Anderson & Holford 2009) was evaluated. The maturation factor (MF) was calculated as:

$$MF = 1/ [1+ (PMA/TM_{50})^{-Hill}]$$

where PMA is age derived by adding 36 weeks to post-natal age, assuming no premature birth. TM_{50} is the age at which maturation reaches 50% of the final value, and Hill is the coefficient that regulates the rate of onset of the maturation. Models with and without the Hill factor fixed to 1 were tested.

In cases where the drug has a metabolite, the above procedure was also applied to build the metabolite model. The exposures of each drug were obtained from NONMEM using the $ABBREVIATED COMRES when required.

4.5.3.2 Parametric survival analysis

The hazard of a treatment failure at time *t* was modeled as: h(t)=Pr(t≤T<(t+dt|T>t); where Pr is the probability of having an event within a time interval dt, give the scenario that that the event did not occur before time *t*. The probability of having favorable outcome was modeled as a function of the cumulative hazard of an unfavorable event (integral of the hazard with respect to time) for each day from start of observation using the following function: $S(t) = e^{-\int_0^t h(t)dt}$. The probability density function (pdf) of having an event at time *t* was modeled as: pdf = h(t) x S(t). The baseline survival models tested where parameterized as follows (Weibull function) as follows: $S(t) = e^{(\lambda t)^{\alpha}}$ where λ is the baseline hazard and α is the shape parameter. If α =1, then the hazard in

constant over time, if $\alpha < 1$, then hazard decreases with time and if $\alpha > 1$ the hazard increases with time.

---

5 Population pharmacokinetics of rifampicin, pyrazinamide and isoniazid in children with tuberculosis, *in silico* evaluation of currently recommended doses

5.1 Introduction

Tuberculosis is the most frequent infectious cause of death worldwide with high impact in developing countries (WHO 2013). In settings with high disease burden such as South Africa, children comprise 15-20% of tuberculosis cases (Marais et al. 2006). Young children (<5 years of age) and children infected with HIV are prone to rapid progression to tuberculosis disease following infection, and frequently experience severe forms of tuberculosis including disseminated disease and meningitis (Marais et al. 2006). Isoniazid and rifampicin are important for their bactericidal activity against metabolically active *M.tuberculosis*. The sterilizing activities of pyrazinamide and rifampicin prevent relapse of disease after treatment (Hu et al. 2006, Steele & Des Prez 1988). Isoniazid plays an important role in preventing the development of resistance to companion drugs such as rifampicin (Mitchison 2000). Dosages of rifampicin higher than those currently employed have been suggested to improve efficacy (Gumbo et al. 2007a).

Until recently, the daily dosages of first-line antituberculosis drugs recommended in children were derived from adult dosage based on the assumption that the same dose per kg is appropriate across all ages of patients. Even though rifampicin, isoniazid and pyrazinamide have been available for many years, the limited pharmacokinetic information in children suggests that young children receiving adult-derived dosages have drug exposures lower than adults (McIlleron et al. 2009, Schaaf et al. 2005, 2009b). In children, factors such as maturation of metabolizing enzymes and transporters, body composition, organ function, nutritional status, and the pathophysiology of severe forms

of tuberculosis may contribute to changes in pharmacokinetics, drug response and toxicity (Kearns et al. 2003). Previous studies have reported reduced tuberculosis drug concentrations in adults with HIV infection (Gurumurthy et al. 2004a) but the effect of HIV infection on the pharmacokinetics of tuberculosis drugs has not been adequately evaluated in children. The WHO has recently recommended increased dosage some of the first-line antituberculosis drugs for children (WHO 2010), which are to be implemented using dispersible FDC tablets for paediatric use, manufactured according to newly recommended specifications, with each tablet containing 50 mg isoniazid, 75 mg rifampicin and 150 mg pyrazinamide (WHO 2012c).

The aim of this study was to describe the population pharmacokinetics of rifampicin, pyrazinamide, and isoniazid in non-linear mixed-effects models, using previously published data from children with tuberculosis aged 2 months to 11.3 years who were given a wide range of dosages (McIlleron et al. 2009, 2011; Schaaf et al. 2009b, Thee et al. 2011). In addition, use final models to predict steady state area AUC and Cmax in a paediatric population and compared them with the corresponding pharmacokinetic measures in ethnically similar adults with tuberculosis.

5.2 Setting and Study Design

Pharmacokinetic data from studies of pharmacokinetics of first-line antituberculosis drugs were used (Section 4.2.1). The studies described the pharmacokinetics of rifampicin, pyrazinamide and isoniazid in children with tuberculosis. A total of 76 children were used in this analysis. On the basis of analysis of genetic polymorphisms determined on NAT2 gene, the children were categorized as slow, intermediate, or fast acetylator genotypes for acetylation of isoniazid. The methods used in classification of NAT2 genotypes have been previously described under Methodology section 4.5.1 for

cohort 1 (Schaaf et al. 2005) and cohort 2 (Thee et al. 2011). The demographic, clinical characteristics and doses given of 76 children are summarized in Table 5.1.

Table 5.1: Demographic and clinical characteristics of children with tuberculosis

Covariate	**Cohort 1[a]**	**Cohort 2[a]**	**Combined**
Number of patients	56	20	76
Sex (M/F)	29/27	11/9	40/36
Genotype (S/I/F/M_s)	20/24/8/4	8/4/8/0	28/28/16/4
HIV positive (M/F)	22 (12/10)	5 (2/3)	27 (14/13)
Age (yrs)	3.22 (0.598, 10.9)	1.10 (0.321, 1.99)	2.17 (0.417, 10.7)
Weight (kg)	12.5 (4.87, 26.9)	7.80 (4.12, 12.8)	10.5 (4.90, 21.8)
RIF dose 1st PK (mg/kg)	9.54 (6.70, 13.3)	10.1 (9.0, 10.5)	9.71 (7.07, 13.2)
RIF dose 2nd PK (mg/kg)	9.57 (5.46, 16.0)	15.4 (10.4, 15.8)	10.3 (6.37, 15.9)
PZA dose 1st PK (mg/kg)	22.7 (15.9, 26.7)	25.2 (22.5, 26.5)	24.6 (17.6, 26.5)
PZA dose 2nd PK (mg/kg)	22.2 (12.2, 26.3)	36.2 (33.4, 39.5)	33.7 (15.6, 39.1)
INH dose 1st PK (mg/kg)	4.92 (3.35, 12.8)	5.04 (4.50, 5.36)	5.03 (3.56, 12.1)
INH dose 2nd PK (mg/kg)	4.95 (2.36, 16.0)	10.2 (8.74, 10.8)	9.77 (2.73, 13.3)

M/F, males/females; M_s, missing covariate data; S/I/F, slow/intermediate/fast arylamine N-acetyltransferase acetylators; RIF stands for rifampicin; PZA for pyrazinamide; INH for isoniazid; 1st PK and 2nd PK stand for first and second PK sampling occasion, respectively; [a] Continuous variable reported as median (2.5th percentile, 97.5th percentile), while the size of each group is reported for categorical covariates (McIlleron et al. 2009, 2011; Schaaf et al. 2009b, Thee et al. 2011).

Daily doses of rifampicin and isoniazid were given for 6 months with pyrazinamide added for the first two months. Dispersible FDC tablets formulated for children were used (McIlleron et al. 2009, 2011; Schaaf et al. 2009b, Thee et al. 2011). At each sampling occasion venous blood was drawn at 0.75, 1.5, 3, 4, and 6 h post-dose. Cohort 2 underwent pharmacokinetic sampling 2 weeks or more after initiation of antituberculosis therapy and sampling was repeated one week later, with samples drawn pre-dose and at 0.5, 1.5, 3, and 5 h after the dose. Plasma rifampicin, pyrazinamide and isoniazid concentrations for each cohort were determined as detailed under section 4.3.

5.2.1 Pharmacokinetic data analysis

The methodology applied for model building has been described in section 4.5.3. In all models, allometric scaling was applied to CL/F and apparent volume of distribution in Vc according to Anderson and Holford (Anderson & Holford 2008). As a reference, the median body weight of 12.5 kg from cohort 1 (Table 5.1) was used and scaled as shown below:

$$CL_i = CLstd \cdot (WT_i/12.5)^{0.75}$$

$$Vc_i = Vstd \cdot (WT_i/12.5)^{1}$$

where CL_i is the scaled typical value of CL/F for individual *i*, CLstd is its typical CL for an individual of median weight of 12.5 kg in the patient population. A similar notation applies to Vc_i. In the case of a two-compartment model, allometric scaling was also applied on Q (similar to CL_i) and on Vp (similar to Vc_i). After allometric scaling was included, the need for including maturation models following the approach previously described by Anderson and Holford (Anderson & Holford 2009) was evaluated. The MF was calculated as:

$$MF = 1/ [1+ (PMA/TM_{50})^{-Hill}]$$

where PMA is age derived by adding 36 weeks to post-natal age, assuming no premature birth. TM_{50} is the age at which maturation reaches 50% of the final value, and Hill is the coefficient that regulates the rate of onset of the maturation. Models with and without the Hill factor fixed to 1 were tested.

The structural models tested included one- and two-compartment with first-order elimination. Different absorption models were explored such as first-order absorption or a sequence of zero- and first-order absorption incorporating either lag times or transit compartment absorption (Savic et al. 2007, Wilkins et al. 2008). The effect of a dose on

the pharmacokinetic parameters was also tested. For relative bioavailability (F), first-order absorption rate constant (ka), mean transit time (MTT) and CL of rifampicin (a substrate of polymorphic OATP1B1 transporter (Chigutsa et al. 2011) and isoniazid (a substrate of polymorphic metabolizing enzyme NAT2), the possibility of subpopulations having different parameter estimates was tested using mixture models. A log-normal model for IIV and IOV was used and shrinkage in the post-hoc estimates was derived. Additive and/or proportional models for the residual unexplained variability (RUV) were evaluated. In Cohort 1, the drug concentrations reported as below the LLOQ were 0.6%, 0%, and 3.4% for rifampicin, pyrazinamide, and isoniazid, respectively. In Cohort 2, the values below the LLOD were 19%, 5.5%, and 17.1% for rifampicin, pyrazinamide, and isoniazid, respectively. Additionally, 4.5%, 3%, and 24.1% of the concentrations of rifampicin, pyrazinamide, and isoniazid, respectively, were in the "low precision" range of the assay, but above LLOD. The larger proportion of low concentrations in Cohort 2 is partly due to the collection of a pre-dose sample. All the data below LLOQ in Cohort 1 was handled by fixing the error structure to additive with size LLOQ/2, to include these samples in the fit while accounting for the lower precision. The lower limit of detection (LLOD) in Cohort 2, under which no concentration was reported, was 0.25, 0.5 and 0.15 mg/L for rifampicin, pyrazinamide and isoniazid, respectively. Moreover, the assay could not guarantee 5% precision between the LLOD (0.75, 1.5 and 1 mg/L for rifampicin, pyrazinamide and isoniazid, respectively) and LLOQ values. The effect of age, sex and HIV infection was tested on F, CL, Vc, Vp, ka and MTT. Arm muscle area (AMA) was tested as a predictor for CL, Vc and Vp while albumin and other nutritional status measures (weight-for-age, weight-for-height and height-for-age z-scores) were tested on F, CL, Vc and Vp.

The AMA was calculated for each child using formula detailed in Section 4.5.2. The reference AMA values were derived from percentiles from the United States Health and Nutrition Examination Survey I from 1971 to 1974 (Heymsfield et al. 1979), and the z-scores were derived from National Center for Health Statistics/Centers for Disease Control and Prevention/World Health Organization (NCHS/CDC/WHO) international reference standards (Gibson 2005). Missing continuous covariate data were replaced with the individual information from the other dosing and sampling occasion, if available. Otherwise, median values from the cohort were used. Missing categorical covariates were replaced with the most common category, except for acetylator genotype. For the missing genotype data (4 individuals), a mixture model was used. The likelihood of belonging to each acetylator status was fixed to the frequency observed in the subjects for whom the information was available.

The effect of continuous and categorical covariates, and model validation were evaluated as described under section 4.5.3.1. Model selection was based on VPC (Holford 2005), CWRES versus time, GOF plots, and ΔOFV. The covariate relationships were tested in the model by stepwise addition (forward step) using a ΔOFV of ≥ 3.84 ($p \leq 0.05$) as the cut-off for inclusion, followed by stepwise deletion (backward step) using ΔOFV of ≥ 6.83 ($p \leq 0.01$) as a requisite for covariate retention.

5.2.2 Simulations

Monte Carlo simulations were used to predict the model-based AUC and Cmax in a paediatric population should they be dosed in pragmatic weight bands (adhering as closely as possible to the revised guidelines in dose per unit weight) using 1 to 4 undivided tablets of a FDC with the newly recommended specifications. Reference AUC and Cmax values in adults with tuberculosis given the doses currently recommended for

adults by the WHO (WHO 2003), were derived using previously published models (Wilkins et al. 2006, 2008, 2011).

Using Monte Carlo simulations, the final models were used to simulate steady state AUC and Cmax for children using pragmatic weight bands (adhering as closely as possible to the revised guidelines in dose per unit weight) (WHO 2010) using 1 to 4 undivided tablets of a FDC with the newly recommended specifications (i.e. 75/50/150 mg rifampicin/isoniazid/pyrazinamide in each FDC tablet) (WHO 2012c). AUC and Cmax were predicted for children weighing 4.0-7.9, 8.0-11.9, 12.0-15.9 and 16.0-24.0 kg receiving respective daily doses of 1, 2, 3 and 4 FDCs. Individual weight and age values were available from historical data of 246 South African children with tuberculosis, 72% infected with HIV (2% with HIV status unknown), and 54% males. Pooling these with the present data from the two cohorts (Table 5.1), we obtained a dataset of baseline values for 312 children. The pharmacokinetic models were applied (1000 repetitions) to this in-silico population, using the WHO-recommended dosing guidelines, and AUC and Cmax values were collected for each weight band. To obtain reference values for comparison, previously published pharmacokinetic models (Wilkins et al. 2006, 2008, 2011) from an ethnically similar population of adult patients were used to simulate AUC and Cmax ranges using the current WHO-recommended dosing guidelines for adults (WHO 2008c). The respective daily doses used for simulations in adults weighing 30.0-37.9, 38.0-54.9, 55.0-69.9, and ≥ 70 kg were: 300, 450, 600 and 750 mg for rifampicin; 800, 1200, 1600 and 2000 mg for pyrazinamide; and 150, 225, 300 and 375 mg for isoniazid.

5.3 Results

Rifampicin. A total of 629 concentration-time data points were available for 67 children (Schaaf et al. 2009b, Thee et al. 2011). 9 Children were resistant to rifampicin. The final

pharmacokinetic model for rifampicin was a one-compartment model with transit compartments absorption (Savic et al. 2007), and first-order elimination. The parameter estimates of the final model are shown in Table 5.2.

The absorption transit model was simplified by fixing ka to the same value as the first-order transit rate constant (ktr), since the two were not found significantly different. HIV status and albumin levels had no influence on the pharmacokinetics of rifampicin. Age maturation was supported on CL and MTT and resulted in a 23 point improvement in OFV, explaining 16 % IIV in CL and 17 % IOV in MTT (no IIV on MTT was present in the model). TM_{50} was estimated to be 58.2 weeks which is 22.2 weeks (0.43 years) after birth for both CL and MTT. The estimate of typical ktr was 7.8 h^{-1}. The proportional change of each parameter with post-natal age is shown in Figure 5.1.

Table 5.2: Parameter estimates of the final rifampicin pharmacokinetic model

Parameter	Typical value (RSE[%])[a]	IIV[b] (RSE[%])[a]	IOV[c] (RSE[%])[a]
CL_{std} (L/h)	8.15 (9.00)	32.6 (27.7)	25.1 (20.0)
Vc_{std} (L)	16.2 (10.2)	43.4 (19.8)	
MTT (h)	1.04 (6.10)		40.6 (8.60)
NN	8.04 (11.9)		
F (%)	1 (fixed)		48.1 (12.7)
TM_{50} (weeks)	58.2 (9.00)		
Hill	2.21 (11.7)		
Additive error, Cohort 1 (mg/L)	0.122 (24.6)		
Additive error, Cohort 2 (mg/L)	0.630 (30.3)		
Proportional error, (%)	23.4 (4.50)		

CL_{std} and Vc_{std} are oral clearance and apparent volume of distribution, respectively. The values reported refer to a 12.5 kg child and for CL at full maturation. MTT, absorption mean transit time, value at full maturation; NN, number of transit compartments; F, relative bioavailability. TM_{50}, post-menstrual age at which 50% of clearance and mean transit time maturation is achieved; Hill, steepness of the maturation function; [a]RSE, relative standard error reported on the approximate standard deviation scale; [b]IIV, inter-individual variability expressed as percent coefficient of variation (% CV); [c]IOV, inter-occasional variability expressed as % CV.

The final model included IIV, expressed as percent coefficient of variation (% CV), on CL (33%) and Vc (43%), while IOV was significant on CL (25%), F (48%) and MTT (40%). The residual error model had both additive (0.122 mg/L for Cohort 1 and 0.63 mg/L for Cohort 2) and proportional terms (23% for both cohorts). The final pharmacokinetic model described the data well, as shown in the VPC (Figure 5.2). When scaled to a 70 kg individual, the typical values for CL and Vc were 29.7 L/h and 90.7 L, respectively. The run record and control stream of final rifampicin pharmacokinetic model are shown in Appendix 1.

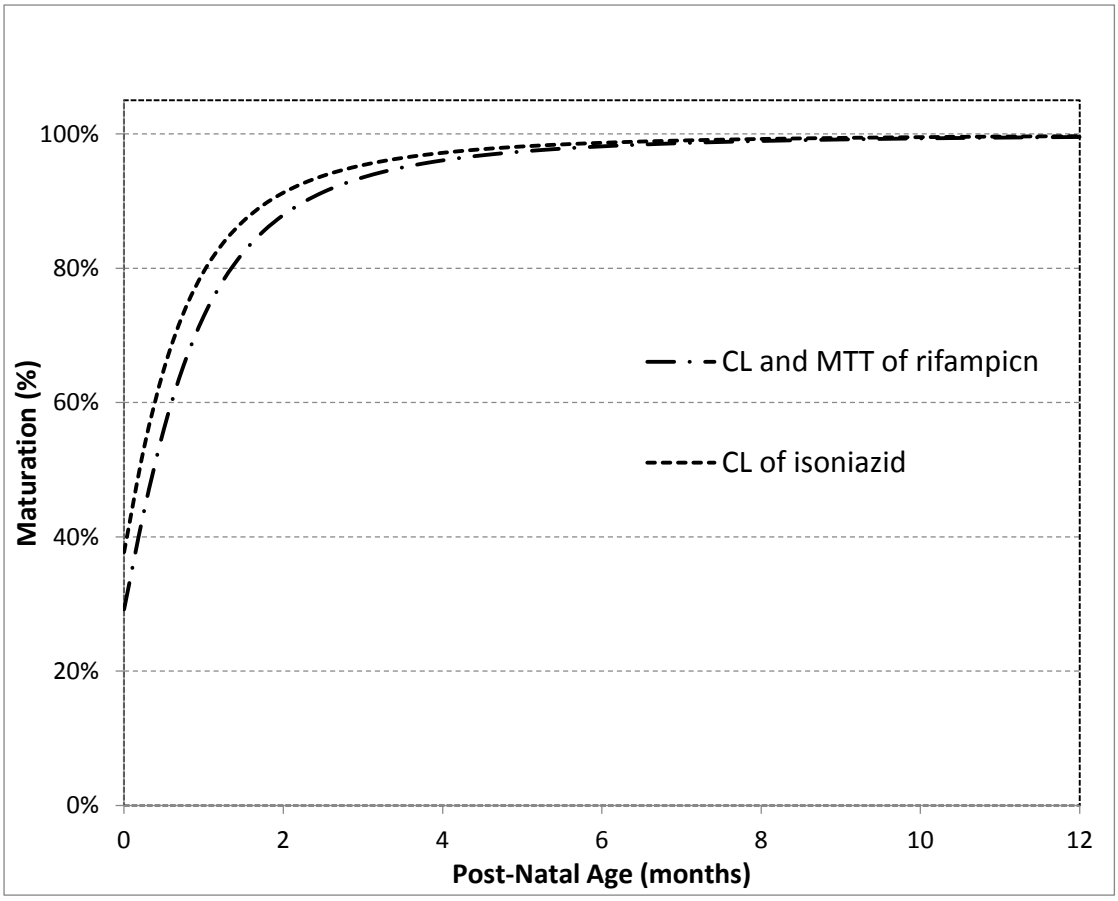

Figure 5.1: Maturation of oral clearance (CL) and mean transit time (MTT) of rifampicin and CL/F of isoniazid in a typical patient with post-natal age. The plot is not adjusted for covariate effects or allometric scaling.

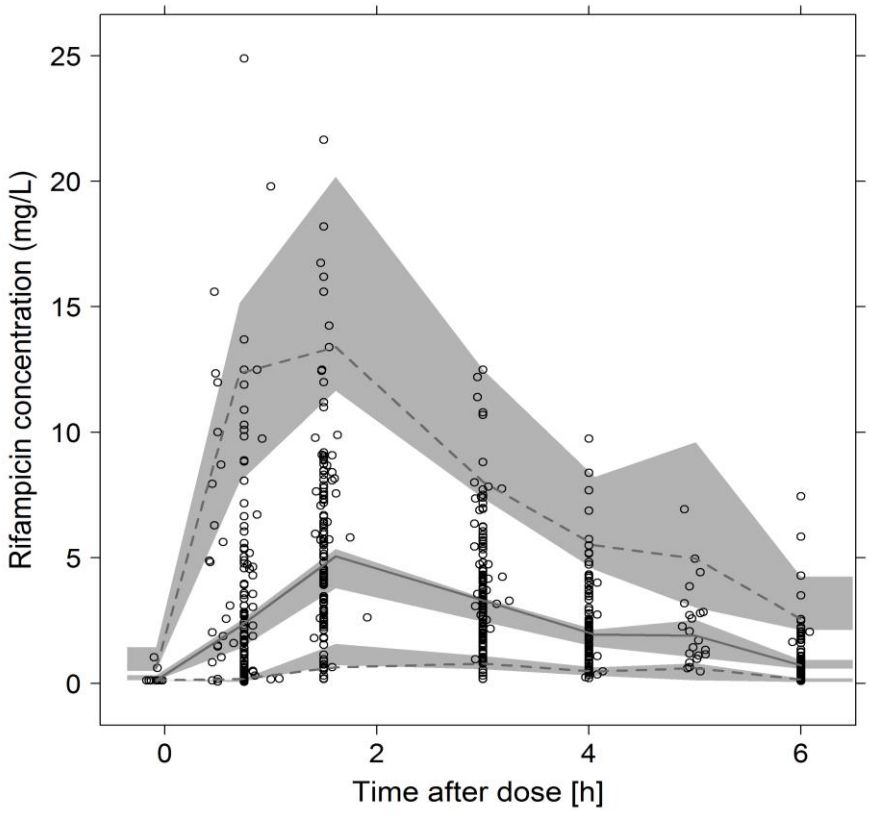

Figure 5.2: Visual predictive checks for the final model of rifampicin. The lower, middle and upper lines (dotted/solid) are the 5th, median, and 95th percentiles of the observed data, respectively. The shaded areas are the 95% confidence intervals for the 5th percentile, median and the 95th percentile of the simulated data.

Pyrazinamide. A total of 518 concentration-time data points were available in 55 children (McIlleron et al. 2011, Thee et al. 2011). The final pharmacokinetic model for pyrazinamide was a one-compartment distribution model with absorption transit compartments, first-order absorption and elimination. Final parameter estimates are shown in Table 5.3. No significant covariate relationships were supported by the data. IIV, expressed as percent coefficient of variation (% CV), was supported on CL (27%), while IOV was significant for CL (26%), ka (86%), F (25%) and MTT (112%). The residual error model was proportional (10% for Cohort 1 and 6% for Cohort 2). The VPC for the final pyrazinamide model is displayed on Figure 5.3, showing that the final model described the data well. The typical values of CL and Vc were 3.9 L/h and 54 L,

respectively, when scaled to a 70 kg individual. The run record and control stream of final pyrazinamide pharmacokinetic model are shown in Appendix 2.

Table 5.3: Parameter estimates of the final pyrazinamide pharmacokinetic model

Parameter	Typical value (RSE [%])[a]	IIV[b] (RSE [%])[a]	IOV[c] (RSE [%])[a]
CL_{std} (L/h)	1.08 (5.60)	27.1 (16.3)	25.5 (11.3)
Vc_{std} (L)	9.64 (2.60)		
k_a (h^{-1})	4.48 (6.10)		86.4 (14.6)
MTT (h)	0.10 (17.7)		112 (22.5)
NN	3.94 (8.00)		
F (%)	1 (fixed)		24.7 (8.40)
Proportional error, Cohort 1 (%)	10.0 (4.90)		
Proportional error, Cohort 2 (%)	5.53 (7.20)		

CL_{std} and Vc_{std} are oral clearance and apparent volume of distribution, respectively. The values reported refer to a 12.5 kg child. k_a, first-order absorption rate constant; MTT, absorption mean transit time, value at full maturation; NN, number of transit compartments; F, relative bioavailability; [a]RSE, relative standard error reported on the approximate standard deviation scale; [b]IIV, inter-individual variability expressed as percent coefficient of variation (% CV); [c]IOV, inter-occasional variability expressed as % CV.

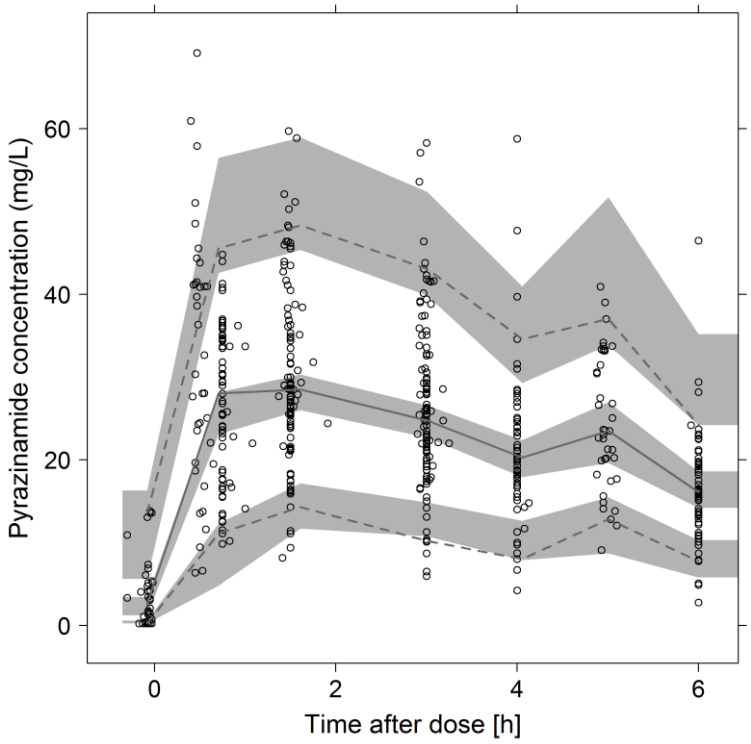

Figure 5.3: Visual predictive checks for the final model of pyrazinamide. The lower, middle and upper lines (dotted/solid) are the 5th, median, and 95th percentiles of the observed data, respectively. The shaded areas are the 95% confidence intervals for the 5th percentile, median and the 95th percentile of the simulated data.

Isoniazid. A total of 715 concentration-time data points were available in all 76 children (McIlleron et al. 2009, Thee et al. 2011). A two-compartment distribution model with absorption transit compartments and first-order elimination best described the pharmacokinetics of isoniazid. Final parameter estimates are shown in Table 5.4.

Table 5.4: Final parameter estimates for isoniazid pharmacokinetics

Parameter	Typical value (RSE [%])[a]	IIV[b] (RSE [%])[a]	IOV[c] (RSE [%])[a]
$CL_{std.sa}$ (L/h)[d]	4.44 (11.6)	25.1 (12.3)	
$CL_{std.ia}$(L/h)[d]	8.94 (13.1)	25.1 (12.3)	
$CL_{std.fa}$(L/h)[d]	11.3 (14.8)	25.1 (12.3)	
Vc_{std} (L)[d]	11.0 (10.2)		
k_a (h^{-1})	2.47 (12.8)		61.6 (12.4)
MTT (h)	0.179 (10.9)		93.9 (17.9)
NN	4 (fixed)		
Q_{std} (L/h)[d]	2.00 (26.3)		
Vp_{std} (L)[d]	5.03 (33.4)		
F_{sa}	1 (fixed)		39.7 (5.80)
$F_{im/fa}$	0.772 (30.3)		39.7 (5.80)
TM_{50} (weeks)	49.0 (13.5)		
Hill	2.19 (46.1)		
Proportional error, Cohort 1 (%)	20.6 (2.80)		
Proportional error, Cohort 2 (%)	7.00 (18.7)		

$CL_{std.sa}$, $CL_{std.ia}$ and $CL_{std.fa}$ are oral clearance for slow, intermediate and fast acetylators, respectively. They refer to a child weighing 12.5 kg and at full maturation; Vc_{std}, apparent volume of distribution in the central compartment for 12.5 kg child; k_a, first order absorption rate constant; MTT, absorption mean transit time; NN, number of hypothetical transit compartments. Q_{std}, inter-compartmental clearance for 12.5 kg child; Vp_{std}, volume of distribution in the peripheral compartment for 12.5 kg child; F_{sa}, relative bioavailability of slow acetylators; $F_{im/fa}$, relative bioavailability of intermediate and fast acetylators relative to slow acetylators; TM_{50}, post-menstrual age at 50% of adult clearance; Hill, steepness of the maturation function; [a]RSE, relative standard error reported on the approximate standard deviation scale; [b]IIV, inter-individual variability expressed percent coefficient of variation (% CV); [c]IOV, inter-occasional variability expressed as % CV; [d]In order to obtain the values of CL/F, Vc/F, Q/F and Vp/F, the values in the Table 5.4 should be divided by the respective value of bioavailability, which changes according to acetylator status. The IIV in CL was set to the same value for irrespective of metaboliser status.

NAT2 genotype was a significant covariate on CL and F. The OFV improved by 55.7 points when including acetylator status, which explained 45% of the IIV in CL. Estimation of F for intermediate and fast acetylators (relative to slow acetylators) and

accounting for age maturation of CL further improved the OFV by 11 and 16 points, respectively. The age maturation explained 6% IIV in CL. With respect to intermediate acetylators (CL=8.94 L/h), slow acetylators had 50% lower CL (4.44 L/h), while fast acetylators had 26% higher CL (11.3 L/h). Also, F in intermediate and fast acetylators was estimated to 77.2% which is 23% lower than in slow acetylators. Thus, combining the genotype effect on CL and bioavailability, the value of CL/F is 4.44, 11.6, and 14.6 L/h for slow, intermediate and fast acetylators, respectively. The final model included IIV, expressed as percent coefficient of variation (% CV), in CL (25%) and IOV in ka (61%), MTT (94%) and F (40%). Maturation of CL is represented in Figure 5.1 and the VPC for the final model is shown in Figure 5.4. When scaled to a 70 kg individual, the typical values of CL (not CL/F, so before adjusting for the effect of NAT2 genotype on F) were 16.2, 32.5, and 41.1 L/h for slow, intermediate and fast acetylators, respectively, and Vc and Vp were 61.6 L and 28.2 L. Appendix 3 shows the run record and control stream of final isoniazid pharmacokinetic model.

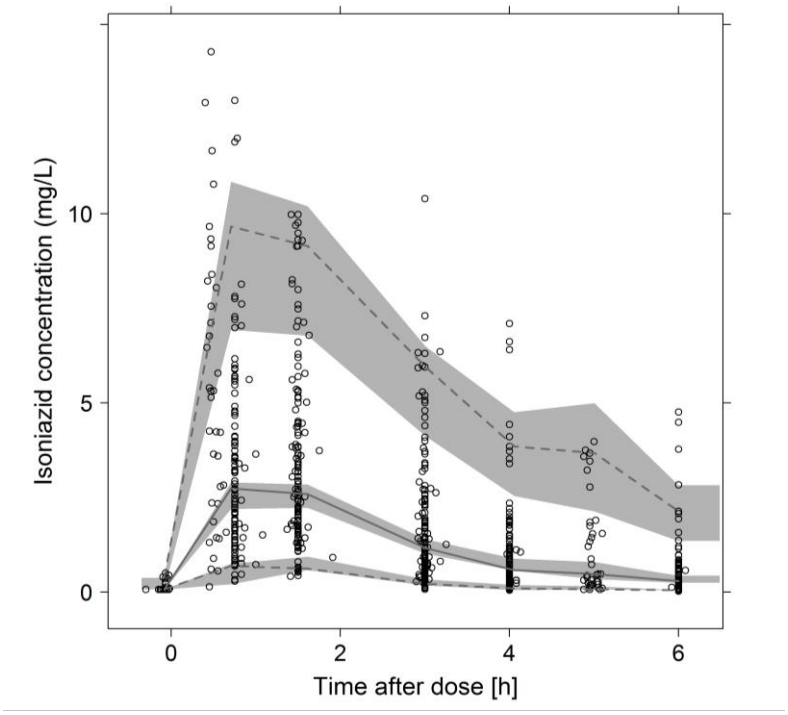

Figure 5.4: Visual predictive checks for the final model of isoniazid. The lower, middle and upper lines (dotted/solid) are the 5th, median, and 95th percentiles of the observed data, respectively. The shaded areas are the 95% confidence intervals for the 5th percentile, median and the 95th percentile of the simulated data.

5.3.1 Simulations

Using the final models and WHO's newly recommended higher dosages utilizing revised FDC recommendations, the predicted steady state AUC for all weight bands are shown in Figures 5.5, 5.6 and 5.7 for rifampicin, pyrazinamide, and isoniazid, respectively. Median rifampicin exposures were similar to those in adults, although wider variability was present in the simulated paediatric AUCs as shown in Figure 5.1. The simulation results suggest that a 50 mg/kg dose for children in the lowest weight band of 5.0-7.9 kg would achieve the same median AUC as that in the adults. Exposure after pyrazinamide and isoniazid were adequate, but younger children, particularly those in the lowest weight band, had lower exposures than those in the reference adult population, and

intermediate and rapid acetylators had reduced isoniazid exposures compared to the majority of adults.

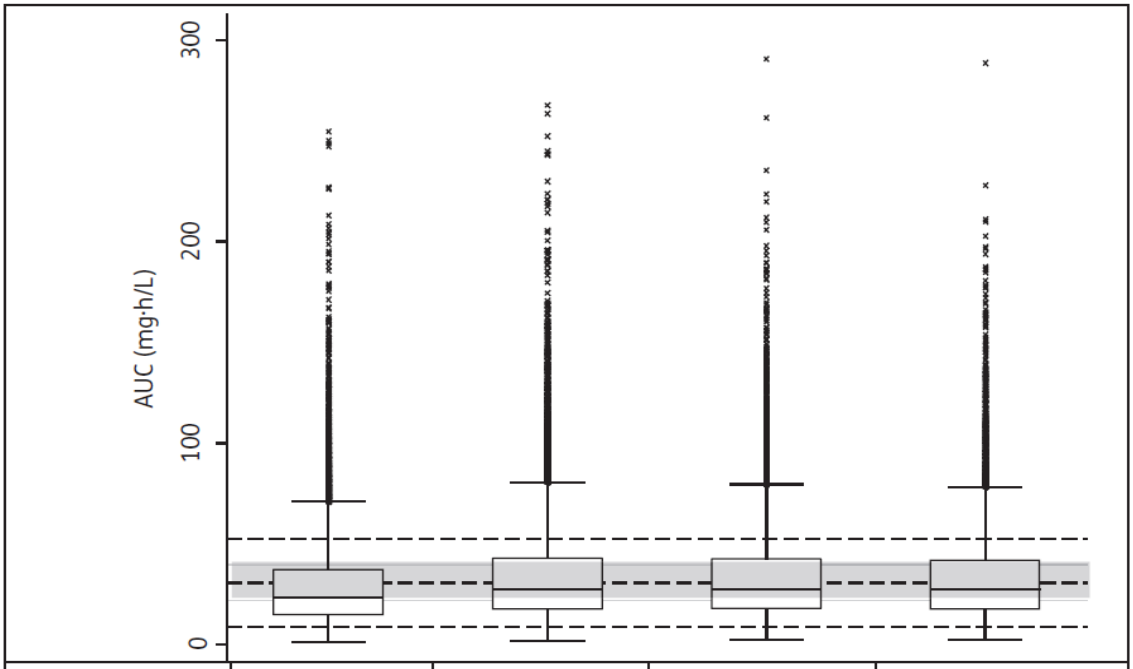

Dose (mg)	75	150	225	300
Dose (mg/kg)	10.7-18.8	13.6-18.8	15.0-18.8	12.5-18.8
>5th, <95th (%)	79.9	79.7	80.5	81.0
<5th (%)	7.7	4.2	3.8	3.8
>95th (%)	12.4	16.1	15.8	15.1
Weight (kg)	5.0-7.9	8.0-11.9	12.0-15.9	16.0-24.0
Age (years)	0.20-2.43	0.42-6.17	2.61-11.08	6.08-13.0

Figure 5.5: Box plot of simulated steady-state area under the concentration-time curve (AUC) of rifampicin across different age and weight bands, obtained adhering as closely as possible to the revised guidelines in dose per unit weight according to World Health Organisation 2010 dosing guidelines. Each box shows the 25th-75th percentile of simulated AUC and the symbol "x" shows data falling outside 1.5 times the interquartile range (25th-75th). The lower, middle, and upper dashed lines are the derived 5th (9.0 mg·h/L), median (30.7 mg·h/L) and 95th (52.4 mg·h/L) percentiles of the adult AUC, respectively. The grey shaded area is the 25th-75th (21.9 -39.5 mg·h/L) percentile of adult AUC.

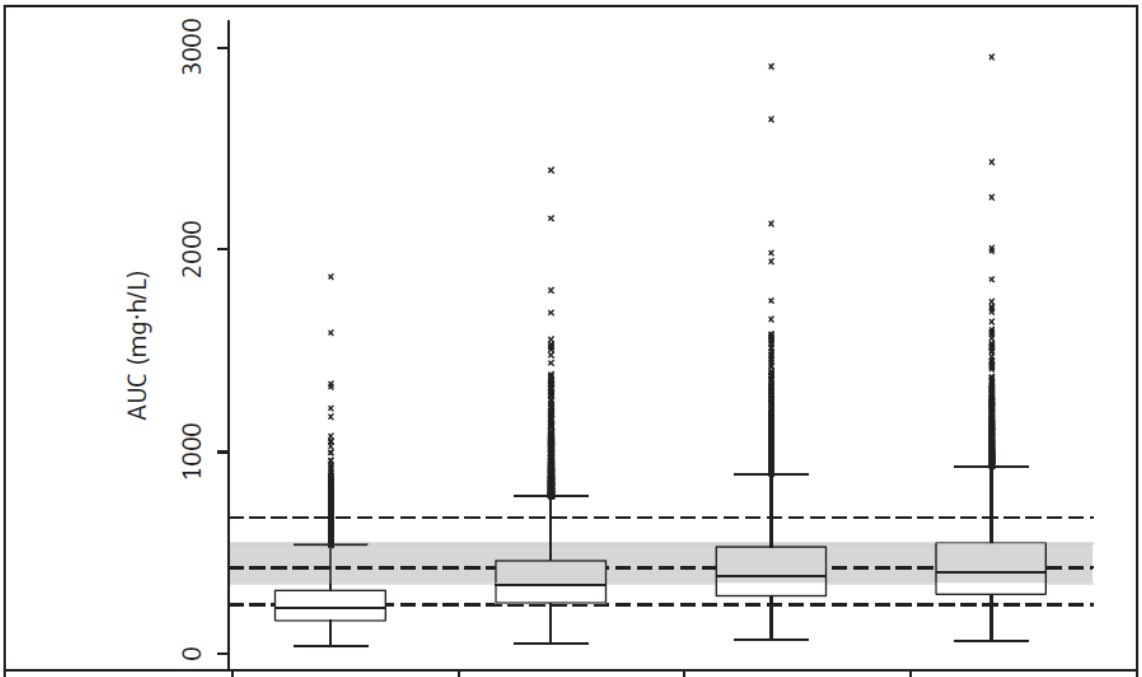

Dose (mg)	150	300	450	600
Dose (mg/kg)	21.4-37.50	27.3-37.7	30.0-37.5	25.0-37.5
>5th, <95th (%)	43.4	69.8	73.2	73.4
<5th (%)	55.4	23.4	15.5	13.6
>95th (%)	1.2	6.7	11.3	13.0
Weight (kg)	5.0-7.9	8.0-11.9	12.0-15.9	16.0-24.0
Age (years)	0.20-2.43	0.42-6.17	2.61-11.08	6.08-13.0

Figure 5.6: Box plot of simulated steady-state area under the concentration-time curve of pyrazinamide across different age and weight bands, obtained adhering as closely as possible to the revised guidelines in dose per unit weight according to World Health Organisation 2010 dosing guidelines. Each box shows the 25^{th}-75^{th} percentile of simulated AUC and the symbol "x" shows data falling outside 1.5 times the interquartile range (25^{th}-75^{th}). The lower, middle, and upper dashed lines are the derived 5^{th} (244.0 mg·h/L), median (427.0 mg·h/L), and 95^{th} (675.0 mg·h/L) percentiles of the adult AUC, respectively. The grey shaded area is the 25^{th}-75^{th} (346-547 mg·h/L) percentile of adult exposure.

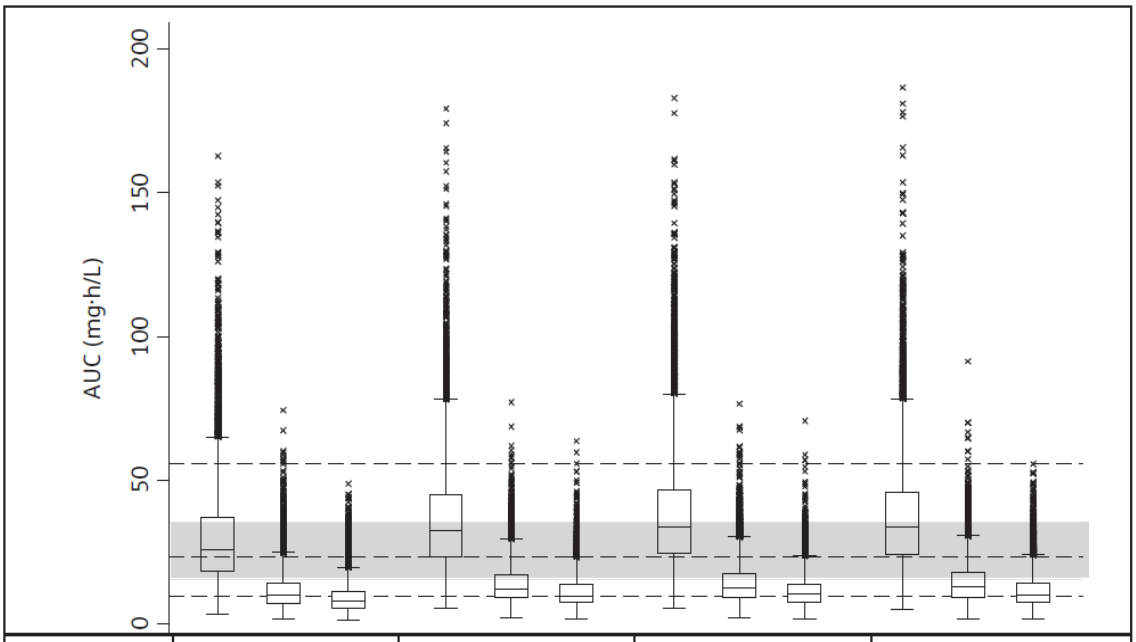

Dose (mg)	50			100			150			200		
Dose (mg/kg)	7.1-12.5			9.1-12.5			10.1-12.5			8.3-12.5		
Genotype	S	I	F	S	I	F	S	I	F	S	I	F
>5th, <95th (%)	89.1	50.7	32.9	85.9	67.2	49.4	85.2	69.2	52.3	86.0	70.9	52.1
<5th (%)	3.3	49.2	67.1	0.63	32.7	50.6	0.4	29.3	47.3	0.4	29.0	47.9
>95th (%)	7.5	0.1	0.0	13.5	0.1	0.0	14.4	1.5	0.5	13.6	0.1	0.0
Weight (kg)	5.0-7.9			8.0-11.9			12.0-15.9			16.0-24.0		
Age (years)	0.20-2.43			0.42-6.17			2.61-11.08			6.08-13.0		

Figure 5.7: Box plot of simulated steady-state area under the concentration-time curve (AUC) of isoniazid in slow (S), intermediate (I) and fast (F) acetylators across different age and weight bands, obtained adhering as closely as possible to the revised guidelines in dose per unit weight according to World Health Organisation 2010 dosing guidelines. Each box shows the 25th-75th percentile of simulated AUC and the symbol "x" shows data falling outside 1.5 times the interquartile range (25th-75th). The lower, middle, and upper dashed lines are the derived 5th (9.8 mg·h/L), median (23.4 mg·h/L), and 95th (55.6 mg·h/L) percentiles of the adult AUC, respectively. The grey shaded area is the 25th-75th (15.6-35.5 mg·h/L) percentile of adult exposure.

The results of this current study also predicted that from 3 months to 2 years of age, the AUC decreased by 56% and 50% for rifampicin and isoniazid, respectively, but only 18% for pyrazinamide (refer to respective Figure 5.8-5.10 below).

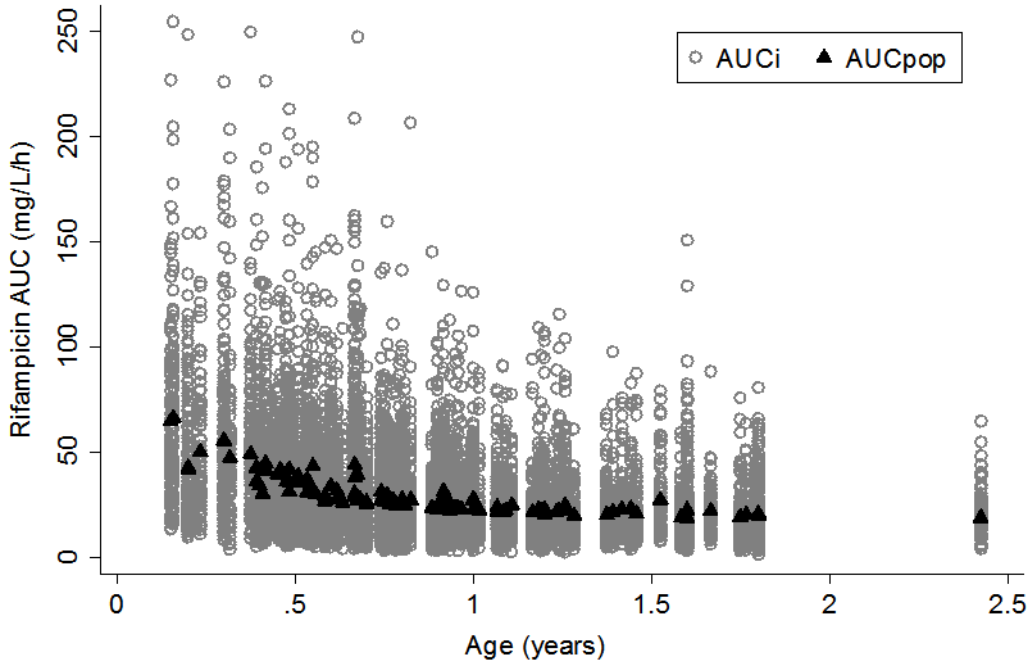

Figure 5.8: Scatter plot of simulated rifampicin steady state area under the concentration-time curve (AUC) versus post-natal age, based on the final model. AUCpop (black triangles) are the population predicted values for each individual, obtained under the assumption that each subject is characterised by the typical parameter values of the population, i.e. no random effects are included. AUCi (grey open circles) are the individual simulated predictions, obtained by including the random effects, generated according to the level of variability identified in the population. Data from the 5.0-7.9 kg weight band is shown. Age was included as a covariate in the final model.

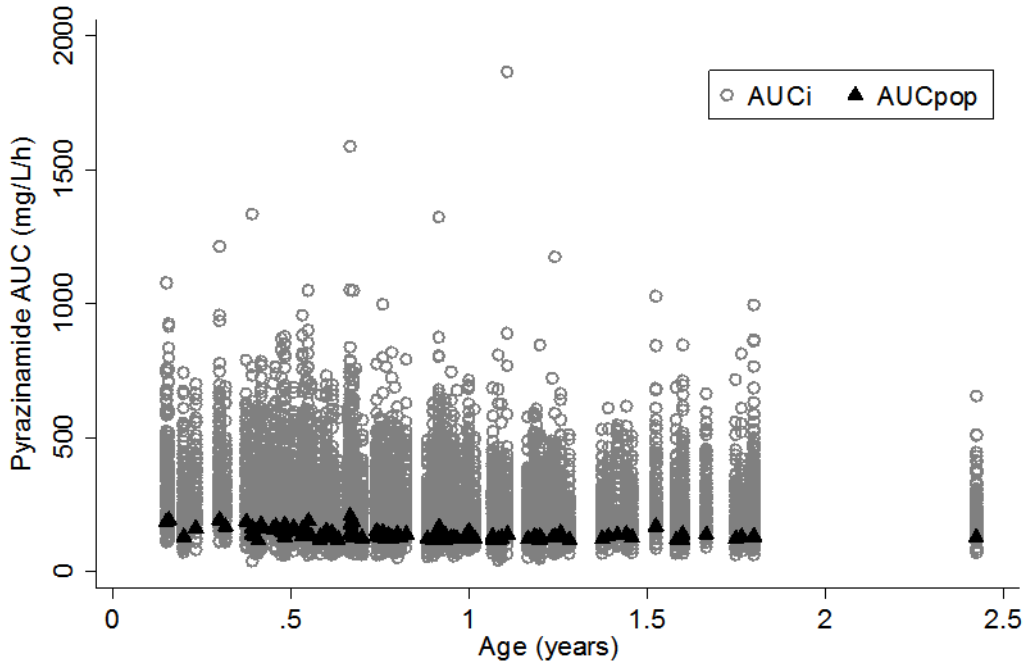

Figure 5.9: Scatter plot of simulated pyrazinamide steady state area under the concentration-time curve (AUC) versus post-natal age, based on the final model. AUCpop (black triangles) are the population predicted values for each individual, obtained under the assumption that each subject is characterised by the typical parameter values of the population, i.e. no random effects are included. AUCi (grey open circles) are the individual simulated predictions, obtained by including the random effects, generated according to the level of variability identified in the population. Data from the 5.0-7.9 kg weight band is shown. Age was included as a covariate in the final model.

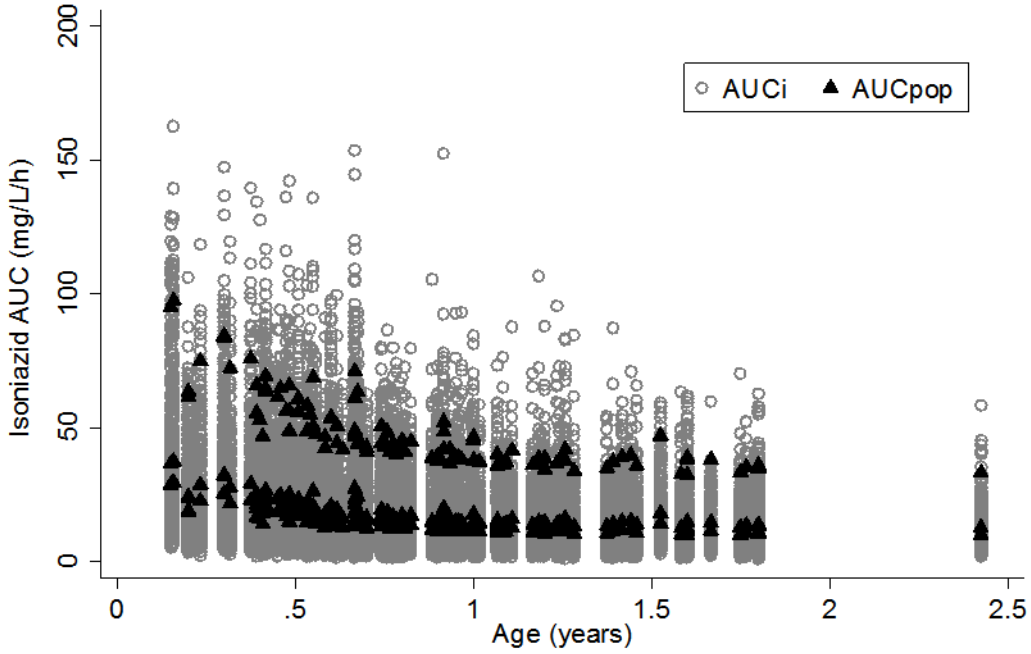

Figure 5.10: Scatter plot of simulated isoniazid steady state area under the concentration-time curve (AUC) versus post-natal age, based on the final model. AUCpop (black triangles) are the population predicted values for each individual, obtained under the assumption that each subject is characterised by the typical parameter values of the population, i.e. no random effects are included. AUCi (grey open circles) are the individual simulated predictions, obtained by including the random effects, generated according to the level of variability identified in the population. Data from the 5.0-7.9 kg weight band is shown. Please note that for isoniazid the simulations were repeated three times, assuming fast, intermediate, or slow metaboliser status, thus the separate trends visible in the charts for AUCpop. Age was included as a covariate in the final model.

5.4 Discussion

We described the population pharmacokinetics of rifampicin, pyrazinamide and isoniazid in South African children treated for tuberculosis. In addition, drug exposures resulting from the dosages recently recommended by the WHO were investigated. In this current study, simulations predicted that, even with the increased dosages, smaller children would achieve relatively low exposures to pyrazinamide and isoniazid. Moreover, intermediate and fast acetylators (together comprising 61% of South African population) may be under-dosed with respect to isoniazid, if exposures in an ethnically similar population of adults are considered therapeutic (Figure 5.7). It should be noted

that the doses of pyrazinamide and isoniazid used for these predictions tended to be somewhat lower than the recommended dose per kg, especially in the youngest children. The choice of weight bands was based on ongoing discussions about the optimal dose of the FDC by weight band, pragmatic considerations, such as the stability and equal distribution of active ingredients in each portion after breaking the FDC tablets, and concern that pharmacokinetic maturation could still be incomplete in young children (Fletcher et al. 2012, Pariente-Khayat et al. 1997, Schaaf et al. 2005). In this current study, the proposed doses were optimized assuming that dividing the FDC tablets should be avoided if possible.

The typical paediatric parameter estimates for rifampicin CL/F and Vc/F are in line with adult values reported in an ethnically similar population (Wilkins et al. 2008). After adjusting for the difference in body size (the median weight of the adult population used for comparison was 50 kg), CL/F was 23.1 L/h in children versus 19.2 L/h in adults and Vc/F was 64.8 L versus 53.2 L, respectively. This suggests that pharmacokinetic differences between children and adults could mainly be explained by differences in body size (which was accounted for by allometric scaling) and enzyme maturation. To date, this is the only paper that that evaluated non-linearity within the current dose range in children. However, the data did not support non-linearity in the pharmacokinetics of rifampicin, even though the doses given ranged from approximately 5 to almost 18 mg/kg daily. These results therefore suggest that at the doses used in the children studied, rifampicin may not display the dose-dependent non-linear pharmacokinetics in children that has been described in adults (Pargal & Rani 2001). However, further studies, including sufficient numbers of children being given the increased dosages, would be needed to confirm this. A Cmax of at least 8 mg/L has been suggested as

therapeutic for rifampicin (Peloquin 2002) although even higher concentrations are likely necessary for maximal bactericidal activity (Gumbo et al. 2007a). However, such concentrations are rarely achieved in children prescribed 8-12 mg/kg/day doses of rifampicin (Schaaf et al. 2009b). If the pharmacokinetics in an ethnically similar adult population (Wilkins et al. 2008) given the currently-recommended doses is used for comparison, the majority of the children fall within the 5^{th}-95^{th} percentile range of exposures in the adult patients (Figure 5.6). The simulated adult exposures were similar to those found in a large pharmacokinetic study conducted in adults with pulmonary tuberculosis in Botswana (Chideya et al. 2009).Simulations for children using newly recommended WHO paediatric guidelines predicted more variable rifampicin exposures than those for the reference adult population (Figure 5.6). Moreover, both the predicted mean Cmax using the revised paediatric guidelines (6.6 mg/L) and the current doses recommended by WHO in the adult reference population (4.8 mg/L) were lower than the proposed minimum Cmax of 8 mg/L (Peloquin 2002), implying that even higher doses of rifampicin should be considered for both children and adults.

Using the final pyrazinamide model and parameter estimates for CL/F and Vc/F scaled to the median weight of the adults population used for comparison (51.5 kg) (Wilkins et al. 2006), the children had similar CL/F (about 3.1 versus 3.42 L/h) and higher Vc/F (39.7 versus 29.2 L) compared to the adults. The higher Vc/F in children could partly be due to malnutrition and severe forms of tuberculosis disease. When previously-reported exposures in an ethnically similar adult population who received doses recommended by WHO are used as targets, simulation results predicted that children weighing 5.0-7.9 kg may be under-dosed (Figure 5.6). As noted above, children in the lowest weight band tended to receive doses somewhat lower than the 30-40 mg/kg target proposed in the

revised guidelines. The pyrazinamide exposures simulated for the reference adult population were similar to those in the large cohort in Botswana (Chideya et al. 2009). In addition, the majority of adults had simulated Cmax within the suggested range of 20-50 mg/L (Peloquin 2002). Importantly, patients in the Botswana cohort with pyrazinamide Cmax lower than 35 mg/L had an increased risk of poor treatment outcome.

Isoniazid pharmacokinetics is highly dependent on the polymorphic NAT2 locus, which is a major determinant of isoniazid plasma concentrations (Parkin et al. 1997). Targeting average exposures simulated for ethnically similar adults following doses currently recommended by WHO, the new doses recommended by the WHO for children are adequate for slow acetylators, but insufficient for intermediate and fast acetylators (Figure 5.7. In this current analysis, there was wide IIVs in the systemic concentrations and AUC mostly because children were not dosed according to NAT2 acetylator genotype. Hence further studies are needed to adequately define the implications of IIVs for safety and efficacy in children. Interestingly, children who were younger than 1 year had higher AUC irrespective of their weight band. In addition, isoniazid CL showed maturation with age and this support the notion that finer weight bands in conjunction with age should be considered to avoid overdosing very young children. The reduced bioavailability for intermediate and fast acetylators is most likely a result of increased pre-systemic metabolism which also correlates with systemic clearance. The lower exposure in intermediate and fast acetylators may predispose to the development of ARR. In the Center for Disease Control (CDC) Study 22 (Weiner et al. 2005) an association was found between low isoniazid plasma concentrations and the occurrence of relapse in patients on a regimen of once weekly rifapentine and isoniazid, suggesting

that isoniazid might have been ineffective in preventing development of rifamycin resistance.

In all the models, clearance and volume were scaled using allometric approach, and this choice over using weight as a linear covariate was also supported by the data following general criteria such as the OFV. The use of allometric to account for differences in pharmacokinetics due to body size is supported by both empirical observation and biological theory, as discussed in depth by Anderson and Holford (Anderson & Holford 2008, 2009).

Although children in this current study received similar formulations across the 2 cohorts, formulation is known to be an important determinant of bioavailability (Agrawal et al. 2004, McIlleron et al. 2006). Other factors encountered when preparing suspensions and administering the drug are likely to play a role in young children who cannot swallow tablets. There is a need for studies to evaluate such sources of variability in paediatric drug exposure and to develop solutions to reduce it. Genetic diversity is also an important consideration when extrapolating the results of pharmacokinetic studies. There is considerable geographic variation in the distribution of NAT2 polymorphisms (Fuselli et al. 2007, Sabbagh et al. 2011). Moreover, recent studies have identified polymorphisms of SLCO1B1 (which encodes the OATP1B1 transporter) occurring in relatively high frequencies in African populations, associated with substantially reduced rifampicin exposure (Chigutsa et al. 2011, Weiner et al. 2010). Hence, pharmacogenetic studies in children may allow further optimization of dosing strategies.

5.4.1 Limitation

Limitations of the pharmacokinetic models include the fact that the AMA values and z-scores used to test anthropometric associations with the pharmacokinetic parameters were not derived specifically from an African population, and thus they may not have correctly described the children used in this analysis. Furthermore, a limitation of simulation approach of this current analysis is that it did not into account for any nonlinearity in the pharmacokinetics that may occur at the higher doses; hence predictions in this analysis should be confirmed in pharmacokinetic studies in children dosed according to the revised guidelines. Also, non-linearity at higher doses could be a toxicity rather than efficacy concern. Finally, the simulations used were against pharmacokinetic and not pharmacodynamics target though it is still debatable.

5.5 Conclusion

In summary, the models in this study described the population pharmacokinetics of rifampicin, pyrazinamide and isoniazid in children with tuberculosis. Simulations based on these models predict that the newly-recommended weight band-based doses in WHO guidelines for children result in rifampicin exposures in paediatric population which are similar to those in adults from the same study population. But, when children are dosed in pragmatic weight bands, there is wide variability in drug exposure, and pyrazinamide and isoniazid exposures in many children will be lower than those in an ethnically similar adult population. Hence, adjustment of the recommended doses may be warranted should the findings be confirmed in other populations.

6 Effects of Four Different Meal Types on the Population Pharmacokinetics of Single-Dose Rifapentine in Healthy Male Volunteers

6.1 Introduction

Rifapentine, a cyclopentyl rifamycin, is an orally administered drug registered by the Food and Drug Administration (FDA) for the treatment of pulmonary tuberculosis. It exerts its antibacterial activity through inhibition of DNA-dependent RNA polymerase in susceptible strains of *Mycobacterium tuberculosis* (Wehrli 1983). Rifapentine has a microbiologically active metabolite, 25-desacetyl rifapentine (Heifets et al. 1990). Rifapentine has a long half-life (Burman et al. 2001, Keung et al. 1999) and superior *in vitro* potency against *M. tuberculosis* in comparison with rifampin (Heifets et al. 1990), making it an attractive candidate for shortening and simplifying antitubercular therapy.

Currently, rifapentine is dosed at 600 mg either once weekly or twice weekly in HIV-negative patients with noncavitary tuberculosis (Blumberg et al. 2003). There is concern that the development of ARR, treatment failure, and relapse may be associated with intermittent dosing (Burman et al. 2006, Menzies et al. 2009), insufficient companion drug exposure (Weiner et al. 2005), or low rifamycin concentrations (Gumbo et al. 2007a, Mitchison 1998). Previously, rifapentine's sterilizing effect has been shown to be dose dependent in murine studies which suggest that daily doses of rifapentine may reduce treatment duration to just 3 months (Rosenthal et al. 2006, 2007; Zhang et al. 2009), and higher doses of rifapentine are associated with improved early bactericidal activity in humans (Sirgel et al. 2005). Clinical trials are currently evaluating new antituberculosis regimens containing

higher doses of rifapentine used intermittently or daily doses of rifapentine. Concomitant food has a marked effect on rifapentine absorption (Chan et al. 1994). The effect of food on systemic rifapentine exposure may therefore impact treatment activity and safety. The aim of this study was to investigate the effect of meals differing in fat and bulk content on the rate and extent of rifapentine absorption and 25-desacetyl rifapentine disposition. The study was designed to include meals comprising largely maize, a staple cereal in many parts of Africa and South America, and a light meal (i.e., a reconstituted powdered chicken soup). The study was conducted in 1999 shortly after the release of results from studies evaluating intermittent 600-mg doses of rifapentine, which displayed unacceptably high relapse rates in patients with lung cavities or immune suppression. It was therefore anticipated that future studies would evaluate higher doses of rifapentine.

6.2 Setting and Study Design

The data used were from the health volunteer study described in Section 4.2.2. Each participant provided written informed consent before being enrolled into the study. The study protocol (M000473/1LO1) was reviewed and approved by the Research Ethics Committee of the University of Cape Town and the Medicines Control Council of South Africa. Table 6.1 shows the composition of the meals ingested.

Table 6.1: Description of different meals ingested 30 minutes before administration of a single 900 mg dose of rifapentine

Meal	Description	Protein (g)	Fat (g)	Carbohydrates (g)	Energy (Kilojoules)	Weight (g)
A (High fat breakfast)	Two rashers of bacon (20 g), 1 fried egg (50 g), one slice white toast (30 g) with butter (7 g) and marmalade (10 g), two cups decaffeinated coffee (400 ml) with full cream milk (100 ml) and two teaspoons of sugar (10 g) (English breakfast)	18.9	27	38	1966	627
B (low fat and bulky breakfast)	One-and-half cups soft maize meal porridge (375 g cooked) with three teaspoons of sugar (15 g), one cup of decaffeinated coffee (200 ml) with full cream milk (50 ml) and one teaspoon of sugar (5 g) (Maize meal porridge)	6	3	66	1285	645
C (high fat and bulky breakfast)	One-and-half cups soft maize meal porridge (375 g cooked) with three teaspoons of sugar (15 g) and five teaspoons of lard (25 g), one cup of decaffeinated coffee (200 ml) with full cream milk (50 ml) and one teaspoon of sugar (5 g) (Maize meal porridge with lard)	6	28	66	2229	670
D (low fat and high fluid breakfast)	Two cups of reconstituted (powder) chicken noodle soup (400 ml), one cup of decaffeinated coffee (200 ml) with skimmed milk (50 ml) and one teaspoon of sugar (5 g)	9	4	28	774	660

Volunteers were eligible if they weighed at least 50 kg, had normal physical examination and baseline laboratory evaluation, and were nonsmokers. Exclusion criteria included a history of TB, active allergies, excessive coffee or alcohol consumption, recent blood donation of more than 500 ml, and clinically relevant cardiovascular, hepatic, neurologic, endocrine, or other major systemic disease. In order to limit the risks of unintended fetal exposure to the unregistered drug, women were excluded. Likewise HIV- or hepatitis B virus (HBV)-infected volunteers were excluded due to the risks of undiagnosed tuberculosis and adverse effects, respectively. Table 6.2 shows clinical and demographic characteristics of healthy male volunteers.

Table 6.2: Demographic and clinical characteristics of healthy male volunteers

Variable[a]	Value
Number of patients	35
Median age, range (years)	23 (18, 46)
Median weight, range (kg)	71.5 (56, 110)
Median height, range (cm)	177(159, 192))
BMI, range (kg/m^2)	22.9 (18.9, 29.8)

[a]BMI, body mass index

After an overnight fast, participants received a single 900-mg dose of rifapentine (200 ml of water with six 150-mg Priftin tablets; Hoechst Marion Roussel, Italy) 30 min after the meal (Table 4.1). Individuals were randomized to receive the rifapentine dose in the fasted state (meal E) on one occasion. Other scheduled meals included a standardized lunch and dinner at 6 or 12 h postdose. At each visit a 20-ml

blood sample was collected prior to drug administration, and 10-ml samples were collected 2, 3, 4, 5, 6, 7, 8, 10, 12, 14, 24, 36, 48, and 72 h after the dose to obtain plasma for quantification of rifapentine and 25-desacety rifapentine. Each dose was separated by a 14-day washout period. Seven participants were randomized to each of five different meal sequences. Due to the large number of potential meal sequences, the design was not fully balanced. The blood samples were collected by venipuncture into lithium-heparin-coated glass tubes and centrifuged at 2,500 rpm within 1 h of collection. The supernatants were transferred into two dry polypropylene tubes and stored at −80°C away from light until analysis.

6.2.1 Population pharmacokinetic analysis

The methodology applied for model building has been described in section 4.5.3 (Population pharmacokinetic analysis). For the rifapentine concentration-time data, various pharmacokinetic models, including one or two compartments with first-order absorption and first- or zero-order elimination (Holford et al. 1992), incorporating either lag times (to describe the delay in the appearance of drug in plasma) or transit absorption compartments (Rousseau et al. 2004, Savic et al. 2007), time-varying clearance (Langdon et al. 2005), and enterohepatic recirculation (Roberts et al. 2002), were fitted to the data during model development.

Time-varying clearance was introduced into the model as:

$$CL_i = TV\left(\frac{CL_1}{F}\right)\cdot \exp\left(\eta_{i,}^{\frac{CL_1}{F}} + \kappa_i^{\frac{CL_1}{F}}\right)\cdot\left(1 - mpast(i)\right) + TV\left(\frac{CL_2}{F}\right)\cdot \exp\left(\eta_i^{\frac{CL_2}{F}} + \kappa_i^{\frac{CL_2}{F}}\right) \cdot mpast(i)$$

where CL_i is the oral clearance for the *i*th individual, $TV(\frac{CL_1}{F})$ is the typical oral clearance which later changes to $TV(\frac{CL_2}{F})$ at MTIME, $mpast(i)$ remains zero until MTIME when it changes to 1, $\eta_i^{\frac{CL_1}{F}}$ represents the IIV and $\kappa_i^{\frac{CL_1}{F}}$ represents the IOV.

Covariates (age and body weight) were evaluated with respect to their impact on IIV in *F* and CL/*F* parameters. The effect of continuous and categorical covariates, and model validation were evaluated as described under section 4.5.3.1 (Model building and validation).

The following equation was used in quantifying meal effects:

$$TVF = \theta_F \cdot (1 - RXF)$$

TVF is the typical bioavailability, *RXF* is the fractional change (all five visits) in F due to a given meal relative to the fasted state, θ_F is the value of F under fasting conditions (fixed to 1). A similar approach was used to evaluate meal effects on the fixed effects for MTT and k_a. The delay in absorption was modeled using a transit absorption model where drug absorption is described as drug movement through a series of hypothetical presystemic compartments, as previously suggested (Savic et al. 2007). Carryover effects on clearance and MTIME values at each treatment period were evaluated relative to the first treatment period using the equation below:

$$\text{TVMT} = \theta_{\text{MTIME}} \cdot (1 - \theta_{\text{mtocc}})$$

where θ_{MTIME} is the typical value of MTIME (TVMT), and θ_{mtocc} is the fractional change in MTIME at a given occasion relative to the first occasion. After developing the model for rifapentine, all the parameter estimates were fixed and a model for the metabolite was developed. The above-mentioned pharmacokinetic models were also

evaluated for the 25-desacetyl rifapentine data. In addition, models accounting for presystemic formation of the metabolite (Kerbusch et al. 2003), loss of the parent drug to other metabolites (Taft et al. 1997), and saturable clearance of the metabolite (Relling et al. 1993) and a two-compartment model with time-varying CL/*F* were tested when developing the 25-desacetyl rifapentine model.

6.3 Results

Rifapentine and 25-desacetyl rifapentine plasma concentrations in 2,272 samples from 34 participants were available. Data for 1 participant, who withdrew after a single visit, were not available. Less than 1% of the concentration-time data were below the limit of quantification and therefore excluded in the pharmacokinetic analysis. A one-compartment model with first-order absorption and time-varying clearance best described the rifapentine data (Figure 6.1).

The delay in absorption was described using a transit absorption model. The residual error model, selected by GOF plots, IWRES versus time, and decrease in OFV, had both additive and proportional error terms. The model described the data well, as shown in Figure 6.2. The population pharmacokinetic parameter estimates for rifapentine and meal effects on rifapentine are tabulated in Tables 6.1 and 6.3, respectively.

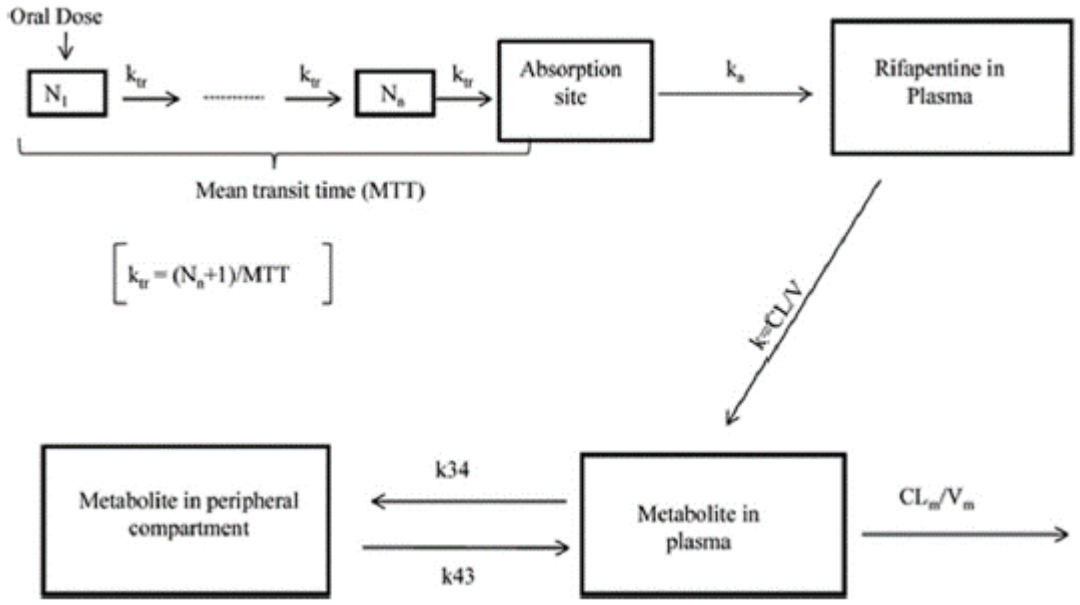

Figure 6.1: Illustration of the parent metabolite model. All rifapentine is assumed to be converted to the major metabolite (25-desacetylrifapentine). N_1represents the first hypothetical transit compartment up to N_n compartment. k_{tr} is the transit rate constant. k_a is the absorption rate constant from the hypothetical drug depot compartment to plasma. k (calculated as CL/Vc) is the elimination rate constant of rifapentine. CLm is the time-varying metabolite clearance. V_m represents volume of distribution of the metabolite. k34 is the first-order rate constant of the metabolite from plasma to the peripheral compartment, and k43 is the first-order rate constant of the metabolite from the peripheral compartment back to plasma.

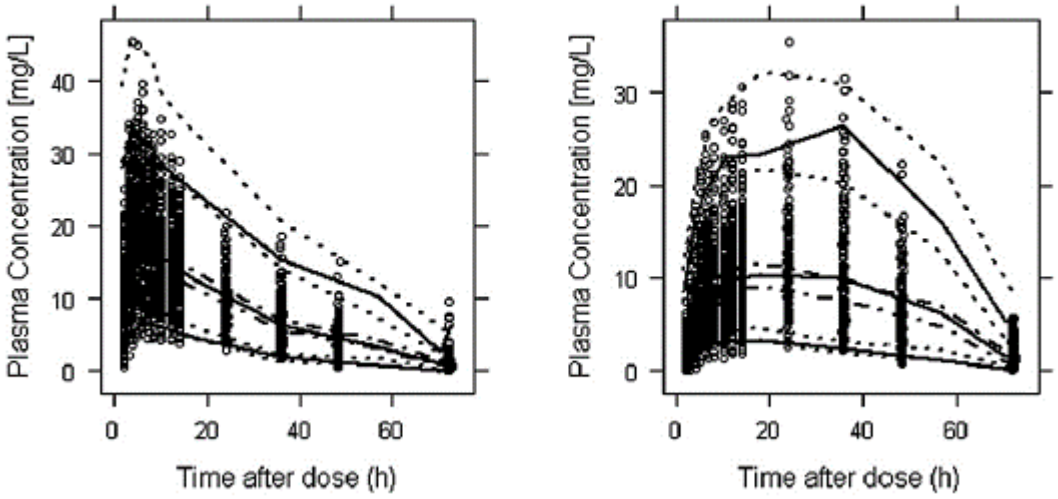

Figure 6.2: Visual predictive check for the final (left) and metabolite (right) models. The lower, middle, and upper solid lines are the 5th, 50th, and 95th percentiles of the observed data, respectively. The dotted and dashed-dotted (50th percentile) lines around each percentile show the 95% confidence interval from the model prediction. The circles are the observed concentration-time data points.

Table 6.3: Final parameter estimates for rifapentine

Parameter	Estimate (RSE[a] [%])	IIV[b] (RSE[a] [%])	IOV[c] (RSE [a][%])
CL_1 (L/h)[d]	2.14 (13.6)	19.2 (24.3)	12.2 (9.1)
CL_2(L/h)[e]	3.22 (11.9)	19.2 (24.3)	12.2 (9.1)
MTT (h)	1.45 (10.8)	9.5 (87)	24.4 (13.4)
F	1 (fixed)	21.4 (35.3)	29.0 (16.6)
MTIME (h)[f]	43 (2.6)		
V/F (L)	60.6 (9.2)		
NN	10.9 (9.6)		
k_a (h^{-1})	1.66 (13.1)		
Residual variability			
Additive error (mg/L)	0.206 (12.3)		
Proportional error (%)	10.6 (1.81)		

[a]RSE, relative standard error expressed as percentage of estimate; [b]IIV, interindividual variability expressed as coefficient of variation (CV); [c]IOV, interoccasional variability expressed as CV; [d]Oral clearance of rifapentine before MTIME; [e]Oral clearance of rifapentine after MTIME; [f]MTIME is the estimated time when oral clearance of rifapentine increases.

Table 6.4: Different meal effects, relative to fasted state, estimated from parent (rifapentine) model

Meal[a]	% increase in oral bioavailability	(% RSE)[b]
Meal A	85.7	20.1
Meal B	32.7	40.4
Meal C	45.7	29.3
Meal D	48.9	30.7

[a] Meals are described in Table 4.1 under Materials and methods. The model was parameterized for meal effects on oral bioavailability (F), first-order absorption rate constant (k_a) and mean transit time (MTT). Meal effects on k_a and MTT were dropped in the final model since they became insignificant. [b]RSE, relative standard error expressed as percentage of estimate

All the meals investigated in this current study increased the bioavailability of rifapentine relative to fasting conditions. No clinically significant demographic covariates were supported by the data. Accounting for the correlation between *F* and MTT (correlation coefficient = 0.65) and between CL/*F* and MTT (correlation coefficient = −0.56) in the RFP model significantly improved the model. The η shrinkage values for RFP CL/*F*, MTT, and *F* were 6%, 40%, and 13%, respectively. For model diagnostic, a VPC was preferred. 25-desacetyl rifapentine pharmacokinetic data were best described by a two-compartment model with time-varying clearance (Figure 6.1). Final PK parameter estimates for 25-desacetyl rifapentine are summarized in Table 6.3 and the VPC is shown in Figure 6.2. The run record and control stream final pharmacokinetic model for rifapentine and 25-desacetyl rifapentine are shown in Appendix 4.

Table 6.5: Final parameter estimates for 25-desacetyl rifapentine

Parameter	Estimate (RSE[a] [%])	IIV[b] (RSE[a] [%])	IOV[c] (RSE [%])
CL_{M1}/F (L/h)[d]	1.81 (8.7)	23.9 (23.9)	30.2 (10.6)
CL_{M2}/F (L/h)[e]	4.63 (8.1)	23.9 (23.9)	30.2 (10.6)
MTIME (h)[f]	46.8 (0.3)		
V_{MC}/F (L)[g]	6.36 (5.8)		
V_{MP}/F (L)[h]	22.1 (4.8)		
QM(/h)[i]	4.4 (6.9)		
Residual variability			
Additive error (mg/L)	0.211 (9.7)		
Proportional error (%)	19.1 (0.7)		

[a] RSE, relative standard error expressed as percentage of estimate; [b]IIV, interindividual variability expressed as coefficient of variation (CV); [c]IOV, interoccasional variability expressed as CV; [d]Oral clearance of 25-desacetyl rifapentine before MTIME; [e]Oral clearance of 25-desacetyl rifapentine after MTIME; [f]MTIME is the estimated time when oral clearance of rifapentine increases. [g]Apparent volume of distribution of 25-DRFP in the central compartment; [h]Apparent volume of 25-desacetyl rifapentine distribution of in the peripheral compartment; [i]intercompartmental clearance of 25-desacetyl rifapentine

Clinical adverse events were mild. Three volunteers were withdrawn due to elevated alanine transaminase (ALT) levels. One volunteer withdrew after the first rifapentine dose and had an ALT level 2 times the upper normal limit (UNL). Two volunteers were withdrawn after the second dose; they had ALT levels 2.2 and 6.9 times the ULN. ALT levels in these 3 participants returned to the normal range after withdrawal, and they remained clinically well and asymptomatic throughout. There was no evidence of a relationship between toxicity and drug concentrations or meal type.

6.4 Discussion

The bioavailability of rifapentine and consequently 25-desacetyl rifapentine exposure were increased when single 900-mg rifapentine oral doses were administrated

immediately after food. The high-fat meal (an English breakfast which included one fried egg) had the greatest effect (Table 6.2), increasing the oral bioavailability by 85.7%. This finding is consistent with previous studies (Chan et al. 1994, Langdon et al. 2005). A study conducted in Hong Kong found that 2 eggs with toast increased the bioavailability of rifapentine to almost the same extent as a high-fat English breakfast (Chan et al. 1994). This meal effect finding forms the basis for the concomitant meal used in the ongoing RIFAQUIN study described in section 4.2.3, in which patients have 2 boiled eggs and bread immediately before each weekly 1,200-mg dose or twice-weekly 900-mg dose of rifapentine. The finding of high-fat breakfast without eggs (meal C) increased bioavailability of rifapentine by only 45.7% supports the notion proposed by Chan et al. (Chan et al. 1994) that eggs may be effective in promoting rifapentine absorption, although the mechanism is unclear. Meal effects on tablet dissolution, gastric emptying time (hence duration of absorption), and pH (which may affect solubility or absorption) may, in part, account for the pharmacokinetic differences observed with the different meals. Surprisingly, the low-fat chicken noodle soup (meal D) increased RFP bioavailability to an extent comparable to that of the maize meal porridge with lard (meal C). Monosodium glutamate (MSG) was one of the ingredients in the chicken noodle soup. MSG accelerates gastric emptying time in a high-energy, high-protein liquid diet (Zai et al. 2009), and we suspect that it could have played a role in meal D's effect. Even though in the final model there was no statistically significant effects of all meals on k_a and MTT, meal D gave the highest increase in k_a (100% against the fasting state), showing its influence on RFP pharmacokinetics.

The pharmacokinetics of rifapentine was best described by a one-compartment model with transit absorption compartments, first-order absorption, and first-order

elimination with time-varying clearance. Time-varying clearance is suggestive of autoinduction (Gordi et al. 2005, Zhu et al. 2009), and this finding is consistent with a recent study by Dooley et al. (Dooley et al. 2008) in which thrice-weekly doses of rifapentine were administered. In this current study, the autoinduction effect was detected with a 2-week washout between single 900-mg doses of rifapentine. The baseline CL/*F* tended to increase slightly in a cumulative manner with subsequent dosing occasions, and there was a tendency for the time of change (i.e., MTIME) to decrease slightly after each subsequent dose. Given that rifapentine and 25-desacetyl rifapentine were still identifiable in plasma up to 72 h postdose and that rifapentine is a potent enzyme inducer, it is not surprising that the duration of its effect on clearance should be similar to that of rifampin (Niemi et al. 2003).

As rifapentine concentrations had a double peak, an enterohepatic recirculation model was investigated. However, based on ΔOFV and other diagnostic procedures the data did not support an enterohepatic recirculation model. Other possible explanations include analytical interference due to food ingested 6 h after the dose, absorption windows, or progressive solubilization along the gastrointestinal tract and variable gastric emptying. The final pharmacokinetics models for both rifapentine and 25-desacetyl rifapentine differ from a previously published model (Langdon et al. 2005). The previous model was developed to describe patient data where the participants were preinduced by rifampin and were on other antituberculosis drugs. Furthermore, wider variability is expected among the patients described in the previous model than in healthy volunteers. We identified a positive correlation between IIV of oral bioavailability and MTT ($r = 0.65$), which was expected since increased MTT allows more time for drug absorption, while negative correlations between η values for

CL/*F* and MTT ($r = -0.56$) were probably due to association between IIVs for CL and *F*.

The prominent food effect has important implications for the interpretation of studies evaluating antituberculosis regimens. Assuming linear pharmacokinetics of rifapentine over different dose ranges (Weiner et al. 2004), the results of this current analysis indicate that drug exposure following a 600-mg dose of rifapentine after a high fat meal is 24% higher than exposure after a 900-mg dose under fasting conditions. While higher rifapentine exposure may be beneficial in enhancing the efficacy of regimens, there is concern that the risk of adverse events is increased (Bock et al. 2002). Thus, rigorous trials of a new dosing regimen would include proof of efficacy and safety when rifapentine is taken with and without food, as is likely to occur under operational conditions.

6.5 Conclusion

In conclusion, as rifapentine has dose-related activity, concomitant food should be considered when evaluating optimal rifapentine doses in rifapentine -based regimens. The effects of rifapentine should be evaluated under the meal conditions that can feasibly be provided by tuberculosis control programs in high-burden countries; in many settings provision of meals may be an unrealistic expectation.

7 Moxifloxacin Population Pharmacokinetics in Patients with Pulmonary Tuberculosis and the Effect of Intermittent High-Dose Rifapentine

7.1 Introduction

The duration of standard therapy for pulmonary tuberculosis is at least 6 months, and direct observation of treatment doses is promoted to support treatment adherence. Strategies aiming to shorten the duration of treatment or reduce the frequency of treatment doses are desirable. Rifapentine has a long half-life (Burman et al. 2001) and has superior *in vitro* activity against *Mycobacterium tuberculosis* compared to rifampin (Heifets et al. 1990). Moxifloxacin has demonstrated potent bactericidal and sterilizing activity against *M. tuberculosis in vitro* and in mouse models (Hu et al. 2003, Ji et al. 1998). Like rifapentine, moxifloxacin has a long half-life (9 to 12 h) (Dooley et al. 2008, Siefert et al. 1999), making it an attractive companion drug to prevent selection of rifapentine-resistant strains when the drugs are administered intermittently. However, moxifloxacin is a substrate of p glycoprotein (Brillault et al. 2009), sulfotransferases (Senggunprai et al. 2009), and glucuronosyltransferases (Tachibana et al. 2005), which may be induced by rifapentine, thus potentially reducing systemic concentrations of moxifloxacin.

The aim of this study was to investigate the effects of rifapentine on moxifloxacin pharmacokinetics, 28 adults diagnosed with pulmonary tuberculosis who were participating in the RIFAQUIN study at the study site in Worcester, South Africa, were enrolled.

7.2 Setting and Study Design

This analysis was a sub-study of RIFAQUIN study detailed in Section 4.2.3. Separate written informed consent for the pharmacokinetic study was obtained from RIFAQUIN study participants who were randomized to the two investigational arms with continuation-phase regimens of 1,200 mg rifapentine and 400 mg moxifloxacin once weekly or 900 mg rifapentine and 400 mg moxifloxacin twice weekly. The study protocol was reviewed and approved by the Research Ethics Committee of the University of Cape Town and the Medicines Control Council of South Africa. Plasma concentration data were collected during coadministration of moxifloxacin and rifapentine in the fourth month of tuberculosis treatment and again after a single 400-mg moxifloxacin dose 4 to 8 weeks after completion of tuberculosis treatment. At each occasion, blood samples were collected immediately before and at 1, 3, 5, 7, 10, 12, 26, and 50 h after the dose.

After blood collection, plasma was separated and immediately stored at -80°C. Moxifloxacin concentrations were determined using LC-MS/MS as previously described section 4.3. The lower limit of quantification was 0.063 mg/L

7.3 Population Pharmacokinetic analysis

Moxifloxacin plasma concentration-time data were determined using LC-MS/MS as previously described in Section 4.3. The lower limit of quantification was 0.063 mg/L. The methodology applied for model building has been described in section 4.5.3. Allometric scaling was explored using either WT, FFM or NFM (calculated separately for each sampling period) on CL/*F*, Q/F, *V*c/*F*, and Vp/F according to Anderson and Holford (Anderson & Holford 2008, 2009). The use of allometric scaling was evaluated as described under section 4.5.3 as shown below:

$$CL_i = CLstd \cdot (WT_i/52)^{0.75}$$

$$V_i = Vstd \cdot (WT_i/52)^{1}$$

where CL_i is the scaled typical value of CL/F for individual i, CLstd is its typical CL for an individual of median weight of 52 kg in the patient population. A similar notation applies to V_i. For a two-compartment model, allometric scaling was also applied on Q and Vp. NFM, FFM and FAT were tested through allometric scaling instead of total body weight.

The FFM was calculated as follows according to Janmahasatien et al (Janmahasatian et al. 2005):

$$FFM = \frac{WHSMAX_{MAX} \times HT^2 \times WT}{WHS_{50} \times HT^2 + WT}$$

where for females $WHSMAX_{MAX}$ = 37.99 and WHS_{50}=35.98 and for males $WHSMAX_{MAX}$ = 42.92 and WHS_{50}=30.93, and HT is height (m) and WT is total body weight (kg). Then $NFM = FFM + ffat(WT - FFM)$. $ffat$ is parameter-specific fat fraction associated with size. If $ffat$ is 1 then WT is used for allometric scaling, if $ffat$ is zero (0) then FFM is used.

The effect of presence of rifapentine was parameterised as presence or absence of rifapentine. The following equation was used:

$$PAR = \theta_P \times (1 + \theta_{cov} \times (COV))$$

where θ_{cov} fractional change in typical value (θ_p) of PAR due to presence of covariate (COV) . The covariate relationships were tested in the model by stepwise addition using a change in objective function value (ΔOFV) of ≥3.84 ($P \leq 0.05$) as the

cutoff for inclusion, followed by stepwise deletion using an ΔOFV of ≥6.83 ($P \leq$ 0.01) for covariate retention.

7.4 Results

The median (5^{th} and 95^{th} percentiles) age, weight, and height of the study patients were 40 (21, 51) years, 52 (42, 71) kg, and 163 (154, 176) cm, respectively.

The pharmacokinetics of moxifloxacin was best described by a model with transit absorption compartments (Savic et al. 2007). The introduction of a second compartment to which distribution appears relatively late (Figure 7.1) resulted in ΔOFV of 99.8 points. The final structural model is represented in Figure 7.1.

Allometric scaling using FFM gave the best fit and was applied on CL/F, Q/F,Vc/F, and Vp/F. Inclusion of the effect of rifapentine on moxifloxacin CL/F further improved the fit (ΔOFV = −29 points) and reduced the IOV in bioavailability from 22.9% to17.5%. Parameter estimates of the final moxifloxacin model are shown in Table 7.1. The co-administration of intermittent high-dose rifapentine increased the CL/*F* of moxifloxacin by 8%, corresponding to a reduction in the AUC from 0 h to infinity hours ($AUC_{0-\infty}$) of approximately the same magnitude (Table 7.2). A one-compartment model was previously used to describe moxifloxacin pharmacokinetics (Peloquin et al. 2008) and reported a somewhat lower half-life (6.53 h), CL/*F* (6.66 liters/h), and apparent volume of distribution (62.79 liters); these differences are probably largely due to a different study design and model structure. Appendix 5 summarises the run record and also shows the control stream of final moxifloxacin pharmacokinetic model. Table 7.2 shows pharmacokinetic values for different moxifloxacin dosing regimens.

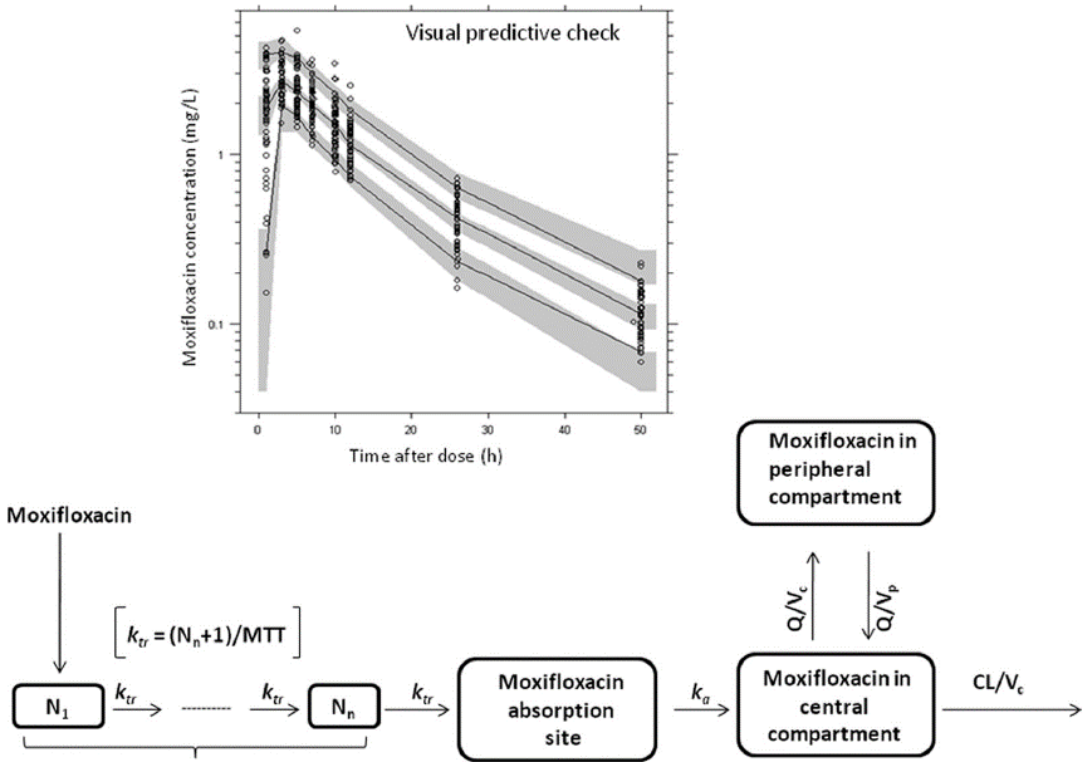

Figure 7.1: Illustration of the final moxifloxacin pharmacokinetic model (bottom). N_1 to $N_n$represents a series of hypothetical transit compartments used to model the delay in onset of absorption, and k_{tr} is the transit rate constant. k_a is the absorption rate constant from the hypothetical drug absorption site (depot) compartment to plasma. V_c, V_p, CL, and Q are the central and peripheral volumes of distribution and the oral and intercompartmental clearance, respectively. (Top) Visual predictive check of the final moxifloxacin pharmacokinetic model. The lower, middle, and upper solid lines are the 5th percentiles, medians, and 95th percentiles of the observed data, respectively. The shaded areas are the 95% confidence intervals for the 5th percentile, median, and 95th percentile of the simulated data. The open black circles are the observed concentrations.

Table 7.1: Parameter estimates of the final moxifloxacin pharmacokinetic model[a]

Parameter	Estimate (RSE [%])	IIV[b] (RSE [%])	IOV[c] (RSE [%])
TV[CL/F] (L/h)	8.50 (4.9)	12.6 (28.1)	
V_c/F (L)	114 (4.0)		
ka (h^{-1})	1.85 (22.3)		74.7 (31.0)
MTT (h)	0.483 (22.4)		70.4 (27.0)
NN	22.5 (44.9)		
Q/F (L/h)	2.90 (12.1)		
V_p/F(L)	41.6 (9.1)		
F	1.00		17.5 (16.3)
EFF_{RFP} (%)[d]	8.03 (21.5)		
$t_{1/2}$[e] (h)	9.23		
Additive residual error (mg/L)	0.0189 (19.5)		
Proportional residual error (%)	8.94 (4.7)		

[a]RSE, relative standard error reported on standard deviation scale (it is approximate for IIV and IOV); CL/F, oral clearance; V_c/F, apparent volume of distribution of the central compartment; k_a, first-order absorption rate constant; MTT, absorption mean transit time; NN, number of hypothetical transit compartments; Q/F, inter-compartmental clearance; V/F_p, apparent volume of distribution of the peripheral compartment; F, oral bioavailability fixed to 1. [b]IIV, inter-individual variability expressed as approximate percent coefficient of variation (% CV). [c]IOV, inter-occasional variability expressed as approximate % CV; [d]CL/F, $TV[CL/F]\cdot(1+EFF_{RFP})$ where TV[CL/F] is the typical value of moxifloxacin CL/F when not coadministered with rifapentine, while EFF_{RFP} is the fractional change in CL/F due to the coadministration of rifapentine; [e]$t_{1/2}$= calculated population elimination half-life when moxifloxacin is not coadministered with rifapentine.

Table 7.2: Pharmacokinetic values for different moxifloxacin dosing regimens

Regimen	Median Cmax[a] (mg/liter), (range)	Median AUC[b] (mg·h/liter) (range)	Number of Participants
Moxifloxacin alone (single dose)	3.8 (2.1,4.6)	50.8 (31.8,65.3)	27
Moxifloxacin once weekly[c]	2.9 (2.0,3.8)	46.2 (29.5,60.6)	13
Moxifloxacin twice weekly[c]	2.8 (2.0,4.5)	45.3 (26.8,65.3)	15

[a]Cmax, maximum plasma concentration; [b]AUC, area under concentration-time curve; [c]moxifloxacin coadministered with rifapentine

7.5 Discussion

This study found that high-dose intermittent rifapentine increased the CL/*F* of moxifloxacin by only 8% (Table 7.2). A direct effect on bioavailability was tested but did not reach statistical significance. The extent of interaction in our study was lower than the 17.2% decrease in moxifloxacin exposure previously reported in healthy volunteers dosed three times a week (Dooley et al. 2008). The discrepancy between these results may be due to differences in physiology between tuberculosis patients and healthy volunteers with respect to the activity of drug-metabolizing enzymes, genetic differences in the study population, or the different dosing strategies. Carry-over effects due to multiple dosing of moxifloxacin during rifapentine administration are unlikely to have affected the results, as predose moxifloxacin concentrations were below the validated range in all patients but two (both received twice-weekly doses, and they had predose concentrations of 0.088 and 0.066 mg/L, respectively). The induction effect of rifapentine on moxifloxacin in this current study was less than that of 450 mg of rifampin dosed three times weekly (Nijland et al. 2007), possibly due to different dosing frequencies. Interestingly, Bliven-Sizemore et al. recently showed

that rifapentine in doses of 10 to 20 mg/kg is as potent an inducer of CYP3A as rifampin (Bliven-Sizemore et al. 2011), all dosed daily. The difference in moxifloxacin exposure or clearance between the regimens used in this current study was not detectable. Importantly, the results in this study showed that rifapentine and moxifloxacin can be used together but the results may not be applicable to other scenario where these drugs are administered more frequently. For these results to be generally applicable to all regimens being currently being contemplated, more studies are needed evaluate the autoinductive effect of rifapentine when administrated more frequently and at different doses, and the extent to which it affect the exposures of moxifloxacin.

7.6 Conclusion

In summary, moxifloxacin exposures were not affected by high doses of rifapentine given to tuberculosis patients in once- or twice-weekly doses, and the potential pharmacokinetic interaction is unlikely to affect treatment outcomes.

8 Moxifloxacin population pharmacokinetics and model-based comparison of efficacy between moxifloxacin and ofloxacin in African patients

8.1 Introduction

Fluoroquinolones play an important role in the treatment of MDR-TB (Falzon et al. 2011) which is defined by resistance to both rifampicin and isoniazid (WHO 2008a). Fluoroquinolones differ from each other in their efficacy against *M.tuberculosis* as measured by the ratio of $fAUC_{0\text{-}24}$/MIC, and also display differences in their clinical pharmacokinetics. The *in vitro* bactericidal activity of moxifloxacin against *M.tuberculosis* is superior to that of ofloxacin (Hu et al. 2003); its improved potency has also been confirmed in mice (Yoshimatsu et al. 2002). The substitution of ethambutol by moxifloxacin, but not ofloxacin, in combination with isoniazid, rifampicin and pyrazinamide in the treatment of susceptible tuberculosis, resulted in faster culture conversion (Conde et al. 2009, Rustomjee et al. 2008). New fluoroquinolones are usually preferred to the earlier-generation ones (WHO 2011), but ofloxacin is still widely used to treat MDR-TB, because of its affordability and availability.

Moxifloxacin is rapidly absorbed and the major fraction of the dose reaches the systemic circulation within 2 h (Dooley et al. 2008, Siefert et al. 1999). It has a long half-life in humans (Dooley et al. 2008, Siefert et al. 1999) with moderate renal excretion of 6-20% of total elimination after intravenous administration (Siefert et al. 1999). Moxifloxacin is a substrate of inducible P-gp (Brillault et al. 2009), sulfotransferases (Senggunprai et al. 2009), and glucuronosyltransferases (Tachibana et al. 2005). Co-administration of moxifloxacin with rifapentine (enzyme and

transporter inducer) gave 17.2% (Dooley et al. 2008) and 8% (Next section of results (Zvada et al. 2012)) decrease in moxifloxacin exposure in healthy volunteers (dosed three times a week) and tuberculosis patients (dosed once/twice weekly), respectively. Ofloxacin is rapidly absorbed with peak concentrations reached within 2 h and with a half-life of 6 h, which is comparable between healthy volunteers (Yuk et al. 1991) and patients (Belousov et al. 1996). Ofloxacin is primarily renally eliminated (Lode et al. 1987); its concentrations were reported to increase linearly with dose, but elimination of ofloxacin decreases with declining renal function and increasing age (Stambaugh et al. 2002).

The critical concentration for drug susceptibility is defined as the lowest concentration of a drug that inhibits ≥95% of wild-type strains lacking acquired or mutational resistance mechanisms to the specific drug (Canetti et al. 1969). Accordingly, the WHO recommends susceptibility testing breakpoint concentrations for moxifloxacin and ofloxacin of 0.25 and 2.0 mg/L, respectively (WHO 2008b). The efficacy of fluoroquinolones has been related to the $f\text{AUC}_{0\text{-}24}$/MIC (Shandil et al. 2007). Based on *in vitro*, murine, and clinical studies, a $f\text{AUC}_{0\text{-}24}$/MIC ratio of at least 100–125 has been proposed as reliable predictor of bactericidal activity against gram-positive and gram-negative bacteria (Schentag et al. 2003a,b). The HFS has suggested a minimum target $f\text{AUC}_{0\text{-}24}$/MIC ratio of 53 for *M.tuberculosis* as the identified target for suppressing the outgrowth of moxifloxacin-resistant mutants and not necessarily optimal bactericidal activity (Gumbo et al. 2004).

This study aimed to describe the population pharmacokinetics of moxifloxacin using data from 241 South African and Zimbabwean patients with pulmonary tuberculosis

who participated in the RIFAQUIN study (Section 4.2.3). Monte Carlo simulations were then employed to assess the probability of reaching the *f*AUC_{0-24}/MIC target using moxifloxacin and ofloxacin at the recommended doses for MDR-TB (WHO 2008a). For ofloxacin pharmacokinetics we used a population model that we reported previously (Chigutsa et al. 2012), while the MIC distribution of moxifloxacin and ofloxacin for drug-resistant *M.tuberculosis* isolates were previously determined (Sirgel et al. 2012).

8.2 Setting and Study Design

This analysis was a sub-study of RIFAQUIN study described in Section 4.2.3. Patients (n=241) with pulmonary TB received an initial intensive phase of therapy including daily rifampicin and moxifloxacin for 2 months. For the continuation phase they were treated with either 400 mg moxifloxacin once weekly together with 1200 mg rifapentine or 400 mg moxifloxacin twice weekly with 900 mg of rifapentine. Pharmacokinetic sampling was carried out during the 4th month of therapy. The doses of rifapentine and moxifloxacin were taken with 240 mL of water 15 minutes after the patients received 2 hard-boiled eggs with bread. Four hours after dosing, a light meal, snacks and fluids were provided. Pharmacokinetic samples were obtained immediately before dosing and at 1, 2, 3, 5, 7, 10, 12, 26 and 50 h after the dose in 28 patients. In the remaining 213 patients samples were obtained at 2 (± 0.5) h, 5 (± 0.5) h, and 24 (± 3) h or 48 (± 3) h after dosing. HIV positive patients who required antiretroviral treatment at randomisation were excluded. Separate written informed consent for the pharmacokinetic study was obtained from the RIFAQUIN study participants in Harare (Zimbabwe), and Johannesburg (Gauteng) and Worcester (Western Cape, South Africa). The study protocol was reviewed and approved by the

London-Surrey Borders Research Ethics Committee (ref: 07/Q0806/58), the Research Ethics Committee of the University of Cape Town, the Medicines Control Council of South Africa, the Medicines Research Council of Zimbabwe, and the Medicines Control Authority of Zimbabwe. After blood collection, plasma was separated and immediately stored at -80°C, and moxifloxacin concentrations were determined using LC-MS/MS as previously described in Section 4.3. The lower limit of quantification was 0.063 mg/L. The MICs of Clinical isolates are shown in Table 8.1. MICs of moxifloxacin and ofloxacin were determined for 197 drug-resistant *M.tuberculosis* isolates from patients in the Western Cape, South Africa by BACTEC MIGIT 960 as previously described in Section 4.2.4. The 0.25 mg/L and 2.0 mg/L concentrations of moxifloxacin and ofloxacin were used as susceptibility breakpoints to differentiate between susceptible and resistant strains as suggested by WHO (WHO 2008b).

8.2.1 Population pharmacokinetic analysis.

The methodology applied for model building has been described in Section 4.5.3 (Population pharmacokinetic analysis). In addition, a lognormal distribution for IIV was assumed and additive and/or proportional models for the RUV were evaluated. LLOQ data were modelled using the M3 method (Bergstrand & Karlsson 2009). The tested covariates included age, HIV status, sex, site, and regimen/arm (once weekly vs. twice weekly). The detected covariate effects were included in the final model if clinically significant (a cut-off of 20% change in the fixed effect of parameter value was used).

Table 8.1: The MIC distribution of moxifloxacin and ofloxacin in 197 *Mycobacterium tuberculosis* isolates

*Resistance Profiles	MIC (mg/L)									
	≤0.125	>0.125 ≤0.25	>0.25 ≤0.5	>0.5 ≤1.0	>1.0 ≤2.0	>2.0 ≤4.0	>4.0 ≤6.0	>6.0 ≤8.0	≥10.0	Total Isolates
Moxifloxacin										
INH	68									68
RIF	5									5
MDR	55	2	1							58
MDR+INJ	12	2	3							17
MDR+FLQ				3	2					5
XDR		2	1	17	22	2				44
Ofloxacin										
INH			59	9						68
RIF			5							5
MDR			47	9	1	1				58
MDR+INJ			9	2	6					17
MDR+FLQ						3		1	1	5
XDR					1	10	6	10	17	44

*Resistance Profiles: Resistance to either isoniazid (INH) or rifampicin (RIF) is mono-resistance; MDR is resistance to both INH and RIF; MDR+INJ, MDR plus resistant to an injectable; MDR+FLQ, MDR plus resistant to either fluoroquinolone; XDR is MDR plus resistance to both a FLQ and an injectable

Precision of parameter estimates were obtained from a non-parametric bootstrap (N=200). The use of allometric scaling was evaluated as described under section 4.5.3. The following equation was used for allometric scaling:

$$CL_i = CLstd \cdot (WT_i/55.8)^{0.75}$$

$$V_i = Vstd \cdot (WT_i/55.8)^{1}$$

where CL_i is the scaled typical value of CL/F for individual *i*, CLstd is its typical CL for an individual of median weight of 55.8 kg in the patient population. A similar notation applies to V_i. For a two-compartment model, allometric scaling was also applied on Q and Vp. NFM, FFM and FAT were tested through allometric scaling instead of total body weight. The FFM was calculated as follows according to Janmahasatien et al (Janmahasatian et al. 2005):

$$FFM = \frac{WHSMAX_{MAX} \times HT^2 \times WT}{WHS_{50} \times HT^2 + WT}$$

where for females $WHSMAX_{MAX}$ = 37.99 and WHS_{50}=35.98 and for males $WHSMAX_{MAX}$ = 42.92 and WHS_{50}=30.93, and HT is height (m) and WT is total body weight (kg). Then $NFM = FFM + ffat(WT - FFM)$. $ffat$ is parameter-specific fat fraction associated with size. If $ffat$ is 1 then WT is used for allometric scaling, if $ffat$ is zero (0) then FFM is used.

8.2.2 Pharmacokinetic simulations and probability of target attainment

The final pharmacokinetic model was used to perform Monte Carlo simulations in 10,000 individuals after multiple daily doses of 400 mg moxifloxacin to obtain steady-state $f\text{AUC}_{0\text{-}24}$. Daily doses of 800 mg of moxifloxacin were also explored. The simulated $f\text{AUC}_{0\text{-}24}$ were obtained by using covariate distributions similar to the population on which the model was developed, and assuming 50% plasma protein

binding for moxifloxacin (Andersson & MacGowan 2003, Siefert et al. 1999, Zhanel et al. 2002). Similar simulations were performed to obtain the *f*$AUC_{0\text{-}24}$ for ofloxacin using a previously published model, developed from South African patients with MDR-TB (Chigutsa et al. 2012), using unbound fraction of 0.75 in humans (Lode et al. 1987).The estimated *f*$AUC_{0\text{-}24}$/MIC ratios were obtained dividing *f*$AUC_{0\text{-}24}$ by MICs ranging from 0.125 to 8 mg/L. MIC distributions of moxifloxacin and ofloxacin of drug-resistant *M.tuberculosis* isolates were from a separate study in patients from the Western Cape, South Africa (Sirgel et al. 2012). For the comparison we used targets *f*$AUC_{0\text{-}24}$/MIC ≥100 and *f*$AUC_{0\text{-}24}$/MIC ≥53. The probability of target attainment (PTA) was calculated as the proportion of individuals achieving *f*$AUC_{0\text{-}24}$/MIC ≥100 (or ≥53) for a specific MIC. The cumulative fraction of response (CFR) (Mouton et al. 2005) was calculated as the weighted average of the PTA across the MIC strata, as shown below:

$$CFR = \sum_{i=1}^{n} PTA(MIC_i) \cdot p(MIC_i) \qquad (1)$$

The PTA at each MIC_i level was multiplied by the relative frequency of that MIC in the study population, $p(MIC_i)$. The used in this current analysis was target was CFR ≥90%.

8.3 Results

Although the RIFAQUIN study patients had drug-susceptible pulmonary tuberculosis, while the patients in the ofloxacin pharmacokinetic study had MDR-TB, their demographic and patient characteristics were similar, and only differed by HIV status and sex (Table 8.2). The 241 patients on moxifloxacin provided 856 concentration-time points and only 4% were below LLOQ. Similar to other analysis (Zvada et al. 2012), the

population pharmacokinetics of moxifloxacin was well described by a two-compartment model with first-order elimination and transit absorption compartments.

Table 8.2: Characteristics of patients who received moxifloxacin in the RIFAQUIN trial, and those who were on ofloxacin in a previous study

[a]Variable	Patients on Moxifloxacin (Jindani et al. 2013, RIFAQUIN 2008, Zvada et al. 2012)	Patients on Ofloxacin N=65 (Chigutsa et al. 2012)
Number of patients	241	65
Males (%)	153 (63)	52 (80)
HIV+ (%)	46 (19)	35 (54)
Median age, range (years)	31.8 (18.5, 79.5)	34 (19, 70)
Median weight, range (kg)	55.8 (37.7, 77.9)	55 (35, 91.8)
Median height, range (cm)	177 (143, 190)	167 (127, 189)
BMI, range (kg/m^2)	17.8 (10.4, 38.0)	19.3 (12.4, 39.3)
Patients on twice weekly doses (%)	114 (47)	N/A

[a]HIV+, patients infected with Human immunodeficiency virus (HIV); BMI, body mass index

FFM was used for allometric scaling of CL, Q and Vc, while Vp was better scaled with FAT. The final parameter estimates are shown in Table 8.3 and a VPC of the final model is shown in Figure 8.1. No significant difference in the pharmacokinetic parameters was found between the once and twice weekly dosing approaches, and no additional covariates were included except for body size, which was incorporated via allometric scaling. The Monte Carlo simulations predicted a median $AUC_{0\text{-}24}$ of 38.7 after 400 mg daily moxifloxacin, while the 2.5^{th} and 97.5^{th} percentiles were 21.9 and 69.6 mg·h/L, respectively. Appendix 5 summarises the run record and also shows the control stream of final moxifloxacin pharmacokinetic model.

Table 8.3: Final parameter estimates for moxifloxacin population pharmacokinetic model

Parameter	Typical value (RSE[%])[a]	IIV [b] (RSE[%])[a]
CL (L/h)[d]	10.6 (2.68)	18.7 (4.05)
Vc (L)[e]	114 (1.36)	
ka (h^{-1})[f]	1.50 (2.15)	69.9 (3.62)
MTT (h)[g]	0.723 (7.02)	73.4 (2.58)
Number of transit compartments	11.6 (2.39)	
Q (L/h)[h]	2.14 (2.92)	32.9 (3.17)
Vp (L)[i]	89.8 (3.66)	
F[j]	1 FIX	17.7 (3.28)
Proportional error (%)	7.85 (1.44)	

[a]RSE, relative standard error reported on the approximate standard deviation scale obtained from a bootstrap sample size of 200; [b]IIV, inter-individual variability expressed as percent coefficient of variation (% CV); [c]CL, oral clearance; [d]Vc, volume of distribution in the central compartment; k_a, first-order absorption rate constant; [f]MTT, absorption mean transit time; [g]Q, inter-compartmental clearance; [h]Vp, volume of distribution in the peripheral compartment; [i]F, oral bioavailability fixed to 1 since we do not have intravenous injection data; In this table the values of parameters directly estimated by the model; To obtain CL/F, the values of CL must be combined with those of F. Since the typical value of F was fixed to 1, the typical value of CL/F has the same value as CL, while the BSV of CL/F needs to keep into account both the BSV in CL and that in F. A similar consideration is valid for Vc/F, Q/F, and Vp/F.

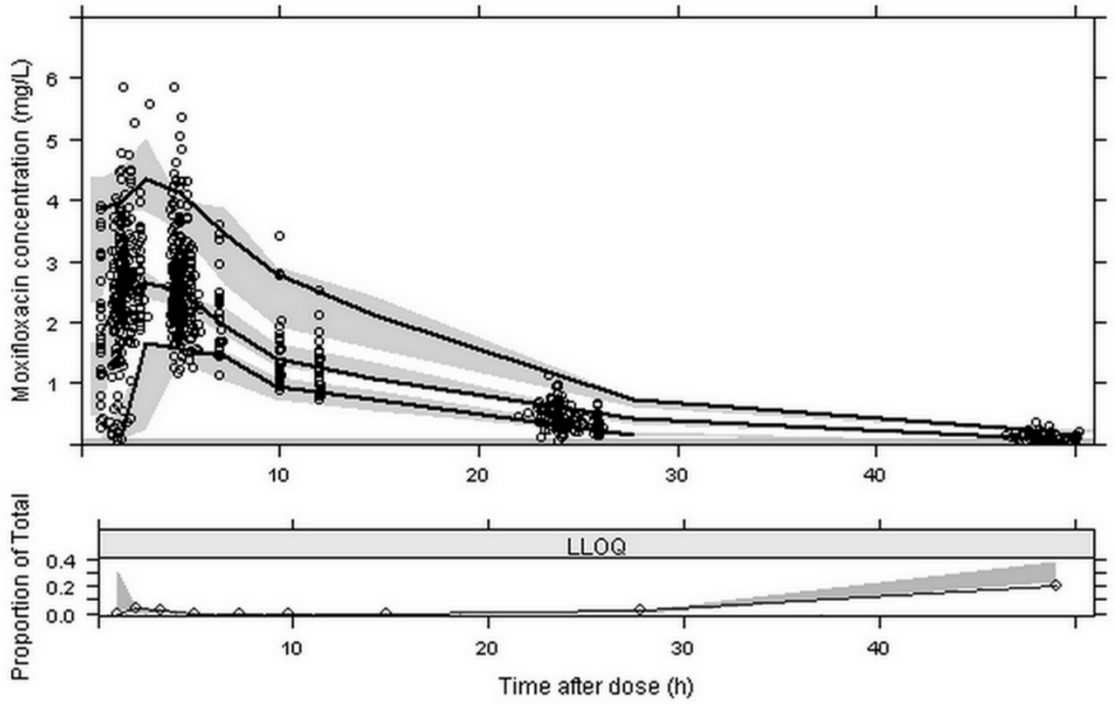

Figure 8.1: Visual predictive check (VPC) for the final moxifloxacin population pharmacokinetic model. In the upper panel, the lower, middle and upper solid lines are the 2.5th, median, and 97.5th percentiles of the observed plasma concentration, respectively, while the shaded areas are the 95% confidence intervals for the same percentiles of the simulated data. The lower panel shows the fraction of observed data below lower limit of quantification (LOQ) which is represented by the solid line. The shaded area shows simulation based 95% confidence interval around the median of LOQ data.

The MIC distributions of moxifloxacin and ofloxacin are listed in Table 8.1. The PTA values for $f\text{AUC}_{0\text{-}24}$/MIC ratio of $\geq$53 and $\geq$100 for both moxifloxacin and ofloxacin are shown in Table 8.4 and corresponding plots are shown in Figure 8.2. The PTA with a target $f\text{AUC}_{0\text{-}24}$/MIC ratio of $\geq$53 across the range of MIC values for daily 400 mg and 800 mg moxifloxacin doses is shown in Figure 8.3, while PTA for daily 800 mg ofloxacin for target 53 and 100 together with range of MIC values is shown in Figure 8.4.

Table 8.4: PTA values of ofloxacin and moxifloxacin for different target ratios

	Target 53		Target 100	
MIC	Ofloxacin	Moxifloxacin	Ofloxacin	Moxifloxacin
0.125	1	1	1	0.970954
0.25	1	0.946058	0.96	0.286307
0.5	1	0.215768	0.51	0
1	0.94	0	0.1	0
2	0.48	0	0	0
4	0.07	0	0	0
8	0	0	0	0

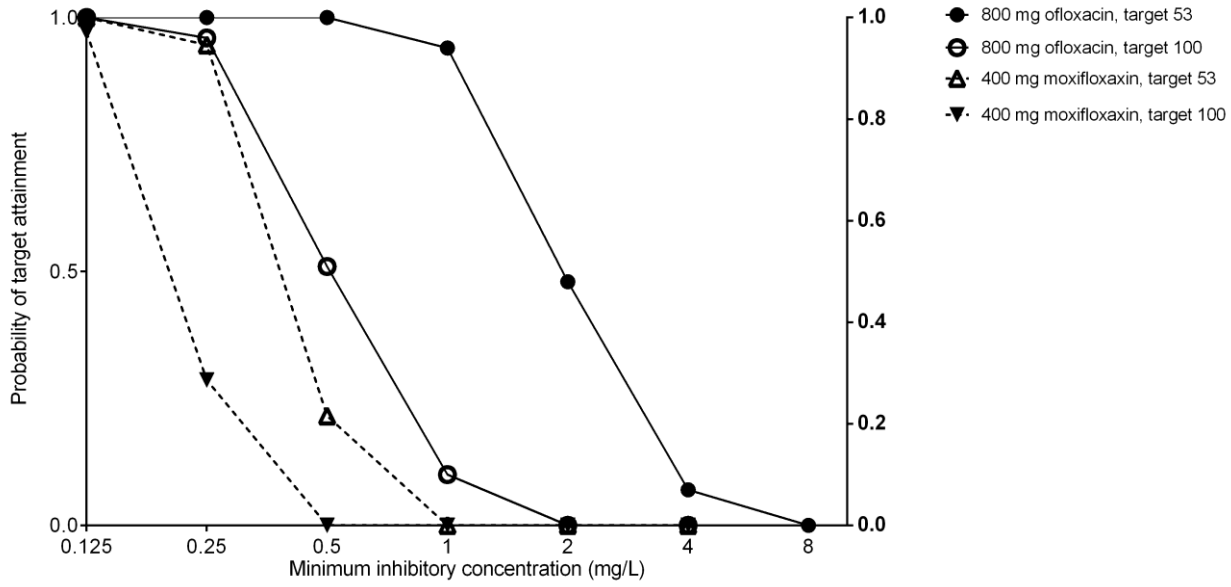

Figure 8.2: Probability of target attainment for 400 mg moxifloxacin and 800 mg ofloxacin.

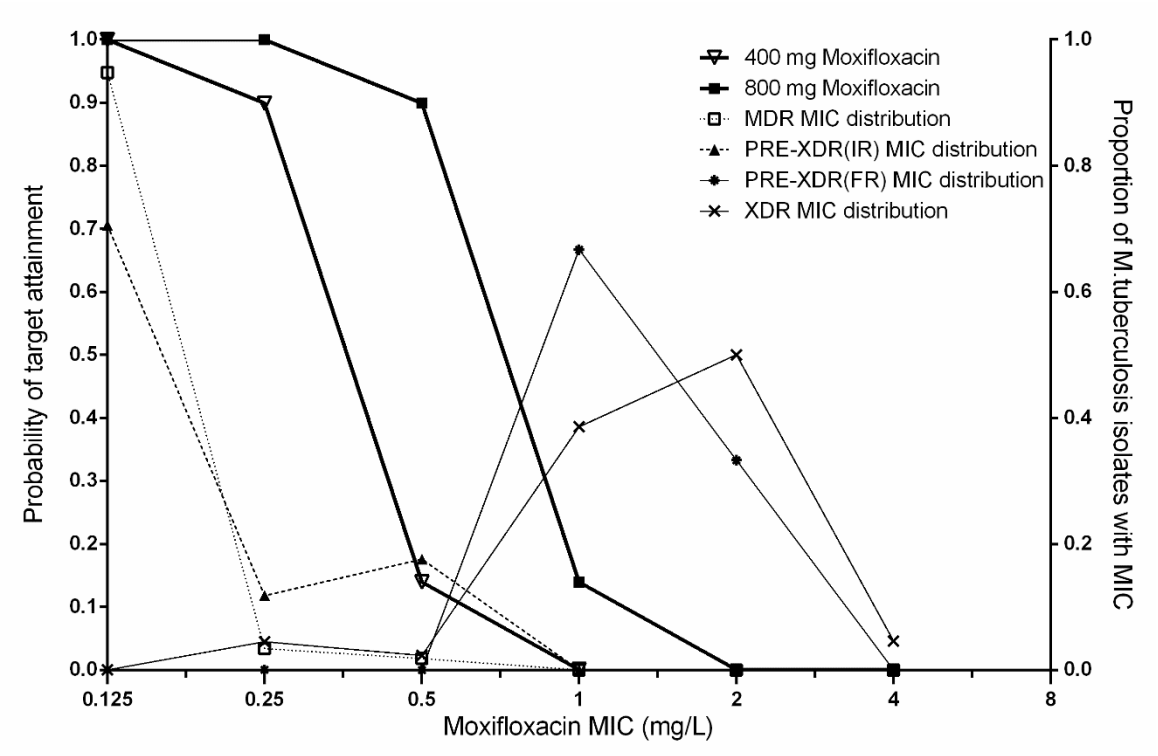

Figure 8.3: Probability of target attainment (target *f*$AUC_{0\text{-}24}$/MIC≥ ratio 53) versus *Mycobacterium tuberculosis* isolates minimum inhibitory concentrations (MIC) for 400 mg and 800 mg moxifloxacin dose. MDR and XDR are MIC distributions from multidrug resistant and extensive drug resistant isolates, respectively. MDR+INJ and MDR+FLQ are MIC distributions from isolates resistant to injectables and fluroroquinolones, respectively. The distributions of these MICs are represented by right side y-axis.

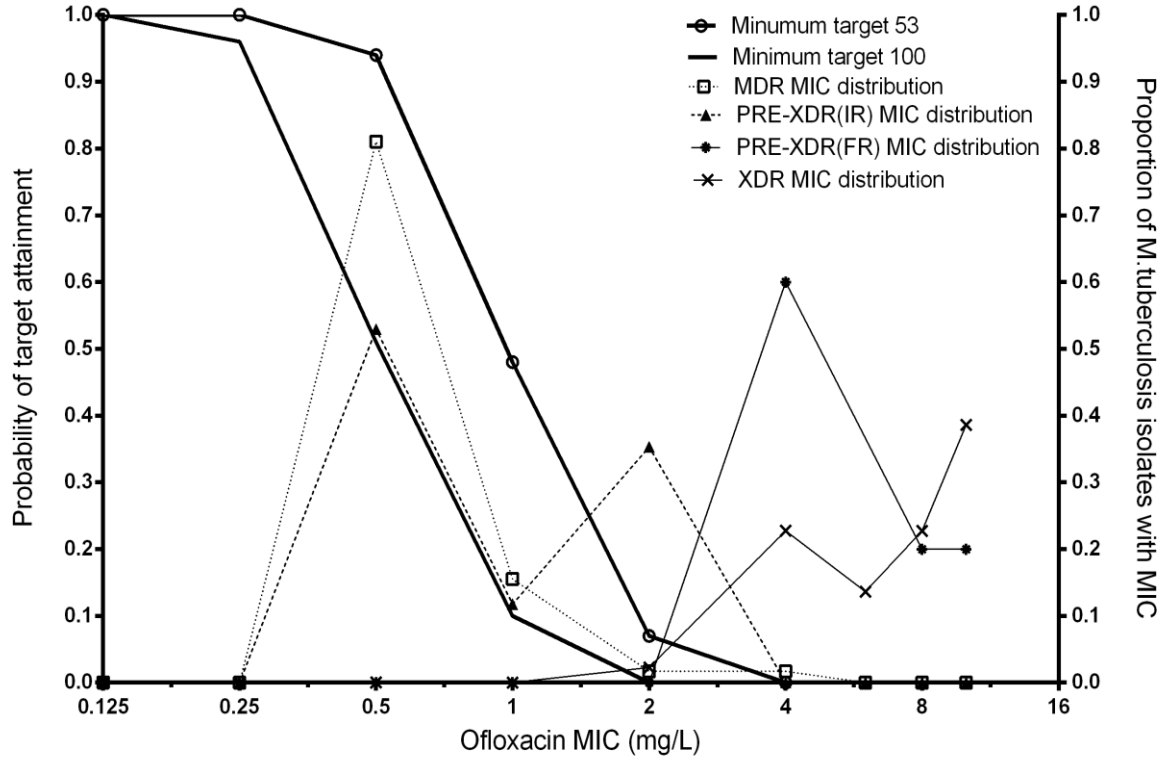

Figure 8.4: Probability of target attainment (target $f\text{AUC}_{0\text{-}24}$/MIC≥ ratio 53 or 100) versus *Mycobacterium tuberculosis* isolates minimum inhibitory concentrations (MIC) for 800 mg ofloxacin dose. MDR and XDR are MIC distributions from multidrug resistant and extensive drug resistant isolates, respectively. MDR+INJ and MDR+FLQ are MIC distributions from isolates resistant to injectables and fluroroquinolones, respectively. The distributions of these MICs are represented by right side y-axis.

Table 8.5 shows the CFR for daily 400 mg and 800 mg moxifloxacin, and daily 800 mg ofloxacin with a target $f\text{AUC}_{0\text{-}24}$/MIC of either $\geq$53 or $\geq$100. Moxifloxacin 400 mg had higher CFR than ofloxacin 800 mg in both scenarios (target ratio of 53 or 100).

Table 8.5: The cumulative fraction of response (CFR) for daily doses of 400 mg and 800mg moxifloxacin, and 800 mg ofloxacin for target *f*AUC_{0-24}/MIC ratio of 53 (Gumbo et al. 2004) and 100 (Schaaf et al. 2009a, Schentag et al. 2003a,b)

M.tuberculosis strain	CFR expectation for 400 mg moxifloxacin	CFR expectation for 800 mg moxifloxacin	CFR expectation for 800 mg ofloxacin
fAUC_{0-24}/MIC≥53			
MDR	0.98	1.00	0.84
MDR+INJ	0.84	0.98	0.58
MDR+FLQ	0.00	0.09	0.00
XDR	0.04	0.12	0.00
fAUC_{0-24}/MIC≥100			
MDR	0.88	0.98	0.43
MDR+INJ	0.68	0.85	0.28
MDR+FLQ	0.00	0.00	0.00
XDR	0.01	0.04	0.00

MDR is resistance to both isoniazid (INH) and rifampicin (RIF); MDR+INJ, MDR plus resistant to an injectable; MDR+FLQ, MDR plus resistant to either fluoroquinolone; XDR is MDR plus resistance to both a FLQ and an injectable.

8.4 Discussion

The results of this analysis revealed that the CFR for 400 mg moxifloxacin was 98% versus 84% for 800 mg ofloxacin by using a target *f*AUC_{0-24}/MIC ratio of ≥53. With the more stringent target ratio of ≥100, the difference in the performance of the drugs was even more marked, and both regimens fell short of the 90% CFR threshold (the CFR for moxifloxacin was 88%, versus 43% for ofloxacin). On the other hand, with 800 mg doses of moxifloxacin in the same patients with MDR-TB and the target ratio of ≥100, a

CFR of 98% would be achieved (Table 8.5). The higher moxifloxacin dose (800 mg) also achieved the pharmacodynamic target ratio of ≥53 in 98% of MDR-TB patients with resistance to an injectable agent whereas the standard 400 mg dose had a marginal CFR of 84% (Table 8.5).

Moxifloxacin has structural differences to ofloxacin at the C-7 position that reduces the ability of the bacterium to efflux moxifloxacin across the cell wall, thus lowering the MIC. Moxifloxacin also has superior intracellular killing kinetics to ofloxacin. Experimental data show that moxifloxacin MICs in macrophages increased by only 2-fold when compared to MIC in extracellular broth, while 4-fold increases were demonstrated for ofloxacin (Shandil et al. 2007).

Using a target $f\text{AUC}_{0\text{-}24}$/MIC ≥53, the currently recommended 400 mg daily dose of moxifloxacin, obtained a PTA greater than 90% when the isolates had MICs ≤0.25 mg/L. On the other hand, ofloxacin failed to achieve a PTA of more than 90% when the MIC was >0.5 mg/L, as found in about 20% of the isolates, classified by standard procedures as resistant to rifampicin and isoniazid but not to injectable second line drugs (such as capreomycin, kanamycin or amikacin), or fluoroquinolones. Hence, findings in this study suggest that a 4-fold reduction in the susceptibility breakpoint for ofloxacin, which is currently set at 2.0 mg/L, may be warranted. However, clinical correlates for the $f\text{AUC}_{0\text{-}24}$/MIC targets are lacking for patients with tuberculosis, and using the target of 100 would suggest revision of the ofloxacin susceptibility breakpoint down to 0.25 mg/L. It should be noted that the target ratio of 53 which we used for comparison of fluoroquinolones was derived only for moxifloxacin and this value is not necessarily applicable to ofloxacin. The current doses for moxifloxacin (400 mg) and ofloxacin (800 mg) may thus be suboptimal for the treatment of drug-resistant tuberculosis if a pharmacodynamic target of $f\text{AUC}_{0\text{-}24}$/MIC ≥100 correlates better with successful clinical

outcomes. Simulations results in this study suggest susceptibility breakpoints of 0.125 mg/L for 400 mg doses of moxifloxacin and 0.25 mg/L for 800 mg ofloxacin. Doubling the dose of ofloxacin is unlikely to achieve acceptable PTA in many patients when a target of 100 and critical concentration of 2.0 mg/L are considered (Table 8.4, Figure 8.2) supporting previous findings (Chigutsa et al. 2012). On the other hand, simulations in this study show that doubling the moxifloxacin dose to 800 mg daily could lead to acceptable PTA (Table 8.4 and Figure 8.2-3), and this is consistent with previous reports (Gumbo et al. 2004). Higher doses of moxifloxacin may increase moxifloxacin side effects including QT interval prolongation (Falagas et al. 2007) and this concern is particularly serious, given the long duration of MDR-TB treatment. However, limited studies seem to suggest safety of higher doses. A recent study by Ruslami et al. (Ruslami et al. 2013) which evaluated daily 800 mg doses of moxifloxacin did not show increased toxicity, while a study by Alffenar et al. showed tolerability at 600 mg and 800 mg moxifloxacin (Alffenaar et al. 2009). An ongoing clinical trial by Alffenar et al. is evaluating the safety of moxifloxacin at escalated doses of 600 and 800 mg (NCT01329250: http://clinicaltrials.gov/show/NCT01329250).

The continued use of fluoroquinolones in suboptimal doses may hinder their use in the future due to the development of fluoroquinolone resistance (Ginsburg et al. 2003). The target $fAUC_{0\text{-}24}$/MIC ratio of $\geq$53 is based on studies showing suppression of resistance emergence with moxifloxacin monotherapy in a HFS (Gumbo et al. 2004). In this current study study, 400 mg moxifloxacin was shown to attain a CFR $\geq$90% for *M.tuberculosis.* strains resistant to isoniazid and rifampicin but not injectable agents, while ofloxacin at 800 mg daily did not. However, for MDR-TB strains resistant to injectable agents only the 800 mg daily doses of moxifloxacin achieved a CFR $\geq$90%.

The target ratio ≥100 is based on review on studies in gram-positive and gram-negative bacteria conducted in animals (Schentag et al. 2003a) and humans (Schentag et al. 2003b). In patients, values of 125–250 were associated with clinical cure and speed of bacterial eradication for gram-negative infections of the respiratory tract (Forrest et al. 1993), and the target value of >100 was linked to decreased emergence of bacterial resistance (Thomas et al. 1998). For gram-negative organisms, a target of 100–125 achieved acceptable activity, although more rapid eradication was achieved with a target *f*AUC_{0-24}/MIC ratio of ≥250 (Forrest et al. 1993), when ciprofloxacin, grepafloxacin, levofloxacin, and gatifloxacin were evaluated. Considering sterilizing activity including killing of the *M.tuberculosis* within macrophages, the target of 100 may be more appropriate, as penetration to the site of action should be considered (Shandil et al. 2007). Fluoroquinolones generally achieve higher concentrations in epithelial lining fluid (ELF) than in plasma (Kiem & Schentag 2008), which means that the PTA and CFR is this study would be higher at the site of action than when plasma concentrations are used. Compared with other fluoroquinolones, moxifloxacin has been found to have greater efficacy than levofloxacin in mice despite a lower plasma AUC/MIC ratio (Ahmad et al. 2013), presumably due to higher intracellular concentrations of moxifloxacin. Levofloxacin, however, penetrates into cerebrospinal fluid of patients with tuberculosis meningitis better than ciprofloxacin and gatifloxacin (Thwaites et al. 2011). In comparison to another moxifloxacin population pharmacokinetic model (Peloquin et al. 2008), we found a reduced IIV on V, but significant IIV on CL and F. In this current study, estimate of CL was 25% higher than that reported by Peloquin et al.; this may be due to the different the study population, but it may also be a consequence of the differences in dosing schedules, sampling times and the structural model used to interpret the data.

8.4.1 Limitations

Due to limited sample size, the MIC data in this analysis may not represent the true distribution for some drug-resistance categories. The *M.tuberculosis* isolates used to determine the MICs originated from patients in the same region as those contributing data to the pharmacokinetic model (Table 8.1). Given the limited geographical distribution of the study population and *M.tuberculosis* isolates contributing to this current analysis, it cannot be assumed that the PTA and especially the CFR analyses will be applicable to other populations outside the region. In addition, this study compares the activities of moxifloxacin with ofloxacin using pharmacodynamic targets derived in experiments using the drugs alone, as monotherapy. Previous studies have shown that a combination of rifampicin (a rifamycin) and moxifloxacin suppresses resistance emergence, but at the price of slightly slowing bacterial kill (Balasubramanian et al. 2012, Drusano et al. 2010). Comparisons in this study did not take into account within regimen synergy or antagonism (Balasubramanian et al. 2012), although these effects are unlikely to differ considerably within the fluoroquinolone class. The pharmacodynamic targets used are based on experimental models which differ from the organism-drug interface in patients. Importantly, the diversity of the *M.tuberculosis* growth states encountered in patients is not accounted for. Moreover, this study assumed unbound plasma concentrations as a marker of exposure, while tissue free drug concentration, would be more appropriate.

8.5 Conclusion

This analysis which is based on the pharmacokinetic and drug susceptibility distributions in African patients indicate that, in currently used doses, moxifloxacin is more efficacious than ofloxacin for the treatment of MDR-TB. Doubling the dose of

moxifloxacin to 800 mg daily improves the CFR. However, further clinical studies are required to evaluate the safety and tolerability of moxifloxacin at higher doses.

9 Investigation of population pharmacokinetic summary variables of rifapentine and moxifloxacin as of predictors of treatment outcome

9.1 Introduction

The duration of standard therapy for tuberculosis of 6 month is lengthy. Novel regimens for the treatment of tuberculosis aiming at potentially reducing the duration of standard therapy from 6 months without compromising the efficacy of the drugs have been proposed based on mouse studies (Rosenthal et al. 2007). These novel combinations involve replacement of isoniazid with moxifloxacin in intensive and continuation phase, and replacement of rifampicin with high-dose daily or intermittent rifapentine in both intensive and continuation phase. The choice of replacing isoniazid with moxifloxacin was based on demonstrated potent bactericidal and sterilizing activity of moxifloxacin *in vitro* and in mouse models (Ji et al. 1998, Yoshimatsu et al. 2002).

Like rifapentine, moxifloxacin has a long half-life (9 to 12 h) (Dooley et al. 2008, Siefert et al. 1999), making it an attractive companion drug to prevent selection of rifapentine-resistant strains when the drugs are administered intermittently. The effect of high dose intermittent rifapentine on moxifloxacin pharmacokinetics has been shown to be clinically insignificant in patients, with only minor drug-drug interaction detected (Zvada et al. 2012). Higher doses of rifamycin have been proposed to be more efficacious and beneficial preventing rifamycin resistance, and this is supported by studies of rifamycin activity in vitro (Gumbo et al. 2007a), murine (Jayaram et al. 2003) and in humans (Sirgel et al. 2005). A previous study evaluating higher doses of rifapentine suggested that they can be tolerated in humans (Weiner et al. 2004). Concomitant food has a marked effect on rifapentine absorption (Chan et al. 1994). Rifapentine has a long half-life (Burman et al. 2001, Keung et al. 1999), superior *in vitro* potency against *M. tuberculosis* in comparison with rifampin (Heifets et al. 1990), and

rifapentine is approximately 4 times more potent (on equivalent 10 mg/kg body weight basis) than rifampicin when used alone and/or in combination with other first-line drugs (Rosenthal et al. 2012). Despite the encouraging results from mouse studies which supported the reduction of duration of therapy to less than 6 months, a Phase 2 study in patients with tuberculosis (TBTC study 29) showed that rifapentine did not improve 2 month culture conversion results (Dorman et al. 2012) as suggested by mouse studies; presumably due to high protein binding (98%) of rifapentine in humans (Mitchison 1998). However, a follow up Phase 2b TBTC study 29X which evaluated daily rifapentine escalating doses up to 20 mg/kg showed superior 2-month culture results compared to standard dose of rifampicin (Savic et al. 2013).

The Phase 3 RIFAQUIN clinical trial (Section 4.2.3) evaluated substitution of isoniazid with moxifloxacin in the intensive phase of tuberculosis treatment coupled with use of high dose intermittent rifapentine with moxifloxacin in the continuation phase of tuberculosis treatment using two different dosing schedules: twice weekly 900 mg rifapentine with moxifloxacin for 2 months in continuation phase or once weekly 1200 mg rifapentine with 400 mg moxifloxacin for 4 months in continuation phase. Each rifapentine dose was administered under observation with a meal of two boiled eggs and bread in order to facilitate rifapentine absorption. Hence, the aim of this study was to investigate the relationship between probability of relapse in the RIFAQUIN study with pharmacokinetics and PKPD parameters (during continuation phase treatment) of rifapentine and moxifloxacin: AUC, Cmax, total AUC for continuation phase of treatment (AUC_{total}), AUC/MIC, Cmax/MIC, TAMIC in modified "intention to treat" (mITT) group of patients in 4-month and 6-month. In order to estimate rifapentine PKPD parameters, a population pharmacokinetic model for rifapentine was developed.

Estimation of moxifloxacin pharmacokinetics and PKPD parameters was done using the moxifloxacin model described in Chapter 7.

9.2 Setting and Study design

The RIFAQUIN study comprised of two experimental arms which were: 1) 4-month arm where isoniazid was substituted with moxifloxacin daily for 2 months during the intensive phase and the continuation phase comprised 2 months of twice-weekly moxifloxacin and 900mg rifapentine; 2) 6-month arm: isoniazid replaced by moxifloxacin daily for the 2-month continuation phase which was followed by 4 months of once-weekly moxifloxacin and 1200mg rifapentine. This analysis is a sub-study of RIFAQUIN trial (Section 4.2.3) which comprised of a subset of 241 patients from two experimental arms and these patients also underwent population pharmacokinetic analysis of rifapentine and moxifloxacin studies. The clinical and demographic characteristics of PKPD patient subset (N=241) included in this analysis are summarized in Table 9.1. Out of 241, a total of 18 patients (7.5%) relapsed (13 and 5 from 4-month and 6-month arm, respectively). The study protocol was reviewed and approved by the Research Ethics Committee of the University of Cape Town, the Medicines Control Council of South Africa, the Medicines Research Council of Zimbabwe, and the Medicines Control Authority of Zimbabwe.

Table 9.1: Baseline characteristics of pharmacokinetic-pharmacodynamic (PKPD) patient subset in 4-month and 6-month arms

Variable[a]	Patients in 4-month and 6-month (Jindani et al. 2013, RIFAQUIN 2008, Zvada et al. 2012)
Number of patients	241
Males (%)	153 (63)
HIV+ (%)	46 (19)
Median age, range (years)	31.8 (18.5, 79.5)
Median weight, range (kg)	55.8 (37.7, 77.9)
Median height, range (cm)	177 (143, 190)
BMI, range (kg/m^2)	17.8 (10.4, 38.0)
Patients on twice weekly doses (%)	114 (47)

[a]HIV+, patients infected with Human immunodeficiency virus (HIV); BMI, body mass index

The doses of rifapentine and moxifloxacin were taken with 240 mL of water 15 minutes after the patients received 2 hard-boiled eggs with bread. Four hours after dosing, a light meal, snacks and fluids were provided. The population pharmacokinetic sampling for both rifapentine and moxifloxacin was done at the 4^{th} month after starting the treatment. A subset of 28 patients underwent intensive pharmacokinetic sampling where blood was drawn before dosing and at 1, 2, 3, 5, 7, 10, 12, 26 and 50 h after the dose. In the remaining 213 patients samples were obtained at 3 time points: 2 (± 0.5) h, 5 (± 0.5) h, and 24 (± 3) h or 48 (± 3) h after dosing. The intensively sampled 28 patients were also brought in 2 months after completion of treatment for additional pharmacokinetic evaluation of moxifloxacin pharmacokinetics without presence of rifapentine and this study is described in Chapter 8 of this thesis.

HIV positive patients who required antiretroviral treatment at randomisation were excluded. After blood collection, plasma was separated and immediately stored at -80°C.

Adequacy of treatment

A patient was considered to have received adequate treatment if both of the following conditions were met: at least 40 doses of intensive phase treatment were taken with 70 days of starting treatment; at least 16 doses were taken within 13 weeks of starting the continuation phase for patients on 4-month arm or within 22 weeks for patients in 6-month arm. The doses were supervised at the clinic or by the domiciliary treatment monitor at home.

Assessment of outcome

Assessable patients were classified as having a favorable or unfavorable status at the end of scheduled follow-up. For the mITT population, unfavorable outcome was classified as: patients requiring an extension, a restart, or a change of treatment for any reason other than to make up missed doses during the intensive or continuation phase or pregnancy; women who become pregnant during treatment whose last culture result was positive; patients who had a positive culture when last seen; patients who died in the follow-up phase with evidence confirmed or suggestive of possible failure or relapse of their tuberculosis. Positive cultures identified as being non-tuberculous mycobacteria were considered as contaminated.

9.3 Population pharmacokinetic analysis

The plasma concentration determination of rifapentine followed procedures described section 4.3. The methodology applied for model building has been described in section 4.5.3 of this thesis.

For rifapentine, there were no samples below limit of quantification. The use of allometric scaling was evaluated as described under section 4.5.3. CL/F and Vc/F were allometrically

scaled using WT according to Anderson and Holford (Anderson & Holford 2008) shown below:

$$CL_i = CLstd \cdot (WT_i/55.8)^{0.75}$$

$$V_i = Vstd \cdot (WT_i/ 55.8)^{1}$$

where CL_i is the scaled typical value of CL/F for individual *i*, CLstd is its typical CL for an individual of median weight of 55.8 in the patient population. A similar notation applies to V_i. Allometric scaling with FFM was also assessed. The tested covariates included age, HIV status, sex, site, and arm (4-month versus 6-month) and evaluated as described in section 4.5.3 of this thesis. The final pharmacokinetic model was used to generate AUC, Cmax, AUC_{total}, AUC/MIC, Cmax/MIC, AUC_{total}/MIC, and cumulative TAMIC; and these pharmacokinetic variables were compared between arms. The MIC value for rifapentine of 0.12 mg/L was obtained from a study conducted in South African patients (Sirgel et al. 2005).

The population pharmacokinetics model of moxifloxacin used in this analysis has been previously described in 241 patients who participated in the RIFAQUIN trial (Chapter 8). Briefly, moxifloxacin pharmacokinetics was best described by a two-compartment model with first-order elimination and transit absorption compartments. FFM was used for allometric scaling of CL, Q and Vc, while Vp was better scaled with FAT. This model was used to estimate pharmacokinetic variables such as AUC, Cmax, AUC_{total}, AUC/MIC, Cmax/MIC, AUC_{total}/MIC, and cumulative TAMIC. The MIC value of 0.25 mg/L was used, which is the susceptibility testing breakpoint concentrations of moxifloxacin recommended by WHO (WHO 2008b).

For each drug, both parametric (t-test) and non-parametric (Mann–Whitney U test) methods were used to compare estimated pharmacokinetic variables between 4-month and 6-month arms. The two-tailed probability of rejecting null hypothesis was set at 5% significance level (p=0.05).

9.4 Parametric hazard modeling (Pharmacokinetic-pharmacodynamic (PKPD) analysis)

A parametric hazard model was fitted to the relapse data combined from the two experimental arms. The hazard of unfavorable outcome at time *t* was modeled as: h(t)=Pr(t≤T<(t+dt|T>t); where Pr is the probability of having an event within the very short time interval dt, provided that one did not have an event before time *t*. The probability of having favorable outcome was modeled as a function of the cumulative hazard of an unfavorable event (integral of the hazard with respect to time) for each day from date of randomization using the following function: $S(t) = e^{-\int_0^t h(t)dt}$. The pdf of having an event at time *t* was modeled as: pdf = h(t) x S(t). The baseline survival models tested were parameterized as follows (Weibull function): $S(t) = e^{(\lambda t)^{\alpha}}$ where λ is the baseline hazard and α is the shape parameter. If α =1, then the hazard in constant over time, if α <1, then hazard decreases with time and if α >1 the hazard increases with time. Model selection and choice was based on VPC and ΔOFV as in pharmacokinetic models.

Continuous covariates tested on λ and α were AUC, Cmax, AUC_{total}, AUC/MIC, Cmax/MIC, AUC_{total}/MIC, and cumulative TAMIC, CD4 count, age, and weight. Categorical covariates tested on λ and α were: treatment duration, cavitation, history of smoking, HIV status and sex. The covariates were parameterized as described in section 4.5.3.1 of this thesis.

9.5 Results

Population pharmacokinetics of rifapentine

A total of 826 plasma concentration-time points were available from 241 patients who participated in the RIFAQUIN population pharmacokinetic study. The population pharmacokinetics of rifapentine was best described with a one compartment model with first-order absorption and transit absorption compartments. Allometric scaling using total body weight on CL/F and Vc/F was best which improved the fit by 40 points ΔOFV, and it explained 4% of variability on either CL/F and 4% on Vc/F. HIV status was found to significantly reduce bioavailability by 27.6% and it reduced correlation between CL/F and Vc/F from 66% to 60%. Sex and arm were also found to exhibit significant effect on CL/F with females showing 15.2% lower CL/F and twice weekly arm exhibiting 10.4% increase in CL/F. Inclusion of sex and regimen effects explained 1% and 0.1% variability in CL/F respectively. The final estimate of correlation between CL/F and Vc/F was 0.6. The final parameter estimates are shown in Table 9.2, and Figure 9.1 shows the VPC stratified by arm. Appendix 6 summarises the run record and also shows the control stream of final rifapentine pharmacokinetic model.

Table 9.2: Final parameter estimates for rifapentine population pharmacokinetic model

Parameter	Estimate (%RSE)[a]	IIV (%RSE)[b]
CL (L/hr)	1.08 (3.0)	28.6 (4.5)
Vc(L)	24.5 (2.4)	23.5 (6.5)
ka (hr^{-1})	0.885 (8.7)	43.8 (17.6)
MTT (hr)	1.45 (4.2)	38.5 (8.1)
NN	8.41 (15.1)	
F	1	
Proportional residual error (%)	10.8 (5.2)	
Additive residual error (mg/L)	0.463 (19.8)	
HIV+ on F	-27.6 (10.3)	
Twice weekly arm on CL	+10.4 (36.7)	
Female on CL	-15.2 (22)	

[a]RSE, relative standard error reported on standard deviation scale (it is approximate for IIV and IOV); CL, oral clearance; V_c, apparent volume of distribution of the central compartment; k_a, first-order absorption rate constant; MTT, absorption mean transit time; NN, number of hypothetical transit compartments; F, oral bioavailability fixed to 1. [b]IIV, inter-individual variability expressed as approximate percent coefficient of variation (% CV).

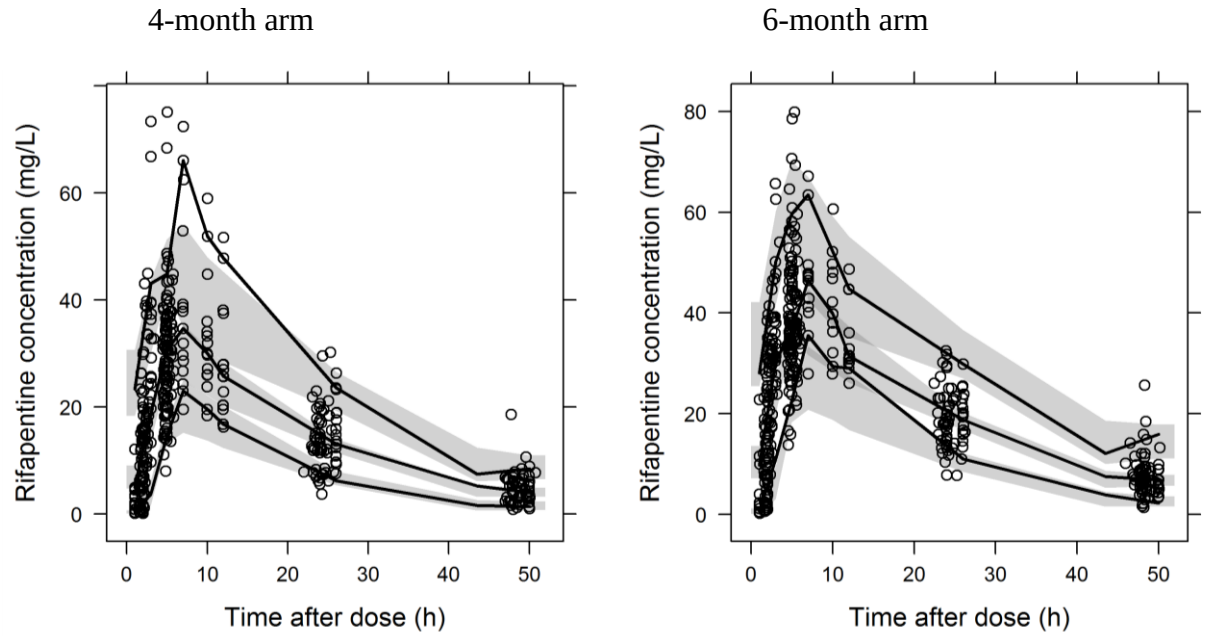

Figure 9.1: Visual predictive check (VPC) for the final rifapentine population pharmacokinetic model. The lower, middle and upper solid lines are the 2.5th, median, and 97.5th percentiles of the observed plasma concentration, respectively, while the shaded areas are the 95% confidence intervals for the same percentiles of the simulated data.

Pharmacokinetic-pharmacodynamic (PKPD) analysis

Out of 241 patients who participated in the pharmacokinetic studies, 186 patients were eligible for mITT analysis. Out of these 186 patients, only 18 experienced relapse. The baseline hazard model for the mITT population (N=186) was best described with a constant hazard model. Time varying hazard model was somewhat better, however improvement in the fit was not significant (p=0.056). In the covariate analysis, the only significant covariate found was treatment duration (p=0.03) with 2 months of continuation phase significantly increasing relapse hazard compared to 4 months of continuation phase. The effect of AUC, Cmax, AUC/MIC, Cmax/MIC, cumulative TAMIC, in addition to patients clinical and demographics information, did not show relationship with treatment outcome in 186 patients subset studied in this current analysis. The final parameter estimates are shown in Table 9.3. An appendix 7 shows the control stream of the final parametric hazard model.

Table 9.3: Parameter estimates for of the final parametric hazard model.

Parameter	Estimate (%RSE)[a]
Baseline	0.00001036 (44)
Impact of treatment duration (%)[b]	+287% (80)

[a]RSE, relative standard error reported on standard deviation scale. The impact is for 4-month on baseline hazard relative to 6-month arm

The only predictor of treatment response identified in this current analysis was treatment duration/arm effect. However given that there were quite few differences between two experimental arms (choice of dose, choice of dosing schedule and choice of treatment duration), the increased hazard in 4 month arm could not have been solely attributable to treatment duration and there is a possibility that this effect had been either co-founded by other pharmacokinetic and PKPD factors or the observable arm effect was as a result of a composite effect of several factors including treatment duration. Therefore, additional investigation to further understand how other pharmacokinetic and PKPD parameters compared between two experimental arms was performed.

Comparison of pharmacokinetic and PKPD parameters between 4-month and 6-month test arms

a) Rifapentine

The AUC and Cmax after 1200 mg (6-month arm) were approximately 1.5 times higher than after 900 mg (4-month arm) for single dosing interval (Figure 9.2 and Table 9.3), and this difference was statistically significant (Table 9.3). The estimates of continuation phase AUC_{total}, AUC/MIC, and TAMIC (even after adjusting for treatment duration and dosing schedule) for rifapentine were all higher in 6-month arm compared with 4-month arm (Figure 9.2 and Table 9.3). Overall, estimates of AUC, Cmax, AUC_{total}, AUC_{total}/MIC, Cmax/MIC,

and cumulative TAMIC were significantly higher in the 6-month arm compared to the 4-month arm, irrespective of less frequent administration of rifapentine.

b) Moxifloxacin

For a single dosing interval, the estimate of moxifloxacin AUC was slightly higher (10%) in the 6-month arm while there was no significant difference in Cmax and Cmax/MIC between two different regimens. Similarly, after adjusting for treatment duration and number of doses, moxifloxacin AUC_{total} was slightly higher in the 6-month arm. Figure 9.3 shows the boxplots of different pharmacokinetic variables of moxifloxacin, and Table 9.3 summarizes the estimates of these variables. Overall, there were only slight differences in moxifloxacin pharmacokinetic and PKPD parameters between two different arms suggesting that twice weekly dosing of rifapentine may affect moxifloxacin exposure more than once weekly regimen.

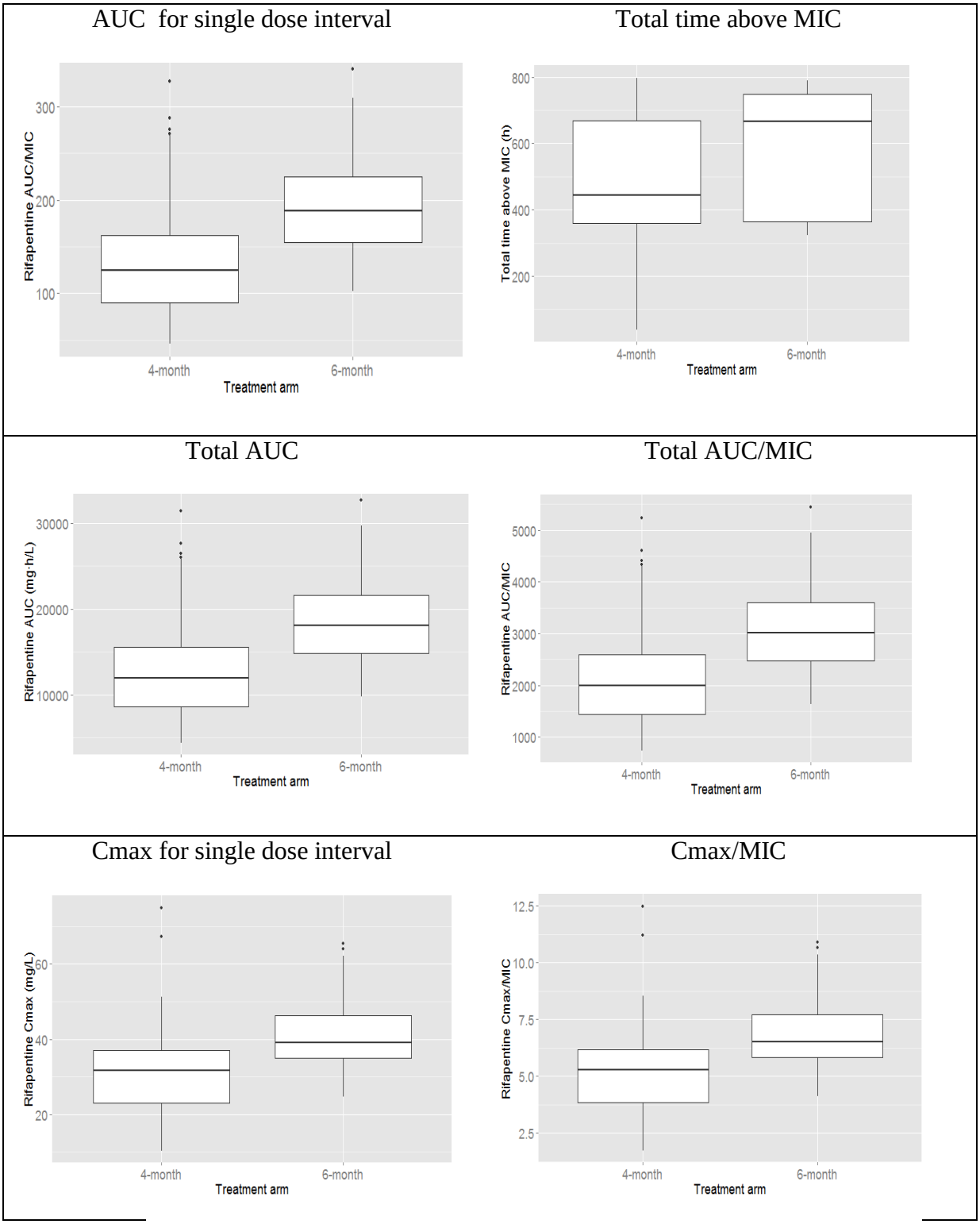

Figure 9.2: Box plots of area under curve (AUC) from 0-infinity hours and peak concentration (Cmax) for rifapentine for different time interval. Each box shows the 25^{th}-75^{th} percentile of AUC and the symbol "·" shows data falling outside 1.5 times the interquartile range (25^{th}-75^{th}). 'Total" refers to whole duration of continuation phase of treatment.

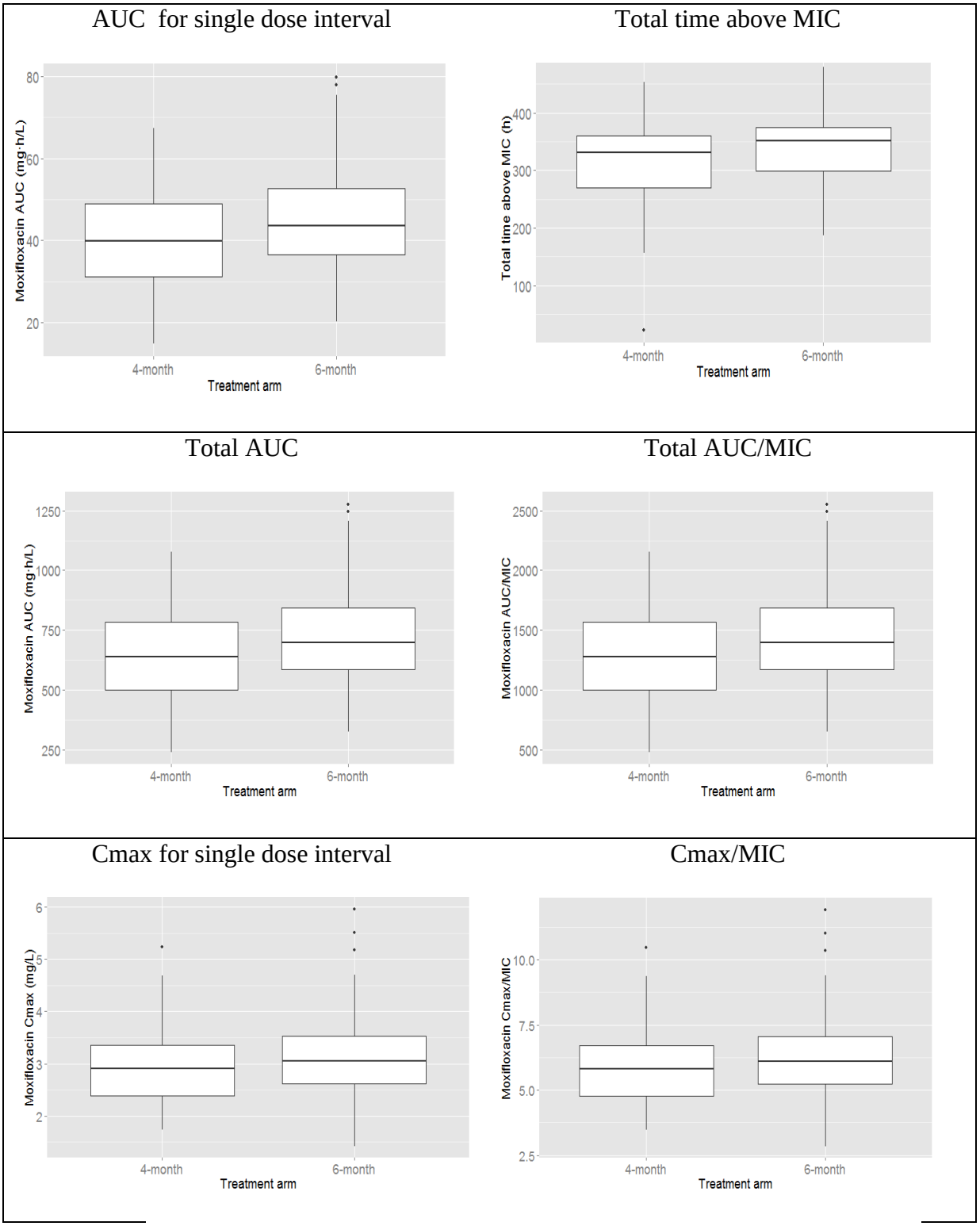

Figure 9.3: Box plots of area under curve (AUC) from 0-infinity hours and peak concentration (Cmax) for moxifloxacin for different time interval. Each box shows the 25^{th}-75^{th} percentile of AUC and the symbol "·" shows data falling outside 1.5 times the interquartile range (25^{th}-75^{th}). 'Total" refers to whole duration of continuation phase of treatment.

Table 9.4: Summary of pharmacokinetic variable for rifapentine and moxifloxacin, and significance test for differences in these variables between 4-month and 6-month arms

Pharmacokinetic Variable[a]	Interval[b]	4-month,		6-month		Mann–Whitney U test[e]
		Median (min, max)[c]	Mean (SD)[d]	Median (min, max)[c]	Mean (SD)[d]	
Rifapentine						
AUC (mg·h/L)	Single dose	746 (277, 1961)	803 (337)	1132 (615, 2043)	1174 (308)	p < 0.0001
TAMIC (h)	Total	445 (39.2, 797)	500 (168)	665 (324, 789)	573 (183)	p = 0.009
AUC (mg·h/L)	Total	11936 (4432, 31376)	12848 (5392)	18112 (9840,32688)	18784 (4928)	p < 0.0001
AUC/MIC	Total	1989 (739, 5229)	2141 (899)	3019 (1640,5448)	3130 (821)	p < 0.0001
Cmax (mg/L)	Single dose	31.7 (10.4, 74.9)	31.1 (10.6)	39.1 (24.6, 65.4)	41.2 (9.5)	p < 0.0001
Cmax/MIC	Single dose	5.28 (1.73, 12.5)	5.18 (1.77)	6.52 (4.10, 10.9)	6.87 (1.58)	p < 0.0001
Moxifloxacin						
AUC (mg·h/L)	Single dose	39.9 (15.0, 67.3)	40.7 (11.8)	43.6 (20.3, 79.7)	45.3 (12.5)	p = 0.013
TAMIC (h)	Total	330 (23.3, 453)	314 (65.5)	352 (187, 479)	341 (59.0)	p = 0.0047
AUC (mg·h/L)	Total	638 (240, 1071)	651 (189)	698 (325, 1275)	725 (200)	p = 0.013
AUC/MIC[e]	Total	1276 (480, 2142)	1302 (378)	1396 (650, 2550)	1450 (400)	p = 0.013
Cmax (mg/L)	Single dose	2.90 (1.73, 5.23)	2.98 (0.72)	3.05 (1.42, 6.00)	3.15 (0.78)	p = 0.129
Cmax/MIC[e]	Single dose	5.80 (3.46, 10.5)	5.96 (1.44)	6.10 (2.84, 12.0)	6.30 (1.56)	p = 0.129

[a]AUC - area under the curve from 0- infinity hours; Cmax - peak plasma concentration; TAMIC - time above MIC. [b]Total - refers to whole duration continuation phase adjusted for dosing schedules. [c]min - minimum; max - maximum. [d]SD - standard deviation. [e]p-probability of rejecting the null hypothesis when it is true (false positive result). [f]When the MIC of ≤0.125 mg/L, value for majority of sensitive strains (Zvada et al. 2014), the estimates of Cmax/MIC and AUC/MIC will double.

9.6 Discussion

Investigation of the role pharmacokinetic variables as predictors of treatment failure/relapse showed no conclusive effect within each experimental arm. This is most likely due to a very small number of patients experiencing unfavorable outcome (5 patients in 6 months arm (2.7%) against 12 patients in 4 month arm (6.45%)). The only observable difference was treatment arm. Even though the treatment duration was the main difference between two experimental arms, given that the RIFAQUIN design altered several things between two investigational arms (dose, dosing frequency and treatment duration), it is hard to conclude if better outcomes seen in 6-month arm were solely due to longer treatment duration. For example, most of the pharmacokinetic summary variables and pharmacokinetic and pharmacodynamics (PKPD) indices for rifapentine were significantly higher in the 6-month arm (Figure 9.2, Table 9.3): Cmax, Cmax/MIC, AUC_{total} and cumulative TAMIC. Therefore significant difference in relapses can likely be attributable to either of these variables including treatment duration or most likely the observed effect is result of combined impact of all these factors (high Cmax, high cumulative AUC and longer treatment duration). These questions require further studies.

Compared with other studies with high dose rifapentine (TBTC Study 29X), the AUC and Cmax in the RIFAQUIN study were significantly higher. For example, in the study 29X, median reported values of AUC following 900 and 1200 mg dose were 472 and 578 mg·h/L respectively (Savic et al. 2013). While in this study these values were 746 and 1132 mg·h/L for 900 and 1200 mg dose respectively. There are two likely reasons for that: auto-induction time course and type of food administered. Patients in the study 29X were given daily rifapentine which leads to full autoinduction with CL values being doubled by end of 2nd week of daily dosing (Savic et al. 2011) . This will have an immediate impact on drug

exposure. Patients in study 29X were given rifapentine with high fat food which did not necessarily include egg, while patients in RIFAQUIN study had 2 boiled eggs and bread before rifapentine was administered. Egg has been shown to increase the bioavailability of rifapentine (Chan et al. 1994) and most likely can boost exposure even further compared to the high fat meal without egg. Importantly, strategies used in the RIFAQUIN study (intermittent dosing and administration of drug with egg) resulted in the highest Cmax and AUC values ever achievable in studies to date.

The population pharmacokinetics of rifapentine was best described with a one compartment model with first-order absorption and elimination. The VPC (Figure 9.1) shows that the model did not fit well higher concentrations in 4-month arm because there were few individuals with very high concentrations in 4-months arm. The estimates of CL and Vc (Table 9.3) were 2 and 1.5 times lower, respectively, than what has been reported previously in patients with tuberculosis from ethnically similar population (Langdon et al. 2005). The difference in these pharmacokinetic estimates is most likely due to differences in dosing frequency and food effect, but could also be partly explained by different severity of disease and inclusion of patients from different sites in RIFAQUIN study. The effect of HIV infection was significant on the bioavailability, where HIV infected patients had 28% lower bioavailability. For rifapentine, studies of differences in pharmacokinetic parameters in HIV-positive and -negative individuals have produced mixed results, with some groups showing significant differences (Peloquin et al. 1996) and others finding no clinically significant effect (Choudhri et al. 1997). A study conducted in South Africa (Langdon et al. 2004) showed good absorption of rifapentine and no differences in pharmacokinetic parameters when compared to HIV-negative patients. Even though these results contradict the results of this current analysis, the detected effect of HIV status was highly significant and this is of clinical

relevance. Interestingly, females had 15% lower CL than males. These results also confirm the sex effect which was shown before (Langdon et al. 2005). Also patients in the twice weekly arm showed 10% higher clearance compared to the once weekly arm. This is most likely due to a partial autoinduction effect which was also reported in the study of thrice weekly rifapentine (Dooley et al. 2008).

Limitations: A major limitation of this study is design, which allowed for simultaneous change of three key factors responsible for treatment response: choice of dose, dosing schedule and treatment duration. Even though, there was a clearly significant difference between the two experimental arms, the design did not allow for identification of the most important out of three responsible factors and/or for quantification of the relative contribution of each of them. Even though, treatment duration is the most plausible one it is not possible to differentiate the effect of time against dose or against dosing schedule. The next major limitation is a relatively small sample size enrolled in the PKPD study where only 18 patients who relapsed leading to lack of power to describe PKPD associations. The sample size could be extended by inclusion of all eligible patients enrolled in the RIFAQUIN study even-though they did not undergo pharmacokinetic sampling. For those patients, pharmacokinetic summary variables can be derived based on the dose and covariate information (HIV status, weight, sex and dose schedule and they can be included into the extended PKPD analysis. Also, the individual data on the actual number of doses and adherence patterns were not used in this analysis. The number of doses taken was supposed to be used to more precisely quantify the cumulative AUCs while adherence patterns were supposed to be used to derive entire continuation phase pharmacokinetic profiles for each patient, which would provide much more granularity and insight into the actual pharmacokinetic plasma variations for both rifapentine and moxifloxacin. Also, the patients were on rifampicin during the intensive phase of the treatment, rifampicin induces its own metabolism. It has been shown that it takes

40 days for the autoinduction of rifampicin to reach its steady-state and causing more than 40% reduction in AUC (Smythe et al. 2013). Little is known about how long this autoinduction takes to clear. Hence, because there was no pharmacokinetic sampling of rifapentine or moxifloxacin on the beginning on continuation phase, it cannot be clearly deduced to what extent the exposures in the 4^{th} months of treatment have altered. Furthermore, this analysis could have been limited by the combined endpoint of failure/relapse/death. Factors like treatment modification could have also confounded the analysis of effect of pharmacokinetic indices of moxifloxacin and rifapentine. Moreso, a handful of HIV positive patients were started on therapy, and there could have been an interaction with investigational drugs. In terms of MIC value of 0.25 mg/L used for moxifloxacin following WHO recommendation; this value was rather at an extreme end of the distribution for patients without pre-XDR or XDR who had MIC ≤0.125 mg/L (Zvada et al. 2014); hence the calculated AUC/MIC, Cmax/MIC and TAMIC for moxifloxacin could be 2 times higher than values shown in Table 9.4.

9.7 Conclusion

This analysis concludes that the composite effect of longer treatment duration, higher rifapentine Cmax and AUC_{total} is associated with better treatment response; however it is not conclusive as to whether longer treatment duration is the major factor needed for successful treatment outcome. Intermittent rifapentine administration and the impact of a meal with egg resulted in the highest rifapentine AUC and Cmax values ever achieved in the patient population; therefore these two strategies can be utilized in future studies to optimize target Cmax and AUC values.

10 Overall discussion and conclusions

Cure rates of more than 95% can be achieved with 6 month long standard therapy using drugs discovered more than 4 decades ago. However, these cure rates may be rarely achieved due to long duration of therapy, drug adverse effects, and complications due to HIV coinfection. All these factors may lead to poor adherence. Hence studies which aim at optimizing these therapies and reducing the duration of therapy or more intermittent administration are very important. Several reports have now suggested that the doses of drugs, particularly the rifamycins, used in the standard therapy of tuberculosis are low, and suggestions for higher doses should be prioritized. Even though the majority of studies have been conducted in adults, a handful of studies conducted in children indicated that children have lower drug exposures rarely achieving concentrations similar to adults. This gives an extra dimension to tuberculosis research where better dose optimization methods should be employed firstly, to establish optimal doses in adults based on pharmacokinetic-pharmacodynamic relationships, and secondly to ensure that children have exposures at least matching those in adults in ethnically similar populations. The most striking factor is that children are not always considered during optimization of drug therapies, yet they frequently experience severe forms of tuberculosis including disseminated disease and meningitis (Marais et al. 2006).

On top of aiming to achieve similar exposures in both adults and children, studies investigating new treatment strategies should be prioritized. The current novel regimens aimed at shortening the duration of tuberculosis treatment or offering intermittent therapy (i.e., once weekly or even less frequently) without compromising efficacy come with the advantages of reducing the burden of supervised drug therapy. Evidence now exists that such regimens could be achieved, but more thorough investigation into why

some these studies fail should be considered, including evaluation of the pharmacokinetic parameters of the drugs together with other risk factors for therapeutic failure or relapse after treatment. Combination of moxifloxacin and rifapentine is complicated by the unknown extent of interaction when these two drugs when they are administered together. The main problem being the possibility of drug-drug interactions where rifapentine may result in decreased exposures of moxifloxacin. Most important approaches towards optimization of the doses rifapentine and moxifloxacin would be to consider their pharmacokinetic correlates with treatment outcome.

Furthermore, there is need to improve 2nd –line regimens used for MDR-TB, where optimal use of the available drugs is prioritized. Fluoroquinolones have wider therapeutic margin than many second line drugs used for the treatment of drug-resistant tuberculosis. The only limitation is that there is limited information regarding their safety at higher doses. It should be noted that fluoroquinolones differ from each other in their efficacy against *M.tuberculosis* as measured by $fAUC_{0\text{-}24}$/MIC, and also display differences in their clinical pharmacokinetics. Even though the *in vitro* bactericidal activity of moxifloxacin against *M.tuberculosis* is superior to that of ofloxacin (Hu et al. 2003), ofloxacin is used widely in developing countries due to its affordability but has very low therapeutic effectiveness. Recommendations made to replace ofloxacin with moxifloxacin should be based on scientific and clinical evaluation of efficacy between these two drugs.

The work in this thesis demonstrates the significant role of pharmacometrics in optimising dosing regimens, understanding what drives the efficacy, and how to improve the treatment of drug-resistant tuberculosis.

10.1 Using population pharmacokinetic models to optimize dosing regimens

The work in this thesis describes the population of pharmacokinetics of rifampicin, pyrazinamide and isoniazid when dosed in children. Limited studies which have evaluated the pharmacokinetics of these drugs in children raised concern of under-dosing. The WHO recommended increased doses based on these studies, but it was necessary to evaluate the adequacy of doses of rifampicin, isoniazid and pyrazinamide in children using the revised doses currently recommended by WHO, and dosed in weight bands suited to FDCs. The key finding in this thesis, following simulations based on the final pharmacokinetic models, predicted that the newly recommended weight band-based doses following WHO guidelines for children would result in rifampicin exposures in similar to those in adults. When these children are dosed in pragmatic weight bands, there is wider variability in rifampicin exposures. The doses of pyrazinamide and isoniazid will give lower exposures than those in an ethnically similar adult population. If similar findings are confirmed in other studies, dose adjustment may be warranted especially when children are dosed using FDCs according to weight bands. The pharmacokinetic models incorporated factors like maturation of drug transporters and/or metabolising enzymes, pharmacogenetic factors, and total body weight which was implemented through allometric scaling. These models could be used to simulate the optimal doses for children across different weight and/or age bands. The results from the patient population studied in this thesis could be generalized across African populations.

It was surprising that dose-dependent non-linearity in pharmacokinetics of rifampicin was not identified, which is different to described in adults (Pargal & Rani 2001). This limits the application of the pharmacokinetic models in simulating optimal doses where higher doses are considered. In children, variability in rifampicin exposures was higher than those for the reference adult population, partly due to physiological differences

between adults and children, and possibly also the severity of the disease in the hospitalized cohort of children. Based on this high variability, there is a need for further studies to evaluate such sources of variability; formulation was reported to alter bioavailability of drugs (Agrawal et al. 2004, McIlleron et al. 2006) and its effect was not identified this analysis. Another important consideration will be evaluation of pharmacokinetic and pharmacogenetic correlates. The differences in the distribution of NAT2 polymorphisms (Fuselli et al. 2007, Sabbagh et al. 2011) may also limit generality of application these models. Further studies which identify more sources of variability in children are warranted factors such as proper anthropometric measurements and reference values derived in for a specific population, and association between pharmacokinetics, efficacy and toxicity.

Other factors which alter drug pharmacokinetics include meal effects. The analysis described in this thesis showed that food intake results in a substantial increase bioavailability of rifapentine and consequently its metabolite, which supports previous findings by Chan et al. (Chan et al. 1994). The most important contribution of the analysis described in this thesis was different categorization of meals which may help policy makers in tuberculosis control programs in selecting the meals, which may be relevant in the clinical program and setting. In addition, this finding is important because high doses of rifapentine (1200 mg) are being investigated in clinical trials which may impact on patient safety. The limitation of this study was that the extent of meal effect was only investigated in healthy volunteers. When rifapentine is dosed daily and for longer durations, autoinduction effects would be more marked (Dooley et al. 2008), and an interaction between the food effect and autoinduction cannot be ruled out. Furthermore, dose nonlinearity in rifapentine exposures have been reported, where doses above 900 mg are administered with decreased bioavailability (Savic et al. 2011), a fact

which the model in this thesis did not account for. Because higher doses of rifapentine give enhanced therapeutic effect, further studies investigating meal effect in combination with dose nonlinearity and indexed against safety are recommended.

Another important contribution of work is that high-dose intermittent rifapentine increased the CL/*F* of moxifloxacin by only 8%, which is clinically insignificant. The change in $AUC_{0-\infty}$ had the same magnitude. This means that the RIFAQUIN study was better designed to reduce the magnitude of effect of rifapentine on the pharmacokinetics of moxifloxacin. This finding is very important for future trials investigating the combination of moxifloxacin and rifapentine. Even though there is a marginal decrease in $AUC_{0-\infty}$ of moxifloxacin, similar results cannot be assumed to circumstances where the drugs are administered more frequently, for example daily. The extent of rifapentine induction potential was reported in doses of 10 to 20 mg/kg, where rifapentine in these doses is as potent an inducer of CYP3A as rifampin (Bliven-Sizemore et al. 2011), a comparison made when the drugs are dosed daily. Also, results from study 29X where patients were given daily rifapentine had CL values of rifapentine being doubled by end of 2nd week of daily dosing (Savic et al. 2011). Therefore, rifapentine effect on moxifloxacin exposure may be higher than what was observed in this work. However, the magnitude of effect should be evaluated in larger sample sizes and consideration of efficacy and safety are also warranted.

10.2 Understanding what drives efficacy

The work in this thesis showed that pharmacokinetics variables had no conclusive effect as predictors of relapse. This is probably due partly to the very small number of patients who relapsed in the 4-month and 6-month arms. Out of 18 patients who relapsed, only 5 were from 6-month arm. It is unclear what contributed towards more relapses in 4-month arm. The differences between the arms were dose, dosing frequency and treatment duration. In

addition, most of the pharmacokinetic summary variables were significantly higher in the 6-month arm. Given the failure to separate which factor contributed towards relapse, the observed effect could be a result of overall impact of all pharmacokinetic summary variables and duration of treatment. The results of this analysis showed that the exposure to rifapentine in the RIFAQUIN trial was significantly higher than those observed in the TBTC study 29X. Importantly, it is reasonable to assume that the difference between the two studies might be attributable to auto-induction and type of food administered. In the study 29X, patients were given high fat food while patients in the RIFAQUIN study had 2 boiled eggs and bread before rifapentine was administered. Hence eggs in the RIFAQUIN probably have enhanced rifapentine absorption. Eggs were has been shown to increase the bioavailability of rifapentine (Chan et al. 1994). However, there were quite a lot of limitations in the study which may have led to lack of pharmacokinetic variables effect. However future studies aiming at evaluating the PKPD should consider the limitation of the analysis which includes: choice of dose, dosing schedule and treatment duration. These factors could have confounded identification of factors or differences between arms that were associated with relapse. Further improvement in the study could be inclusion of data from all patients in the RIFAQUIN study such as including those who did not participate in population pharmacokinetic study. In addition, data on adherence patterns should evaluated in order to improve the analysis on top of data on actual number of doses. This will help in evaluation concentration and actual AUC profiles.

10.3 How to improve treatment of drug resistant tuberculosis

The main contribution of the work described in this thesis was that when using a target $fAUC_{0\text{-}24}$/MIC ratio of $\geq$53, the CFR for 400 mg moxifloxacin was 98% versus 84% for 800 mg ofloxacin in patients with MDR-TB. When a more stringent target of target ratio of $\geq$100 was considered, both regimens did not achieve a threshold of 90% CFR.

Importantly, simulation results showed that when the dose of moxifloxacin is doubled to 800 mg, a CFR of 98% would be achieved same patients with MDR-TB when the target ratio of ≥100 is used. Hence the results of the analysis suggest that doubling the dose of moxifloxacin is beneficial. However, what is not known is the safety of moxifloxacin at these higher doses. Therefore further studies evaluating moxifloxacin efficacy at these higher doses should also evaluate toxicities. However, even though these results are encouraging, the limitation of the study was the MIC data used which may not represent the true distribution for some drug-resistance categories due to small sample size. Furthermore the PTA and CFR analyses may not be applicable to other populations outside the region, hence further studies where there are larger sample sizes of MICs will help in the application of these findings to other regions. Also, these future studies should consider free drug concentration in tissues, which would be more appropriate than plasma concentration used in this thesis. Lastly, there is need for validation of AUC/MIC targets in relevant population in studies verifying clinical and bacteriological outcome.

10.4 Conclusion

In summary, the population pharmacokinetics analysis in children demonstrated the utility of modeling and simulation in testing new guidelines based on expert opinion but not substantiated by evidence. The simulations showed that, even with the increased dosages, the majority of younger children would achieve relatively low exposures to pyrazinamide and isoniazid. Furthermore, intermediate and fast acetylators may be under-dosed with respect to isoniazid, if exposures in an ethnically similar population of adults are considered therapeutic. The models developed in this study could have been used to simulate optimal doses in children. However, if higher doses of pyrazinamide are

suggested, there could be potential overdosing in children on rifampicin and slow metabolisers of isoniazid when FDC are given. This study could also be tied up with other studies evaluating the pharmacokinetics in children at higher doses. Further recommended work could perform a meta-analysis of the all the studies in children evaluating higher doses, where the models developed in the study could also be employed to simulate the likely optimal doses in children.

In terms of the population pharmacokinetics of rifapentine in healthy volunteers, the analysis showed that food increases the bioavailability and exposures of rifapentine. The high exposures found in the RIFAQUIN study compared to other studies could be due to eggs which were used. Even though highest exposures are desirable which could be achieved through the use meals as shown in health volunteers study, the immediate and reasonable dilemma is the use of these meals which may not be practical in Tuberculosis control programs especially in high burdened areas. In terms of interaction between high dose rifapentine and moxifloxacin, these results in this thesis showed that rifapentine effect detectable was but clinically insignificant. This result cannot be assumed to be the same where rifapentine is used in combination with moxifloxacin dosed daily hence further studies will need to confirm this finding.

The study of evaluation of efficacy between moxifloxacin and ofloxacin supports that moxifloxacin can be used instead of ofloxacin. The study also showed important benefit of higher doses of moxifloxacin. However, further studies would need to evaluate the safety of moxifloxacin at higher doses. In addition, the study demonstrates the successful application of pharmacometrics in comparison of 2 drugs against a pre-defined pharmacodynamics target.

Furthermore, investigation of pharmacokinetic and PKPD variable suggest that the combined effect of longer treatment duration, higher rifapentine Cmax and AUC_{total} is associated with better treatment response; the analysis is not conclusive regarding longer treatment duration as a main factor required to enhance successful treatment outcome. There was a noticeable impact of meal (eggs) effect which gave very high rifapentine AUC and Cmax values. Further studies may therefore use this strategy to boost the Cmax and AUC values of rifapentine. However this finding is based on a number of limitations which include small sample size, major simultaneous changes in choice of dose, dosing schedule and treatment duration.

REFERENCES

Acocella G. 1978. Clinical pharmacokinetics of rifampicin. *Clin Pharmacokinet*. 3(2):108–27

Acocella G. 1983. Pharmacokinetics and metabolism of rifampin in humans. *Rev Infect Dis*. 5(Suppl 3):S428–32

Acocella G, Pagani V, Marchetti M, Baroni GC, Nicolis FB. 1971. Kinetic studies on rifampicin. i. serum concentration analysis in subjects treated with different oral doses over a period of two weeks. *Chemotherapy*. 16(6):356–70

Agrawal S, Singh I, Kaur KJ, Bhade S, Kaul CL, Panchagnula R. 2004. Bioequivalence trials of rifampicin containing formulations: extrinsic and intrinsic factors in the absorption of rifampicin. *Pharmacol Res*. 50(3):317–27

Ahmad Z, Tyagi S, Minkowski A, Peloquin CA, Grosset JH, Nuermberger EL. 2013. Contribution of moxifloxacin or levofloxacin in second-line regimens with or without continuation of pyrazinamide in murine tuberculosis. *Am J Respir Crit Care Med*. 188(1):97–102

Al Tawil Y, Berseth CL. 1996. Gestational and postnatal maturation of duodenal motor responses to intragastric feeding. *J. Pediatr.* 129:374–81

Alffenaar JW, van Altena R, Bokkerink HJ, Luijckx GJ, van Soolingen D, et al. 2009. Pharmacokinetics of moxifloxacin in cerebrospinal fluid and plasma in patients with tuberculous meningitis. *Clin Infect Dis*. 49(7):1080–82

Almeida Da Silva PE, Palomino JC. 2011. Molecular basis and mechanisms of drug resistance in mycobacterium tuberculosis: classical and new drugs. *J. Antimicrob. Chemother.* 66:1417–30

Altet-Gômez MN, Alcaide J, Godoy P, Romero MA, Hernández del Rey I. 2005. Clinical and epidemiological aspects of smoking and tuberculosis: a study of 13,038 cases. *Int. J. Tuberc. Lung Dis.* 9(4):430–36

Anderson BJ, Holford NH. 2008. Mechanism-based concepts of size and maturity in pharmacokinetics. *Annu Rev Pharmacol Toxicol*. 48:303–32

Anderson BJ, Holford NH. 2009. Mechanistic basis of using body size and maturation to predict clearance in humans. *Drug Metab Pharmacokinet.* 24(1):25–36

Andersson MI, MacGowan AP. 2003. Development of the quinolones. *J Antimicrob Chemother*. 51 Suppl 1:1–11

Andrews JR, Noubary F, Walensky RP, Cerda R, Losina E, Horsburgh CR. 2012. Risk of progression to active tuberculosis following reinfection with mycobacterium tuberculosis. *Clin Infect Dis*. 54(6):784–91

Andrews RH, Devadatta S, Fox W, Radhakrishna S, Ramakrishnan C V, Velu S. 1960. Prevalence of tuberculosis among close family contacts of tuberculous patients in south india, and influence of segregation of the patient on early attack rate. *Bull World Heal. Organ*. 23:463–510

Back DJ, Rogers SM. 1987. Review: first-pass metabolism by the gastrointestinal mucosa. *Aliment. Pharmacol. Ther.* 1:339–57

Balasubramanian V, Solapure S, Gaonkar S, Mahesh Kumar KN, Shandil RK, et al. 2012. Effect of coadministration of moxifloxacin and rifampin on mycobacterium tuberculosis in a murine aerosol infection model. *Antimicrob Agents Chemother*. 56(6):3054–57

Beal S, Sheiner LB, Boeckmann A, Bauer RJ. 2009. Nonmem user's guides. (1989-2009), icon development solutions, ellicott city, md, usa

Beal SL. 2001. Ways to fit a pk model with some data below the quantification limit. *J Pharmacokinet Pharmacodyn*. 28(5):481–504

Belousov OB, Gutkin AB, Sokolov A V, Tishchenkova IF, Efremenkova O V. 1996. [clinical and pharmacokinetic evaluation of ofloxacin under various regimens of administration in patients with bronchopulmonary infections]. *Antibiot Khimioter*. 41(9):47–49

Benator D, Bhattacharya M, Bozeman L, Burman W, Cantazaro A, et al. 2002. Rifapentine and isoniazid once a week versus rifampicin and isoniazid twice a week for treatment of drug-susceptible pulmonary tuberculosis in hiv-negative patients: a randomised clinical trial. *Lancet*. 360(9332):528–34

Bergstrand M, Karlsson MO. 2009. Handling data below the limit of quantification in mixed effect models. *AAPS J*. 11(2):371–80

Bliven-Sizemore E, Kashuba ADM, Malone S, Weiner M, Nuermberger E, et al. 2011. Cyp3a induction by rifampin and rifapentine: which drug and dose does it best?. 4th international workshop on clinical pharmacology of tuberculosis drugs -16 sepetermber 2011 - chicago il, usa. abstract: o_04. http://regist2.virology-education.com/abstrac

Blumberg HM, Burman WJ, Chaisson RE, Daley CL, Etkind SC, et al. 2003. American thoracic society/centers for disease control and prevention/infectious diseases society of america: treatment of tuberculosis. *Am J Respir Crit Care Med*. 167(4):603–62

Bock NN, Sterling TR, Hamilton CD, Pachucki C, Wang YC, et al. 2002. A prospective, randomized, double-blind study of the tolerability of rifapentine 600, 900, and 1,200 mg plus isoniazid in the continuation phase of tuberculosis treatment. *Am J Respir Crit Care Med*. 165(11):1526–30

Bonah C. 2005. The "experimental stable" of the bcg vaccine: safety, efficacy, proof, and standards, 1921-1933. *Stud Hist Philos Biol Biomed Sci*. 36(4):696–721

Brillault J, De Castro W V, Harnois T, Kitzis A, Olivier JC, Couet W. 2009. P-glycoprotein-mediated transport of moxifloxacin in a calu-3 lung epithelial cell model. *Antimicrob Agents Chemother*. 53(4):1457–62

Brindle R, Odhiambo J, Mitchison D. 2001. Serial counts of mycobacterium tuberculosis in sputum as surrogate markers of the sterilising activity of rifampicin and pyrazinamide in treating pulmonary tuberculosis. *BMC Pulm Med*. 1:2

Burman W, Benator D, Vernon A, Khan A, Jones B, et al. 2006. Acquired rifamycin resistance with twice-weekly treatment of hiv-related tuberculosis. *Am J Respir Crit Care Med*. 173(3):350–56

Burman WJ, Gallicano K, Peloquin C. 2001. Comparative pharmacokinetics and pharmacodynamics of the rifamycin antibacterials. *Clin Pharmacokinet*. 40(5):327–41

Canetti G, Fox W, Khomenko A, Mahler HT, Menon NK, et al. 1969. Advances in techniques of testing mycobacterial drug sensitivity, and the use of sensitivity tests in tuberculosis control programmes. *Bull World Heal. Organ*. 41(1):21–43

Chan SL, Yew WW, Porter JH, McAdam KP, Allen BW, et al. 1994. Comparison of chinese and western rifapentines and improvement of bioavailability by prior taking of various meals. *Int J Antimicrob Agents*. 3(4):267–74

Chen J, Raymond K. 2006. Roles of rifampicin in drug-drug interactions: underlying molecular mechanisms involving the nuclear pregnane x receptor. *Ann. Clin. Microbiol. Antimicrob.* 5:3

Chideya S, Winston CA, Peloquin CA, Bradford WZ, Hopewell PC, et al. 2009. Isoniazid, rifampin, ethambutol, and pyrazinamide pharmacokinetics and treatment outcomes among a predominantly hiv-infected cohort of adults with tuberculosis from botswana. *Clin Infect Dis*. 48(12):1685–94

Chigutsa E, Meredith S, Wiesner L, Padayatchi N, Harding J, et al. 2012. Population pharmacokinetics and pharmacodynamics of ofloxacin in south african patients with multidrug-resistant tuberculosis. *Antimicrob Agents Chemother*. 56(7):3857–63

Chigutsa E, Pasipanodya J, Visser ME, Sirgel FA, Gumbo T, McIlleron H. 2013. Multivariate adaptive regression splines analysis of the effect of drug concentration and mic on sterilizing activity in patients on multidrug therapy. program and abstracts of the 6th international workshop on clinical pharmacology of tuberculosis drugs;

Chigutsa E, Visser ME, Swart EC, Denti P, Pushpakom S, et al. 2011. The slco1b1 rs4149032 polymorphism is highly prevalent in south africans and is associated with reduced rifampin concentrations: dosing implications. *Antimicrob Agents Chemother*. 55(9):4122–27

Choudhri SH, Hawken M, Gathua S, Minyiri GO, Watkins W, et al. 1997. Pharmacokinetics of antimycobacterial drugs in patients with tuberculosis, aids, and diarrhea.

Conde MB, Efron A, Loredo C, De Souza GR, Graca NP, et al. 2009. Moxifloxacin versus ethambutol in the initial treatment of tuberculosis: a double-blind, randomised, controlled phase ii trial. *Lancet*. 373(9670):1183–89

Corbella X, Vadillo M, Cabellos C, Fernandez-Viladrich P, Rufi G. 1995. Hypersensitivity hepatitis due to pyrazinamide. *Scand. J. Infect. Dis.* 27(1):93–94

Craig WA. 1998. Pharmacokinetic/pharmacodynamic parameters: rationale for antibacterial dosing of mice and men. *Clin. Infect. Dis.* 26:1–10; quiz 11–12

Curci G, Bergamini N, Delli Veneri F, Ninni A, Nitti V. 1972. Half-life of rifampicin after repeated administration of different doses in humans. *Chemotherapy*. 17(6):373–81

Daniel TM. 2006. The history of tuberculosis. *Respir Med*. 100(11):1862–70

De Steenwinkel JEM, Aarnoutse RE, de Knegt GJ, ten Kate MT, Teulen M, et al. 2013. Optimization of the rifampin dosage to improve the therapeutic efficacy in tuberculosis treatment using a murine model. *Am. J. Respir. Crit. Care Med.* 187(10):1127–34

Devadatta S, Gangadharam PR, Andrews RH, Fox W, Ramakrishnan C V, et al. 1960. Peripheral neuritis due to isoniazid. *Bull. World Health Organ.* 23:587–98

Diacon AH, Patientia RF, Venter A, van Helden PD, Smith PJ, et al. 2007. Early bactericidal activity of high-dose rifampin in patients with pulmonary tuberculosis evidenced by positive sputum smears. *Antimicrob Agents Chemother*. 51(8):2994–96

Donald PR, Maritz JS, Diacon AH. 2011. The pharmacokinetics and pharmacodynamics of rifampicin in adults and children in relation to the dosage recommended for children. *Tuberc.* 91(3):196–207

Donald PR, Maritz JS, Diacon AH. 2012. Pyrazinamide pharmacokinetics and efficacy in adults and children. *Tuberc.* 92(1):1–8

Donald PR, Sirgel FA, Botha FJ, Seifart HI, Parkin DP, et al. 1997. The early bactericidal activity of isoniazid related to its dose size in pulmonary tuberculosis. *Am J Respir Crit Care Med*. 156(3 Pt 1):895–900

Donald PR, Sirgel FA, Venter A, Smit E, Parkin DP, et al. 2001. The early bactericidal activity of a low-clearance liposomal amikacin in pulmonary tuberculosis. *J Antimicrob Chemother*. 48(6):877–80

Dooley K, Flexner C, Hackman J, Peloquin CA, Nuermberger E, et al. 2008. Repeated administration of high-dose intermittent rifapentine reduces rifapentine and moxifloxacin plasma concentrations. *Antimicrob Agents Chemother*. 52(11):4037–42

Dorman SE, Goldberg S, Stout JE, Muzanyi G, Johnson JL, et al. 2012. Substitution of rifapentine for rifampin during intensive phase treatment of pulmonary tuberculosis: study 29 of the tuberculosis trials consortium. *J. Infect. Dis.* 206(7):1030–40

Drusano GL, Sgambati N, Eichas A, Brown DL, Kulawy R, Louie A. 2010. The combination of rifampin plus moxifloxacin is synergistic for suppression of resistance but antagonistic for cell kill of mycobacterium tuberculosis as determined in a hollow-fiber infection model. *MBio*. 1(3):

Dutta NK, Illei PB, Peloquin CA, Pinn ML, Mdluli KE, et al. 2012. Rifapentine is not more active than rifampin against chronic tuberculosis in guinea pigs. *Antimicrob. Agents Chemother.* 56(7):3726–31

Ellard GA. 1969. Absorption, metabolism and excretion of pyrazinamide in man. *Tubercle*. 50:144–58

Escalante P. 2009. In the clinic. tuberculosis. *Ann Intern Med*. 150(11):ITC61–614; quiz ITV616

Falagas ME, Rafailidis PI, Rosmarakis ES. 2007. Arrhythmias associated with fluoroquinolone therapy. *Int J Antimicrob Agents*. 29(4):374–79

Falzon D, Jaramillo E, Schunemann HJ, Arentz M, Bauer M, et al. 2011. Who guidelines for the programmatic management of drug-resistant tuberculosis: 2011 update. *Eur Respir J*. 38(3):516–28

Favez G, Chioléro R, Willa C. 1972. Rifampin-isoniazid compared with streptomycin-isoniazid in the original treatment of infectious pulmonary tuberculosis. results of a controlled study. *Chest*. 61(6):583–86

FDA. 2010. "Pharmacometrics at fda." http://www.fda.gov/aboutfda/centersoffices/officeofmedicalproductsandtobacco/cder/ucm167032.htm. (10 january 2014, date last accessed)

Fletcher C V., Seifart HI, Zhu R, Mitchell CD, D'Argenio DZ, et al. 2012. The pharmacogenetics of nat2 enzyme maturation in perinatally hiv exposed infants receiving isoniazid

Flynn JL. 2006. Lessons from experimental mycobacterium tuberculosis infections. *Microbes Infect*. 8(4):1179–88

Forrest A, Nix DE, Ballow CH, Goss TF, Birmingham MC, Schentag JJ. 1993. Pharmacodynamics of intravenous ciprofloxacin in seriously ill patients. *Antimicrob Agents Chemother*. 37(5):1073–81

Fox W, Ellard GA, Mitchison DA. 1999. Studies on the treatment of tuberculosis undertaken by the british medical research council tuberculosis units, 1946-1986, with relevant subsequent publications. *Int J Tuberc Lung Dis*. 3(10 Suppl 2):S231–79

Fox W, Sutherland I, Daniels M. 1954. A five-year assessment of patients in a controlled trial of streptomycin in pulmonary tuberculosis; report to the tuberculosis chemotherapy trials committee of the medical research council. *Q J Med*. 23(91):347–66

Fuselli S, Gilman RH, Chanock SJ, Bonatto SL, De Stefano G, et al. 2007. Analysis of nucleotide diversity of nat2 coding region reveals homogeneity across native american populations and high intra-population diversity. *Pharmacogenomics J*. 7(2):144–52

Gagneux S, Small PM. 2007. Global phylogeography of mycobacterium tuberculosis and implications for tuberculosis product development. *Lancet Infect Dis*. 7(5):328–37

Gangadharam PRJ, Devadatta S, Fox W, Nair CN, Selkon JB. 1961. Rate of inactivation of isoniazid in south indian patients with pulmonary tuberculosis*. *Bull. World Health Organ.* 25:793–806

Gibson RS. 2005. Anthropometric assessment of body size. in: principles of nutritional assessment, 2nd edition. new york: oxford university press, 2005: 255-6. , pp. 255–56

Gieschke R, Steimer J-L. 2000. Pharmacometrics: modelling and simulation tools to improve decision making in clinical drug development. *Eur J Drug Metab Pharmacokinet*. 25(1):49–58

Ginsburg AS, Grosset JH, Bishai WR. 2003. Fluoroquinolones, tuberculosis, and resistance. *Lancet Infect Dis*. 3(7):432–42

Gordi T, Xie R, Huong N V, Huong DX, Karlsson MO, Ashton M. 2005. A semiphysiological pharmacokinetic model for artemisinin in healthy subjects incorporating autoinduction of metabolism and saturable first-pass hepatic extraction. *Br J Clin Pharmacol*. 59(2):189–98

Goutelle S, Bourguignon L, Maire PH, Van Guilder M, Conte JE, Jelliffe RW. 2009. Population modeling and monte carlo simulation study of the pharmacokinetics and antituberculosis pharmacodynamics of rifampin in lungs. *Antimicrob. Agents Chemother.* 53(7):2974–81

Graham SM, Bell DJ, Nyirongo S, Hartkoorn R, Ward SA, Molyneux EM. 2006a. Low levels of pyrazinamide and ethambutol in children with tuberculosis and impact of age, nutritional status, and human immunodeficiency virus infection. *Antimicrob Agents Chemother*. 50(2):407–13

Graham SM, Bell DJ, Nyirongo S, Hartkoorn R, Ward SA, Molyneux EM. 2006b. Low levels of pyrazinamide and ethambutol in children with tuberculosis and impact of age, nutritional status, and human immunodeficiency virus infection. *Antimicrob. Agents Chemother.* 50:407–13

Grig ERN. 1958. The arcana of tuberculosis. with a brief epidemiologic history of the disease in the u.s.a. *Amer Rev Tuberc Pulm Dis*. 78(151-72):

Grosset J, Truffot-Pernot C, Lacroix C, Ji B. 1992. Antagonism between isoniazid and the combination pyrazinamide-rifampin against tuberculosis infection in mice. *Antimicrob. Agents Chemother.* 36(3):548–51

Gumbo T, Dona CSWS, Meek C, Leff R. 2009. Pharmacokinetics-pharmacodynamics of pyrazinamide in a novel in vitro model of tuberculosis for sterilizing effect: a paradigm for faster assessment of new antituberculosis drugs. *Antimicrob. Agents Chemother.* 53:3197–3204

Gumbo T, Louie A, Deziel MR, Liu W, Parsons LM, et al. 2007a. Concentration-dependent mycobacterium tuberculosis killing and prevention of resistance by rifampin. *Antimicrob Agents Chemother*. 51(11):3781–88

Gumbo T, Louie A, Deziel MR, Parsons LM, Salfinger M, Drusano GL. 2004. Selection of a moxifloxacin dose that suppresses drug resistance in mycobacterium tuberculosis, by use of an in vitro pharmacodynamic infection model and mathematical modeling. *J Infect Dis*. 190(9):1642–51

Gumbo T, Louie A, Liu W, Brown D, Ambrose PG, et al. 2007b. Isoniazid bactericidal activity and resistance emergence: integrating pharmacodynamics and pharmacogenomics to predict efficacy in different ethnic populations. *Antimicrob Agents Chemother*. 51(7):2329–36

Gupta P, Roy V, Sethi GR, Mishra TK. 2008. Pyrazinamide blood concentrations in children suffering from tuberculosis: a comparative study at two doses. *Br. J. Clin. Pharmacol.* 65:423–27

Gurumurthy P, Ramachandran G, Hemanth Kumar AK, Rajasekaran S, Padmapriyadarsini C, et al. 2004a. Decreased bioavailability of rifampin and other antituberculosis drugs in patients with advanced human immunodeficiency virus disease. *Antimicrob Agents Chemother*. 48(11):4473–75

Gurumurthy P, Ramachandran G, Hemanth Kumar AK, Rajasekaran S, Padmapriyadarsini C, et al. 2004b. Malabsorption of rifampin and isoniazid in hiv-infected patients with and without tuberculosis. *Clin Infect Dis*. 38(2):280–83

Haas CJ, Zink A, Molnar E, Szeimies U, Reischl U, et al. 2000. Molecular evidence for different stages of tuberculosis in ancient bone samples from hungary. *Am J Phys Anthr.* 113(3):293–304

Havlir D, Barnes P. 1999. Tuberculosis in patients with human immunodeficiency virus infection. *N. Engl. J. Med.* 340:367–73

Heifets LB, Lindholm-Levy PJ, Flory MA. 1990. Bactericidal activity in vitro of various rifamycins against mycobacterium avium and mycobacterium tuberculosis. *Am Rev Respir Dis*. 141(3):626–30

Heymsfield SB, Olafson RP, Kutner MH, Nixon DW. 1979. A radiographic method of quantifying protein-calorie undernutrition. *Am J Clin Nutr*. 32(3):693–702

Holford N. 2005. The visual predictive check - superiority to standard diagnostic (rorschach) plots. in abstracts of the fourteenth population approach group in europe meeting, pamploma, 2005. abstract 738. http://www.page-meeting.org/?abstract=738 (date last accessed, 10

Holford NH, Ambros RJ, Stoeckel K. 1992. Models for describing absorption rate and estimating extent of bioavailability: application to cefetamet pivoxil. *J Pharmacokinet Biopharm*. 20(5):421–42

Hu Y, Coates AR, Mitchison DA. 2003. Sterilizing activities of fluoroquinolones against rifampin-tolerant populations of mycobacterium tuberculosis. *Antimicrob Agents Chemother*. 47(2):653–57

Hu Y, Coates AR, Mitchison DA. 2006. Sterilising action of pyrazinamide in models of dormant and rifampicin-tolerant mycobacterium tuberculosis. *Int J Tuberc Lung Dis*. 10(3):317–22

Hu Y, Mangan JA, Dhillon J, Sole KM, Mitchison DA, et al. 2000. Detection of mrna transcripts and active transcription in persistent mycobacterium tuberculosis induced by exposure to rifampin or pyrazinamide. *J Bacteriol*. 182(22):6358–65

Huyen MNT, Buu TN, Tiemersma E, Lan NTN, Dung NH, et al. 2013. Tuberculosis relapse in vietnam is significantly associated with mycobacterium tuberculosis beijing genotype infections. *J. Infect. Dis.* 207(10):1516–24

Janmahasatian S, Duffull SB, Ash S, Ward LC, Byrne NM, Green B. 2005. Quantification of lean bodyweight. *Clin. Pharmacokinet.* 44(10):1051–65

Jayaram R, Gaonkar S, Kaur P, Suresh BL, Mahesh BN, et al. 2003. Pharmacokinetics-pharmacodynamics of rifampin in an aerosol infection model of tuberculosis. *Antimicrob Agents Chemother*. 47(7):2118–24

Ji B, Lounis N, Maslo C, Truffot-Pernot C, Bonnafous P, Grosset J. 1998. In vitro and in vivo activities of moxifloxacin and clinafloxacin against mycobacterium tuberculosis. *Antimicrob Agents Chemother*. 42(8):2066–69

Jindani A, Aber VR, Edwards EA, Mitchison DA. 1980. The early bactericidal activity of drugs in patients with pulmonary tuberculosis. *Am Rev Respir Dis*. 121(6):939–49

Jindani A, Dore CJ, Mitchison DA. 2003. Bactericidal and sterilizing activities of antituberculosis drugs during the first 14 days. *Am J Respir Crit Care Med*. 167(10):1348–54

Jindani A, Hatherill M, Charalambous S, Mungofa S, Zizhou S, et al. 2013. A multicentre randomized clinical trial to evaluate high-dose rifapentine with a quinolone for treatment of pulmonary tb: the rifaquin trial. paper #147lb. 20th conference on retrovirus and opportunistic infections. georgia world congress center, atlanta

Jindani A, Nunn AJ, Enarson DA. 2004. Two 8-month regimens of chemotherapy for treatment of newly diagnosed pulmonary tuberculosis: international multicentre randomised trial. *Lancet*. 364(9441):1244–51

Jonsson EN, Karlsson MO. 1999. Xpose--an s-plus based population pharmacokinetic/pharmacodynamic model building aid for nonmem. *Comput Methods Programs Biomed*. 58(1):51–64

Kalliokoski A, Neuvonen PJ, Niemi M. 2010. Slco1b1 polymorphism and oral antidiabetic drugs. *Basic Clin. Pharmacol. Toxicol.* 107:775–81

Karlsson MO, Savic RM. 2007. Diagnosing model diagnostics. *Clin Pharmacol Ther*. 82(1):17–20

Karlsson MO, Sheiner LB. 1993. The importance of modeling interoccasion variability in population pharmacokinetic analyses. *J Pharmacokinet Biopharm*. 21(6):735–50

Kearns GL. 2000. Impact of developmental pharmacology on pediatric study design: overcoming the challenges. *J. Allergy Clin. Immunol.* 106:S128–S138

Kearns GL, Abdel-Rahman SM, Alander SW, Blowey DL, Leeder JS, Kauffman RE. 2003. Developmental pharmacology--drug disposition, action, and therapy in infants and children. *N Engl J Med*. 349(12):1157–67

Kenny MT, Strates B. 1981. Metabolism and pharmacokinetics of the antibiotic rifampin. *Drug Metab. Rev.* 12:159–218

Kerbusch T, Wahlby U, Milligan PA, Karlsson MO. 2003. Population pharmacokinetic modelling of darifenacin and its hydroxylated metabolite using pooled data, incorporating saturable first-pass metabolism, cyp2d6 genotype and formulation-dependent bioavailability. *Br J Clin Pharmacol*. 56(6):639–52

Keung A, Eller MG, McKenzie KA, Weir SJ. 1999. Single and multiple dose pharmacokinetics of rifapentine in man: part ii. *Int J Tuberc Lung Dis*. 3(5):437–44

Khan FA, Minion J, Pai M, Royce S, Burman W, et al. 2010. Treatment of active tuberculosis in hiv-coinfected patients: a systematic review and meta-analysis. *Clin Infect Dis*. 50:1288–99

Kiem S, Schentag JJ. 2008. Interpretation of antibiotic concentration ratios measured in epithelial lining fluid. *Antimicrob Agents Chemother*. 52(1):24–36

Kiser JJ, Zhu R, D'Argenio DZ, Cotton MF, Bobat R, et al. 2012. Isoniazid pharmacokinetics, pharmacodynamics, and dosing in south african infants. *Ther. Drug Monit.* 34(4):446–51

Krishnaswamy K. 1989. Drug metabolism and pharmacokinetics in malnourished children. *Clin. Pharmacokinet.* 17 Suppl 1:68–88

Kumar V, Abbas AK, Fausto N, Mitchell RN. 2007. Robbins basic pathology (8th ed.). saunders elsevier. pp. 516–522. isbn 978-1-4160-2973-1.

Lacroix C, Hoang TP, Nouveau J, Guyonnaud C, Laine G, et al. 1989. Pharmacokinetics of pyrazinamide and its metabolites in healthy subjects. *Eur. J. Clin. Pharmacol.* 36:395–400

Langdon G, Wilkins J, McFadyen L, McIlleron H, Smith P, Simonsson US. 2005. Population pharmacokinetics of rifapentine and its primary desacetyl metabolite in south african tuberculosis patients. *Antimicrob Agents Chemother*. 49(11):4429–36

Langdon G, Wilkins JJ, Smith PJ, McIlleron H. 2004. Consecutive-dose pharmacokinetics of rifapentine in patients diagnosed with pulmonary tuberculosis. *Int J Tuberc Lung Dis*. 8(7):862–67

Larcombe L, Rempel JD, Dembinski I, Tinckam K, Rigatto C, Nickerson P. 2005. Differential cytokine genotype frequencies among canadian aboriginal and caucasian populations. *Genes Immun*. 6(2):140–44

Lawn SD, Zumla AI. 2012. Tuberculosis. *Lancet*. 378(9785):57–72

Lee D. 2001. Principles of nutritional assessment. 3rd edition

Lei B, Wei CJ, Tu SC. 2000. Action mechanism of antitubercular isoniazid. *J. Biol. Chem.* 275:2520

Lheureux P, Penaloza A, Gris M. 2005. Pyridoxine in clinical toxicology: a review. *Eur. J. Emerg. Med.* 12(2):78–85

Li AP, Reith MK, Rasmussen A, Gorski JC, Hall SD, et al. 1997. Primary human hepatocytes as a tool for the evaluation of structure-activity relationship in cytochrome p450 induction potential of xenobiotics: evaluation of rifampin, rifapentine and rifabutin. *Chem. Biol. Interact.* 107:17–30

Lindbom L, Pihlgren P, Jonsson EN. 2005. Psn-toolkit--a collection of computer intensive statistical methods for non-linear mixed effect modeling using nonmem. *Comput Methods Programs Biomed*. 79(3):241–57

Lode H, Hoffken G, Olschewski P, Sievers B, Kirch A, et al. 1987. Pharmacokinetics of ofloxacin after parenteral and oral administration. *Antimicrob Agents Chemother*. 31(9):1338–42

Long MW, Snider DE, Farer LS. 1979. U.s. public health service cooperative trial of three rifampin-isoniazid regimens in treatment of pulmonary tuberculosis.

Long R, Shwartzman K. 2007. Transmission and pathogenesis of tuberculosis. in long, r. & ellis, e. (eds) canadian tuberculosis standards 6th ed. public health agency of canada

Lonnroth K, Castro KG, Chakaya JM, Chauhan LS, Floyd K, et al. 2010. Tuberculosis control and elimination 2010-50: cure, care, and social development. *Lancet*. 375(9728):1814–29

Lonnroth K, Jaramillo E, Williams BG, Dye C, Raviglione M. 2009. Drivers of tuberculosis epidemics: the role of risk factors and social determinants. *Soc Sci Med*. 68(12):2240–46

Loos U, Musch E, Jensen JC, Mikus G, Schwabe HK, Eichelbaum M. 1985. Pharmacokinetics of oral and intravenous rifampicin during chronic administration. *Klin Wochenschr*. 63:1205–11

Lounis N, Bentoucha A, Truffot-Pernot C, Ji B, O'Brien RJ, et al. 2001. Effectiveness of once-weekly rifapentine and moxifloxacin regimens against mycobacterium tuberculosis in mice. *Antimicrob Agents Chemother*. 45(12):3482–86

Marais BJ, Hesseling AC, Gie RP, Schaaf HS, Beyers N. 2006. The burden of childhood tuberculosis and the accuracy of community-based surveillance data. *Int J Tuberc Lung Dis*. 10(3):259–63

Martineau AR, Timms PM, Bothamley GH, Hanifa Y, Islam K, et al. 2011. High-dose vitamin d(3) during intensive-phase antimicrobial treatment of pulmonary tuberculosis: a double-blind randomised controlled trial. *Lancet*. 377(9761):242–50

Matimba A, Del-Favero J, Van Broeckhoven C, Masimirembwa C. 2009. Novel variants of major drug-metabolising enzyme genes in diverse african populations and their predicted functional effects. *Hum. Genomics*. 3:169–90

McCracken GH, Ginsburg CM, Zweighaft TC, Clahsen J. 1980. Pharmacokinetics of rifampin in infants and children: relevance to prophylaxis against haemophilus influenzae type b disease. *Pediatrics*. 66:17–21

McIlleron H, Norman J, Kanyok TP, Fourie PB, Horton J, Smith PJ. 2007. Elevated gatifloxacin and reduced rifampicin concentrations in a single-dose interaction study amongst healthy volunteers. *J Antimicrob Chemother*. 60(6):1398–1401

McIlleron H, Rustomjee R, Vahedi M, Mthiyane T, Denti P, et al. 2012. Reduced antituberculosis drug concentrations in hiv-infected patients who are men or have low weight: implications for international dosing guidelines. *Antimicrob. Agents Chemother.* 56(6):3232–38

McIlleron H, Wash P, Burger A, Norman J, Folb PI, Smith P. 2006. Determinants of rifampin, isoniazid, pyrazinamide, and ethambutol pharmacokinetics in a cohort of tuberculosis patients. *Antimicrob Agents Chemother*. 50(4):1170–77

McIlleron H, Willemse M, Schaaf HS, Smith PJ, Donald PR. 2011. Pyrazinamide plasma concentrations in young children with tuberculosis. *Pediatr Infect Dis J*. 30(3):262–65

McIlleron H, Willemse M, Werely CJ, Hussey GD, Schaaf HS, et al. 2009. Isoniazid plasma concentrations in a cohort of south african children with tuberculosis: implications for international pediatric dosing guidelines. *Clin Infect Dis*. 48(11):1547–53

McLay RN, Drake A, Rayner T. 2005. Persisting dementia after isoniazid overdose. *J. Neuropsychiatry Clin. Neurosci.* 17(2):256–57

Mehta S. 1990. Malnutrition and drugs: clinical implications. *Dev. Pharmacol. Ther.* 15:159–65

Menzies D, Benedetti A, Paydar A, Martin I, Royce S, et al. 2009. Effect of duration and intermittency of rifampin on tuberculosis treatment outcomes: a systematic review and meta-analysis. *PLoS Med*. 6(9):e1000146

Miller R, Ewy W, Corrigan B w, Ouellet D, Hermann K, et al. 2005. How modeling and simulation have enhanced decision making in new drug development. *J Pharmacokinet Pharmacodyn*. 32(2):185–97

Mitchison DA. 1998. Development of rifapentine: the way ahead. *Int J Tuberc Lung Dis*. 2(8):612–15

Mitchison DA. 2000. Role of individual drugs in the chemotherapy of tuberculosis. *Int J Tuberc Lung Dis*. 4(9):796–806

Mitchison DA. 2012. Pharmacokinetic/pharmacodynamic parameters and the choice of high-dosage rifamycins. *Int J Tuberc Lung Dis*. 16(9):1186–89

Mitchison DA, Selkon JB. 1956. The bactericidal activities of antituberculous drugs. *Am Rev Tuberc*. 74(2 Part 2):109–16; discussion, 116–23

Mor N, Simon B, Mezo N, Heifets L. 1995. Comparison of activities of rifapentine and rifampin against mycobacterium tuberculosis residing in human macrophages. *Antimicrob. Agents Chemother.* 39(9):2073–77

Mouton JW, Dudley MN, Cars O, Derendorf H, Drusano GL. 2005. Standardization of pharmacokinetic/pharmacodynamic (pk/pd) terminology for anti-infective drugs: an update. *J Antimicrob Chemother*. 55(5):601–7

MRC. 1948. Streptomycin treatment of pulmonary tuberculosis. *BMJ*. 2:769–82

Nakajima A, Yokoi T, Nakajima M, Kobayashi Y, Fukami T, Watanabe A. 2011. Human arylacetamide deacetylase is responsible for deacetylation of rifamycins: rifampicin, rifabutin, and rifapentine

Nicol MP, Zar HJ. 2011. New specimens and laboratory diagnostics for childhood pulmonary tb: progress and prospects. *Paediatr Respir Rev*. 12(1):16–21

Niemi M, Backman JT, Fromm MF, Neuvonen PJ, Kivistö KT. 2003. Pharmacokinetic interactions with rifampicin : clinical relevance. *Clin. Pharmacokinet.* 42:819–50

Nijland HM, Ruslami R, Suroto AJ, Burger DM, Alisjahbana B, et al. 2007. Rifampicin reduces plasma concentrations of moxifloxacin in patients with tuberculosis. *Clin Infect Dis*. 45(8):1001–7

Notterman DA, Nardi M, Saslow JG. 1986. Effect of dose formulation on isoniazid absorption in two young children. *Pediatrics*. 77:850–52

Orenstein EW, Basu S, Shah NS, Andrews JR, Friedland GH, et al. 2009. Treatment outcomes among patients with multidrug-resistant tuberculosis: systematic review and meta-analysis. *Lancet Infect Dis*. 9(3):153–61

Pargal A, Rani S. 2001. Non-linear pharmacokinetics of rifampicin in healthy asian indian volunteers. *Int J Tuberc Lung Dis*. 5(1):70–79

Pariente-Khayat A, Rey E, Gendrel D, Vauzelle-Kervroëdan F, Crémier O, et al. 1997. Isoniazid acetylation metabolic ratio during maturation in children. *Clin. Pharmacol. Ther.* 62:377–83

Parkin DP, Vandenplas S, Botha FJ, Vandenplas ML, Seifart HI, et al. 1997. Trimodality of isoniazid elimination: phenotype and genotype in patients with tuberculosis. *Am J Respir Crit Care Med*. 155(5):1717–22

Pasanen MK, Neuvonen M, Neuvonen PJ, Niemi M. 2006. Slco1b1 polymorphism markedly affects the pharmacokinetics of simvastatin acid. *Pharmacogenet. Genomics*. 16:873–79

Pasipanodya JG, Gumbo T. 2010. Clinical and toxicodynamic evidence that high-dose pyrazinamide is not more hepatotoxic than the low doses currently used. *Antimicrob. Agents Chemother.* 54(7):2847–54

Pasipanodya JG, McIlleron H, Burger A, Wash PA, Smith P, Gumbo T. 2013. Serum drug concentrations predictive of pulmonary tuberculosis outcomes. *J. Infect. Dis.* 208(9):1464–73

Peloquin C. 2003. What is the "right" dose of rifampin? *Int J Tuberc Lung Dis*. 7(1):3–5

Peloquin CA. 2002. Therapeutic drug monitoring in the treatment of tuberculosis. *Drugs*. 62(15):2169–83

Peloquin CA, Hadad DJ, Molino LP, Palaci M, Boom WH, et al. 2008. Population pharmacokinetics of levofloxacin, gatifloxacin, and moxifloxacin in adults with pulmonary tuberculosis. *Antimicrob Agents Chemother*. 52(3):852–57

Peloquin CA, Jaresko GS, Yong CL, Keung AC, Bulpitt AE, Jelliffe RW. 1997. Population pharmacokinetic modeling of isoniazid, rifampin, and pyrazinamide.

Peloquin CA, Namdar R, Singleton MD, Nix DE. 1999. Pharmacokinetics of rifampin under fasting conditions, with food, and with antacids.

Peloquin CA, Nitta AT, Burman WJ, Brudney KF, Miranda-Massari JR, et al. 1996. Low antituberculosis drug concentrations in patients with aids. *Ann Pharmacother*. 30(9):919–25

Perlman DC, Segal Y, Rosenkranz S, Rainey PM, Peloquin CA, et al. 2004. The clinical pharmacokinetics of pyrazinamide in hiv-infected persons with tuberculosis. *Clin. Infect. Dis.* 38:556–64

Perlman DC, Segal Y, Rosenkranz S, Rainey PM, Remmel RP, et al. 2005. The clinical pharmacokinetics of rifampin and ethambutol in hiv-infected persons with tuberculosis.

Rae JM, Johnson MD, Lippman ME, Flockhart DA. 2001. Rifampin is a selective, pleiotropic inducer of drug metabolism genes in human hepatocytes: studies with cdna and oligonucleotide expression arrays. *J. Pharmacol. Exp. Ther.* 299:849–57

Rajman I. 2008. Pk/pd modelling and simulations: utility in drug development. *Drug Discov Today*. 13(7-8):341–46

Ramachandran G, Hemanth Kumar a K, Bhavani PK, Poorana Gangadevi N, Sekar L, et al. 2013. Age, nutritional status and inh acetylator status affect pharmacokinetics of anti-tuberculosis drugs in children. *Int. J. Tuberc. lung Dis.* 17:800–806

Reiling N, Homolka S, Walter K, Brandenburg J, Niwinski L, et al. 2013. Clade-specific virulence patterns of mycobacterium tuberculosis complex strains in human primary macrophages and aerogenically infected mice. *MBio*. 4(4):e00250–13–

Reith K, Keung A, Toren PC, Cheng L, Eller MG, Weir SJ. 1998. Disposition and metabolism of 14c-rifapentine in healthy volunteers. *Drug Metab Dispos*. 26(8):732–38

Rekha B, Swaminathan S. 2007. Childhood tuberculosis - global epidemiology and the impact of hiv. *Paediatr. Respir. Rev.* 8:99–106

Relling M V, Evans RR, Groom S, Crom WR, Pratt CB. 1993. Saturable elimination and saturable protein binding account for flavone acetic acid pharmacokinetics. *J Pharmacokinet Biopharm*. 21(6):639–51

RIFAQUIN. 2008. An international multicentre controlled clinical trial to evaluate high dose rifapentine and a quinolone in the treatment of pulmonary tuberculosis. isrctn 44153044; http://ipc.nxgenomics.org/intertb/download/rifaquin_protocol_v_1.8_15_april_2011_final.pd

Roberts MS, Magnusson BM, Burczynski FJ, Weiss M. 2002. Enterohepatic circulation: physiological, pharmacokinetic and clinical implications. *Clin Pharmacokinet*. 41(10):751–90

Rosenthal IM, Tasneen R, Peloquin CA, Zhang M, Almeida D, et al. 2012. Dose-ranging comparison of rifampin and rifapentine in two pathologically distinct murine models of tuberculosis. *Antimicrob. Agents Chemother.* 56(8):4331–40

Rosenthal IM, Williams K, Tyagi S, Peloquin CA, Vernon AA, et al. 2006. Potent twice-weekly rifapentine-containing regimens in murine tuberculosis. *Am J Respir Crit Care Med*. 174(1):94–101

Rosenthal IM, Zhang M, Williams KN, Peloquin CA, Tyagi S, et al. 2007. Daily dosing of rifapentine cures tuberculosis in three months or less in the murine model. *PLoS Med*. 4(12):e344

Rousseau A, Leger F, Le Meur Y, Saint-Marcoux F, Paintaud G, et al. 2004. Population pharmacokinetic modeling of oral cyclosporin using nonmem: comparison of absorption pharmacokinetic models and design of a bayesian estimator. *Ther Drug Monit.* 26(1):23–30

Ruslami R, Ganiem AR, Aarnoutse RE, van Crevel R, study team. 2013. Rifampicin and moxifloxacin for tuberculous meningitis--authors' reply. *Lancet Infect Dis*. 13(7):570

Rustomjee R, Lienhardt C, Kanyok T, Davies GR, Levin J, et al. 2008. A phase ii study of the sterilising activities of ofloxacin, gatifloxacin and moxifloxacin in pulmonary tuberculosis. *Int J Tuberc Lung Dis*. 12(2):128–38

Sabbagh A, Darlu P, Crouau-Roy B, Poloni ES. 2011. Arylamine n-acetyltransferase 2 (nat2) genetic diversity and traditional subsistence: a worldwide population survey. *PLoS One*. 6:e18507

Sabbagh A, Langaney A, Darlu P, Gérard N, Krishnamoorthy R, Poloni ES. 2008. Worldwide distribution of nat2 diversity: implications for nat2 evolutionary history. *BMC Genet.* 9:21

Sakula A. 1982. Robert koch: centenary of the discovery of the tubercle bacillus, 1882. *Thorax*. 37(4):246–51

Sato K, Inoue Y, Fujii T, Aoyama H, Mitsuhashi S. 1986. Antibacterial activity of ofloxacin and its mode of action. *Infection.* 14 Suppl 4:S226–S230

Savic RM, Bliven-Sizemore E, Weiner M, Nuermberger E, Burman W, et al. 2011. Population pharmacokinetics of rifapentine and its active metabolite in healthy volunteers: nonlinearities in clearance and bioavailability

Savic RM, Jonker DM, Kerbusch T, Karlsson MO. 2007. Implementation of a transit compartment model for describing drug absorption in pharmacokinetic studies. *J Pharmacokinet Pharmacodyn*. 34(5):711–26

Savic RM, Weiner M, Mac Kenzie W, Helig C, Dooley K, et al. 2013. Pkpd analysis of rifapentine in patients during intensive phase treatment for tuberculosis from tuberculosis trial consortium studies 29 and 29x. 6th international workshop on clinical pharmacology of tuberculosis drugs. denver, co, usa. abstract 11.

Schaaf HS, Marais BJ, Hesseling AC, Brittle W, Donald PR. 2009a. Surveillance of antituberculosis resistance amonnst children from the western cape province of south africa- an upward trend. *Am. J. Public Health*. 99:1486–90

Schaaf HS, Parkin DP, Seifart HI, Werely CJ, Hesseling PB, et al. 2005. Isoniazid pharmacokinetics in children treated for respiratory tuberculosis. *Arch Dis Child*. 90(6):614–18

Schaaf HS, Willemse M, Cilliers K, Labadarios D, Maritz JS, et al. 2009b. Rifampin pharmacokinetics in children, with and without human immunodeficiency virus infection, hospitalized for the management of severe forms of tuberculosis. *BMC Med*. 7:19

Schatz A, Bugie E, Waksman S. 1944. Streptomycin, a substance exhibiting antibiotic activity against gram-positive and gram-negative bacteria. *Proc. Soc. Exp. Biol. Med.* 55:66–69

Schentag JJ, Meagher AK, Forrest A. 2003a. Fluoroquinolone auic break points and the link to bacterial killing rates. part 1: in vitro and animal models. *Ann Pharmacother*. 37(9):1287–98

Schentag JJ, Meagher AK, Forrest A. 2003b. Fluoroquinolone auic break points and the link to bacterial killing rates. part 2: human trials. *Ann Pharmacother*. 37:1478–88

Seifart HI, Gent WL, Parkin DP, van Jaarsveld PP, Donald PR. 1995. High-performance liquid chromatographic determination of isoniazid, acetylisoniazid and hydrazine in biological fluids. *J. Chromatogr. B Biomed. Sci. Appl.* 674(2):269–75

Senggunprai L, Yoshinari K, Yamazoe Y. 2009. Selective role of sulfotransferase 2a1 (sult2a1) in the n-sulfoconjugation of quinolone drugs in humans. *Drug Metab Dispos*. 37(8):1711–17

Shandil RK, Jayaram R, Kaur P, Gaonkar S, Suresh BL, et al. 2007. Moxifloxacin, ofloxacin, sparfloxacin, and ciprofloxacin against mycobacterium tuberculosis: evaluation of in vitro and pharmacodynamic indices that best predict in vivo efficacy. *Antimicrob Agents Chemother*. 51(2):576–82

Sheiner LB, Beal SL. 1980. Evaluation of methods for estimating population pharmacokinetics parameters. i. michaelis-menten model: routine clinical pharmacokinetic data. *J Pharmacokinet Biopharm*. 8(6):553–71

Sheiner LB, Beal SL. 1983. Evaluation of methods for estimating population pharmacokinetic parameters. iii. monoexponential model: routine clinical pharmacokinetic data. *J Pharmacokinet Biopharm*. 11(3):303–19

Shi W, Zhang X, Jiang X, Yuan H, Lee JS, et al. 2011. Pyrazinamide inhibits trans-translation in mycobacterium tuberculosis. *Science*. 333:1630–32

Siefert HM, Domdey-Bette A, Henninger K, Hucke F, Kohlsdorfer C, Stass HH. 1999. Pharmacokinetics of the 8-methoxyquinolone, moxifloxacin: a comparison in humans and other mammalian species. *J Antimicrob Chemother*. 43 Suppl B:69–76

Sirgel FA, Donald PR, Odhiambo J, Githui W, Umapathy KC, et al. 2000. A multicentre study of the early bactericidal activity of anti-tuberculosis drugs. *J Antimicrob Chemother*. 45(6):859–70

Sirgel FA, Fourie PB, Donald PR, Padayatchi N, Rustomjee R, et al. 2005. The early bactericidal activities of rifampin and rifapentine in pulmonary tuberculosis. *Am J Respir Crit Care Med*. 172(1):128–35

Sirgel FA, Warren RM, Streicher EM, Victor TC, van Helden PD, Bottger EC. 2012. Gyra mutations and phenotypic susceptibility levels to ofloxacin and moxifloxacin in clinical isolates of mycobacterium tuberculosis. *J Antimicrob Chemother*. 67(5):1088–93

Slama K, Chiang C-Y, Enarson DA, Hassmiller K, Fanning A, et al. 2007. Tobacco and tuberculosis: a qualitative systematic review and meta-analysis. *Int. J. Tuberc. Lung Dis.* 11(10):1049–61

Smythe W, Khandelwal A, Merle C, Rustomjee R, Gninafon M, et al. 2012. A semimechanistic pharmacokinetic-enzyme turnover model for rifampin autoinduction in adult tuberculosis patients. *Antimicrob Agents Chemother*. 56(4):2091–98

Smythe W, Merle CS, Rustomjee R, Gninafon M, Lo MB, et al. 2013. Evaluation of single and steady-state gatifloxacin pharmacokinetics and dose in pulmonary tuberculosis patients using monte carlo simulations. *Antimicrob Agents Chemother*

Southwick F. 2007. Chapter 4: pulmonary infections". infectious diseases: a clinical short course, 2nd ed. mcgraw-hill medical publishing division. pp. 104, 313–4. isbn 0-07-147722-5.

Sreevatsan S, Pan X, Zhang Y, Kreiswirth BN, Musser JM. 1997. Mutations associated with pyrazinamide resistance in pnca of mycobacterium tuberculosis complex organisms. *Antimicrob. Agents Chemother.* 41:636–40

Stambaugh JJ, Berning SE, Bulpitt AE, Hollender ES, Narita M, et al. 2002. Ofloxacin population pharmacokinetics in patients with tuberculosis. *Int J Tuberc Lung Dis*. 6(6):503–9

Steele MA, Des Prez RM. 1988. The role of pyrazinamide in tuberculosis chemotherapy. *Chest*. 94(4):845–50

Steingart KR, Jotblad S, Robsky K, Deck D, Hopewell PC, et al. 2011. Higher-dose rifampin for the treatment of pulmonary tuberculosis: a systematic review. *Int J Tuberc Lung Dis*. 15(3):305–16

Strolin Benedetti M, Dostert P. 1994. Induction and autoinduction properties of rifamycin derivatives: a review of animal and human studies. *Environ. Health Perspect.* 102 Suppl :101–5

Tachibana M, Tanaka M, Masubuchi Y, Horie T. 2005. Acyl glucuronidation of fluoroquinolone antibiotics by the udp-glucuronosyltransferase 1a subfamily in human liver microsomes. *Drug Metab Dispos*. 33(6):803–11

Taft DR, Iyer GR, Behar L, DiGregorio R V. 1997. Application of a first-pass effect model to characterize the pharmacokinetic disposition of venlafaxine after oral administration to human subjects. *Drug Metab Dispos*. 25(10):1215–18

Tam CM, Chan SL, Kam KM, Goodall RL, Mitchison DA. 2002. Rifapentine and isoniazid in the continuation phase of a 6-month regimen. final report at 5 years: prognostic value of various measures. *Int J Tuberc Lung Dis*. 6(1):3–10

Tam CM, Chan SL, Lam CW, Leung CC, Kam KM, et al. 1998. Rifapentine and isoniazid in the continuation phase of treating pulmonary tuberculosis. initial report. *Am J Respir Crit Care Med*. 157(6 Pt 1):1726–33

Tappero JW, Bradford WZ, Agerton TB, Hopewell P, Reingold AL, et al. 2005. Serum concentrations of antimycobacterial drugs in patients with pulmonary tuberculosis in botswana. *Clin Infect Dis*. 41:461–69

Telzak EE, Fazal BA, Pollard CL, Turett GS, Justman JE, Blum S. 1997. Factors influencing time to sputum conversion among patients with smear-positive pulmonary tuberculosis. *Clin. Infect. Dis.* 25(3):666–70

Thee S, Detjen A, Wahn U, Magdorf K. 2008. Pyrazinamide serum levels in childhood tuberculosis. *Int J Tuberc Lung Dis*. 12(9):1099–1101

Thee S, Detjen A, Wahn U, Magdorf K. 2009. Rifampicin serum levels in childhood tuberculosis. *Int J Tuberc Lung Dis*. 13(9):1106–11

Thee S, Detjen AA, Wahn U, Magdorf K. 2010. Isoniazid pharmacokinetic studies of the 1960s: considering a higher isoniazid dose in childhood tuberculosis. *Scand J Infect Dis*. 42(4):294–98

Thee S, Seddon JA, Donald PR, Seifart HI, Werely CJ, et al. 2011. Pharmacokinetics of isoniazid, rifampin, and pyrazinamide in children younger than two years of age with tuberculosis: evidence for implementation of revised world health organization recommendations. *Antimicrob Agents Chemother*. 55(12):5560–67

Thomas JK, Forrest A, Bhavnani SM, Hyatt JM, Cheng A, et al. 1998. Pharmacodynamic evaluation of factors associated with the development of bacterial resistance in acutely ill patients during therapy. *Antimicrob Agents Chemother*. 42(3):521–27

Thwaites GE, Bhavnani SM, Chau TT, Hammel JP, Torok ME, et al. 2011. Randomized pharmacokinetic and pharmacodynamic comparison of fluoroquinolones for tuberculous meningitis. *Antimicrob Agents Chemother*. 55(7):3244–53

Van Deun A, Salim MA, Das AP, Bastian I, Portaels F. 2004. Results of a standardised regimen for multidrug-resistant tuberculosis in bangladesh. *Int J Tuberc Lung Dis*. 8(5):560–67

Van Ingen J, Aarnoutse RE, Donald PR, Diacon AH, Dawson R, et al. 2011. Why do we use 600 mg of rifampicin in tuberculosis treatment? *Clin. Infect. Dis.* 52(9):e194–9

Vatsis KP, Weber WW, Bell DA, Dupret JM, Evans DA, et al. 1995. Nomenclature for n-acetyltransferases. *Pharmacogenetics*. 5(1):1–17

Vijayakumar M, Bhaskaram P, Hemalatha P. 1990. Malnutrition and childhood tuberculosis. *J Trop Pediatr*. 36(6):294–98

Visser ME, Stead MC, Walzl G, Warren R, Schomaker M, et al. 2012. Baseline predictors of sputum culture conversion in pulmonary tuberculosis: importance of cavities, smoking, time to detection and w-beijing genotype. *PLoS One*. 7(1):e29588

Wahlby U, Jonsson EN, Karlsson MO. 2001. Assessment of actual significance levels for covariate effects in nonmem. *J Pharmacokinet Pharmacodyn*. 28(3):231–52

Walls T, Shingadia D. 2004. Global epidemiology of paediatric tuberculosis. *J Infect*. 48(1):13–22

Wang TT, Nestel FP, Bourdeau V, Nagai Y, Wang Q, et al. 2004. Cutting edge: 1,25-dihydroxyvitamin d3 is a direct inducer of antimicrobial peptide gene expression. *J Immunol*. 173(5):2909–12

Warren RM, Streicher EM, Gey van Pittius NC, Marais BJ, van der Spuy GD, et al. 2009. The clinical relevance of mycobacterial pharmacogenetics. *Tuberculosis (Edinb).* 89(3):199–202

Wayne LG, Hayes LG. 1996. An in vitro model for sequential study of shiftdown of mycobacterium tuberculosis through two stages of nonreplicating persistence. *Infect Immun*. 64(6):2062–69

Weber F. 1948. Decline of tuberculosis mortality. *Public Health Rep.* 63(6):

Weber WW, Hein DW. 1979. Clinical pharmacokinetics of isoniazid. *Clin. Pharmacokinet.* 4(6):401–22

Wehrli W. 1983. Rifampin: mechanisms of action and resistance. *Rev Infect Dis*. 5 Suppl 3:S407–11

Weiner M, Benator D, Burman W, Peloquin CA, Khan A, et al. 2005. Association between acquired rifamycin resistance and the pharmacokinetics of rifabutin and isoniazid among patients with hiv and tuberculosis. *Clin Infect Dis*. 40(10):1481–91

Weiner M, Bock N, Peloquin CA, Burman WJ, Khan A, et al. 2004. Pharmacokinetics of rifapentine at 600, 900, and 1,200 mg during once-weekly tuberculosis therapy. *Am J Respir Crit Care Med*. 169(11):1191–97

Weiner M, Peloquin C, Burman W, Luo CC, Engle M, et al. 2010. Effects of tuberculosis, race, and human gene slco1b1 polymorphisms on rifampin concentrations. *Antimicrob Agents Chemother*. 54(10):4192–4200

WHO. 2003. Treatment of tuberculosis: guidelines for national programmes, 3rd ed. world health organization, geneva, switzerland. http://whqlibdoc.who.int/hq/2003/who_cds_tb_2003.313_eng.pdf. (18 february 2013, date last accessed)

WHO. 2008a. Guidelines for the programmatic management of drug-resistant tuberculosis. 2008. http://whqlibdoc.who.int/publications/2008/9789241547581_eng.pdf. (23 march 2013, date last accessed)

WHO. 2008b. Policy guidance on drug-susceptibility testing (dst) of second-line antituberculosis drugs.world health organization, geneva, switzerland. who/htm/tb/2008.392, http://www.who.int/tb/publications/2008/whohtmtb_2008_392/en/index.html. accessed 27 february 2

WHO. 2008c. National tuberculosis management guidelines 2008. http://www.who.int/hiv/pub/guidelines/south_africa_tb.pdf (10 frebruary 2013, date last accessed)

WHO. 2009. Who. global tuberculosis control: a short update to the 2009 report. geneva: world health organization, 2009. http://www.who.int/tb/publications/global_report/2009/update/tbu9.pdf (date last accessed, 04 july 2013)

WHO. 2010. Rapid advice: treatment of tuberculosis in children. world health organization, geneva 2010. http://whqlibdoc.who.int/publications/2010/9789241500449_eng.pdf. accessed (14 september 2011, date last accessed)

WHO. 2011. Guidelines for the programmatic management of drug-resistant tuberculosis 2011 update. world health organisation, geneva, switzerland. http://whqlibdoc.who.int/publications/2011/9789241501583_eng.pdf (14 may 2013, date last accessed)

WHO. 2012a. Global tuberculosis report 2012. world health organization, geneva, switzerland. http://apps.who.int/iris/bitstream/10665/91355/1/9789241564656_eng.pdf (date last accessed, 31 december 2013)no title

WHO. 2012b. Definitions and reporting framework for tuberculosis – 2013 revision. http://apps.who.int/iris/bitstream/10665/79199/1/9789241505345_eng.pdf (date last accessed, 23 june 2013)

WHO. 2012c. Annual meeting of the childhood tb subgroup, hotel maya, kuala lumpur, malaysia, 11 november 2012. meeting report. world health organization, stop tb partnership, geneva, switzerland, 2012.

WHO. 2013. Global tuberculosis report 2013. world health organization, geneva, switzerland. http://apps.who.int/iris/bitstream/10665/91355/1/9789241564656_eng.pdf (date last accessed, 31 december 2013)

Wilkins JJ. 2005. Nonmemory: a run management tool for nonmem. *Comput Methods Programs Biomed*. 78(3):259–67

Wilkins JJ, Langdon G, McIlleron H, Pillai GC, Smith PJ, Simonsson USH. 2006. Variability in the population pharmacokinetics of pyrazinamide in south african tuberculosis patients. *Eur J Clin Pharmacol*. 62(9):727–35

Wilkins JJ, Langdon G, McIlleron H, Pillai G, Smith PJ, Simonsson USH. 2011. Variability in the population pharmacokinetics of isoniazid in south african tuberculosis patients. *Br J Clin Pharmacol*. 72(1):51–62

Wilkins JJ, Savic RM, Karlsson MO, Langdon G, McIlleron H, et al. 2008. Population pharmacokinetics of rifampin in pulmonary tuberculosis patients, including a semimechanistic model to describe variable absorption. *Antimicrob Agents Chemother*. 52(6):2138–48

Wong EB, Cohen K a, Bishai WR. 2013. Rising to the challenge: new therapies for tuberculosis. *Trends Microbiol.* 21:493–501

Yim JJ, Selvaraj P. 2010. Genetic susceptibility in tuberculosis. *Respirology*. 15(2):241–56

Yoshimatsu T, Nuermberger E, Tyagi S, Chaisson R, Bishai W, Grosset J. 2002. Bactericidal activity of increasing daily and weekly doses of moxifloxacin in murine tuberculosis. *Antimicrob Agents Chemother*. 46(6):1875–79

Yuk JH, Nightingale CH, Quintiliani R, Sweeney KR. 1991. Bioavailability and pharmacokinetics of ofloxacin in healthy volunteers. *Antimicrob Agents Chemother*. 35(2):384–86

Zai H, Kusano M, Hosaka H, Shimoyama Y, Nagoshi A, et al. 2009. Monosodium l-glutamate added to a high-energy, high-protein liquid diet promotes gastric emptying. *Am J Clin Nutr*. 89(1):431–35

Zent C, Smith P. 1995. Study of the effect of concomitant food on the bioavailability of rifampicin, isoniazid and pyrazinamide.

Zhanel GG, Ennis K, Vercaigne L, Walkty A, Gin AS, et al. 2002. A critical review of the fluoroquinolones: focus on respiratory infections. *Drugs*. 62(1):13–59

Zhang T, Zhang M, Rosenthal IM, Grosset JH, Nuermberger EL. 2009. Short-course therapy with daily rifapentine in a murine model of latent tuberculosis infection. *Am J Respir Crit Care Med*

Zhang Y, Mitchison D. 2003. The curious characteristics of pyrazinamide: a review. *Int. J. Tuberc. Lung Dis.* 7:6–21

Zhu M, Kaul S, Nandy P, Grasela DM, Pfister M. 2009. Model-based approach to characterize efavirenz autoinduction and concurrent enzyme induction with carbamazepine. *Antimicrob Agents Chemother*. 53(6):2346–53

Zhu M, Starke JR, Burman WJ, Steiner P, Stambaugh JJ, et al. 2002. Population pharmacokinetic modeling of pyrazinamide in children and adults with tuberculosis. *Pharmacotherapy*. 22(6):686–95

Zink AR, Sola C, Reischl U, Grabner W, Rastogi N, et al. 2003. Characterization of mycobacterium tuberculosis complex dnas from egyptian mummies by spoligotyping. *J Clin Microbiol*. 41(1):359–67

Zvada SP, Denti P, Geldenhuys H, Meredith S, van As D, et al. 2012. Moxifloxacin population pharmacokinetics in patients with pulmonary tuberculosis and the effect of intermittent high-dose rifapentine. *Antimicrob Agents Chemother*. 56(8):4471–73

Zvada SP, Denti P, Sirgel FA, Chigutsa E, Hatherill M, et al. 2014. Moxifloxacin population pharmacokinetics and model-based comparison of efficacy between moxifloxacin and ofloxacin in african patients. *Antimicrob. Agents Chemother.* 58(1):503–10

APPENDICES

Appendix 1- Rifampicin run record and control stream

a) Rifampicin run record

Model	Description [a]	Comment[b]	OFV
1	One compartment, first-order absorption, first order elimination. IIV on CL, Vc, ka, F	Base model	1035
2	Add lag time to model 1	The model high imprecision on estimate of lag time, hence dropped	1028
3	Use transit absorption compartment on model 1 instead of lag time, IIV CL, Vc, F, MTT	The model had good precision in parameter estimates, but IIV in ka was almost zero(0) and was dropped	1023
4	Add IOV in F on model 3. IIV CL, Vc, F, MTT	Improvement in the fit but IIV in F dropped and had high RSE.	988
5	Add IOV in CL on model 4	Improvement in fit.	980
6	Add IOV in MTT on model 4, IIV in CL, Vc, IOV in CL, MTT and F	Improvement in the fit but IIV in MTT dropped and had high RSE	967
7	Add IOV in V on model 5	No significant improvement in fit	961
8	Add IOV in ka on model 6	No significant improvement in fit	960
9	Run 6 plus covariance between IIV for CL and Vc	Improvement in fit	963
10	Run 9 plus dose-nonlinearity	Very high RSE on estimates of CL, Vc	958
11	Run 9 plus saturable clearance	Imprecision in estimates of Km and Vmax	962
12	Run 9 and add weight as linear covariate on CL	Huge improvement in fit	898
13	Run 12 plus add weight as covariate on Vc	improvement in fit	891
14	Run 9 plus allometric scaling with weight on CL and Vc. Therefore selected. IIV in CL, Vc, IOV in CL, MTT and F	Improvement in fit. This run was preferred than run13 based on well-established principles (Anderson & Holford 2008) and parsimony	893
15	Run 9 plus allometric scaling with fat free mass on CL and Vc	Was worse than run 14	898
16	Run 9 plus allometric scaling with fat mass mass on CL and Vc	Was than run 14	901
17	Run 14 plus test HIV on F	Slight improvement in fit compared with run 14	891
18	Run 14 plus HIV on CL	No improvement in fit compared with run 14	892
19	Run 14 plus HIV on Vc	No improvement in fit compared with run 14	893
20	Run 14 plus SEX on F	No improvement in fit compared with run 14	890
21	Run 14 plus SEX on CL	No improvement in fit compared with run 14	890
22	Run 14 plus SEX on Vc	Improvement in fit compared with run 14, but was dropped because it was being confounded with kwashiorkor status. Females 17% had higher Vc and estimates had high RSE	888
23	Run 14 plus albumin on Vc	No improvement in fit compared with run 14	893
24	Run 14 plus maturation of CL	Improvement in fit and better RSE	874
25	Run 14 plus maturation on Vc	No improvement in fit	880
26	Run 14 pus maturation on MTT	Improvement in fit and better RSE	875
27	Combine maturation effect in MTT and CL	Improvement in fit	870
28	Add hill factor on run 26	Final model	866

[a]CL and Vc are oral clearance and apparent volume of distribution in plasma, respectively. MTT, absorption mean transit time, value at full maturation; NN, number of transit compartments; F, relative bioavailability; Hill, steepness of the maturation function; IIV, inter-individual variability; IOV, inter-occasional variability. [b]RSE, relative standard error.

b) Rifampicin run record

```
$PROBLEM  RIF PAEDIATRICS
$ABBREVIATED COMRES=2
$INPUT ID OCC TIME DVO=DROP DV AMT DOSE AGE KWS HIV WT EVID SEX HT PRB SITE BLQ
$DATA simba_rif_2013_09_20.csv IGNORE=# IGNORE=(PRB.EQ.1)
$SUBROUTINE ADVAN13 TOL=8

$MODEL NCOMPARTMENTS=1
COMP=(CENTRAL DEFDOSE DEFOBSERVATION)

$PK
IF (AMT.GT.0.OR.EVID.GE.3) THEN
            TDOSE=TIME
            TAD=0
ENDIF
TAD=TIME-TDOSE

IF (TIME<72.AND.TIME>71) TAD=TIME-72 ; Fix the TAD for pre-doses

; Maturation
HILL   = THETA(9)
TM50   = THETA(8)

PMA    = AGE + (9/12)
FMAT =1/(1+(PMA/TM50)**(-HILL))

OC1=0
OC2=0
OC3=0
OC4=0

IF(OCC.EQ.1) OC1 =1
IF(OCC.EQ.2) OC2 =1
IF(OCC.EQ.3) OC3 =1
IF(OCC.EQ.4) OC4 =1

IOVBIO  = OC1*(ETA(3)) + OC2*(ETA(4))+ OC3*(ETA(5)) + OC4*(ETA(6))
IOVCL   = OC1*(ETA(7)) + OC2*(ETA(8))+ OC3*(ETA(9)) + OC4*(ETA(10))
IOVMTT  = OC1*(ETA(11)) + OC2*(ETA(12))+ OC3*(ETA(13)) + OC4*(ETA(14))

BSVCL=ETA(1)
BSVV2=ETA(2)

 TVCL  = THETA(1)*((WT/12.5)**0.75)*FMAT
 CL    = TVCL *EXP(BSVCL+IOVCL)

 TVV  = THETA(2) *(WT/12.5)
 V    = TVV*EXP(BSVV2)

 TVMTT  = THETA(3)*FMAT
 MTT    = TVMTT*EXP(IOVMTT)

 TVBIO  = THETA(4)
 BIO    = TVBIO*EXP(IOVBIO)

 TVNN   =THETA(5)
 NN     =TVNN

K=CL/V
S1=V
F1=0 ; set bioavailability in compartment 1 to 0 when using transit compartment

KTR = (NN+1)/MTT

IF (NEWIND.NE.2.OR.EVID.GE.3) THEN
            TNXD=TIME
```

```
        PNXD=AMT
ENDIF

TDOS=TNXD
PD=PNXD

IF(AMT.GT.0) THEN ;
        TNXD=TIME
        PNXD=AMT
ENDIF


LNGAM = NN*LOG(NN)-NN+LOG(NN*(1+4*NN*(1+2*NN)))/6+0.572364942
PIZZA=LOG(BIO*PD*KTR+0.00001)-LNGAM


IF (NEWIND.LE.1.OR.EVID.GE.3) THEN ; assign negative Cmax Tmax for the new subject
        COM(1)=-1 ; holder of Cmax
        COM(2)=-1 ; holder of Tmax
ENDIF


$DES
TEMPO=T-TDOS ; this is time after dose, it should always be >= 0
DADT(1)=0
KTT=0

IF(TEMPO.GT.0) THEN
        KTT=KTR*TEMPO
        DADT(1)=EXP(PIZZA+NN*LOG(KTT)-KTT)-K*A(1)
ENDIF

;------CMAX AND TMAX
CT=A(1)/V
IF(CT.GT.COM(1)) THEN
        COM(1)=CT
        COM(2)=T
ENDIF

$ERROR
IPRED =A(1)/V
PROP  =THETA(6)*IPRED
ADD   =THETA(7)
IF (SITE==2) ADD=THETA(10)


W = SQRT(PROP**2+ADD**2)
IF (W.LE.0.0001) W=0.0001
IF(BLQ==1.AND.SITE==1) W = 0.05
IF(BLQ==1.AND.SITE==2) W = 0.375

IRES  = DV-IPRED
IWRES = IRES/W
Y     = IPRED+W*EPS(1)


IF (ICALL==4.AND.SITE==1.AND.Y.LE.0.1) Y = 0.05
IF (ICALL==4.AND.SITE==2.AND.Y.LE.0.75) Y = 0.375

AUC  = BIO*AMT/CL
CMAX = COM(1)
TMAX = COM(2)

AA1=A(1)

;-------initial estimates_ theta
$THETA  (0,8.14633,20) ; 1_TVCL
```

```
$THETA  (0,16.238,30) ; 2_TVV2
$THETA  (0,1.03838,3) ; 3_TVMTT
$THETA  1 FIX ; 4_BIO
$THETA  (0,8.04401,30) ; 5_NN
$THETA  (0,0.233525,0.5) ; 6_PROP
$THETA  (0,0.121799,1) ; 7_ADD
$THETA  (0,1.12139,5) ; 8_TM50
$THETA  (0,2.2141,5) ; 9_HILL
$THETA  (0,0.629802,1) ; 10_ADD2
$OMEGA  BLOCK(2)
 0.106349  ;   1_IIV_CL
 0.125873 0.188156  ;    2_IIV_V

$OMEGA  BLOCK(1)  0.230832
$OMEGA  BLOCK(1) SAME
$OMEGA  BLOCK(1) SAME
$OMEGA  BLOCK(1) SAME

$OMEGA  BLOCK(1)  0.0631686
$OMEGA  BLOCK(1) SAME
$OMEGA  BLOCK(1) SAME
$OMEGA  BLOCK(1) SAME

$OMEGA  BLOCK(1) 0.160309
$OMEGA  BLOCK(1) SAME
$OMEGA  BLOCK(1) SAME
$OMEGA  BLOCK(1) SAME

$SIGMA  1  FIX
$ESTIMATION MAXEVAL=9999 PRINT=1 SIGDIG=3 SIGL=9 POSTHOC METH=COND INTER NOABORT
MSFO=msf1020 ATOL=4
$COVARIANCE PRINT=E MATRIX=S ATOL=4

$TABLE FILE=sdtab1020 ID CMAX OCC TIME TAD DV IPRED PRED IWRES WRES CWRES NPDE AA1 NOPRINT
ONEHEADER NOAPPEND ESAMPLE=1000 FORMAT=,
$TABLE FILE=patab1020 ID OCC CL V BIO BSVCL BSVV2 IOVCL IOVBIO NOPRINT ONEHEADER NOAPPEND
FORMAT=,
$TABLE FILE=cotab1020 ID OCC WT AGE NOPRINT ONEHEADER NOAPPEND FORMAT=,
$TABLE FILE=catab1020 ID OCC KWS HIV SEX SITE NOPRINT ONEHEADER NOAPPEND FORMAT=,
$TABLE FILE=mytab1020 ID CMAX OCC TIME TAD DV IPRED PRED IWRES WRES CWRES NPDE AA1
CL V BIO BSVCL BSVV2 IOVCL IOVBIO
WT AGE KWS HIV SEX SITE CMAX TMAX AUC NOPRINT ONEHEADER NOAPPEND FORMAT=,
```

Appendix 2- Pyrazinamide run record and control stream

a) Pyrazinamide run record

Model	Description [a]	Comment[b]	OFV
1	One compartment, first-order absorption, first order elimination. IIV on CL, Vc, ka, F	Base model	2030
2	Add lag time to model 1	No improvement in fit	2030
3	Use transit absorption compartment on model 1 instead of lag time, IIV CL, Vc, F, MTT, ka	Improvement in fit	2022
4	Add IOV in F on model 3. IIV CL, Vc, F, MTT	Improvement in the fit but IIV in F and Vc zeros	2002
5	Add IOV in CL on model 4	Improvement in fit.	1992
6	Add IOV in MTT on model 5	Improvement in the fit but IIV in MTT zeros	1985
7	Add IOV in V on model 6	No improvement in fit	1983
8	Add IOV in ka on model 6	Improvement in fit	1974
9	Run 8 plus covariance between IIV for CL and Vc	No improvement in fit	1974
10	Run 8 plus dose-nonlinearity	Very RSE on estimates of CL, Vc	1973
11	Run 8 plus saturable clearance	Imprecision in estimates of Km and Vmax	1971
12	Run 8 and add weight as linear covariate on CL	Improvement in fit	1965
13	Run 12 plus add weight as covariate on Vc	improvement in fit, but not significant	1963
14	Run 8 plus allometric scaling with weight on CL and Vc. Therefore selected. IIV in CL, IOV in CL, MTT , F, ka	Improvement in fit. This run was preferred than run13 based on well-established principles (Anderson & Holford 2008) and parsimony. FINAL model	1960
15	Run 8 plus allometric scaling with fat free mass on CL and Vc	Worse fit	1969
16	Test allometric scaling with fat mass mass on CL and Vc	Worse fit	1967
17	Run 14 plus test HIV on F	Not significant	1958
18	Run 14 plus HIV on CL	Not significant	1959
19	Run 14 plus HIV on Vc	Not significant	1959
20	Run 14 plus SEX on F	High RSE in estimate of sex effect	1955
21	Run 14 plus SEX on CL	Not significant	1960
22	Run 14 plus SEX on Vc	Not significant	1960
23	Run 14 plus albumin on Vc	Not significant	1960

[a]CL and Vc are oral clearance and apparent volume of distribution in plasma, respectively. MTT, absorption mean transit time, value at full maturation; NN, number of transit compartments; F, relative bioavailability; IIV, inter-individual variability; IOV, inter-occasional variability. [b]RSE, relative standard error.

b) Pyrazinamide run record

```
$PROBLEM  PZA  pediatrics
$INPUT ID OCC TIME ORG_DV=DROP DV AMT MDV EVID AGE KWS HIV WT SEXM PRB SITE BLQ

$DATA PZA_2013-09-20.csv IGNORE=@ IGNORE=(PRB.EQ.1)

$ABBREVIATED COMRES=2
$SUBROUTINE ADVAN13 TOL=9
$MODEL NCOMP=2
COMP(ABSORB, DEFDOSE)
COMP(CENTRAL, DEFOBS)

$PK
IF (AMT.GT.0.OR.EVID.GE.3) THEN
        TDOSE=TIME
        TAD=0
ENDIF
TAD=TIME-TDOSE
IF (TIME<72.AND.TIME>71) TAD=TIME-72


BSVCL=ETA(1)
BSVV2=ETA(2)

IOVCL=ETA(3)
IOVF=ETA(7)
IOVKA=ETA(11)
IOVMTT=ETA(15)
IF(OCC==2) THEN
        IOVCL=ETA(4)
        IOVF=ETA(8)
        IOVKA=ETA(12)
        IOVMTT=ETA(16)
ENDIF
IF(OCC==3) THEN
        IOVCL=ETA(5)
        IOVF=ETA(9)
        IOVKA=ETA(13)
        IOVMTT=ETA(17)
ENDIF
IF(OCC==4) THEN
        IOVCL=ETA(6)
        IOVF=ETA(10)
        IOVKA=ETA(14)
        IOVMTT=ETA(18)
ENDIF

TVWT=12.5
ALLMCL=(WT/TVWT)**0.75
ALLMV=WT/TVWT

TVCL = THETA(1)*ALLMCL
CL   = TVCL*EXP(BSVCL+IOVCL)

TVV2 = THETA(2)*ALLMV
V2    = TVV2*EXP(BSVV2)

TVKA = THETA(3)
KA   = TVKA*EXP(IOVKA)

TVBIO =1
BIO   =TVBIO*EXP(IOVF)

TVMTT  = THETA(6)
MTT    = TVMTT*EXP(IOVMTT)
```

```
TVNN   =THETA(7)
NN     =TVNN


K    = CL/V2
F1=0
KTR = (NN+1)/MTT

IF (NEWIND.NE.2.OR.EVID.GE.3) THEN
            TNXD=TIME
            PNXD=AMT
ENDIF

TDOS=TNXD
PD=PNXD

IF(AMT.GT.0) THEN
            TNXD=TIME
            PNXD=AMT
ENDIF

LNGAM = NN*LOG(NN)-NN+LOG(NN*(1+4*NN*(1+2*NN)))/6+0.572364942
PIZZA=LOG(BIO*PD*KTR+0.00001)-LNGAM

IF(NEWIND.NE.2.OR.EVID.GE.3) THEN
            COM(1)=-1 ; holder of Cmax
            COM(2)=-1 ; holder of Tmax
ENDIF

$DES
TEMPO=T-TDOS

DADT(1)=0
KTT=0
IF(TEMPO.GT.0) THEN
            KTT=KTR*TEMPO
            DADT(1)=EXP(PIZZA+NN*LOG(KTT)-KTT)-KA*A(1)
ENDIF

DADT(2) = KA*A(1)-K*A(2)

CT=A(2)/V2
IF(CT.GT.COM(1)) THEN
            COM(1)=CT
            COM(2)=T
ENDIF

$ERROR
IPRED = A(2)/V2
PROP = THETA(4)*IPRED
ADD = THETA(5)
IF (SITE==2) PROP = THETA(8)*IPRED

W =SQRT(PROP**2+ADD**2)
IF (W.LT.0.001) W = 0.001
IF (BLQ==1.AND.SITE==1.AND.ICALL.EQ.2) W=0.05
IF (BLQ==1.AND.SITE==2.AND.ICALL.EQ.2) W=0.75

IRES=DV-IPRED
IWRES=IRES/W
Y = IPRED + W*EPS(1)

IF (ICALL==4.AND.SITE==1.AND.Y.LE.0.1) Y = 0.05
IF (ICALL==4.AND.SITE==2.AND.Y.LE.0.5) Y = 0.25

CMAX = COM(1)
TMAX = COM(2)
```

```
AUC  = BIO*AMT/CL

$THETA  (0,1.08297,5) ; 1_CL
$THETA  (0,9.64465,20) ; 2_V
$THETA  (0,4.48056,10) ; 3_KA
$THETA  (0,0.0999155,0.5) ; 4_PROP_RUV_SITE1
$THETA  0 FIX ; 5_ADD_RUV
$THETA  (0,0.095077,2) ; 6_MTT
$THETA  (0,3.93896,50) ; 7_NN
$THETA  (0,0.0553184,0.5) ; 8_PROP_RUV_SITE2
$OMEGA  0.0733772  ;    1 IIVCL
$OMEGA  0  FIX  ;     2 IIVV

$OMEGA  BLOCK(1)  0.0647795  ;    3 IOVCL
$OMEGA  BLOCK(1) SAME
$OMEGA  BLOCK(1) SAME
$OMEGA  BLOCK(1) SAME

$OMEGA  BLOCK(1)  0.0610214  ;     7 IOVF
$OMEGA  BLOCK(1) SAME
$OMEGA  BLOCK(1) SAME
$OMEGA  BLOCK(1) SAME

$OMEGA  BLOCK(1)  0.745937  ;   11 IOVKA
$OMEGA  BLOCK(1) SAME
$OMEGA  BLOCK(1) SAME
$OMEGA  BLOCK(1) SAME

$OMEGA  BLOCK(1)  1.25559  ;  15 IOVMTT
$OMEGA  BLOCK(1) SAME
$OMEGA  BLOCK(1) SAME
$OMEGA  BLOCK(1) SAME

$SIGMA  1  FIX
$ESTIMATION MSFO=msf129 MAXEVAL=9999 PRINT=1 SIGDIG=3 SIGL=9 POSTHOC METH=COND ATOL=4
INTER NOABORT
$COVARIANCE ATOL=4 PRINT=E MATRIX=S

$TABLE FILE=sdtab129 ID CMAX OCC TIME TAD DV IPRED PRED IWRES WRES CWRES NPDE AA1 AA2
NOPRINT ONEHEADER NOAPPEND ESAMPLE=1000 FORMAT=,
$TABLE FILE=patab129 ID OCC CL V2 KA F1 BSVCL BSVV2 IOVCL IOVKA IOVF NOPRINT ONEHEADER
NOAPPEND FORMAT=,
$TABLE FILE=cotab129 ID OCC WT AGE NOPRINT ONEHEADER NOAPPEND FORMAT=,
$TABLE FILE=catab129 ID OCC KWS HIV SEXM SITE NOPRINT ONEHEADER NOAPPEND FORMAT=,
$TABLE FILE=mytab129 ID CMAX OCC TIME TAD DV IPRED PRED IWRES WRES CWRES NPDE AA1 AA2 CL
V2 KA F1
        BSVCL BSVV2 IOVCL IOVKA IOVF WT AGE KWS HIV SEXM SITE CMAX TMAX AUC NOPRINT
ONEHEADER NOAPPEND FORMAT=,
```

Appendix 3 - Isoniazid run record and control stream

a) Isoniazid run record

Model	Description [a]	Comment[b]	OFV
1	One compartment, first-order absorption, first order elimination. IIV on CL, Vc, ka, F	Base model	-90
2	Add lag time to model 1	High RSE on lag time	-98
3	Use transit absorption compartment on model 1 instead of lag time, IIV CL, Vc, F, MTT,ka	Better than run 2 in term of fit and diagnostics	-110
4	Add IOV in F on model 3. IIV CL, MTT, ka	Improvement in the fit but IIV in F was small while in Vc had high RSE.	-125
5	Add IOV in MTT on model 4	Improvement in fit. The IIV in MTT drops to zero (0).	-135
6	Add IOV in CL on model 5	No improvement in the fit	-138
7	Add IOV in Vc on model 5	No significant improvement in fit	-137
8	Add IOV in ka on model 5.	Improvement in fit, IIV in ka zeros	-150
9	Run 6 plus covariance between IIV for CL and Vc	No improvement in fit. Estimates of RSE increased	-152
10	Run 8 plus dose-nonlinearity	Very high RSE on estimates of CL, Vc	-146
11	Run 8plus saturable clearance	Imprecision in estimates of Km and Vmax	-146
12	Run 8 and add weight as linear covariate on CL	Huge improvement in fit	-188
13	Run 12 plus add weight as covariate on Vc	improvement in fit	-200
14	Run 8 plus allometric scaling with weight on CL and Vc. Therefore selected. IIV in CL, Vc, IOV in CL, MTT and F	Improvement in fit. This run was preferred than run13 based on well-established principles (Anderson & Holford 2008) and parsimony	-200
15	Run 8 plus allometric scaling with fat free mass on CL and Vc	Was worse than run 14	-195
16	Run 8 scaling with fat mass mass on CL and Vc	Was better than run 14	-185
17	Run 14 plus genotype on CL	Huge improvement in fit. The genenotypes were fast, intermediate and slow acetylators.	-246
18	Run 14 plus test HIV on F	Slight improvement in fit compared with run 14	-248
18	Run 14 plus HIV on CL	insignificant	-248
19	Run 14 plus HIV on Vc	insignificant	-247
20	Run 14 plus SEX on F	insignificant	-246
21	Run 14 plus SEX on CL	insignificant	-246
22	Run 14 plus SEX on Vc	insignificant	-246
23	Run 14 plus albumin on Vc	insignificant	-247
24	Run 14 plus maturation of CL	insignificant	-251
25	Run 14 plus maturation on Vc	No improvement in fit	-249
26	Run 14 pus maturation on MTT	insignificant	-246
27	Test different F on genotype	significant	-269
28	Combine estimate of F for fast and intermediate acetylators. Final model (plus Hill)	Significant. Final model	-267

[a]CL and Vc are oral clearance and apparent volume of distribution in plasma, respectively. MTT, absorption mean transit time, value at full maturation; NN, number of transit compartments; F, relative bioavailability; Hill, steepness of the maturation function; IIV, inter-individual variability; IOV, inter-occasional variability. [b]RSE, relative standard error.

b) Isoniazid control stream

```
$SIZES MAXFCN=100000000
$PROBLEM PEDS INH

$INPUT ID OCC TIME AMT DV AGE KWS HIV WT EVID SEX HT PRB SITE GENO MDV BLQ
BLQ_VALUE=DROP
$DATA  PEDS_INH_2013-09-20.csv IGNORE=# IGNORE=(PRB.EQ.1)

$ABBREVIATED COMRES=2
$SUBROUTINE ADVAN13 TOL=6

$MODEL NCOMPARTMENTS=3
COMP=(ABSORB DEFDOSE)
COMP=(CENTRAL DEFOBS)
COMP=(PERI)

$THETA  (0,4.43579) ; 1_CL_SLOW
$THETA  (0,8.9373) ; 2_CL_INT
$THETA  (0,11.3482) ; 3_CL_FAST
$THETA  (0,11.035) ; 4_TVV2
$THETA  (0,2.46631) ; 5_TVKA
$THETA  (0,5.02587) ; 6_V3
$THETA  (0,1.99841) ; 7_Q
$THETA  (0,0.205733) ; 8_PROP
$THETA  0 FIX ; 9_ADD
$THETA  (0,0.179338) ; 10_MTT
$THETA  (0,0.942572) ; 11_TM50
$THETA  (0,2.19) ; 12_HILL
$THETA  (-0.99,-0.228087,1) ; 13_F_INTER&FAST
$THETA  0.402777778 FIX ; 14_P1_SLOW
$THETA  0.402777778 FIX ; 15_P2_INTER
$THETA  0.194444444 FIX ; 16_P3_FAST
$THETA  4 FIX ; 17_NN
$THETA  (0,0.0699578,0.5) ; 18_PROP2

$OMEGA  0.0630975  ;    1_IIVCL
$OMEGA  0  FIX  ;    2 DUMMY

$OMEGA  BLOCK(1)  0.157738  ;     3_IOVF
$OMEGA  BLOCK(1) SAME
$OMEGA  BLOCK(1) SAME
$OMEGA  BLOCK(1) SAME

$OMEGA  BLOCK(1)  0.378515  ;    5_IOVKA
$OMEGA  BLOCK(1) SAME
$OMEGA  BLOCK(1) SAME
$OMEGA  BLOCK(1) SAME

$OMEGA  BLOCK(1)  0.882379  ;  11_IOVMTT
$OMEGA  BLOCK(1) SAME
$OMEGA  BLOCK(1) SAME
$OMEGA  BLOCK(1) SAME

$SIGMA  1  FIX

$PK

IF (AMT.GT.0.OR.EVID.GE.3) THEN
        TDOSE=TIME
        TAD=0
ENDIF
TAD=TIME-TDOSE

IF (TIME<72.AND.TIME>71) TAD=TIME-72 ; Fix the TAD for pre-doses

HILL   = THETA(12)
```

```
TM50   = THETA(11)
PMA    = AGE + (9/12)
FMAT   = 1/(1+(PMA/TM50)**(-HILL))

OC1=0
OC2=0
OC3=0
OC4=0

IF(OCC.EQ.1) OC1 =1
IF(OCC.EQ.2) OC2 =1
IF(OCC.EQ.3) OC3 =1
IF(OCC.EQ.4) OC4 =1

IOVBIO   = ETA(3)*OC1 + ETA(4)*OC2 + ETA(5)*OC3 + ETA(6)*OC4
IOVKA  = ETA(7)*OC1 + ETA(8)*OC2 + ETA(9)*OC3 + ETA(10)*OC4
IOVMTT = ETA(11)*OC1 + ETA(12)*OC2 + ETA(13)*OC3 + ETA(14)*OC4

EST=MIXEST

IF (GENO.NE.-99) THEN
        GENOME=GENO
ELSE
        IF (MIXNUM.EQ.1) GENOME=0
        IF (MIXNUM.EQ.2) GENOME=1
        IF (MIXNUM.EQ.3) GENOME=2
ENDIF


IF(GENOME.EQ.0) THEN
 TVCL  = THETA(1)*((WT/12.5)**0.75)*FMAT   ;SLOW
 TVBIO  = 1
ENDIF


IF(GENOME.EQ.1) THEN
 TVCL  = THETA(2)*((WT/12.5)**0.75)*FMAT    ;INTER
 TVBIO  = 1+THETA(13)
ENDIF


IF(GENOME.EQ.2) THEN
 TVCL  = THETA(3)*((WT/12.5)**0.75)*FMAT    ;FAST
 TVBIO  = 1+THETA(13)
ENDIF

  BSVCL  = ETA(1)
  CL     = TVCL*EXP(BSVCL)
  BIO    = TVBIO*EXP(IOVBIO)

 TVV2   = THETA(4)*(WT/12.5)         ;volume of the central compartment
 V2     = TVV2

 TVKA   = THETA(5)
 KA     = TVKA*EXP(IOVKA)


TVV3    = THETA(6)*(WT/12.5)                ;4_V3
V3      = TVV3

TVQ     = THETA(7)*((WT/12.5)**0.75)         ;5_Q
Q       = TVQ

TVMTT   = THETA(10)
MTT     = TVMTT*EXP(ETA(2)+IOVMTT)

NN      = THETA(17)
```

```
 S2   = V2
 K  = CL/V2
 K23  = Q/V2
 K32  = Q/V3



F1=0

KTR = (NN+1)/MTT

IF (NEWIND.NE.2.OR.EVID.GE.3)
            TNXD=TIME
            PNXD=AMT
ENDIF

TDOS=TNXD
PD=PNXD

IF(AMT.GT.0) THEN
            TNXD=TIME
            PNXD=AMT
ENDIF

LNGAM = NN*LOG(NN)-NN+LOG(NN*(1+4*NN*(1+2*NN)))/6+0.572364942 ; approximation of log of gamma(n),
0.572364942 is LOG(PI)/2
PIZZA=LOG(BIO*PD*KTR+0.00001)-LNGAM ; without +0.00001, it won't work with ETAs in bioavailability

   IF(NEWIND.LE.1.OR.EVID.GE.3) THEN ; assign negative Cmax Tmax for the new subject
     COM(1)=-1 ; holder of Cmax
     COM(2)=-1 ; holder of Tmax
    ENDIF


$MIX
       NSPOP=3
       P(1)=THETA(14)
       P(2)=THETA(15)
     P(3)=THETA(16)

$DES
TEMPO=T-TDOS ; this is time after dose, it should always be >= 0
KTT=0
DADT(1)=0 ; I believe this is executed only when TEMPO=0, or before the first dose is given

IF(TEMPO.GT.0) THEN
            KTT=KTR*TEMPO
            DADT(1)=EXP(PIZZA+NN*LOG(KTT)-KTT)-KA*A(1)
ENDIF

DADT(2) =  K32*A(3)- K23*A(2) + KA*A(1)-K*A(2)
DADT(3) =  K23*A(2)-K32*A(3)

;------CMAX AND TMAX
CT=A(2)/V2 ; (or other expression for concentration)
IF(CT.GT.COM(1)) THEN
            COM(1)=CT
            COM(2)=T
ENDIF


$ERROR
IPRED=A(2)/V2
PROP=THETA(8)*IPRED
ADD=THETA(9)
```

```
IF(SITE==2) THEN
        PROP=THETA(18)*IPRED
ENDIF

W =SQRT(PROP**2+ADD**2)

IF(W.LT.0.0001) W = 0.0001

IF(BLQ==1.AND.SITE==1) W = 0.05
IF(BLQ==1.AND.SITE==2) W = 0.5

Y = IPRED + W*EPS(1)
IRES=DV-IPRED
IWRES=IRES/W

IF(ICALL.EQ.4.AND.Y.LE.0.1) Y=0.05

IF (AMT.GT.0) T_DOSE=TIME
TAD=TIME-T_DOSE


$ESTIMATION MSFO=run1601.msf MAXEVAL=9999 PRINT=1 SIGDIG=2 SIGL=8 POSTHOC METH=COND INTER
NOABORT

$COVARIANCE PRINT=E MATRIX=S

$TABLE FILE=sdtab1601 ID OCC TIME TAD IPRED PRED IWRES WRES CWRES NPDE NOPRINT NOAPPEND
ONEHEADER
$TABLE FILE=patab1601 ID OCC CL V2 KA Q V3 BIO MTT BSVCL IOVBIO IOVKA IOVMTT NOPRINT
NOAPPEND ONEHEADER
$TABLE FILE=cotab1601 ID OCC WT AGE HT NOPRINT NOAPPEND ONEHEADER
$TABLE FILE=catab1601 ID OCC HIV SEX GENO GENOME SITE NOPRINT NOAPPEND ONEHEADER
$TABLE FILE=mytab1601 ID OCC TIME TAD IPRED PRED IWRES WRES CWRES NPDE CL V2 KA Q V3 BIO MTT
BSVCL IOVBIO IOVKA IOVMTT WT AGE HT HIV SEX GENO GENOME SITE NOPRINT NOAPPEND
ONEHEADER
```

Appendix 4- Rifapentine and 25-desacetyl rifapentine in healthy volunteer run record and control stream

a) Rifapentine and 25-desacetyl rifapentine run record

Model	Description [a]	Comment[b]	OFV
Rifapentine			
1	One compartment, first-order absorption, first order elimination. IIV on CL, Vc, ka, F	Base model	6087
2	Add lag time to model 1	No improvement in fit	6066
3	Use transit absorption compartment on model 1 instead of lag time, IIV CL, Vc, F, MTT, ka	Improvement in fit	6011
4	Add IOV in F on model 3. IIV CL, Vc, F, MTT	IIV if F zeros	5084
5	Add IOV in CL on model 4	Improvement in fit.	5077
6	Add IOV in MTT on model 5	Improvement in the fit but IIV in MTT zeros	5060
7	Add IOV in V on model 6	No improvement in fit	5058
8	Add IOV in ka on model 6	Improvement in fit	5060
9	Run 6 plus covariance between IIV for CL and Vc	No improvement in fit	5060
10	Run 6 plus dose-nonlinearity	All the estimates had high RSE and estimate of CL increased 10 times	5054
11	Run 6 plus saturable clearance	Significant improvement in fit	5054
12	Run 6 and add weight as linear covariate on CL	No improvement in fit	5057
13	Run 6 plus weight as covariate on Vc	improvement in fit, but not significant	5060
14	Run 6 plus allometric scaling with body weight	No significant improvement in fit	5057
15	Run 6 plus allometric scaling with fat free mass on CL and Vc	Worse fit	5064
16	Run6 plus allometric scaling with fat mass mass on CL and Vc	Worse fit	5063
17	Run 6 plus time varying clearance	Better than run 11, and had improved goodness of fit plots	5040
18	Run 17 plus Meal effect of F	Significant covariate	5020
19	Run 18 plus meal effect on MTT	insignificant	5018
20	Run 18 plus meal effect on ka	Insignificant and high RSE	5019
Rifapentine plus 25-desacetyl rifapentine			
run 21	Fix estimate from run 20 then first order elimination of rifapentine to form metabolite, IIV on CLm of metabolite (one compartment)		9377
run 22	Run 21 plus IIV Vm of metabolite	Insignificant improvement in fit	1974
Run 22	Two compartment model for metabolite plus IIV CLm, Vm	Improvement in fit	1969
Run23	Run22 plus IIV Qm	Insignificant improvement in fit	1968
Run24	Run22 plus IIV Vpm	Insignificant improvement in fit	1969
Run 25	Run22 plus IOV CLm	Improvement in fit	1953
Run 26	Run 25 plus IOV Vm	Insignificant improvement in fit	
Run27	Run 22 plus time-varying clearance of metabolite	Improvement in fit. Final model	1947

[a]CL and Vc are oral clearance and apparent volume of distribution in plasma, respectively. MTT, absorption mean transit time; NN, number of transit compartments; F, relative bioavailability; IIV, inter-individual variability; IOV, inter-occasional variability; Vm, volume of metabolite in plasma; Vpm, volume of metabolite on peripheral

compartment; CLm, clearance of metabolite; Qm, intercompartmental clearance of metabolite. [b]RSE, relative standard error.

b) Rifapentine and 25-desacetyl rifapentine control stream (healthy volunteer study)

```
$PROBLEM    RIFAPENTINE SINGLE-DOS FIVE WAY CROSSOVER
$INPUT      ID PTIM=DROP TIME TAD=DROP DV AMT DOSE EVID OCC MDV AGE WT HT              RACE RX
            EXID=DROP CMT FLAG
$DATA Final_par_met2.csv IGNORE=#


$SUBROUTINE ADVAN6 TRANS1 TOL=6
$MODEL      NCOMP=4 COMP=(DEPOT,DEFDOSE) COMP=(CENTRAL) COMP=(METAB) COMP=(PERI)
$ABBREVIATED DERIV2=NO

$PK
;----------------meal effect
RXBIO = 0  ; reference meal
IF(RX.EQ.4) RXBIO = THETA(9)
IF(RX.EQ.3) RXBIO = THETA(10)
IF(RX.EQ.2) RXBIO = THETA(11)
IF(RX.EQ.1) RXBIO = THETA(12)

;---------------occasions
OCC5=0
OCC2=0
OCC3=0
OCC4=0
OCC1=0
IF(OCC.EQ.1)OCC1=1
IF(OCC.EQ.2)OCC2=1
IF(OCC.EQ.3)OCC3=1
IF(OCC.EQ.4)OCC4=1
IF(OCC.EQ.5)OCC5=1

IIVCL1 = ETA(1)
IIVMTT = ETA(2)
IIVBIO = ETA(3)
BOVCL  = ETA(4)*OCC1+ ETA(5)*OCC2+ ETA(6)*OCC3+ ETA(7)*OCC4+ ETA(8)*OCC5
BOVBIO = ETA(9)*OCC1+ ETA(10)*OCC2+ETA(11)*OCC3+ETA(12)*OCC4+ETA(13)*OCC5
BOVMTT = ETA(14)*OCC1+ETA(15)*OCC2+ETA(16)*OCC3+ETA(17)*OCC4+ETA(18)*OCC5
IIVCLM = ETA(19)

BOVCLM  = ETA(20)*OCC1+ ETA(21)*OCC2+ ETA(22)*OCC3+ ETA(23)*OCC4+ ETA(24)*OCC5



;------changing CL, typical values
MTIME(1)= THETA(13) ;*EXP(IMTM)
TVCL1   = THETA(1)*EXP(IIVCL1+BOVCL)
TVCL2   = THETA(14)*EXP(IIVCL1+BOVCL)
CL      = TVCL1*(1-MPAST(1))+TVCL2*(MPAST(1))

TVV2    = THETA(2)
TVKA    = THETA(3)
TVMTT   = THETA(5)
TVBIO   = THETA(4)*(1+RXBIO)

V2     = TVV2
KA     = TVKA
BIO    = TVBIO*EXP(IIVBIO+BOVBIO)
MTT    = TVMTT*EXP(IIVMTT+BOVMTT)
TVNN   = THETA(6)
NN     = TVNN


KTR = (NN+1)/MTT
F1=0
S2=V2
K=CL/V2
```

```
;--metabolite
MTIME(2)= THETA(21) ;*EXP(IMTM)
TVCLM1  = THETA(15)
TVCLM2  = THETA(22)

CLM1   = TVCLM1*EXP(IIVCLM+BOVCLM)
CLM2   = TVCLM2*EXP(IIVCLM+BOVCLM)
CLM    = CLM1*(1-MPAST(2))+CLM2*(MPAST(2))
TVV3   = THETA(16)
TVQM   = THETA(19)
TVVPM  = THETA(20)


V3   = TVV3
QM   = TVQM
VPM  = TVVPM


KMET = CLM/V3
S3   = V3
K34  =QM/V3
K43  =QM/VPM


;----------
LNFAC=LOG(2.5066)+(NN+0.5)*LOG(NN)-NN
;----------

IF(AMT.GT.0)DAMT=AMT

A_0(1) = 0
A_0(2) = 0
A_0(3) = 0

$DES
DADT(1)=EXP(LOG(BIO*DAMT+.00001)+LOG(KTR)+NN*LOG(KTR*T+.00001)-KTR*T-LNFAC)-KA*A(1)
DADT(2)=KA*A(1)-K*A(2)
DADT(3)=K*(A(2))-(KMET+K34)*A(3)+K43*A(4)
DADT(4)=K34*A(3)-K43*A(4)


$ERROR
CP2=A(2)/V2
CP3=A(3)/V3
IPREDP = CP2 ; parent
IPREDM = CP3 ; metabolite
IF(FLAG.EQ.2)IPRED = IPREDP   ; parent
IF(FLAG.EQ.3)IPRED = IPREDM   ; metabolite

PROPP=IPREDP*THETA(7)
ADDP=THETA(8)
PROPM=IPREDM*THETA(17)
ADDM=THETA(18)

IRES = DV - IPRED
IF(FLAG.EQ.2)W2 = SQRT(PROPP**2 + ADDP**2)   ; RUV parent--corrected paranthesis
IF(FLAG.EQ.3)W3 = SQRT(PROPM**2 + ADDM**2) ; RUV metabolite
IF(W2.EQ.0) W2 = 1
IF(W3.EQ.0) W3 = 1

IF(FLAG.EQ.2)IWRES = IRES/W2
IF(FLAG.EQ.3)IWRES = IRES/W3
IF(FLAG.EQ.2)Y = IPREDP + W2*EPS(1)  ; parent
IF(FLAG.EQ.3)Y = IPREDM + W3*EPS(2)  ; metabolite
```

```
;----strata
STRT = 0
;--parent
IF(FLAG.EQ.2.AND.RX.EQ.1)STRT = 1
IF(FLAG.EQ.2.AND.RX.EQ.2)STRT = 2
IF(FLAG.EQ.2.AND.RX.EQ.3)STRT = 3
IF(FLAG.EQ.2.AND.RX.EQ.4)STRT = 4
IF(FLAG.EQ.2.AND.RX.EQ.5)STRT = 5

;--metabolite
IF(FLAG.EQ.3.AND.RX.EQ.1)STRT = 6
IF(FLAG.EQ.3.AND.RX.EQ.2)STRT = 7
IF(FLAG.EQ.3.AND.RX.EQ.3)STRT = 8
IF(FLAG.EQ.3.AND.RX.EQ.4)STRT = 9
IF(FLAG.EQ.3.AND.RX.EQ.5)STRT = 10


$THETA  2.14 FIX ; 1 POP_CL
$THETA  60.6 FIX ; 2 POP_V
$THETA  1.66 FIX ; 3  POP_KA
$THETA  1 FIX ; 4 POP_BIO
$THETA  1.45 FIX ; 5 POP_MTT
$THETA  10.9 FIX ; 6 POP_NN number of transit compartments
$THETA  0.106 FIX ; 7 PROPP RUV
$THETA  0.206 FIX ; 8 ADDP RUV
$THETA  .489 FIX ; 9 Meal = 4 on BIO - bioavailability
$THETA  .457 FIX ; 10 Meal = 3 on bio
$THETA  .327 FIX ; 11  Meal = 2 on bio
$THETA  .857 FIX ; 12 Meal = 1 on bio
;-------CL2
$THETA  43 FIX ; 13_change_point_time
$THETA  3.22 FIX ; 14_POP_CL
;--metabolite
$THETA  (0,1.810000) ; 15_CLM
$THETA  (1,6.360000) ; 16_V3
$THETA  (0,0.191000) ; 17 PROPM RUV
$THETA  (0,0.211000) ; 18 ADDM RUV
$THETA  (0,4.400000) ; 19_TVQ3
$THETA  (0,22.10000) ; 20_TVVPM
$THETA  (0,46.80000) ; 21_T2_CLM
$THETA  (0,4.630000) ; 22_CLM2
;-------
$OMEGA  0.0367  FIX  ; 1 BETWEEN SUBJECT VARIABILITY BSVCL
$OMEGA  0.00904  FIX  ; 2 BETWEEN SUBJECT VARIABILITY BSVMTT
$OMEGA  0.0458  FIX  ; 3 BETWEEN SUBJECT VARIABILITY BSVBIO

$OMEGA  BLOCK(1) FIX  0.015  ; 4 BOVCL OCC=1
$OMEGA  BLOCK(1) SAME
$OMEGA  BLOCK(1) SAME
$OMEGA  BLOCK(1) SAME
$OMEGA  BLOCK(1) SAME

$OMEGA  BLOCK(1) FIX 0.0586  ; 9  BOV_BIO OCC =1
$OMEGA  BLOCK(1) SAME
$OMEGA  BLOCK(1) SAME
$OMEGA  BLOCK(1) SAME
$OMEGA  BLOCK(1) SAME

$OMEGA  BLOCK(1) FIX  0.0839  ; 14 BOVMTT OCC=1
$OMEGA  BLOCK(1) SAME
$OMEGA  BLOCK(1) SAME
$OMEGA  BLOCK(1) SAME
$OMEGA  BLOCK(1) SAME

$OMEGA  0.056900  ;  19_IIVCLM
```

```
$OMEGA  BLOCK(1)  0.091200  ; 4 BOVCLM OCC=1
$OMEGA  BLOCK(1) SAME
$OMEGA  BLOCK(1) SAME
$OMEGA  BLOCK(1) SAME
$OMEGA  BLOCK(1) SAME

$SIGMA  1  FIX
$SIGMA  1  FIX
$ESTIMATION METHOD=1 INTER MAXEVAL=9999 PRINT=1 POSTHOC    NOABORT
MSFO=run30.msf
$COVARIANCE  PRINT=E MATRIX=S
$TABLE ID TIME DV DAMT PRED OCC STRT ETA19 ETA20 CL TVCLM1 TVCLM2 QM K43 K34 VPM V2 K MTT
KTR NN BIO BOVCL BOVMTT BOVBIO
                                    CMT  RXBIO AGE WT HT RACE RX IPRED IRES IWRES              NOPRINT
ONEHEADER FILE=sdtab30
$TABLE ID TIME CL V2 K MTT NN QM K43 K34 VPM ETA19 ETA20 BIO KTR BOVCL BOVMTT BOVBIO PRED
IPRED IRES IWRES        NOPRINT ONEHEADER FILE=patab30
$TABLE ID TIME AGE WT HT PRED IPRED IRES IWRES                                                NOPRINT
ONEHEADER FILE=cotab30
$TABLE ID TIME RACE RX OCC PRED IPRED IRES IWRES                                               NOPRINT
ONEHEADER FILE=catab30
```

Appendix 5- Moxifloxacin run records and control streams

a) Moxifloxacin run records

Model	Description [a]	Comment[b]	OFV
Moxifloxacin in 28 patients from RIFAQUIN study			
1	One compartment, first-order absorption, first order elimination. IIV on CL, Vc, ka, F	Base model	-720
2	Add lag time to model 1	No improvement in fit	-730
3	Use transit absorption compartment on model 1 instead of lag time, IIV CL, Vc, F, MTT, ka	Improvement in fit	-795
4	Run 3 plus two compartment model	Improvement in fit	-894
5	Run 4 plus IOV in F	IIV in V and F zeros	-936
6	Run 5 plus IOV MTT	Significant improvement in fit, IIV in MTT zeros	-954
7	Run 6 plus IOV in CL	No improvement if fit	-958
8	Run6 plus IOV in Vc	No improvement if fit	-955
9	Run 6 plus IOV in Vp	No improvement if fit	-955
10	Run 6 plus IOV in ka	Significant improvement in fit, IIV in had high RSE (120%)	-960
11	Run 10 plus allometric scaling scaling with body weight on Clearance and Volume terms	insignificant	-962
12	Run 10 plus allometric scaling scaling with fat-free mass on Clearance and Volume terms, IIV on CL and IOV F, MTT, ka	significant	-966
13	Run 10 plus allometric scaling scaling with fat mass on Clearance and Volume terms	Significant but scaling with fat-free mass was better	-964
14	Run 12 plus rifapentine effect on CL	Significant and Final model	-995

Continues on next page

Model	Description [a]	Comment[b]	OFV
Moxifloxacin in 241 patients from RIFAQUIN study			
50	Run 12 structural model plus IIV in CL, ka, F, MTT	The model had one occasion	-1137
52	Run 50 plus IIV in Q	significant	-1144
53	Run 52 plus allometric scaling with total body weight	Worse fit	-1125
54	Scaling with fat-free mass on CL, Vc, Q and fat mass on Q	Improved fit	-1148
55	Run 54 plus HIV on CL	insignificant	-1151
56	Run 54 plus HIV on Vc	insignificant	-1148
57	Run 54 plus HIV on Vp	insignificant	-1148
58	Run 54 plus HIV on CL	insignificant	-1148
59	Run 54 plus HIV on Vc	insignificant	-1148
60	Run 54 plus HIV on Vc	insignificant	-1148
61	Run 54 plus HIV on F	insignificant	-1148
62	Run 54 plus ARM on CL	insignificant	-1148
63	Run 54 plus ARM on Vc	insignificant	-1148
64	Run 54 plus ARM on Vp	insignificant	-1148
65	Run 54 plus ARM on CL	insignificant	-1148
66	Run 54 plus ARM on Vc	insignificant	-1148
67	Run 54 plus ARM on F	insignificant	-1148
68	Run 54 plus sex on CL	insignificant	-1151
69	Run 54 plus sex on Vc	insignificant	-1148
70	Run 54 plus sex on Vp	insignificant	-1148
71	Run 54 plus sex on CL	insignificant	-1148
72	Run 54 plus sex on Vc	insignificant	-1148
73	Run 54 plus sex on F	insignificant	-1148
74	Run 54 plus age on CL	insignificant	-1148

75	Run 54 plus age on Vc	insignificant	-1148
76	Run 54 plus age on Vp	insignificant	-1148
77	Run 54 plus age on CL	insignificant	-1148
78	Run 54 plus age on Vc	insignificant	-1148
79	Run 54 plus age on F	insignificant	-1148
80	Run 54 estimated using LAPLACE method	The method was used when fitting data which was below lower limit of quantification	-832

[a]CL and Vc are oral clearance and apparent volume of distribution in plasma, respectively. MTT, absorption mean transit time; NN, number of transit compartments; F, relative bioavailability; IIV, inter-individual variability; IOV, inter-occasional variability; Vp, volume of distribution in peripheral compartment; Q, intercompartmental clearance. [b]RSE, relative standard error.

b) Moxifloxacin control stream (241 Patients)

```
$PROBLEM    ;FINAL M3 method
$ABBREVIATED COMRES=2
$INPUT      ID RFP=DROP SID DV1=DROP DVO=DROP DATE=DROP TIME
            ATIME=DROP EVID MDV OCC SS II BLQ DAY ARM HT WT AGE HIV
            SEX PROB_RPT PSID=DROP DV AMT PROB SPARSE

$DATA       MXF20130529M3.csv IGNORE=@ IGNORE=(PROB.EQ.1)
$SUBROUTINE ADVAN13 TOL=9
$MODEL      NCOMPARTMENTS=4 COMP=(ABS DEFDOSE) ; Actually the dose won't go there. F1=0
            COMP=(CENTRAL DEFOBSERVATION) COMP=(PERI) COMP=(AUC)
$PK
IF(SEX.EQ.0) THEN    ;females in my dataset
WHSMAX = 37.99
WHS50  = 35.98
  ELSE  ;           ;males in my dataset
WHSMAX = 42.98
WHS50  = 30.93
ENDIF

HTT=HT/100
FFM    = WHSMAX*(HTT**2)*WT/(WHS50*(HTT**2)+WT)
FAT=WT-FFM
FFMC=FFM/44.87
FATV3= FAT/11.29

OC1=0
OC2=0

IF(OCC.EQ.1) OC1 =1
IF(OCC.EQ.2) OC2 =1
IOVF   = OC1*(ETA(7))  + OC2*(ETA(8))
IOVMTT = OC1*(ETA(9))  + OC2*(ETA(10))
IOVKA  = OC1*(ETA(11)) + OC2*(ETA(12))

BSVCL=ETA(1)
BSVV2=ETA(2)
BSVQ=ETA(13)
BSVV3=ETA(4)


 TVCL   = THETA(1) *(FFMC**0.75)
 CL     = TVCL*EXP(BSVCL)

 TVV2   = THETA(2) *FFMC              ;volume of the central compartment
 V2     = TVV2*EXP(BSVV2)

 TVKA   = THETA(3)
 KA     = TVKA*EXP(IOVKA+ETA(3))

TVV3   = THETA(4) *FATV3 ;FFMC                ;4_V3
V3     = TVV3*EXP(BSVV3)

TVQ    = THETA(5) *(FFMC**0.75)           ;5_Q
Q      = TVQ*EXP(BSVQ)

TVMTT = THETA(8)
 MTT = TVMTT*EXP(IOVMTT+ETA(5))

TVNN  = THETA(9)
 NN  = TVNN

 S2   = V2
 K    = CL/V2
 K2T3 = Q/V2
 K3T2 = Q/V3
 KTR  = (NN+1)/MTT
```

```
F1=0
TVBIO =THETA(10)
BIO  =TVBIO*EXP(IOVF+ETA(6))

LNGAM = NN*LOG(NN)-NN+LOG(NN*(1+4*NN*(1+2*NN)))/6+0.572364942

IF (NEWIND.NE.2.OR.EVID.GE.3) THEN
            TNXD=TIME
            PNXD=AMT
ENDIF

TDOS=TNXD
PD=PNXD

IF(AMT.GT.0) THEN
            TNXD=TIME
            PNXD=AMT
ENDIF

PIZZA=LOG(BIO*PD*KTR+0.00000001)-LNGAM

  IF(NEWIND.LE.1.OR.EVID.GE.3) THEN
    COM(1)=-1 ; holder of Cmax
    COM(2)=-1 ; holder of Tmax
   ENDIF

$DES


TEMPO=T-TDOS ; this is time after dose, it should always be >= 0

IF(PD.GT.0.AND.TEMPO.GT.0) THEN ; This happens only id PD>0, so only if a dose has been detected
            KTT=KTR*(TEMPO)
            DADT(1)=EXP(PIZZA+NN*LOG(KTT)-KTT)-KA*A(1)
ENDIF

DADT(2) = KA*A(1)-K*A(2) - K2T3*A(2) + K3T2*A(3)
DADT(3) = K2T3*A(2) - K3T2*A(3)



;------CMAX AND TMAX
  CT=A(2)/S2 ; (or other expression for concentration)
  IF(CT.GT.COM(1)) THEN
       COM(1)=CT
       COM(2)=T
  ENDIF


;-------AUC 0-50
DADT(4) = A(2)/S2

$ERROR


IPRED=F
PROP=THETA(6)*IPRED
ADD=THETA(7)
IRES=DV-IPRED
W =SQRT(PROP**2+ADD**2)

IF(W.EQ.0) W=1
IWRES=IRES/W


IF(AMT.GT.0) TIM_DOS=TIME
```

```
TAD=TIME-TIM_DOS


;-------M3 METHOD FOR BLQ DATA----------

LOQ    = 0.063          ;
DUM    = (LOQ - IPRED) / W
CUMD   = PHI(DUM)

; TREAT DV AS AN OBSERVATION BY DEFAULT
Y = IPRED + W*EPS(1)
; !!! CAREFUL TO IGNORE BLQ==-1 WHICH ARE SUSPICIOUS SAMPLES !!!

;Sim_start
IF (BLQ>0) THEN          ; TREAT DV AS A LIKELIHOOD
            F_FLAG = 1
            Y = CUMD
ENDIF
;IF (ICALL==4.AND.Y.LE.0.0315) THEN
;           Y=0.0315 ; For the BLQ values in simulation (VPC)
;ENDIF
;Sim_end



AUC50 = A(4)
AUCINF= BIO*AMT/CL
CMAX = COM(1)
TMAX = COM(2)

$THETA  (0,10.6) ; 1_CL
$THETA  (0,114) ; 2_V
$THETA  (0,1.5) ; 3_KA
$THETA  (0,89.8) ; 4_V3
$THETA  (0,2.14) ; 5_Q
$THETA  (0,0.0785) ; 6_PROP
$THETA  0 FIX ; 7_ADD
$THETA  (0,0.723) ; 8_MTT
$THETA  (0,11.6) ; 9_NN
$THETA  1 FIX ; 10_TVBIO
$OMEGA  0.0351  ;    1_IIVCL
$OMEGA  0  FIX  ;    2_IIVV
$OMEGA  0  FIX  ;    3_IIVKA
$OMEGA  0  FIX  ;    4_IIVV3
$OMEGA  0  FIX  ;   5_IIVMTT
$OMEGA  0  FIX  ;   6_IIVBIO
$OMEGA  BLOCK(1)
 0.0314  ;    7_IOVF
$OMEGA  BLOCK(1) SAME

$OMEGA  BLOCK(1)
 0.539  ;   9_IOVMTT
$OMEGA  BLOCK(1) SAME

$OMEGA  BLOCK(1)
 0.489  ;   11_IOVKA
$OMEGA  BLOCK(1) SAME

$OMEGA  0.108  ;   13 BSV Q
$SIGMA  1  FIX
;Sim_start
$ESTIMATION MAXEVAL=9999 PRINT=1 SIGDIG=3 SIGL=8 POSTHOC METHOD=1
          ATOL=4 INTER LAPLACE NUMERICAL SLOW NOABORT
          MSFO=run145.msf
$COVARIANCE PRINT=E MATRIX=S ATOL=4
;$SIMULATION (12345) ONLYSIMULATION
$TABLE      ID TIME DV AUCINF AUC50 CMAX TMAX FAT TAD OCC ARM WT HT
```

```
        FFM MTT NN CL V2 KA Q V3 BSVCL BSVV2 BSVQ BSVV3 IOVF W
        IOVMTT IOVKA WT CWRES NPDE PRED IPRED PREDI RESI WRESI
        IPRED IWRES NOPRINT ONEHEADER FILE=sdtab145
$TABLE      ID TIME TAD OCC CL V2 KA Q V3 MTT NN BSVCL BSVV2 BSVQ
        BSVV3 IOVF IOVKA IOVMTT PRED CWRES NPDE IPRED PREDI RESI
        WRESI NOPRINT ONEHEADER FILE=patab145
$TABLE      ID FAT HT WT FFM AGE NOPRINT ONEHEADER FILE=cotab145
$TABLE      ID ARM SEX HIV SID NOPRINT ONEHEADER FILE=catab145
$TABLE      ID TIME DV W AUCINF AUC50 CMAX FAT FFM TMAX OCC WT TAD
        IOVF IOVMTT IOVKA ARM HT CL V2 KA Q V3 MTT NN BSVCL BSVV2
        BSVQ BSVV3 CWRES PRED IPRED PREDI RESI WRESI NOPRINT
        ONEHEADER FILE=mytab145
; $TABLE FILE=simtab144 ID OCC TIME DV AMT MDV EVID IPRED PRED IWRES WRES CWRES NPDE
; CL V2 KA MTT NN BIO Q V3 BSVBIO BSVCL BSVV BSVQ BSVV3
; SEX AGE WT HT FFM FAT AUC NOPRINT NOAPPEND ONEHEADER
;Sim_end
```

c) Moxifloxacin control stream (28 Patients)

```
$PROBLEM   ;Moxifloxacin 28 patients
$INPUT      ID AMT TIM=DROP TIME PTIM=DROP DV MDV ARM OCC WT AGE
          HT HIV  SEX EVID PRB SS=DROP II=DROP RFP GRP FFM
$DATA       MOXI_02062011.csv IGNORE=@
$DATA       IGNORE=(PRB.EQ.1)


$ABBREVIATED COMRES=2

$SUBROUTINE ADVAN13 TOL=9
$MODEL      NCOMPARTMENTS=4
                COMP=(ABS DEFDOSE) ; Actually the dose won't go there. F1=0
                COMP=(CENTRAL DEFOBSERVATION)
                   COMP=(PERI)
                COMP=(AUC)

$PK
IF(RFP.EQ.1) CLRFP = 1  ; presence of rifapentine
IF(RFP.EQ.2) CLRFP = ( 1 + THETA(11))
CLCOV=CLRFP

OC1=0
OC2=0

IF(OCC.EQ.1) OC1 =1
IF(OCC.EQ.2) OC2 =1
IOVF   = OC1*(ETA(4))  + OC2*(ETA(5))
IOVMTT = OC1*(ETA(6))  + OC2*(ETA(7))
IOVKA  = OC1*(ETA(8)) + OC2*(ETA(9))


 TVCL   = THETA(1)*((FFM/44.784)**0.75)
TVCL = CLCOV*TVCL
  CL    = TVCL*EXP(ETA(1))

 TVV2   = THETA(2)*(FFM/44.784)
 V2     = TVV2*EXP(ETA(2))

 TVKA   = THETA(3)
 KA     = TVKA*EXP(IOVKA)

TVV3   = THETA(4)*(FFM/44.784)                ;4_V3

TVV3 = V3COV*TVV3
V3     = TVV3*EXP(ETA(3))

TVQ   = THETA(5)*((FFM/44.784)**0.75)            ;5_Q
Q     = TVQ

TVMTT = THETA(8)
  MTT = TVMTT*EXP(IOVMTT)

TVNN  = THETA(9)
  NN  = TVNN

 S2   = V2
 K    = CL/V2
 K2T3 = Q/V2
 K3T2 = Q/V3
 KTR  = (NN+1)/MTT

F1=0
TVBIO =THETA(10)

TVBIO = BIOCOV*TVBIO
```

```
BIO  =TVBIO*EXP(IOVF)

LNGAM = NN*LOG(NN)-NN+LOG(NN*(1+4*NN*(1+2*NN)))/6+0.572364942

IF (NEWIND.NE.2.OR.EVID.GE.3) THEN
            TNXD=TIME
            PNXD=AMT
ENDIF

TDOS=TNXD
PD=PNXD

IF(AMT.GT.0) THEN
            TNXD=TIME
            PNXD=AMT
ENDIF
PIZZA=LOG(BIO*PD*KTR+0.00000001)-LNGAM
  IF(NEWIND.LE.1.OR.EVID.GE.3) THEN
    COM(1)=-1 ; holder of Cmax
    COM(2)=-1 ; holder of Tmax
   ENDIF

$DES

TEMPO=T-TDOS

IF(PD.GT.0.AND.TEMPO.GT.0) THEN
            KTT=KTR*(TEMPO)
            DADT(1)=EXP(PIZZA+NN*LOG(KTT)-KTT)-KA*A(1)
ENDIF

DADT(2) = KA*A(1)-K*A(2) - K2T3*A(2) + K3T2*A(3)
DADT(3) = K2T3*A(2) - K3T2*A(3)



;------CMAX AND TMAX
  CT=A(2)/S2 ; (or other expression for concentration)
  IF(CT.GT.COM(1)) THEN
       COM(1)=CT
       COM(2)=T
  ENDIF

;-------AUC 0-50
DADT(4) = A(2)/S2

$ERROR

IPRED=F
PROP=THETA(6)*IPRED
ADD=THETA(7)
IRES=DV-IPRED
W =SQRT(PROP**2+ADD**2)
IF(W.LE.0.000001) W=0.000001
IWRES=IRES/W
Y = IPRED + W*EPS(1)
IF(ICALL.EQ.4.AND.Y.LT.0.04) Y=0.04

AUC50 = A(4)
AUCINF= BIO*AMT/CL
CMAX = COM(1)
TMAX = COM(2)

$THETA  (0,10.6449) ; 1_CL
$THETA  (0,114.162) ; 2_V
$THETA  (0,1.85084) ; 3_KA
$THETA  (0,41.5755) ; 4_V3
```

```
$THETA  (0,2.89708) ; 5_Q
$THETA  (0,0.0894374) ; 6_PROP
$THETA  (0,0.0189204) ; 7_ADD
$THETA  (0,0.482942) ; 8_MTT
$THETA  (0,22.4926) ; 9_NN
$THETA  1 FIX ; 10_TVBIO
$THETA  (-1,-0.0802717,5) ;11CLRFP1

$OMEGA  0.0158083  ;    1_IIVCL
$OMEGA  0  FIX  ;     2_IIVV
$OMEGA  0  FIX  ;    3_IIVV3

$OMEGA  BLOCK(1)  0.0306359
$OMEGA  BLOCK(1) SAME
$OMEGA  BLOCK(1) 0.495098
$OMEGA  BLOCK(1) SAME
$OMEGA  BLOCK(1) 0.557799
$OMEGA  BLOCK(1) SAME

$SIGMA  1  FIX
$ESTIMATION MAXEVAL=9999 PRINT=1 SIGDIG=3 SIGL=9 POSTHOC METH=COND  INTER NOABORT
MSFO=run69.msf
$COVARIANCE PRINT=E MATRIX=S
$TABLE  ID TIME DV AUCINF AUC50 CMAX TMAX  OCC SEX ARM AGE HIV WT HT MTT NN CL V2 KA Q V3
ETA1 ETA2 ETA3 IOVF W IOVMTT IOVKA  WT HIV CWRES NPDE  PRED IPRED PREDI RESI WRESI IPRED
IWRES   NOPRINT ONEHEADER FILE=sdtab69
$TABLE  ID TIME CL V2 KA Q V3 MTT NN ETA1 ETA2 ETA3  IOVF  IOVMTT IOVKA PRED CWRES NPDE
IPRED PREDI RESI WRESI          NOPRINT ONEHEADER FILE=patab69
$TABLE  ID TIME PRED WT AGE HT  NOPRINT ONEHEADER FILE=cotab69
$TABLE  ID TIME PRED HIV SEX ARM     NOPRINT ONEHEADER FILE=catab69
$TABLE  ID TIME DV W RFP AUCINF AUC50 CMAX TMAX OCC HIV SEX WT IOVF IOVMTT IOVKA ARM
AGE HT CL V2 KA Q V3 MTT NN ETA1 ETA2 ETA3  CWRES PRED IPRED PREDI RESI WRESI NOPRINT
ONEHEADER FILE=mytab69.tab69
```

Appendix 6- Rifapentine run records and control streams (RIFAQUIN study)

a) Rifapentine run records

Model	Description [a]	Comment[b]	OFV
Rifapentine			
1	Run 16 from Health volunteer study only IIV in CL, Vc, ka, MTT,		3855
2	Run 1 plus covariance on CL and Vc		3847
3	Two compartment model	Estimate of V3 has 120% RSE	3845
4	run 2 plus allometric scaling with body weight		3807
5	run 2 plus allometric scaling with fat-free mass		3810
SCM	Run 4 was used for SCM run		
540	IIV on CL, Vc, ka, MTT plus effect of HIV on F, and significant covariates on CL were regimen an Sex effects	HIV positive patients had lower F, females had lower CL than males, and patients on 4-month arm had higher clearance	3727

b) Rifapentine SCM log file.

```
Model directory /home/simba/RFPUCSF/scm_dir1/m1

MODEL           TEST     BASE OFV     NEW OFV         TEST OFV (DROP)    GOAL     dDF    SIGNIFICANT PVAL
BIOAGE-2        PVAL   3807.32200  3805.93600             1.38600  >   3.84150    1              0.239080
BIOARM-2        PVAL   3807.32200  3806.87900             0.44300  >   3.84150    1              0.505680
BIOHIV-2        PVAL   3807.32200  3753.58800            53.73400  >   3.84150    1        YES!  2.30e-13
BIOSEX-2        PVAL   3807.32200  3807.05100             0.27100  >   3.84150    1              0.602660
CLAGE-2         PVAL   3807.32200  3807.25400             0.06800  >   3.84150    1              0.794270
CLARM-2         PVAL   3807.32200  3798.04200             9.28000  >   3.84150    1        YES!  0.002317
CLHIV-2         PVAL   3807.32200  3796.03200            11.29000  >   3.84150    1        YES!  0.000779
CLSEX-2         PVAL   3807.32200  3792.79100            14.53100  >   3.84150    1        YES!  0.000138
KAAGE-2         PVAL   3807.32200  3803.48700             3.83500  >   3.84150    1              0.050193
KAARM-2         PVAL   3807.32200  3807.26500             0.05700  >   3.84150    1              0.811300
KAHIV-2         PVAL   3807.32200  3795.02800            12.29400  >   3.84150    1        YES!  0.000454
KASEX-2         PVAL   3807.32200  3800.85000             6.47200  >   3.84150    1        YES!  0.010959
MTTAGE-2        PVAL   3807.32200  3801.93800             5.38400  >   3.84150    1        YES!  0.020322
MTTARM-2        PVAL   3807.32200  3803.15900             4.16300  >   3.84150    1        YES!  0.041316
MTTHIV-2        PVAL   3807.32200  3806.09800             1.22400  >   3.84150    1              0.268580
MTTSEX-2        PVAL   3807.32200  3804.65800             2.66400  >   3.84150    1              0.102640
V2AGE-2         PVAL   3807.32200  3805.57900             1.74300  >   3.84150    1              0.186760
V2ARM-2         PVAL   3807.32200  3803.26100             4.06100  >   3.84150    1        YES!  0.043885
V2HIV-2         PVAL   3807.32200  3791.62400            15.69800  >   3.84150    1        YES!  0.000074
V2SEX-2         PVAL   3807.32200  3799.38200             7.94000  >   3.84150    1        YES!  0.004835

Parameter-covariate relation chosen in this forward step: BIO-HIV-2
CRITERION              PVAL < 0.05
BASE_MODEL_OFV        3807.32200
CHOSEN_MODEL_OFV      3753.58800
Relations included after this step:
BIO     HIV-2
CL
KA
MTT
V2
--------------------

Model directory /home/simba/RFPUCSF/scm_dir1/forward_scm_dir1/m1

MODEL           TEST     BASE OFV     NEW OFV         TEST OFV (DROP)    GOAL     dDF    SIGNIFICANT PVAL
BIOAGE-2        PVAL   3753.58800  3751.26100             2.32700  >   3.84150    1              0.127150
BIOARM-2        PVAL   3753.58800  3753.38600             0.20200  >   3.84150    1              0.653110
BIOSEX-2        PVAL   3753.58800  3750.54200             3.04600  >   3.84150    1              0.080936
CLAGE-2         PVAL   3753.58800  3753.60800            -0.02000  >   3.84150    1
9999
CLARM-2         PVAL   3753.58800  3747.30300             6.28500  >   3.84150    1        YES!  0.012176
CLHIV-2         PVAL   3753.58800  3753.28100             0.30700  >   3.84150    1              0.579530
CLSEX-2         PVAL   3753.58800  3735.40800            18.18000  >   3.84150    1        YES!  0.000020
KAAGE-2         PVAL   3753.58800  3749.35300             4.23500  >   3.84150    1        YES!  0.039599
KAARM-2         PVAL   3753.58800  3753.58200             0.00600  >   3.84150    1              0.938260
KAHIV-2         PVAL   3753.58800  3752.63200             0.95600  >   3.84150    1              0.328200
```

```
KASEX-2          PVAL   3753.58800  3748.93500             4.65300  >   3.84150    1         YES!  0.030999
MTTAGE-2         PVAL   3753.58800  3748.09100             5.49700  >   3.84150    1         YES!  0.019049
MTTARM-2         PVAL   3753.58800  3749.47400             4.11400  >   3.84150    1         YES!  0.042530
MTTHIV-2         PVAL   3753.58800  3752.37300             1.21500  >   3.84150    1               0.270340
MTTSEX-2         PVAL   3753.58800  3750.65600             2.93200  >   3.84150    1               0.086840
V2AGE-2          PVAL   3753.58800  3751.04500             2.54300  >   3.84150    1               0.110780
V2ARM-2          PVAL   3753.58800  3746.69300             6.89500  >   3.84150    1         YES!  0.008644
V2HIV-2          PVAL   3753.58800  3753.26900             0.31900  >   3.84150    1               0.572210
V2SEX-2          PVAL   3753.58800  3749.79600             3.79200  >   3.84150    1               0.051498

Parameter-covariate relation chosen in this forward step: CL-SEX-2
CRITERION             PVAL < 0.05
BASE_MODEL_OFV       3753.58800
CHOSEN_MODEL_OFV     3735.40800
Relations included after this step:
BIO     HIV-2
CL      SEX-2
KA
MTT
V2
--------------------

Model directory /home/simba/RFPUCSF/scm_dir1/forward_scm_dir1/scm_dir1/m1

MODEL            TEST     BASE OFV     NEW OFV         TEST OFV (DROP)    GOAL     dDF    SIGNIFICANT PVAL
BIOAGE-2         PVAL   3735.40800  3732.58200             2.82600  >   3.84150    1               0.092749
BIOARM-2         PVAL   3735.40800  3735.26800             0.14000  >   3.84150    1               0.708280
BIOSEX-2         PVAL   3735.40800  3735.32600             0.08200  >   3.84150    1               0.774600
CLAGE-2          PVAL   3735.40800  3735.34900             0.05900  >   3.84150    1               0.808080
CLARM-2          PVAL   3735.40800  3726.97500             8.43300  >   3.84150    1         YES!  0.003685
CLHIV-2          PVAL   3735.40800  3734.13700             1.27100  >   3.84150    1               0.259580
KAAGE-2          PVAL   3735.40800  3731.23400             4.17400  >   3.84150    1         YES!  0.041049
KAARM-2          PVAL   3735.40800  3735.41800            -0.01000  >   3.84150    1
9999
KAHIV-2          PVAL   3735.40800  3734.74900             0.65900  >   3.84150    1               0.416910
KASEX-2          PVAL   3735.40800  3733.53700             1.87100  >   3.84150    1               0.171360
MTTAGE-2         PVAL   3735.40800  3729.78300             5.62500  >   3.84150    1         YES!  0.017706
MTTARM-2         PVAL   3735.40800  3731.36500             4.04300  >   3.84150    1         YES!  0.044355
MTTHIV-2         PVAL   3735.40800  3734.14900             1.25900  >   3.84150    1               0.261840
MTTSEX-2         PVAL   3735.40800  3732.61100             2.79700  >   3.84150    1               0.094441
V2AGE-2          PVAL   3735.40800  3732.91400             2.49400  >   3.84150    1               0.114280
V2ARM-2          PVAL   3735.40800  3727.58800             7.82000  >   3.84150    1         YES!  0.005167
V2HIV-2          PVAL   3735.40800  3734.11500             1.29300  >   3.84150    1               0.255500
V2SEX-2          PVAL   3735.40800  3735.36300             0.04500  >   3.84150    1               0.832000

Parameter-covariate relation chosen in this forward step: CL-ARM-2
CRITERION             PVAL < 0.05
BASE_MODEL_OFV       3735.40800
CHOSEN_MODEL_OFV     3726.97500
Relations included after this step:
BIO     HIV-2
CL      ARM-2   SEX-2
KA
MTT
V2
--------------------

Model directory /home/simba/RFPUCSF/scm_dir1/forward_scm_dir1/scm_dir1/scm_dir1/m1

MODEL            TEST     BASE OFV     NEW OFV         TEST OFV (DROP)    GOAL     dDF    SIGNIFICANT PVAL
BIOAGE-2         PVAL   3726.97500  3724.75000             2.22500  >   3.84150    1               0.135790
BIOARM-2         PVAL   3726.97500  3724.48900             2.48600  >   3.84150    1               0.114860
BIOSEX-2         PVAL   3726.97500  3726.97700            -0.00200  >   3.84150    1
9999
CLAGE-2          PVAL   3726.97500  3726.88600             0.08900  >   3.84150    1               0.765450
CLHIV-2          PVAL   3726.97500  3726.50000             0.47500  >   3.84150    1               0.490700
KAAGE-2          PVAL   3726.97500  3722.68500             4.29000  >   3.84150    1         YES!  0.038337
KAARM-2          PVAL   3726.97500  3726.70200             0.27300  >   3.84150    1               0.601330
KAHIV-2          PVAL   3726.97500  3726.18000             0.79500  >   3.84150    1               0.372590
KASEX-2          PVAL   3726.97500  3725.18800             1.78700  >   3.84150    1               0.181290
MTTAGE-2         PVAL   3726.97500  3721.51000             5.46500  >   3.84150    1         YES!  0.019401
MTTARM-2         PVAL   3726.97500  3722.67700             4.29800  >   3.84150    1         YES!  0.038157
MTTHIV-2         PVAL   3726.97500  3725.78600             1.18900  >   3.84150    1               0.275530
MTTSEX-2         PVAL   3726.97500  3724.29200             2.68300  >   3.84150    1               0.101420
V2AGE-2          PVAL   3726.97500  3724.08600             2.88900  >   3.84150    1               0.089186
V2ARM-2          PVAL   3726.97500  3724.48100             2.49400  >   3.84150    1               0.114280
V2HIV-2          PVAL   3726.97500  3726.49700             0.47800  >   3.84150    1               0.489330
V2SEX-2          PVAL   3726.97500  3726.96900             0.00600  >   3.84150    1               0.938260

Parameter-covariate relation chosen in this forward step: MTT-AGE-2
CRITERION             PVAL < 0.05
BASE_MODEL_OFV       3726.97500
CHOSEN_MODEL_OFV     3721.51000
Relations included after this step:
BIO     HIV-2
CL      ARM-2   SEX-2
KA
MTT     AGE-2
```

```
V2
--------------------

Model directory /home/simba/RFPUCSF/scm_dir1/forward_scm_dir1/scm_dir1/scm_dir1/scm_dir1/m1

MODEL            TEST     BASE OFV     NEW OFV         TEST OFV (DROP)    GOAL     dDF    SIGNIFICANT PVAL
BIOAGE-2         PVAL   3721.51000  3719.25400              2.25600  >   3.84150    1              0.133100
BIOARM-2         PVAL   3721.51000  3718.97400              2.53600  >   3.84150    1              0.111280
BIOSEX-2         PVAL   3721.51000  3721.62000             -0.11000  >   3.84150    1
9999
CLAGE-2          PVAL   3721.51000  3721.37000              0.14000  >   3.84150    1              0.708280
CLHIV-2          PVAL   3721.51000  3720.98800              0.52200  >   3.84150    1              0.469990
KAAGE-2          PVAL   3721.51000  3720.40000              1.11000  >   3.84150    1              0.292080
KAARM-2          PVAL   3721.51000  3721.31300              0.19700  >   3.84150    1              0.657150
KAHIV-2          PVAL   3721.51000  3720.56100              0.94900  >   3.84150    1              0.329970
KASEX-2          PVAL   3721.51000  3719.68500              1.82500  >   3.84150    1              0.176720
MTTAGE-3         PVAL   3721.51000  3717.70700              3.80300  >   3.84150    1              0.051161
MTTARM-2         PVAL   3721.51000  3717.78500              3.72500  >   3.84150    1              0.053604
MTTHIV-2         PVAL   3721.51000  3719.98500              1.52500  >   3.84150    1              0.216860
MTTSEX-2         PVAL   3721.51000  3719.13400              2.37600  >   3.84150    1              0.123210
V2AGE-2          PVAL   3721.51000  3718.98900              2.52100  >   3.84150    1              0.112340
V2ARM-2          PVAL   3721.51000  3718.92600              2.58400  >   3.84150    1              0.107950
V2HIV-2          PVAL   3721.51000  3721.00700              0.50300  >   3.84150    1              0.478190
V2SEX-2          PVAL   3721.51000  3721.46400              0.04600  >   3.84150    1              0.830180

Parameter-covariate relation chosen in this forward step: --
CRITERION              PVAL < 0.05
--------------------
--------------------
Forward search done. Starting backward search inside forward top level directory
Model directory /home/simba/RFPUCSF/scm_dir1/backward_scm_dir1/m1

MODEL            TEST     BASE OFV     NEW OFV         TEST OFV (DROP)    GOAL     dDF  INSIGNIFICANT PVAL
BIOHIV-1         PVAL   3721.51000  3775.95200            -54.44200  >  -6.63490   -1              1.60e-13
CLARM-1          PVAL   3721.51000  3729.70700             -8.19700  >  -6.63490   -1              0.004196
CLSEX-1          PVAL   3721.51000  3741.56700            -20.05700  >  -6.63490   -1              0.000008
MTTAGE-1         PVAL   3721.51000  3727.04800             -5.53800  >  -6.63490   -1        YES!  0.018608

Parameter-covariate relation chosen in this backward step: MTT-AGE-1
CRITERION              PVAL > 0.01
BASE_MODEL_OFV        3721.51000
CHOSEN_MODEL_OFV      3727.04800
Relations included after this step:
BIO      HIV-2
CL       ARM-2    SEX-2
KA
V2
--------------------

Model directory /home/simba/RFPUCSF/scm_dir1/backward_scm_dir1/scm_dir1/m1

MODEL            TEST     BASE OFV     NEW OFV         TEST OFV (DROP)    GOAL     dDF  INSIGNIFICANT PVAL
BIOHIV-1         PVAL   3727.04800  3781.25800            -54.21000  >  -6.63490   -1              1.80e-13
CLARM-1          PVAL   3727.04800  3735.39100             -8.34300  >  -6.63490   -1              0.003872
CLSEX-1          PVAL   3727.04800  3747.14100            -20.09300  >  -6.63490   -1              0.000007

Parameter-covariate relation chosen in this backward step: --
```

c) Rifapentine Control stream (RIFAQUIN study)

```
$PROBLEM   ;RIFAPENTINE

$ABBREVIATED COMRES=2
$INPUT     ID       AMT      SID        DV        DVO=DROP DATE=DROP  TIME     ATIM=DROP       EVID
        MDV        OCC      SS=DROP          II=DROP BQL      DAY=DROP ARM HT         WT        AGE       HIV
          SEX      PROB
                            PSID=DROP        MXF=DROP        DOSM=DROP       PROB_MXF=DROP
          SPARSE
$DATA      20131003RFP.csv IGNORE=#
$DATA      IGNORE=(PROB.EQ.1)
$SUBROUTINE ADVAN13 TOL=9
$MODEL     NCOMPARTMENTS=4 COMP=(ABS DEFDOSE)
                      COMP=(CENTRAL DEFOBSERVATION)
                            COMP=(TBMIC)
                            COMP=(TAMIC)

$PK

IF(SEX.EQ.1) CLSEX = 1  ; Males
IF(SEX.EQ.0) CLSEX = ( 1 + THETA(11))
IF(ARM.EQ.6) CLARM = 1  ; Most common
```

```
IF(ARM.EQ.4) CLARM = ( 1 + THETA(10))

CLCOV=CLARM*CLSEX

IF(HIV.EQ.0) BIOHIV = 1  ; Most common
IF(HIV.EQ.1) BIOHIV = ( 1 + THETA(9))

BIOCOV=BIOHIV


TVCL    = THETA(1)*((WT/55.2)**0.75)

TVCL = CLCOV*TVCL
CL      = TVCL*EXP(ETA(1))

TVV2   = THETA(2)*(WT/55.2)
 V2     = TVV2*EXP(ETA(2))

TVKA   = THETA(3)
 KA     = TVKA*EXP(ETA(3))

TVMTT = THETA(4)
  MTT = TVMTT*EXP(ETA(4))

F1=0 ;
TVBIO = THETA(5)

TVBIO = BIOCOV*TVBIO
BIO   = TVBIO*EXP(ETA(5))

TVNN  = THETA(6)
  NN  = TVNN

 S2   = V2
 K    = CL/V2
 KTR  = (NN+1)/MTT


LNGAM = NN*LOG(NN)-NN+LOG(NN*(1+4*NN*(1+2*NN)))/6+0.572364942

IF (NEWIND.NE.2.OR.EVID.GE.3) THEN
              TNXD=TIME
              PNXD=AMT
ENDIF

TDOS=TNXD
PD=PNXD

IF(AMT.GT.0) THEN
              TNXD=TIME
              PNXD=AMT
ENDIF

PIZZA=LOG(BIO*PD*KTR+0.00000001)-LNGAM

IF(NEWIND.LE.1.OR.EVID.GE.3) THEN
     COM(1)=-1 ; holder of Cmax
     COM(2)=-1 ; holder of Tmax
   ENDIF

$DES

TEMPO=T-TDOS

IF(PD.GT.0.AND.TEMPO.GT.0) THEN
              KTT=KTR*(TEMPO)
              DADT(1)=EXP(PIZZA+NN*LOG(KTT)-KTT)-KA*A(1)
```

```
ENDIF

DADT(2) = KA*A(1)-K*A(2)

  CT=A(2)/S2 ; (or other expression for concentration)
  IF(CT.GT.COM(1)) THEN
      COM(1)=CT
      COM(2)=T
  ENDIF

  MIC=6 ; MIC adjusted for protein binding
  BMIC=0
  AMIC=0
  IF(CT.LT.MIC) BMIC=1
  IF(CT.GE.MIC) AMIC=1
  DADT(3)=BMIC ; time below threshold
  DADT(4)=AMIC ;cumulative time above MIC

$ERROR

IPRED=F
PROP=THETA(7)*IPRED
ADD=THETA(8)
IRES=DV-IPRED
W =SQRT(PROP**2+ADD**2)
IF(W.LE.0.000001) W=0.000001

IWRES=IRES/W
IF(BQL.EQ.0) THEN
Y = IPRED + W*EPS(1)
ELSE
Y=0.078
ENDIF

IF(ICALL.EQ.4.AND.Y.LE.0.156) Y=0.078

IF (AMT.GT.0.OR.EVID.GE.3) THEN
            TDOSE=TIME
            TAD=0
ENDIF
TAD=TIME-TDOSE



AUC    = BIO*AMT/CL
CMAX   = COM(1)
TMAX   = COM(2)
TBMIC  =A(3)  ;cumulative time below MIC
TAMIC  =A(4)  ;cumulative above below MIC
AUCMIC =A(3)*A(2)/S2

$THETA  (0,1.07616) ; 1 POP_CL
$THETA  (0,24.4966) ; 2 POP_V
$THETA  (0,0.8851) ; 3  POP_KA
$THETA  (0,1.45013) ; 4 POP_MTT
$THETA  1 FIX ; 4 POP_BIO
$THETA  (0,8.41091) ; 6 POP_NN number of transit compartments
$THETA  (0,0.107836) ; 7 PROPP RUV
$THETA  (0,0.462632) ; 8 ADDP RUV
$THETA  (-1,-0.276084,5) ; BIOHIV1
$THETA  (-1,0.103575,5) ; CLARM1
$THETA  (-1,-0.151606,5) ; CLSEX1

$OMEGA  BLOCK(2)
 0.0818678  ;     1BSVCL
 0.0403007 0.0551038  ;      2BSVV
$OMEGA  0.192439  ;     3BSVKA
```

```
$OMEGA  0.14761 ;    4BSVMTT
$OMEGA  0  FIX ;    5BSVBIO

$OMEGA  BLOCK(1) FIX
 0 ;     6_IOVF
$OMEGA  BLOCK(1) SAME

$OMEGA  BLOCK(1) FIX
 0 ;   8_IOVMTT
$OMEGA  BLOCK(1) SAME

$OMEGA  BLOCK(1) FIX
 0 ;   10_IOVKA
$OMEGA  BLOCK(1) SAME

$SIGMA  1  FIX
$ESTIMATION MAXEVAL=9999 PRINT=1 SIGDIG=3 SIGL=9 POSTHOC METH=COND
 ATOL=4 INTER NOABORT
MSFO=run540.msf
$COVARIANCE PRINT=E MATRIX=S ATOL=4
$TABLE  ID TIME DV CL V2 KA MTT NN BIO ETA1 ETA2 ETA4 ETA5 ETA5 TAD SID TMAX CMAX TBMIC
TAMIC AUCMIC AUC
CWRES NPDE  PRED IPRED PREDI RESI WRESI IPRED IWRES                                    NOPRINT
ONEHEADER FILE=sdtab540
$TABLE  ID TIME CL V2 KA MTT NN TAD BIO ETA1 ETA2 ETA3 ETA4 ETA5 ETA5 PRED CWRES NPDE IPRED
PREDI RESI WRESI         NOPRINT ONEHEADER FILE=patab540
$TABLE  ID TIME PRED WT  HT AGE                                                NOPRINT ONEHEADER
FILE=cotab540
$TABLE  ID TIME PRED ARM HIV SEX                                                NOPRINT ONEHEADER
FILE=catab540
$TABLE  ID TIME DV CL V2 KA MTT NN TAD TMAX CMAX TBMIC TAMIC AUCMIC AUC SID BIO
AGE HIV SEX  ETA1 ETA2 ETA3 ETA4 ETA5 ETA5 WT ARM HT CWRES PRED IPRED PREDI RESI WRESI
NOPRINT ONEHEADER FILE=mytab540
```

Appendix 7- Parametric hazard modeling

a) Control stream of final model

```
$PROB Time To Event data ; TIME VARYING HAZARD SAME

$INPUT ID CAV SEX WEIGHT RACE=DROP CD4=DROP SMOKED SMOKER MITT_STATUS TTE_MITT
        PP_STATUS TTE_PP TMAXRFP=DROP CMAXRFP AUCRFP CMAXMX TMAXMX AUCMX
CMAXWTMXF TMAXWTMXF=DROP AUCWTMX AUCMICMX1=DROP AUCMICMX2=DROPAUCMICRFP
CMAXMICMX1=DROP CMAXMICMX2=DROP CMAXMICRFP AUCMICWTMX1 AUCMICWTMX2
CMAXMICWTMX1 CMAXMICWTMX2 IDENTIFIER HIV SITE ARM AUCRFP_WT CMAXRFP_WT
AUCMXF_WT CMAXMXF_WT        TIME MARKER1 DVONE  MARKER2 DV AGE          EVID
        MARKER TOTAL_AUCRFP RFP_AUCMIC CMAXRFP_MIC TAMIC_RFP MXFAUCT
MXFAUC_MIC CMAXMXF_MIC TAMICMXF


$DATA TWO_ARMS.csv  IGNORE=@  ACCEPT=(TIME==0)  ACEPT=(MARKER1==1)

$SUBR ADVAN=6 TOL=6
$MODEL COMP=(RISK)

$PK

IF(ARM.EQ.2) COVDUR = 1  ; Males
IF(ARM.EQ.1) COVDUR = ( 1 + THETA(3))

IF(NEWIND.NE.2) TP=0
 TVLAM = THETA(1)*COVDUR
 TVSHP = THETA(2) ; shape (FIXED TO 1)

 LAM=TVLAM*EXP(ETA(1))  ;the ETA is a placeholder here
 SHP=TVSHP

$DES
 DEL=1E-6
 DADT(1) = LAM*SHP*(T-TP+DEL)**(SHP-1)

$ERROR
;----------RTTE Model------------------------------
 IF(NEWIND.NE.2) OLDCHZ=0  ;reset the cumulative hazard
 CHZ = A(1)-OLDCHZ        ;cumulative hazard
                ;from previous time point
                ;in data set
 OLDCHZ = A(1)          ;rename old cumulative hazard
 SUR = EXP(-CHZ)         ;survival probability
 DELX = 1E-6
 HAZNOW=LAM*SHP*(TIME-TP+DELX)**(SHP-1)
                ;rate of event
                ;NB: update with each new model

 IF(DV.EQ.0)   Y=SUR   ;censored event (prob of survival)
 IF(DV.NE.0)   Y=SUR*HAZNOW  ;prob of event at time=TIME


$THETA  (0,0.000102896) ; 1.BASE
$THETA  1 FIX ; 2.ALPHA
$THETA  (0,1.87119) ; 3.COVDUR
$OMEGA  0  FIX
$ESTIM MAXEVAL=9990 METHOD=0 LIKE PRINT=1 NOABORT MSFO=msfb34
$COV PRINT=E

$TABLE ID TIME EVID SUR NOPRINT ONEHEADER FILE=sdtab34
$TABLE ID NOPRINT ONEHEADER FILE=patab34
$TABLE ID   NOPRINT ONEHEADER FILE=cotab34
$TABLE ID CAV SEX HIV SMOKED SMOKER ARM   SITE PP_STATUS   NOPRINT ONEHEADER
FILE=catab34
```

_____END OF THESIS_____